

CCFS *Whole-of-Centre* Meeting

27-29 November 2017

Cairns, Australia



Abstracts



The Australian Research Council Centre of Excellence for Core to Crust Fluid Systems

2017 CCFS *Whole-of-Centre* Meeting

**Cairns, Australia,
27-29 November 2017**

Abstract Volume



*Abstracts are arranged alphabetically by the presenting author's name.
Presentations and posters are listed by author on pp. 121-122.*



**2017 CCFS Whole-of-Centre Meeting,
Cairns, Australia, 27-29 November 2017
Abstract Volume**

ISSN 2208-7230

Citations of abstracts in this volume should be referenced as follows:

<Authors> 2017. <Title>. Abstract, 2017 CCFS Whole of Centre Meeting, p.<page>. CCFS, Australia, pp. 122.

CCFS information is accessible at:
<http://www.ccfs.mq.edu.au/>



Contact CCFS via email at:
ccfs.admin@mq.edu.au



© CCFS

ARC Centre of Excellence for Core to Crust Fluid Systems (CCFS)

Front cover designed by Sally-Ann Hodgekiss.

Taming the impossible: Multiobservable thermochemical tomography at global scale

J.C. AFONSO^{1,2}

¹Australian Research Council Centre of Excellence for Core to Crust Fluid Systems (CCFS) and GEMOC, Department of Earth and Planetary Sciences, Macquarie University, Sydney, NSW 2109, Australia (juan.afonso@mq.edu.au)

²Centre for Earth Evolution and Dynamics (CEED), Department of Geosciences, University of Oslo, NO-0315, Norway

Multiobservable thermochemical tomography (MTT) is a recent method specifically designed to obtain estimates of the physical state (e.g. temperature distribution, compositional structure, stress/strain distributions, etc.) of the lithosphere and sublithospheric upper mantle [1-3]. MTT is framed within a probabilistic framework that requires long Markov Chain Monte Carlo (MCMC) simulations. As such, it is computationally demanding, and at least in principle, subject to the curse of dimensionality. Computational cost arises primarily from the need to solve complex forward problems (e.g. Stokes flow, waveforms, Maxwell's equations, etc.) millions of times, whereas the dimensionality problem is related to the fact that in high-dimensional parameter spaces it becomes increasingly difficult to 1) locate the regions of high probability and 2) sample these regions densely enough to obtain representative estimates of the true posterior probability density function.

Previous work showed that MTT is a practical option for high-resolution regional studies (e.g. 2000 x 2000 km) with ~10,000 parameters, requiring relatively modest computational resources (i.e. a few hundred cores). However, the extension of the method to larger areas, or even at global scale, presents a vastly different problem. The number of parameters in a global study can easily reach one million and the solution of the forward problems becomes significantly more involved. Solving such a probabilistic problem is typically considered unachievable. It is clear therefore that if the method is to become a reality, novel ways of solving these difficulties need to be devised. Incidentally, if this is achieved, it will be the biggest probabilistic inversion ever attempted.

In this presentation I will discuss some of the new approaches we are taking to tackle the above difficulties and produce the first global MTT. Taming this problem clearly needs an “army” of techniques carefully assembled and used in parallel. We rely on 1) a “multi-method” approach that uses state-of-the-art MCMC methodologies, specifically tailored to our needs, to solve the sampling problem and 2) novel reduced-order modelling techniques to make the solution of the forward problems more efficient. While the estimated computational resources remains somewhat daunting to the average practitioner, we are starting to reach core numbers well within the capabilities of the largest supercomputers in many institutions around the world.

REFERENCES

- [1] Afonso, J.C. et al. 2013. 3D multi-observable probabilistic inversion for the compositional and thermal structure of the lithosphere and upper mantle I: a priori information and geophysical observables. *Journal of Geophysical Research*, doi:10.1002/jgrb.50124.
- [2] Afonso, J.C. et al. 2013. 3D multi-observable probabilistic inversion for the compositional and thermal structure of the lithosphere and upper mantle II: General methodology and resolution analysis. *Journal of Geophysical Research*, doi:10.1002/jgrb.50123.
- [3] Afonso, J.C. et al. 2016. 3D multi-observable probabilistic inversion for the compositional and thermal structure of the lithosphere and upper mantle III: Thermochemical Tomography in the Western-Central US. *Journal of Geophysical Research*, 121, doi:10.1002/2016JB013049.

Reappraisal of MORB redox state using both Fe and S speciation

O. ALARD¹, C. BAUDOUIN², M. CHASSÉ^{1,3}, F. PARAT² AND M. MUÑOZ²

¹Australian Research Council Centre of Excellence for Core to Crust Fluid Systems (CCFS) and GEMOC, Department of Earth and Planetary Sciences, Macquarie University, Sydney, NSW 2109, Australia (olivier.alard@mq.edu.au)

²Géosciences Montpellier, CNRS UMR5243, France

³IMPMC UMR7590, Paris 6, France

The oxidation state of MORB (fO_2) has been vividly debated these recent years and several studies have yielded distinct values ranging from FMQ-1.2 to +1 and conclusions regarding the (lack of) variability and/or correlation with other geochemical indexes [1-3]. Historically, the oxidation state of Fe ($Fe^{3+}/\Sigma Fe$) in glasses has been used to assess fO_2 of magma. While less abundant than Fe, S oxidation shifts sharply from S^{2-} to S^{6+} at FMQ+1.0±0.5 [4], thus ideal to constrain MORB fO_2 . $Fe^{3+}/\Sigma Fe$ and S^{6+}/SS were determined by micro X-ray absorption near edge structure (ID21 ESRF) on the same shard of fresh MORB glasses (N=38). Lithophile and chalcophile trace elements by LA-ICP-MS have also been also obtained on the same glasses.

The average $Fe^{3+}/\Sigma Fe = 0.137 \pm 0.006$ yielding an average fO_2^{Fe} ca. FMQ-0.10±0.16. fO_2^{Fe} is positively correlated with V/Sc and S content. No other significant correlation with trace element fractionation (e.g. La/Sm, Nb/Zr) or radiogenic isotope compositions (e.g. $^{206}Pb/^{204}Pb$, $^{143}Nd/^{144}Nd$) have been found so far. S^{6+}/SS ranges between 0.03 and 0.17 average is 0.09±0.02 yielding fO_2^S ca. FMQ+0.01±0.1 within error of the Fe based estimate. However, S^{6+}/SS is poorly correlated with $Fe^{3+}/\Sigma Fe$ nor with V/Sc.

REFERENCES

- [1] Christie, D.M. et al. 1986. Oxidation states of mid-ocean ridge basalt glasses. *Earth and Planetary Science Letters*, 79, 397-411.
- [2] Bézous, A. and Humler, E. 2005. The $Fe^{3+}/\Sigma Fe$ ratios of MORB glasses and their implications for mantle melting. *Geochimica et Cosmochimica Acta*, 69, 711-725.
- [3] Cottrell, E. and Kelley, K.A. 2013. Redox heterogeneity in mid-ocean ridge basalts as a function of mantle source. *Science*, 340, 1314-1317.
- [4] Jugo, P.J. et al. 2010. Sulfur K-edge XANES analysis of natural and synthetic basaltic glasses: Implications for S speciation and S content as function of oxygen fugacity. *Geochimica et Cosmochimica Acta*, 74, 5926-5938.

Microbial diversity at the rise of atmospheric oxygen: Two distinct microfossil communities from the Turee Creek Group, Western Australia

E.V. BARLOW AND M.J. VAN KRANENDONK

Australian Research Council Centre of Excellence for Core to Crust Fluid Systems (CCFS), and the Australian Centre for Astrobiology and PANGAEA Research Centre, School of Biological, Earth and Environmental Sciences, University of New South Wales, Kensington, NSW 2052, Australia (e.barlow@unsw.edu.au; m.vankranendonk@unsw.edu.au)

The c. 2.4 Ga Turee Creek Group (TCG) from the Hamersley Ranges in Western Australia preserves a snapshot of a whole ecosystem from a shallow water stromatolite-thrombolite reef, to deeper water microfossiliferous black chert units [1]. That this sequence occurs across one continuous outcrop provides a unique opportunity to study a range of life from multiple different habitats within the same system, allowing insight into the diversity of life present during the rise of atmospheric oxygen (Great Oxidation Event: GOE).

The recently discovered suite of microfossils [2, 3, 4] is preserved in deep water nodular and bedded black chert units, and now encompasses at least 18 different morphotypes including two forms new to the geobiological record [5]. The two types of black chert contain communities of microfossils from different environments: a primarily benthic, *in situ*, deep water assemblage from the nodular chert, and a transported, originally shallow-water (likely phototrophic) community in the bedded black chert (Fig. 1) [5].

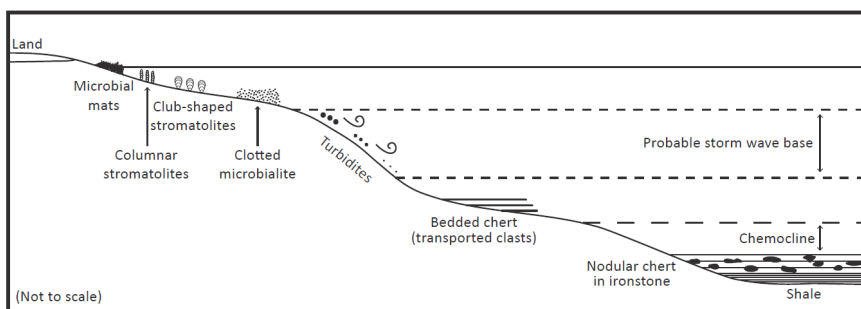


Figure 1. Model of the TCG environment, showing the relative position of the inter-tidal microbialites and the deeper-water microfossiliferous bedded and nodular black cherts [5].

The deep water bedded black chert consists of rounded organic clasts transported from the shallower water. Numerous

microfossil forms within these clasts bear similarity to the well-known microfossil assemblage of the c. 1.8 Ga Gunflint Iron Formation, Canada [6]. Gunflint-type microbiota are preserved in multiple localities worldwide, ranging from c. 1.6-2.1 Ga, and examples are representative of similar shallow-water environments rather than one common stratigraphic horizon [7]. Thus, the assemblage of Gunflint-type microfossils presented here from the TCG further highlights the persistence of silica-rich, subtidal microbial environments throughout the Paleoproterozoic, and forms the oldest known examples of the Gunflint microbiota worldwide.

The two communities of microfossils from the nodular and bedded black cherts of the TCG, when combined with the wide array of stromatolitic microbialites preserved in the intertidal zone [1], provide a snapshot of a c. 2.4 Ga ecosystem (Fig. 1). The TCG microfossil assemblage also creates a substantial reference point in the sparse fossil record of the earliest Paleoproterozoic, and illustrates that microbial life diversified quite rapidly from the simple forms preserved in the Archean.

REFERENCES

- [1] Barlow, E.V. et al. 2016. Lithostratigraphic analysis of a new stromatolite-thrombolite reef from across the rise of atmospheric oxygen in the Paleoproterozoic Turee Creek Group, Western Australia. *Geobiology*, 14, 317-343.
- [2] Van Kranendonk, M.J. et al. 2012. A 2.3 Ga sulfuretum at the GOE: Microfossils and organic geochemistry evidence from the Turee Creek Group, Western Australia. *Astrobiology Science Conference Abstract*, Atlanta, Georgia.
- [3] Schopf, J.W. et al. 2015. Sulfur-cycling fossil bacteria from the 1.8-Ga Duck Creek Formation provide promising evidence of evolution's null hypothesis. *Proceedings of the National Academy of Sciences*, 112, 7, 2087-2092.
- [4] Fadel, A. et al. 2017. Iron mineralization and taphonomy of microfossils of the 2.45-2.21 Ga Turee Creek Group, Western Australia. *Precambrian Research*, 298, 530-551.
- [5] Barlow, E.V. and Van Kranendonk, M.J. In review. Snapshot of a c. 2.4 Ga ecosystem: Two diverse microfossil communities from the Turee Creek Group, Western Australia. *Geobiology*.
- [6] Barghoorn, E.S. and Tyler, S.A. 1965. Microorganisms from the Gunflint Chert. *Science*, 147, 3658, 563-575.
- [7] Knoll, A.H. and Simonson, B. 1981. Early Proterozoic microfossils and penecontemporaneous quartz cementation in the Sokoman Iron Formation, Canada. *Science*, 211, 4481, 478-480.

Nano-scale biosignatures preserved in sulfidised stromatolites of the 3.5 Ga Dresser Formation

R.J. BAUMGARTNER¹, M. FIORENTINI¹, M. VAN KRANENDONK² AND D. WACEY³

¹ARC Centre of Excellence for Core to Crust Fluid Systems (CCFS), The University of Western Australia, 35 Stirling Highway, Crawley, WA 6009, Australia (raphael.baumgartner@uwa.edu.au; marco.fiorentini@uwa.edu.au)

²ARC Centre of Excellence for Core to Crust Fluid Systems (CCFS), School of Biological, Earth and Environmental Sciences, University of New South Wales, NSW 2052, Australia (m.vankranendonk@unsw.edu.au)

³ARC Centre of Excellence for Core to Crust Fluid Systems (CCFS) and Centre for Microscopy, Characterisation and Analysis, The University of Western Australia, 35 Stirling Highway, Crawley, WA 6009, Australia (david.wacey@uwa.edu.au)

The ~3.5 Ga old stromatolites of the Dresser Formation, Pilbara Craton, are among the oldest known fossiliferous rocks on the Earth. They presumably formed by chemoautotrophic microbes that grew in proximity to shallow marine or surficial hot spring vents of steam-heated acid-sulfate geothermal systems in a volcanic caldera [1, 2]. A drilling initiative in the Dresser Formation in 2004 uncovered barite-chert-hosted stromatolites defined by unweathered pyrite \pm sphalerite laminae [1]. While recent quadruple sulfur isotope analysis of the contained pyrite provided subtle, but inconclusive indications for sulfur-based biogenesis (i.e. sulfate and/or elemental sulfur metaboliser [3]), coupled multi-scale textural, mineralogical, and chemical characterisations, which are crucial to test the hypothesis of microbial metabolism involved during sulfidisation, are absent. Hence, this study examines the sulfides for micron- to nano-scale co-variations of potential microbial fabrics, chemical biosignatures (e.g. isotopes of S, C and N), and transition metals such as Ni and Zn that are known to be vital for biotic reactions.

Micron- to nano-scale investigations (FESEM, FIBS-SEM and TEM) reveal a diverse array of millimetre- to submicron-scale variations in textures and (trace) element signatures of pyrite, suggesting consecutive crystallisation in contrasting realms; i.e. potentially ranging from hydrothermally-influenced crystallisation during sedimentation/diagenesis, to exclusively hydrothermal overgrowth. Notable observations are early-stage framboidal pyrite associations, defined by dispersed nano-crystals in variably recrystallised, Ni- and C-rich, spongy/porous pyrite matrix material, and which are overgrown by irregularly annealed and non-porous late-stage pyrite. Comparable textures, suggesting porous pyritisation in an organic matrix, were reported from younger bio-mediated pyrite framboids [4, 5]. Indeed, nitric-acid (HNO₃) etching of the spongy pyrite uncovered uncorroded filamentous and sheath-like carbon-rich structures that are in places speckled/encrusted by platy nanocrystals and irregular concretions of barite. Similar associations in younger cold and hot sulfur-rich spring deposits (e.g. Flyby Springs, Canada [6]) were linked to precipitation in microbial mats; an interpretation that could hold true for the investigated Dresser Formation material.

Detailed SIMS and NanoSIMS analysis for the isotopes of S, N, and C, is underway to test the hypothesis of whether the observed morphological biosignatures can be linked with microbial sulfur-metabolism during formation of the sulfidised Dresser Formation stromatolites. This study highlights the importance of combining micron- to nano-scale textural and chemical techniques in the study of sulfur metabolism and the global sulfur cycle on the early Earth.

REFERENCES

- [1] Van Kranendonk, M. et al. 2008. Geological setting of Earth's oldest fossils in the ca. 3.5 Ga Dresser Formation, Pilbara Craton, Western Australia. *Precambrian Research*, 167, 93-124.
- [2] Djokic, T. et al. 2017. Earliest signs of life on land preserved in 3.5 Ga hot spring deposits. *Nature Communications*, DOI: 10.1038/ncomms15263.
- [3] Shen, Y. et al. 2009. Evaluating the role of microbial sulfate reduction in the early Archean using quadruple isotope systematics. *Earth and Planetary Science Letters*, 279, 383-391.
- [4] MacLean, L.C. et al. 2008. A high-resolution chemical and structural study of framboidal pyrite formed within a low-temperature bacterial biofilm. *Geobiology*, 6, 471-480.
- [5] Wacey, D. et al. 2007. Uncovering framboidal pyrite biogenicity using nano-scale CN_{org} mapping. *Geology*, 35, 27-30.
- [6] Bonny, S.M. and Jones, B. 2007. Barite (BaSO₄) biomineralization at Flyby Springs, a cold sulphur spring system in Canada's Northwest Territories. *Canadian Journal of Earth Sciences*, 44, 835-856.

Numerical modelling of erosion and assimilation of sulfur-rich substrate by martian lava flows: Implications for the genesis of massive sulfide mineralisation on Mars

R.J. BAUMGARTNER¹, D. BARATOUX², F. GAILLARD³ AND M. FIORENTINI¹

¹ARC Centre of Excellence for Core to Crust Fluid Systems (CCFS), The University of Western Australia, 35 Stirling Highway, Crawley, WA 6009, Australia (raphael.baumgartner@uwa.edu.au; marco.fiorentini@uwa.edu.au)

²Géosciences Environnement Toulouse, CNRS, IRD and University of Toulouse, 31400 Toulouse, France (david.baratoux@gmail.com)

³Institut des Sciences de la Terre d'Orléans, CNRS/INSU, Université d'Orléans, 41071 Orléans, France (fabrice.gaillard@cnrs-orleans)

Mantle-derived volcanic rocks on Mars display physical and chemical commonalities with mafic- ultramafic ferropicrite and komatiite volcanism on the Earth. Terrestrial komatiites are common hosts of massive sulfide mineralisation enriched in siderophile-chalcophile precious metals (i.e. Ni, Cu, and the platinum-group elements). These deposits correspond to the batch segregation and accumulation of immiscible sulfide liquids as a consequence of mechanical/thermo-mechanical erosion and assimilation of sulfur-rich bedrock during the turbulent flow of high-temperature and low-viscosity komatiite lava flows. We adopt this mineralisation model and present numerical simulations of erosion and assimilation of sulfide- and sulfate-rich sedimentary substrates during the dynamic emplacement of (channelled) mafic-ultramafic lava flows on Mars.

For sedimentary substrates containing adequate sulfide proportions (e.g. 1 wt% S), our simulations suggest that sulfide supersaturation in low-temperature (<1350 °C) flows could be attained at <200 km distance, but may be postponed in high-temperature lavas flows (>1400 °C). The precious-metals tenor in immiscible sulfide liquids derived by the above process may be significantly upgraded as a result of their prolonged equilibration with large volumes of silicate melts along flow conduits. The influence of sulfate assimilation on sulfide supersaturation in martian lava flows is addressed by simulations of melt-gas equilibration in the C–H–O–S fluid system. However, prolonged sulfide segregation and deposit genesis by means of sulfate assimilation appears to be limited by lava oxidation and the release of sulfur-rich gas.

The identification of massive sulfide endowments on Mars is not possible from remote sensing data. Yet the results of this study aid to define regions for the potential occurrence of such mineral systems, which may be the large canyon systems Noctis Labyrinthus and Valles Marineris, or the Hesperian channel systems of Mars' highlands (e.g. Kasei Valles), most of which have been periodically draped by mafic-ultramafic lavas.

New insights into mantle-crustal interaction in the Finero lithosphere from zircon and laurite isotopic studies

E.A. BELOUSOVA¹, K.N. MALITCH², W.L. GRIFFIN¹, I.YU. BADANINA², S.Y. O'REILLY¹ AND N.J. PEARSON¹

¹Australian Research Council Centre of Excellence for Core to Crust Fluid Systems (CCFS) and GEMOC, Department of Earth and Planetary Sciences, Macquarie University, Sydney, NSW 2109, Australia (elena.belousova@mq.edu.au)

²Department of Geochemistry and Ore-Forming Processes, A.N. Zavaritsky Institute of Geology and Geochemistry, Ural Branch of the Russian Academy of Sciences, Vonsovsky str. 15, Ekaterinburg 620016, Russia (dunite@yandex.ru)

The Ivrea-Verbano Zone in northwest Italy to southern Switzerland represents a section of middle and lower continental crust and lithospheric mantle that accreted onto the Austro-Alpine domain and the European plate during the Alpine orogeny. Three mantle peridotite bodies (Finero, Balmuccia and Baldissero) are considered to represent obducted slices of the continental mantle [1, 2]. The Finero phlogopite-peridotite massif is a metasomatised residual mantle harzburgite, exposed at the base of the lower-crustal section in the northern part of the Ivrea Zone. Chromitites enclosed within the metasomatised Finero phlogopite peridotite contain accessory platinum-group minerals, base metal sulfides, baddeleyite, zircon, zirconolite, uraninite and thorianite. In order to gain further insights into the genesis of chromitite in the subcontinental mantle we have carried out a combined study of zircon and laurite from two chromitite localities at Finero, Italy (i.e. Alpe Polunia and Rio Creves). We integrate Re-Os LA-MC-ICP-MS analyses of laurite to date melt extraction and possible metasomatic events in the Finero lithospheric mantle, and U-Pb, Lu-Hf and trace-element LA-ICP-MS analyses of zircon to constrain the age, nature and evolution of this fragment of the subcontinental mantle.

Re-Os model ages of laurite reflect an Early Paleozoic partial melting event (ca 450 Ma or older), presumably before the Variscan orogeny. The Os isotopic composition of laurite/chromitite probably preserves their mantle signature and was not affected by later metasomatic processes.

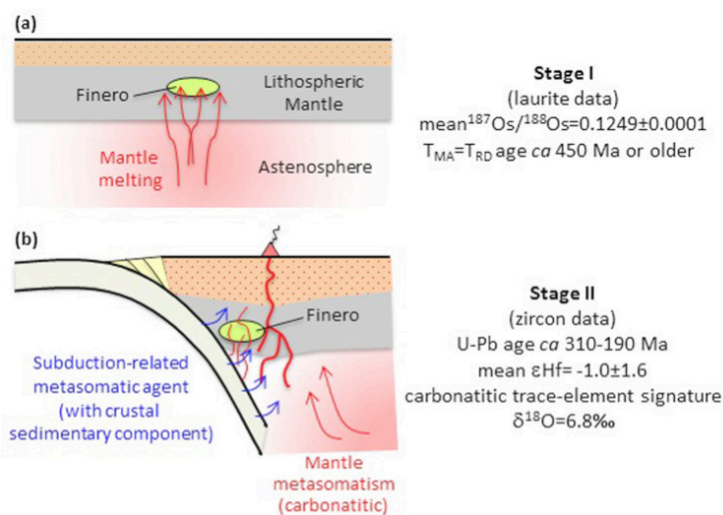


Figure 1. Two-stage geodynamic evolution model for the genesis of chromitites at Finero [1, 2]. Red arrows represent partial melt; blue arrows in (b) represent fluids released by slab devolatilisation.

U-Pb and Hf-isotope studies identified several distinct zircon populations with characteristic crystal morphology, cathodoluminescence features, trace-element composition and an overall U-Pb age span from ~310 Ma to 190 Ma. Three age peaks at Rio Creves (220 ± 4 Ma, 234.2 ± 4.5 Ma and 277.5 ± 3.2 Ma) are consistent with a prolonged formation and

multistage zircon growth, in contrast to the common assumption of a single metasomatic event during chromitite formation. Our findings imply that mantle rocks and metasomatic events at Finero have a far more complex geological history than commonly assumed.

REFERENCES

- [1] Zanetti, F. et al. 2016. Origin and age of zircon-bearing chromitite layers from the Finero phlogopite peridotite (Ivrea-Verbano Zone, Western Alps) and geodynamic consequences. *Lithos*, 262, 58-74.
- [2] Malitch, K.N. et al. 2017. Laurite and zircon from the Finero chromitites (Italy): New insights into evolution of the subcontinental mantle. *Ore Geology Reviews* (in press).

A fluid inclusion microthermometric record and interpretation of the magmatic-hydrothermal mineralisation processes during growth of a single cassiterite crystal

J. BENNETT¹, S. HAGEMANN², T. KEMP³ AND M. FIORENTINI¹

¹Centre for Exploration Targeting (CET) and ARC Centre of Excellence in Core to Crust Fluid Systems (CCFS), University of Western Australia, 35 Stirling Highway, Crawley, WA 6009, Australia (jason.bennett@research.uwa.edu.au; marco.fiorentini@uwa.edu.au)

²Centre for Exploration Targeting (CET), University of Western Australia, 35 Stirling Highway, Crawley, WA 6009, Australia (steffen.hagemann@uwa.edu.au)

³School of Earth Sciences, University of Western Australia, 35 Stirling Highway, Crawley, WA 6009, Australia (tony.kemp@uwa.edu.au)

The 21st century is seeing an increased demand for metals such as Li, Nb, Ta, W, Mo and In. These metals are commonly associated with Sn mineralisation, which predominantly crystallises as cassiterite (SnO₂). Cassiterite has the potential to be an important multi-process recorder of the physical and chemical conditions of formation, as any cassiterite present in an ore assemblage (or even an alluvial sample) is a direct result of the mineralising processes. This work is a facet of a larger study assessing the capabilities of cassiterite in this regard.

Here we show the results of a fluid inclusion microthermometric study on a single crystal of cassiterite from the Blue Tier tin field in north-eastern Tasmania. The crystal was collected alluvially, so the exact placement in the mineralising system is unknown. However, the largest cassiterite crystals described from this region are predominantly hosted in quartz -mica -(topaz) greisen veins and alteration associated with the latest stage of magmatic evolution of the Blue Tier Batholith [1, 2].

The crystal shows fine scale oscillatory zoning in thin section (Fig. 1) which is reflected optically with alternating bands of brown and red-colourless pleochroism. The oscillatory zoning continues to the micrometre

scale with cathodoluminescent (CL) bands 10 to 20 µm across. Changes in minor element composition detectable by Electron Probe Microanalysis (EPMA) also show variable contents of Ti, Fe, Ta and Nb that correlate well with the CL signal, but not with the optical colouration.

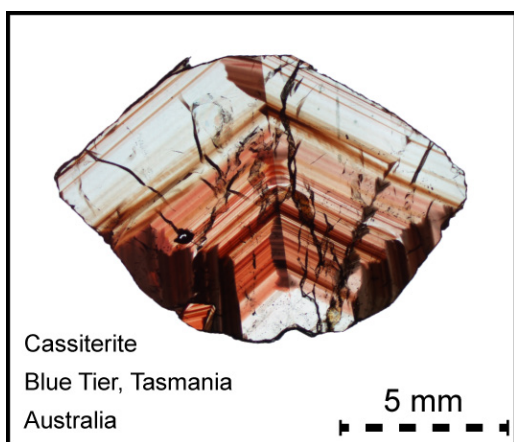


Figure 1. Plane polarised light image of one of the thin sections used in this study. The cassiterite crystal exhibits a twin plane and sector zoning along with the oscillatory zoning discussed in the text.

The optical zoning has been used to define an internal stratigraphy for correlation of fluid inclusions across four consecutive thin section slices of the crystal. This results in a relative petrogenetic sequence for each primary assemblage across the bands that can be used to show changes in the

fluid properties during active cassiterite growth. Previous studies [3] in the Erzgebirge (Ore Mountains) have examined entire petrogenetic stages of the mineralising system in comparable Sn greisens, and these report a complex fluid evolution due to late stage volatile exsolution and subsequent phase separation (boiling) reactions combined with mixing of meteoric waters. The results of this study (still in progress) compare the variability of fluid properties with changes in the microchemistry and optical character of the cassiterite during growth under these complex magmatic-hydrothermal conditions. Discussion of these results will highlight implications for our understanding of fluid behaviour in these mineralising systems.

REFERENCES

- [1] Reid, A.M. and Henderson, Q.J. 1928. The Blue Tier tin field. Geological Survey of Tasmania, Bulletin, 38.
- [2] Groves, D.I. et al. 1977. The Blue Tier Batholith. Geological Survey of Tasmania, Bulletin, 55.
- [3] Dolníček, Z. et al. 2012. Fluid evolution of the Hub Stock, Horní Slavkov-Krásno Sn-W ore district, Bohemian Massif, Czech Republic. Mineralium Deposita, 47, 7, 821-833.

Deciphering the fluid evolution of the Nimbus Ag-Zn-(Au) VHMS deposit, Yilgarn Craton, Western Australia

S. CARUSO¹, C. LAFLAMME¹, R.J. BAUMGARTNER¹, M.L. FIORENTINI¹, S.P. HOLLIS² AND L. MARTIN³

¹Centre for Exploration Targeting (CET) and ARC Centre of Excellence in Core to Crust Fluid Systems (CCFS), University of Western Australia, 35 Stirling Highway, Crawley, WA 6009, Australia (stefano.caruso@research.uwa.edu.au; crystal.laflamme@uwa.edu.au; raphael.baumgartner@uwa.edu.au; marco.fiorentini@uwa.edu.au)

²ICRAG (Irish Centre for Research in Applied Geosciences), University College Dublin, Ireland

³CMCA/CCFS, The University of Western Australia, Perth, WA (laure.martin@uwa.edu.au)

In the Yilgarn Craton, volcanic-hosted massive sulfide (VHMS) mineralisation is mainly restricted to zones of thin juvenile crust as recently identified by regional (Nd, Pb and Hf) isotope studies [2,3]. Interpreted as Archaean paleo-rift zones, one such zone trends N-S through the Eastern Goldfields Superterrane and is associated with the high-grade ca. 2690 Ma Teutonic Bore, Jaguar and Bentley VHMS deposits [1]. Until recently, the plume-related lower portions of the stratigraphy were considered non-prospective since only minor barren pyritic lenses were recognised.

The Nimbus Ag-Zn-(Au) VHMS deposit represents the first notable exception to this paradigm. It is located 250 km south of Teutonic Bore, near the margin of the paleo-rift zone, but in comparison with the aforementioned occurrences, it preserves strikingly different features, in particular, the tectono-stratigraphic position and its age, defined by two new U-Pb zircon SHRIMP ages of 2703±5 Ma and 2702±4 Ma, that associate Nimbus with the 2.7 Ga plume magmatism responsible for world-class Ni-komatiite mineralisation. The ore mineralogy is characterised by an abundance of Ag-Sb-Pb-As bearing sulfosalts, high Hg and low Cu contents, and is hosted in a sericite-dominated alteration assemblage. Nimbus may be interpreted as a shallow water and low temperature VHMS deposit with epithermal characteristics.

In this study, we take advantage of state-of-the-art *in-situ* techniques to investigate the fluid evolution of this peculiar VHMS system. From the trace element compositions and S-isotope signatures we suggest that Nimbus experienced a bimodal fluid evolution consisting of (i) an initial intense interaction between deep-magmatic fluids and seawater that developed barren pyritic lenses, and (ii) a subsequent closure of the hydrothermal system during which the Ag-rich ore formed sourcing sulfur almost entirely from a deep-magmatic source. We also provide evidence supporting a widespread presence of bacterial colonies that promoted the formation of the barren pyrite lenses.

REFERENCES

- [1] Hollis, S. et al. 2015. A review of volcanic-hosted massive sulfide (VHMS) mineralization in the Archaean Yilgarn Craton, Western Australia: Tectonic, stratigraphic and geochemical associations. *Precambrian Research Elsevier*, 260, 113-135.
- [2] Huston, D.L. et al. 2014. Tectonic controls on the endowment of Neoproterozoic cratons in volcanic-hosted massive sulfide deposits: evidence from lead and neodymium isotopes. *Economic Geology*, 109, 11-26.
- [3] Mole, D.R. et al. 2014. Archean komatiite volcanism controlled by the evolution of early continents. *PNAS*, 111, 10083-10088.

Atmospheric sulfur in the orogenic gold deposits of the Archean Yilgarn Craton

V. SELVARAJA^{1,2}, S. CARUSO^{1,2}, M.L. FIORENTINI^{1,2}, C.K. LAFLAMME^{1,2} AND T.-H. BUI³

¹Centre for Exploration Targeting, University of Western Australia, 35 Stirling Highway, Crawley, 6009 WA, Australia

²ARC Centre of Excellence for Core to Crust Fluid Systems (CCFS), University of Western Australia

³McGill University and GEOTOP, 3450, University Street, Montreal, Quebec, Canada

The elusive source of sulfur in Archean orogenic gold deposits is a highly-contested area of research, with different models of deposit formation calling on a variety of crustal and mantle sources to explain the anomalous (10-100 x average crustal abundance) amounts of sulfur in these systems. Possible sources of sulfur in Archean orogenic gold deposits include supracrustal rocks [1], mid crustal magmatic hydrothermal systems [2] or even deeper reservoirs, such as the lower crust or mantle [3].

Our natural laboratory to address this knowledge gap is the highly metal endowed Yilgarn Craton, where we measured the multiple sulfur isotope signature of representative sulfide-bearing auriferous samples from 24 Archean orogenic gold deposits varying in size and geological setting. Utilising the chemically conservative mass-independently fractionated sulfur (MIF-S) isotope signatures, we fingerprinted a major source of sulfur in these deposits. Contrary to previous studies, our data show that they display very strong MIF-S isotope anomalies, with $\Delta^{33}\text{S}$ values ranging from -1.18‰ to 2.04‰, with most of the studied deposits showing a sulfur signature that is consistent with a crustally derived source. Unlike smaller deposits, which may form with sulfur derived from a single sedimentary sulfur source, hence providing a coherent Archean atmospheric signal in their $\Delta^{33}\text{S}$ - $\Delta^{36}\text{S}$ slope (~0.9 - 1.5), the formation of giant deposits may require sourcing of a wider range of sulfur reservoirs, as reflected in their apparently random $\Delta^{33}\text{S}$ - $\Delta^{36}\text{S}$ slopes.

REFERENCES

- [1] Tomkins, A.G. 2013. On the source of orogenic gold. *Geology* 41, 1255-1256. doi:10.1130/focus122013.1
- [2] Xue, Y. et al. 2013. No mass-independent sulfur isotope fractionation in auriferous fluids supports a magmatic origin for Archean gold deposits. *Geology* 41, 791-794. doi:10.1130/G34186.1
- [3] Hronsky, J.M.A. et al. 2012. A unified model for gold mineralisation in accretionary orogens and implications for regional-scale exploration targeting methods. *Mineralium Deposita*, 47, 339-358. doi:10.1007/s00126-012-0402-y

The origin(s) of carbonates in kimberlites: isotopic constraints

M. CASTILLO-OLIVER¹, W.L. GRIFFIN¹, S.Y. O'REILLY¹, A. GIULIANI^{1,2}, R.N. DRYSDALE² AND E. THOMASSOT³

¹Australian Research Council Centre of Excellence for Core to Crust Fluid Systems (CCFS) and GEMOC, Department of Earth and Planetary Sciences, Macquarie University, Sydney, NSW 2109, Australia

(montgarri.castillo-oliver@mq.edu.au; bill.griffin@mq.edu.au; sue.oreilly@mq.edu.au; andrea.giuliani@mq.edu.au)

²School of Earth Sciences, The University of Melbourne, Parkville, 3010 Victoria, Australia (rnd@unimelb.edu.au)

³Centre de Recherches Pétrographiques et Géochimiques, CNRS, Nancy, France (emilie@crpg.cnrs-nancy.fr)

Introduction

The composition of kimberlite parental magmas is typically modified by a wide spectrum of processes, such as mantle assimilation, crustal contamination, degassing and hydrothermal or meteoric alteration. As a consequence, the original composition of these melts, including their volatile contents (i.e. CO₂ and H₂O), still remains an unsolved puzzle. Primary carbonate could help to elucidate the C-O isotopic composition of kimberlite parental melts, although comprehensive petrographic and compositional characterisation is essential. This project not only shows the potential of combining detailed petrographic studies with *in situ* Sr and SIMS O- and C-isotope analysis, but also narrows the C and O isotopic values of primitive kimberlite melts based on the study of fresh hypabyssal kimberlites worldwide.

Results and discussion

Magmatic carbonate in kimberlites commonly occurs as fine-grained interstitial calcite between other groundmass crystals such as olivine, monticellite, apatite or perovskite. It can also be found as randomly oriented calcite laths (~150 x 1500 µm), segregations or euhedral crystals. Although there are a few exceptions, a typical feature of these carbonates is their enrichment in SrO₂ (1-2.7 wt%), while Na, Ba, and REE concentrations commonly remain low. Their CL response is usually low, showing a characteristic dark brown colour. Sr-isotope analysis reveals that a majority have a primary (i.e. magmatic) signature (average ⁸⁷Sr/⁸⁶Sr = 7.0459±30).

Secondary carbonates may occur either replacing the original groundmass phases or as crosscutting veins. In most cases, they have a very bright (orange-yellow) CL response. Some of the secondary carbonates (calcite and, less commonly, Mg-rich calcite or dolomite) carry abundant inclusions, such as barite, apatite, halides or fluorite. Their composition differs from that of the primary carbonates, showing either negligible or very high Sr contents, but it varies from kimberlite to kimberlite. This reflects their crystallisation from late fluids that were strongly influenced by the composition of local crustal fluids and wall rocks. Consistently, Sr-isotope analysis of these veins is quite variable (e.g. ⁸⁷Sr/⁸⁶Sr = 0.70482±19 vs 0.70922±57), indicating that they could either be related to deuteritic fluids or result from meteoric alteration or crustal assimilation.

In-situ C-O-isotope analyses confirm that different carbonate generations have clearly distinct origins. Primary carbonates are characterised by δ¹⁸O = 6-9‰ and δ¹³C = -4 to -6.5‰, whereas secondary carbonates commonly have higher O and slightly lower C values (δ¹⁸O = 12-23‰; δ¹³C = -5 to -8‰). The significant δ¹⁸O -and, to a lesser extent, δ¹³C- differences between primary carbonates and bulk carbonate analysis undoubtedly shows that the latter is not representative of the composition of the parental kimberlitic melt, even for the least-altered kimberlites. Instead, this work stresses the necessity of *in-situ* characterisation of each carbonate type, to identify its paragenesis and ultimately define the isotopic composition of magmatic carbonates.

The study of the Benfontein kimberlite sills (South Africa) could be a textbook example of the approach presented here. The combination of all the *in-situ* techniques has enabled us to correctly identify, for the first time, different stages of carbonate formation, including: i. crystallisation of at least 2 generations of primary carbonate; ii. carbonate diapirism after crustal contamination from the host shales; iii. crystallisation of late veins from deuteritic fluids and iv. meteoric alteration leading to secondary groundmass and veins.

Conclusions

Combined *in-situ* C, O and Sr isotope analysis of kimberlitic carbonates, supported by detailed petrographic and compositional characterisation, is a powerful method to describe kimberlite evolution and constrain its parental melt composition and it could thus be used to better understand the deep Earth carbon cycle.

Sedimentary limestone recycling and its role in lithospheric refertilisation

C. CHEN^{1,2}, Y. LIU¹, S.F. FOLEY² AND M.W. FÖRSTER²

¹State Key Laboratory of Geological Processes and Mineral Resources, School of Earth Sciences, China University of Geosciences, Wuhan 430074, China (chunfei.chen@mq.edu.au; stephen.foley@mq.edu.au)

²ARC Centre of Excellence for Core to Crust Fluid Systems (CCFS), Dept. of Earth and Planetary Sciences, Macquarie University, North Ryde, New South Wales 2109, Australia

Sedimentary carbonate rocks, which exist extensively in the oceanic realm, are subducted to differing degrees during the closure of oceanic basins. However, very few observational data exist to provide details on the mechanisms of transport of carbonate materials from the surface to mantle depths and back to the Earth's surface. Recently, we reported on a carbonatite intruding Neogene alkali basalts in the Hannuoba region, close to the northern margin of the North China Craton (NCC) [1]. This carbonatite intrusion shows geochemical features of recycled limestone, indicating that this carbonatite had a sedimentary limestone precursor. The presence of coarse-grained mantle-derived clinopyroxene, orthopyroxene and olivine, and chemical features of the carbonates (high Ni content and $^{143}\text{Nd}/^{144}\text{Nd}$ ratio) indicate that the carbonate melts were derived from the mantle. These observations suggest that the carbonatite probably formed by melting of subducted sedimentary carbonate rocks in the mantle. In addition, U-Pb geochronology and Hf isotopic ratios in detrital zircons from the carbonatite intrusion, which show a wide range of ages ranging from Precambrian to Phanerozoic, are used to trace the origin of the subducted limestone precursor [2]. The age spectrum of the Precambrian zircons in the carbonatites exhibits similar age peaks to those of the southern Central Asian Orogenic belt (CAOB), but is not compatible with a northern NCC lithosphere source. The 300-400 Ma Phanerozoic zircons show positive Hf isotopic compositions similar to those of the southern CAOB, but contrast strongly with those from the northern NCC. These features suggest that the limestone precursor was derived from the Paleo-Asian Ocean and show that this carbonatite intrusion marks the subduction of a carbonate platform of the Paleo-Asian Oceanic slab to mantle depths beneath the NCC.

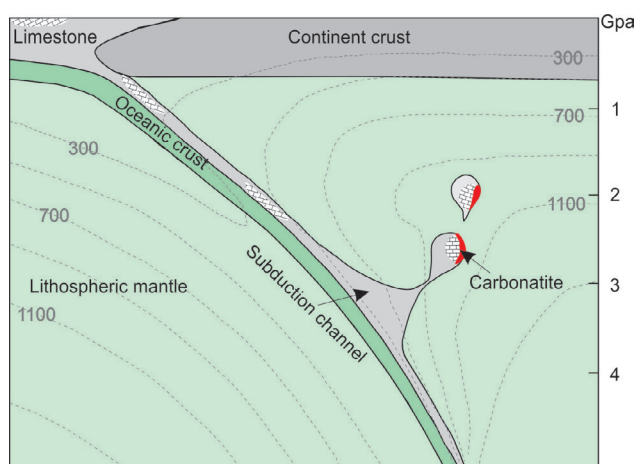


Figure 1. Schematic illustration of recycling of sedimentary limestone. Limestones may detach from the subducted slab to form solid buoyant diapirs. Reaction with peridotite could trigger melting of limestone diapirs, resulting in carbonatite.

Melting of limestone is commonly regarded to be restricted to unusually hot regimes ($>1520\text{ }^{\circ}\text{C}$ at 2-3 GPa; [3]), which could not occur in subduction-zone forearcs. Subducted limestone may penetrate the mantle wedge in the form of solid buoyant diapirs due to lower density and viscosity [4] (Fig. 1). However, the behaviour of the limestone in the mantle is unclear. Here, we use laboratory experiments to show

that carbonatite melt can form at temperatures as low as $950\text{--}1050\text{ }^{\circ}\text{C}$ and 2-3 GPa during interaction between limestone and olivine. We find that reaction with olivine strongly depresses the solidus for subducted limestone ($\text{Calcite} + \text{Olivine} \Rightarrow \text{Clinopyroxene} + \text{Carbonate melt}$), creating calcium-rich carbonatite melt in the shallow mantle (60-90 km). Our results suggest that carbonatite melt could originate from the mantle depths as shallow as 60 km. These carbonatite melts react with the mantle during ascent and transform the dunite or lherzolite to clinopyroxenite or wehrlite. Hence, reaction melting of limestone diapirs may dominate the recycling of limestone in the mantle and contribute to lithospheric refertilisation.

REFERENCES

- [1] Chen, C.F. et al. 2016. Paleo-Asian oceanic slab under the North China craton revealed by carbonatites derived from subducted limestones. *Geology*, 44(12), 1039-1042.
- [2] Chen, C.F. et al. 2017. Zircons in carbonatites establish recycling of a carbonate rock from the Paleo-Asian ocean under the North China Craton. Submitted to *Earth and Planetary Science Letters*.
- [3] Irving, A.J. and Wyllie, P. J. 1975. Subsolidus and melting relationships for calcite, magnesite and the join $\text{CaCO}_3\text{--MgCO}_3$ 36 kb. *Geochimica et Cosmochimica Acta*, 39, 35-53.
- [4] Behn, M.D. et al. 2011. Diapirs as the source of the sediment signature in arc lavas. *Nature Geoscience*, 4, 641-646.

3-D crustal and upper mantle velocity structure beneath Wudalianchi volcanic field

Y. CHEN^{1,2,3}, Y. AI^{1,2}, Y. YANG³ AND J. LEI⁴

¹Key Laboratory of Earth and Planetary Physics, Institute of Geology and Geophysics, Chinese Academy of Sciences, Beijing 100029, China

²University of Chinese Academy of Sciences, Beijing 100049, China

³ARC Centre of Excellence for Core to Crust Fluid Systems (CCFS) and GEMOC, Dept. Earth and Planetary Sciences, Macquarie University, North Ryde, NSW 2109, Australia (ying.chen@mq.edu.au)

⁴Key Laboratory of Crustal Dynamics, Institute of Crustal Dynamics, China Earthquake Administration, Beijing 100085, China

Most of the Earth's volcanoes erupt at plate boundaries. There are also other volcanoes located thousands of kilometres away from plate margins. These group of volcanoes are called intraplate volcanoes. The origin of most intraplate volcanoes still remains elusive. The Cenozoic intraplate volcanic belt (CIVB) in northeast China, consisting of the Erkeshan volcanic field (EVF), the Wudalianchi volcanic field (WVF) and the Keluo volcanic field (KVF), are typically intraplate volcanoes mostly comprised of highly potassic basalts. This group of volcanoes erupted from the Pleistocene to about 300 years ago and is located about 1800 km east from the Japan Trench and 800 km southeast from the Changbai volcano. To date, the source and origin of high-K basalts in the CIVB have remained controversial.

Seismic tomography by imaging 3D seismic structures is a useful method to investigate the origin of volcanism. However, previous seismic results in the CIVB is very limited because of the limitations of sparse distribution or poor coverage of seismic stations. Therefore, in order to image the detailed crustal and upper mantle structures beneath the CIVB, we deployed a high-density seismic array consisting of 42 stations in the study region. By combining our own deployment with other previously deployed stations, we have a total of 203 stations, with an average station spacing of ~30 km and a minimum station spacing of ~10 km, around the centre of the study region.

By combining the Ambient Noise tomography (ANT) and Two-plane surface wave tomography (TPWT) methods, surface wave phase velocity maps at 6-130 s periods are generated. Then, the local dispersion curves are extracted from these surface-wave phase velocity maps and inverted for 3D S-wave velocity structures by a Markov chain Monte Carlo (MCMC) method. Our resulting 3D model reveals a number of interesting velocity features. In the shallow/middle crust, velocity anomalies are highly correlated with geological terranes. High S-wave velocity anomalies dominate in the Great Xing'an and Lesser Xing'an range; while low S-wave velocity anomalies appear in the northern Songliao Basin. In the lower crust and uppermost mantle, WVF is characterised by a low S-wave velocity anomaly, which may be related to magmatism. This low-velocity anomaly extends from the Moho to ~90 km depth, maybe suggesting partial melting of the sub-continental lithospheric mantle. From the S-wave velocity profile, we infer that the high-K basalts may be derived from the upper mantle at the depths of 80–120 km. Furthermore, the low velocity beneath the CIVB may indicate a local asthenospheric upwelling, probably triggered by the Cenozoic NNW strike intracontinental rift extension and the small-scale mantle convection in northeast China.

Probe into the lithospheric mantle: platinum-group and trace element geochemistry of alkaline magmas in Yilgarn Craton, Western Australia

E. CHOI¹, M.L. FIORENTINI¹, A. GIULIANI² AND S. FOLEY²

¹ARC Centre of Excellence in Core to Crust Fluid Systems (CCFS), University of Western Australia, 35 Stirling Highway, Crawley, WA 6009, Australia (eunjoo.choi@research.uwa.edu.au; marco.fiorentini@uwa.edu.au)

²Australian Research Council Centre of Excellence for Core to Crust Fluid Systems (CCFS) and GEMOC, Department of Earth and Planetary Sciences, Macquarie University, Sydney, NSW 2109, Australia (andrea.giuliani@unimelb.edu.au; stephen.foley@mq.edu.au)

The Yilgarn Craton in Western Australia is a world-class metallogenic Archean craton hosting numerous metal resources, including komatiite-associated Ni-sulfide, orogenic Au and base metal volcanogenic massive sulfide systems. Interest in the geodynamic evolution of the crust and upper mantle in the craton has increased greatly over the last decade. Our current understanding of the whole- lithosphere architecture is predominantly based on the image provided by a number of geophysical datasets and on the radiogenic isotope (e.g. Lu-Hf, Sm-Nd) composition of felsic, mafic and ultramafic rocks. This research aims to integrate existing knowledge by investigating the poorly documented mineralogical, geochemical and petrogenetic features of alkaline rocks, in order to define the composition of both the asthenospheric and lithospheric mantle under the Yilgarn Craton.

The Yilgarn Craton contains various types of alkaline magmas, including kimberlites, carbonatites and two types of lamprophyres - ultramafic lamprophyres (UML) and calc-alkaline lamprophyres (CAL) - in the eastern area and margins of the craton. Results of whole-rock analysis of the Yilgarn alkaline rocks exhibit different geochemical characteristics of major, trace and platinum group elements (PGE) for the different alkaline rock types. CAL show significant depletion in high-field-strength elements (HRSE; e.g. Nb, Ta, Ti) compared to other alkaline rocks. Strong Th, U, Nb and LREE enrichment of UML is revealed in primitive mantle normalised incompatible element patterns, whereas relative depletions are apparent for HREE.

Primitive-mantle normalised PGE patterns of CAL show strong fractionation with relative depletion in Ir and Ru (IPGE), enrichment in Rh, Pt, and Pd (PPGE) and high (Pd/Ir)_N from 11.64 to 24.58, reflecting a less primitive PGE component. In contrast, other alkaline rocks such as carbonatites, UML and kimberlites are characterised by much less fractionation of PPGE from IPGE with low (Pd/Ir)_N values (< 10.60), and have lower PGE contents than alkaline rocks in South Africa and Brazil [1, 2].

These characteristics of CAL are similar to off-craton alkaline rocks and alkali volcanics, while UML and kimberlites show similar PGE patterns of on-craton kimberlites reported by McDonald et al. [2]. This may indicate that the source of CAL was shallower in the upper mantle than the other alkaline rocks of the Yilgarn Craton. The lower PGE contents of UML and kimberlites could be explained by the lithospheric mantle under the Yilgarn Craton having lower PGE contents than South Africa and Brazil.

REFERENCES

- [1] Maier, W. et al. 2017. Platinum-group element contents of Karelian kimberlites: Implications for the PGE budget of the subcontinental lithospheric mantle. *Geochimica et Cosmochimica Acta*, 216, 358-371.
- [2] McDonald, I. et al. 1995. The geochemistry of the platinum-group elements in Brazilian and southern African kimberlites. *Geochimica et Cosmochimica Acta*, 59, 2883-2903.

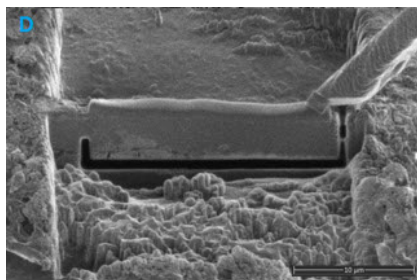
A new method to measure iron self diffusion at high pressure and temperature

M. STEWART¹, M.R. KILBURN², O. LORD³ AND S.M. CLARK¹

¹Australian Research Council Centre of Excellence for Core to Crust Fluid Systems (CCFS) and GEMOC, Department of Earth and Planetary Sciences, Macquarie University, Sydney, NSW 2109, Australia (simon.clark@mq.edu.au)

²Centre for Microscopy, Characterisation and Analysis and CCFS, M010, The University of Western Australia, 35 Stirling Highway, Crawley, WA 6009, Australia (matt.kilburn@uwa.edu.au)

³School of Earth Science, Bristol University, Wills Memorial Building, Bristol, BS8, UK

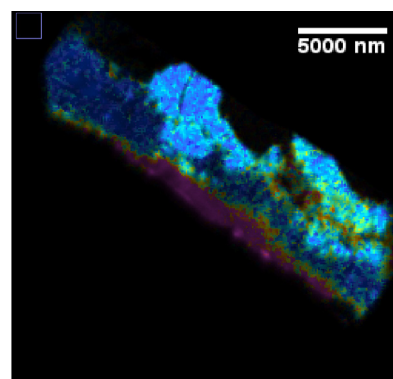


Diffusion plays a key role in planetary processes. It controls solid state fractionation which determines the distribution of elements and it is the rate limiting step for creep which determines the rheology.

Figure 1. Sample being cut and lifted out in the FIB.

Many processes occur deep within planetary bodies so we need to understand the effect of pressure on diffusion rates. Iron is abundant throughout the Earth so an appreciation of the self-diffusion rate of iron is of particular relevance. Previous studies [1, 2] have focussed on determining diffusion coefficients in iron-nickel alloys. These studies determined diffusivities by placing two metals in contact (iron and nickel), pressurising in a piston cylinder or multi-anvil high-pressure cell, heating, quenching and then cutting and polishing the sample before measuring concentration as a function of distance using an electron micro-probe. These studies successfully quantified the effect of temperature on the diffusion coefficient, but were unable to detect any effect of pressure possibly due to the relatively low pressure range achievable using piston cylinder and multi-anvil devices. To extend the pressure range we need to move to diamond anvil high-pressure cells, but the extremely small sample size (typically 20-50 μm in diameter) makes the method of using the electron microprobe (with a beam size of around 5 μm) infeasible.

Figure 2. Ratio of ^{57}Fe to ^{56}Fe . Red is higher and blue is lower.



This limitation has now been overcome with the advent of new instruments such as the nano-SIMS with a beam size of around 100 nm. We have therefore carried out a demonstration measurement of iron self-diffusion in the bcc phase of iron using samples prepared at high-pressure and temperature in a laser heated diamond anvil cell. Samples were prepared by taking a 6 μm thick sheet of ^{56}Fe and coating it on one side with a 70 nm thick layer of ^{57}Fe . 60 μm diameter disks were cut from this sheet and loaded into a 60 μm hole in a Re gasket in a diamond anvil cell together with a 60 μm diameter, 10 μm thick disk of KCl on either side as insulating layers. The sample was then pressurised and the centre of the sample was heated using the laser heating system in the Department of Earth Sciences, Bristol University. The pressure was released, the samples recovered and the KCl insulating layers removed. Slices were cut from the centre of the sample using a Helios NanoLab G3 CX focused ion beam mill and the concentration of ^{56}Fe and ^{57}Fe measured using a Cameca NanoSIMS 50L. Both of these instruments are housed in the Centre for Microscopy, Characterisation and Analysis at the University of Western Australia. Diffusion coefficients of $1.46 \times 10^{-14} \text{ m}^2/\text{s}^{-1}$ at 43.6 GPa and 2100 K and $9.92 \times 10^{-14} \text{ m}^2/\text{s}^{-1}$ at 43.6 GPa and 2000 K were determined. These were combined with the previous data [1, 2] and found to give a satisfactory fit to the Sammis and Smith model [3] with an activation volume of $1.43 \text{ cm}^3/\text{mol}$ and an activation energy of 431 kJ/mol.

REFERENCES

- [1] Goldstein, J. et al. 1965. Diffusion in the Fe-Ni system at 1 atm and 40 kbar pressure (Interdiffusion coefficients for Fe-Ni alloy as function of composition in alpha and gamma phases at 1 atm and 40 kbar pressure). AIME, Transactions, 233, 812-820.
- [2] Yunker, M.L. and Van Orman, J.A. 2007. Interdiffusion of solid iron and nickel at high pressure. Earth and Planetary Science Letters, 254, 203-213.
- [3] Sammis, C.G. et al. 1981. A critical assessment of estimation methods for activation volume. Journal of Geophysical Research: Solid Earth, 86, B11, 10707-10718.

Melt flux through the root of a magmatic arc under static versus dynamic conditions

N.R. DACZKO¹, S. PIAZOLO^{1,2}, C. STUART¹ AND U. MEEK¹

¹Australian Research Council Centre of Excellence for Core to Crust Fluid Systems (CCFS) and GEMOC, Department of Earth and Planetary Sciences, Macquarie University, Sydney, NSW 2109, Australia (nathan.daczko@mq.edu.au; cait.stuart@mq.edu.au; uvana.meek@hdr.mq.edu.au)

²School of Earth and Environment, University of Leeds, Leeds, England (S.Piazolo@leeds.ac.uk)

Melt-rock interaction delineate melt pathways

Melt-rock interaction in crustal rocks is rarely documented due to the inherent complexity of crustal rock types and melt compositions, and a lack of criteria for identification of the former flux of melt [1]. We contrast static [2, 3] versus dynamic [1] styles of melt flux throughout a homogeneous host rock, the Pembroke Granulite in Fiordland, New Zealand. Field relationships and microstructures demonstrate that melt-rock interaction involved little to no crystallisation of melt within the modified rocks, and the mineral assemblages and microstructures that were produced during melt-rock interaction are common in lower crustal rocks [1-3]. Key changes common to both melt flux styles involve hydration and an increase in the mode of amphibole. All rock types contain microstructures indicative of the former presence of melt. The static melt flux styles involved widespread growth of pargasite-bearing coronae around pyroxene throughout the entire Pembroke Granulite [2] followed by the development of localised tschermakite-clinozoisite gneiss and migmatite [3]. The dynamic styles of melt-rock interaction formed distinct minor rock types hosted within the Pembroke Granulite, including melt-bearing high-grade shear zones and hornblendite [1]. The static melt flux styles are inferred to involve diffuse porous melt flow with low melt flux occurring at the kilometre scale [2] and channelled high melt-flux occurring at the metre scale, leading to local migmatisation [3]. In contrast, the dynamic styles of melt flux only occurred at the metre scale, hosted in shear zones. Significant metasomatism to form hornblendite [1] in some shear zones indicates an increased cumulate flux in these examples, in comparison to the static styles of melt flux.

REFERENCES

- [1] Daczko, N.R. et al. 2016. Hornblendite delineates zones of mass transfer through the lower crust. *Scientific Reports*, 6, Article number: 31369, doi:10.1038/srep31369, 1-6. [<http://www.nature.com/articles/srep31369>]
- [2] Stuart, C.A. et al. 2016. Mass transfer in the lower crust: evidence for incipient melt assisted flow along grain boundaries in the deep arc granulites of Fiordland, New Zealand. *Geochemistry, Geophysics, Geosystems (G3)*, 17, 1-21. doi: 10.1002/2015GC006236
- [3] Stuart, C.A. et al. 2017. Local partial melting of the lower crust triggered by hydration through melt-rock interaction: an example from Fiordland, New Zealand. *Journal of Metamorphic Geology*, 35, 213-230. doi:10.1111/jmg.12229

The growth of continental crust at arcs, revealed by high-precision geochronology

S.W. DENYSZYN, J.E. STIRLING, A.I.S. KEMP, R.R. LOUCKS, M.L. FIORENTINI AND J. HAMMERLI

Australian Research Council Centre of Excellence for Core to Crust Fluid Systems (CCFS) and School of Earth Sciences, University of Western Australia, Perth, WA 6009, Australia (steven.denyszyn@uwa.edu.au; jack.stirling@research.uwa.edu.au; tony.kemp@uwa.edu.au; robert.loucks@uwa.edu.au; marco.fiorentini@uwa.edu.au; johannes.hammerli@uwa.edu.au)

Subduction-related processes are important elements in the growth of continental crust. Magmatic rocks generated within subduction-related volcanic arcs typically have geochemical compositions similar to that of andesitic bulk continental crust, though the composition of the lower crust within subduction-related volcanic arcs is more mafic than that of the upper arc crust. Therefore, there must be modification of lower arc crust if continental crust is generated in island arcs. Various mechanisms for the responsible processes have been proposed, including considering lower arc crust to be a residue following partial melting; a cumulate fraction of crystallisation processes that produced the andesitic upper crust; or the formation of a basaltic proto-continental crust at subduction zones with subsequent refinement via partial melting. Some emphasise crystal fractionation as the dominant crust-forming mechanism, while others favour models of delamination and foundering of dense ultramafic residuals which drives the composition of upper arc crust towards more andesitic compositions.

The Kohistan Arc Complex (KAC) of northeastern Pakistan provides a rare opportunity to study these processes. It is the world's best-preserved and -exposed section of arc-generated crust, about 40 km thick and including the lower crust which comprises a series of layered packages (complexes) of cumulate rocks. Previous geochemical and geochronological research permit two mutually-exclusive models for the formation of the KAC: Either each complex represents an episode of underplating, accretion, fractionation, and partial delamination, or the KAC was formed by a more punctuated pattern of accretion, with the cumulate complexes being emplaced at varying depths and with discrete histories of modification. Precise and accurate geochronology is capable of resolving this controversy, as the progressive underplating of the former model would indicate younger rocks emplaced under older ones while the discrete magmatic events of the latter model would not produce any such age gradient.

The five cumulate complexes of the KAC (from top to bottom: Chilas, Dasu, Kayal, Patan, Jijal) were sampled for radio-isotopic geochronology by the UWA group. The upper four complexes yielded zircons and were dated using the ID-TIMS U-Pb method, while the Jijal complex was dated by the Lu-Hf and Sm-Nd isochron method on whole-rock, garnet, and clinopyroxene separates. The results clearly indicate a progressively younging-downward age pattern. Weighted-mean $^{206}\text{Pb}/^{238}\text{U}$ ages (2σ uncertainty) for the Dasu, Kayal, and Patan complexes were 108.1 ± 0.3 Ma, 107.0 ± 0.2 Ma, and 100.2 ± 0.4 Ma, respectively, and the Jijal complex was dated to 92.4 ± 1.9 Ma (model 1 Sm-Nd isochron) and 94.3 ± 1.0 Ma (model 1 Lu-Hf isochron). The Chilas complex did not yield a meaningful magmatic age, but it does contain inherited Proterozoic zircons that indicate that the KAC is not a juvenile arc as previously interpreted, but may represent an extension of older terranes to the east.

Taken together with previously-published data, our new geochronological results support the model of progressive underplating, fractionation, and delamination for the growth of continental crust at island arcs. This represents the first conclusive test of the competing models, and reveals a fundamental process in the production and growth of continental crust.

Arrested in the Ivrea Zone: Ni sulfide mineralisation in lower continental crust, La Balma igneous complex (NW Italian Alps)

G.M. DERING¹, M. FIORENTINI¹, C.M. GONZALEZ¹ AND A. DAVIS²

¹ARC Centre of Excellence in Core to Crust Fluid Systems (CCFS), University of Western Australia, 35 Stirling Highway, Crawley, WA 6009, Australia (gregory.dering@research.uwa.edu.au; marco.fiorentini@uwa.edu.au; christopher.gonzalez@uwa.edu.au)

²School of Earth, Atmosphere & Environment, Monash University, 9 Rainforest Walk Clayton, VIC 3800 Australia (alison.davis@monash.edu)

Identifying sites of magma arrest in the deep crust

A common conceptual model for emplacement of intrusion-hosted magmatic Ni-Cu-PGE sulfide deposits emphasises ascent of mantle-derived magmas along large, steeply dipping, planar discontinuities (i.e. translithospheric faults and shear zones) [1]. However, our understanding of how mantle-derived magmas are transferred to sites of ore formation is limited by the accessibility of intrusion networks at crustal roots. The Ivrea Zone (NW Italian Alps) represents a largely intact section of Paleozoic lower to middle continental crust modified in composition and structure by voluminous mantle melts, ca. 288 Ma. Exhumation and tilting of the Ivrea Zone reveals an elongate mafic-ultramafic intrusive complex in cross section that hosts Ni-sulfide mineralisation, termed here the La Balma igneous complex, where we investigate mechanisms of magma arrest and sill formation. Recent ID-TIMS geochronology reveals the La Balma igneous complex to have been emplaced ~88 Ma after the main magmatic underplating event, and therefore motivates this reappraisal of its structural relation to adjacent bodies and mode of emplacement. The igneous complex comprises one or more sills composed of peridotite, with lessor gabbro and pyroxenite, and a cumulative length of at least 9 km and thickness of 400 m. These composite mafic-ultramafic bodies are thought to be the product of *in-situ* differentiation of a high-Mg magma. Detailed mapping of host rocks and internal architecture of the igneous complex reveals the mineralising magmas to be emplaced at a physico-chemical transition in lower continental crust, where garnet gabbro gives way to an overlying package of granulite-facies metasedimentary rocks, dominated by quartzofeldspathic gneiss. Given this strong physical contrast in host rocks, we evaluate the role of density and buoyancy force in the emplacement of the La Balma igneous complex with a 1D density profile of the Ivrea Zone lower crust. The model incorporates published bulk densities for gabbros (n=40) and overlying granulite-facies gneiss (n=17) and is compared with calculated density for a range of estimated primary melt compositions (n=13) for the La Balma igneous complex. The density model uses Gibbs free minimisation and thermodynamic modelling to determine rock densities based on empirically determined P-T parameters [2] using *Perple_X*. The model shows the average density of the La Balma parental melt (2810 kg m⁻³) to be less than the average densities of both the footwall gabbros (3190 kg m⁻³) and hanging wall felsic gneisses (2990 kg m⁻³). It is notable that despite significant differences in mineralogy and bulk composition, the differences between hanging wall and footwall rock densities are small, on the order of 3-8%. Only the most mafic (45 wt% SiO₂) parental melts exhibit densities that lie in the narrow range of values such that a hypothetical melt would reach a level of neutral buoyancy between the footwall gabbros and slightly less dense overlying felsic gneiss. The model suggests that positive buoyancy force would have driven La Balma parental melts shallower in the crust than the structural transition zone at which the intrusions were arrested. Therefore, we suggest mechanical contrast between differing host rock types, and not density, is the primary control on deep magma arrest. This study shows that, in addition to corridors defined by steep translithospheric structures, compositional contrasts influence the transfer of magmas and metals through the deep crust. Therefore, the study of magma arrest mechanisms has implications for the identification (and exploration) of fertile crustal domains within these corridors.

REFERENCES

- [1] Begg, G.C. et al. 2010. Lithospheric, Cratonic, and Geodynamic Setting of Ni-Cu-PGE Sulfide Deposits. *Economic Geology*, 105, 1057-1070.
- [2] Demarchi G. et al. 1998. Pressure gradient and original orientation of a lower-crustal intrusion in the Ivrea-Verbano Zone, northern Italy. *The Journal of Geology*, 106, 609-622.

Earliest signs of life on land in ~3.5 Ga hot spring deposits

T. DJOKIC^{1,2}, M.J. VAN KRANENDONK^{1,2,3}, K.A. CAMPBELL⁴, M.R. WALTER¹ AND C.R. WARD⁵

¹Australian Centre for Astrobiology, PANGAEA Research Centre and School of Biological, Earth and Environmental Sciences, University of New South Wales, Kensington, New South Wales 2052, Australia

²Australian Research Council Centre of Excellence for Core to Crust Fluid Systems (CCFS), Macquarie University, New South Wales 2109, Australia

³Big Questions Institute, University of New South Wales Australia, Kensington, New South Wales, 2052 Australia

⁴School of Environment, University of Auckland, Private Bag 92019, Auckland 1142, New Zealand. ⁵School of Biological, Earth and Environmental Sciences, University of New South Wales Australia, Kensington, New South Wales 2052, Australia. Correspondence and requests for materials should be addressed to T.D. (t.djokic@unsw.edu.au)

The ca. 3.48 Ga Dresser Formation, Pilbara Craton, Western Australia hosts some of the oldest evidence for life on Earth. Recent discoveries showed evidence for life living at hot springs and therefore established these deposits as the oldest evidence for life on land, while extending the record of life in hot springs by ~3 billion years. Findings include geyserite and sinter terracettes observed with a number of biosignatures including stromatolites, microbial palisade fabric and preserved gas bubbles inferring a sticky microbial substance was present. The findings provide support for the search for life in ancient martian hot springs and have implications for origins of life on Earth.

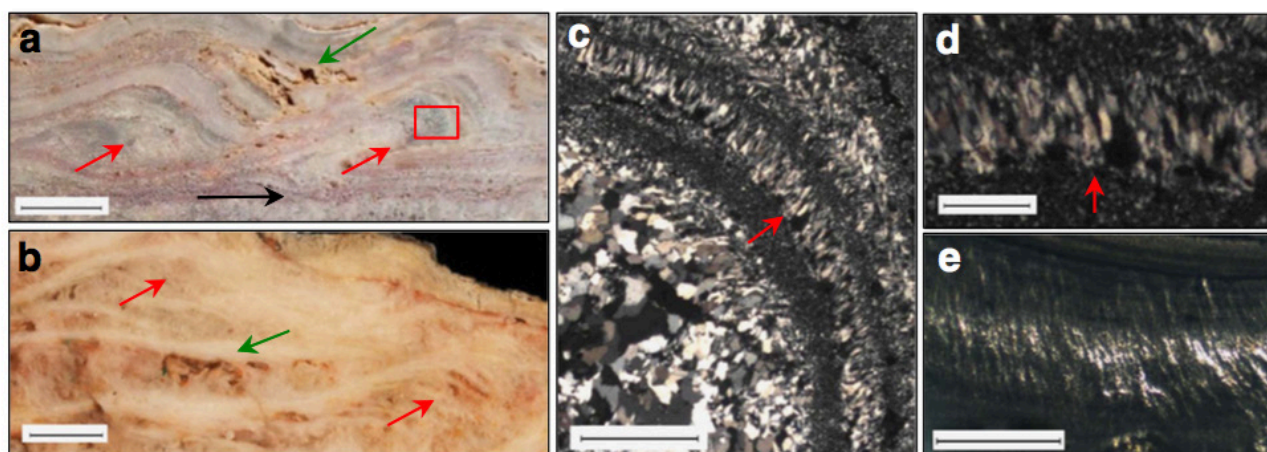


Figure 1. Sinter terracettes and microbial palisade fabric. Scale bar measurements indicated. (a) Dresser terracettes (red arrows) with preserved primary porosity (green arrow) and a horizon containing Dresser stratiform geyserite (black arrow). Scale bar, 1 cm. Inset box of c. displays palisade fabric. (b) 41,800-year-old sinter terracettes (red arrows) with preserved primary porosity (green arrow) from a sinter buttress at Te Kopia, New Zealand. Scale bar, 1 cm. Micrographs in XPL of (c) Dresser palisade fabric oriented vertical to bedding (scale bar, 1 mm) and (d) close-up (scale bar, 250 mm). (e) Sinter with preserved palisade fabric, Te Kopia, New Zealand. Scale bar, 1 mm.

Process complexity, interactions and feedbacks during lower crustal melting

M. ETHERIDGE^{1,2}, N.R. DACZKO² AND C. STUART²

¹Tectonex Geoconsultants Pty Ltd, Sydney, Australia (Mike@tectonex.com.au)

²Australian Research Council Centre of Excellence for Core to Crust Fluid Systems (CCFS) and GEMOC, Department of Earth and Planetary Sciences, Macquarie University, Sydney, NSW 2109, Australia (nathan.daczko@mq.edu.au; cait.stuart@mq.edu.au)

Rock mechanics at high melt pressure

Partial melting in the lower crust is initiated mainly at grain boundaries, edges and corners. There is broad agreement that, as melting progresses, microfracture processes initiated at these sites can lead to grainscale interconnected porosity and permeability that can in turn enable melt migration and extraction. There is also widespread evidence from exhumed examples and some experiments that deformation during melting is in some way important in channelling melt migration. However, there is no unifying mechanistic framework that connects melting and deformation to enable efficient drainage and accumulation of melt.

We examine the mechanical processes that are likely to take place in a lower crustal melt source region during progressive melting. In particular, we examine the likely interactions and feedbacks between melt porosity formation, melt pore pressures, hydraulic (melt) fracturing, rock deformation, permeability enhancement and melt migration/extraction.

Migmatite delineates zones of melt flux in the upper crust, Wongwibinda, NSW

M. FARMER¹, N. DACZKO¹ AND S. PIAZOLO^{1,2}

¹Australian Research Council Centre of Excellence for Core to Crust Fluid Systems (CCFS) and GEMOC, Department of Earth and Planetary Sciences, Macquarie University, Sydney, NSW 2109, Australia (michael.farmer@students.mq.edu.au; nathan.daczko@mq.edu.au)

²School of Earth and Environment, University of Leeds, Leeds, England (S.Piazolo@leeds.ac.uk)

The small (<20 km wide) high-temperature – low-pressure (HTLP) Wongwibinda Metamorphic Complex (WMC), southern New England Orogen, is characterised by an irregular elevated metamorphic field gradient (<100°C/km). An examination of the migmatite rocks shows they did not experience significant *in-situ* partial melting, suggesting the abundant leucocratic veins and dykes observed in outcrop are externally derived. Using a combined field and petrographic study, augmented by targeted electron backscatter diffraction (EBSD) and whole-rock geochemical analyses, two types of melt pathways through the migmatite have been identified: (i) veining and dyking, and (ii) grain-scale channelled porous flow. The pathways of porous flow are recognised across the field area as cm- to outcrop-scale channels, characterised by rare-earth element (REE) metasomatism, mineral mode changes, a randomisation of host crystallographic preferred orientation fabrics and the presence of cusped K-feldspar pockets. The identification of collapse structures, due to volume loss as melt-filled dykes and voids drained, demonstrates that some of the injected melt escaped to structurally higher levels. The two types of melt pathways and their characteristics supports a melt flux hypothesis, which is interpreted to drive migmatisation and promote the formation of the elevated thermal field gradient.

CCFS Flagship Program 2: Advances in understanding the multi-scale four-dimensional genesis, transfer and focus of fluids and metals

M.L. FIORENTINI

Centre for Exploration Targeting, School of Earth Sciences, ARC Centre of Excellence for Core to Crust Fluid Systems (CCFS), University of Western Australia, 35 Stirling Highway, Crawley, WA 6009, Australia (marco.fiorentini@uwa.edu.au)

This project tests the hypothesis that the genesis of sizeable mineral deposits is the end product of self-organised critical systems operating from the scale of the planet all the way to the very focused environment where ore deposits can form. The ability to discover new mineral resources is very challenging today partly due to the limited predictive capability of the traditional analogue deposit model approach. Recently, a new conceptual framework, the mineral system approach, has been proposed, which enables more powerful predictive capability for mineral exploration. The mineral system approach represents a step change in the way we investigate ore-forming processes, whereby we look at the evolving relationship between the localised setting of anomalous metal resources and processes operating at the scale of the planet.

Prior to the advent of the concept of mineral system framework, single deposits were documented in detail as unique occurrences. However, this approach failed to focus on the commonalities among various occurrences and the larger scale architectural framework that hosts them. The new rationale now takes on a more holistic approach acknowledging that the genesis of mineral occurrences required the conjunction in time and space of three main independent parameters, including *fertility*, *lithosphere-scale architecture*, and *favourable transient geodynamics*. An integrated focus on multiple mineral systems has generated new understanding on the multi-scale four-dimensional genesis, transfer and focus of fluids and metals.

Exciting results from integrated geochemical and isotopic studies from porphyry copper systems in subduction and post-subduction tectonic settings (Chile, Argentina, Australia, China) have tested the exciting hypothesis that copper fertility is associated with long term storage of magma chambers at lower crustal depths, where magmatic fluids can be enriched in metals prior to being injected in the upper crust. These processes have been investigated with a strong architectural focus, with new high-precision geochronological results supporting the model of progressive underplating, fractionation, and delamination for the growth of continental crust. Geological proxies to image the evolving nature of the lithospheric architecture and track the changing composition of magmatic-hydrothermal systems (through fingerprinting of mass independent sulfur isotope fractionation in sulfides and integrated minero-chemical and isotopic analysis of zircon and apatite) have been developed to aid the exploration industry.

Integrated work on the lower crust in the Ivrea Zone natural laboratory (Italy) has shown that mafic and ultramafic magmas can preserve evidence for metal and sulfur flux from the lithospheric mantle. It is now thought that the lower continental crust can be fertilised with mantle-derived metals and volatiles, which are available for later remobilisation into upper-crustal ore systems. With the renewed understanding of magmatic processes at the base of the continental crust, it is proposed that world-class mineral deposits along the margins of lithospheric blocks may be the result of both favourable crustal architecture (focussing of magmas and fluids) and localised volatile and metal enrichment of the lower crust related to mantle-derived hydrous (and carbonated) metasomatism. This work has emphasised the need to further constrain the Earth's volatile budgets (H_2O , CO_2 , and SO_2), which are important to understanding the evolution of our habitable and tectonically active planet.

Carbon recycling during plate tectonics has been considered as an important process driving both chemical heterogeneity and changes in the redox state of the mantle. More recently, fluxes of carbon from a subducting slab to the lithospheric and asthenospheric mantle have been reevaluated suggesting that nearly all carbon is remobilised at upper mantle conditions within our colder, present-day subduction environment. However, these calculations are often done only for stable and average condition subduction zones. To gain a better understanding on the dynamics of carbon recycling, recent work in this Flagship Program has used numerical modelling to assess mobilisation of carbon at three significant tectonic settings: CO_2 devolatilisation and melting at subduction zone; CO_2 degassing and melting at lithosphere rifting; CO_2 melting of remnant carbon-rich sediments at stagnating slabs at mid-mantle conditions. Investigation of these three settings allows for a better understanding of the full carbon cycle.

This work couples together state-of-the-art geodynamical numerical codes and petrological modelling to include carbon flux calculations and carbonate melting, which are key to better understanding the deepest probes of the terrestrial carbon cycle: kimberlite and carbonatite magmas. Additional geochemical and isotopic work on selected Australian and Russian alkaline systems elucidate the role of metasomatic processes in controlling localised gold and platinum-group element enrichment in cratonic lithospheric mantle domains.

Post-collisional alkaline magmatism as gateway for metal and sulfur enrichment of the continental lower crust

M.L. FIORENTINI¹, C. LAFLAMME¹, S. DENYSZYN¹, D. MOLE², R. MAAS³, M. LOCMEIS⁴, S. CARUSO¹ AND T.-H. BUI⁵

¹Centre for Exploration Targeting, School of Earth Sciences, ARC Centre of Excellence in Core to Crust Fluid Systems (CCFS), University of Western Australia, 35 Stirling Highway, Crawley, WA 6009, Australia
(marco.fiorentini@uwa.edu.au)

²CSIRO Mineral Resources, 26 Dick Perry Avenue, Kensington, WA 6151, Australia

³School of Earth Sciences, University of Melbourne, VIC 3010, Australia

⁴Department of Geosciences and Geological and Petroleum Engineering, Missouri University of Science & Technology, Rolla, Missouri 65409, USA

⁵Department of Earth and Planetary Sciences, McGill University, 3450 University St., Montreal, QC H3A 0E8, Canada

Mafic and ultramafic magmas that intrude into the lower crust can preserve evidence for metal and sulfur transfer from the lithospheric mantle into the lower continental crust. Here we focus on a series of ultramafic, alkaline pipes in the Ivrea Zone (NW Italy), which exposes deeply buried (6-11 kbar), migmatitic metasedimentary rocks intruded by voluminous basaltic magmas of the Mafic Complex, a major crustal underplating event precisely dated via U/Pb CA-IDTIMS on zircon at 286.8 ± 0.4 Ma. The ultramafic pipes postdate the Mafic Complex and form 100-300 m wide cumulate-rich conduits. They are hydrated and carbonated, have unusually high incompatible element concentrations and contain blebby and semi-massive Ni-Cu-PGE sulfide mineralisation. The sulfides occur as coarse intergranular nodules (>10 mm) and as small intragranular blebs (<1 mm) hosted in olivine, and have homogeneous, mantle-like $\delta^{34}\text{S}$ ($+1.35 \pm 0.25\%$). This homogeneity suggests that the pipes reached sulfide supersaturation without addition of crustal sulfur, and that the $\delta^{34}\text{S}$ signature is representative of the continental lithospheric mantle. One of the pipes, the 249 Ma Valmaggia pipe, carries a very distinctive Sr-Nd-Hf-Pb isotopic composition in its core ($^{87}\text{Sr}/^{86}\text{Sr}$ 0.70250, ϵ_{Nd} -18, ϵ_{Hf} -18, $^{206}\text{Pb}/^{204}\text{Pb}$ 16.0, $^{207}\text{Pb}/^{204}\text{Pb}$ 15.16, $^{208}\text{Pb}/^{204}\text{Pb}$ 35.87), very different from the margin of this pipe and from other pipes that have higher $^{87}\text{Sr}/^{86}\text{Sr}$, ϵ_{Nd} and $^{206}\text{Pb}/^{204}\text{Pb}$. The unusual isotopic composition of the Valmaggia pipe requires a source with long-term (2500-1500 million years) U-, Th- and Rb-depletion and LREE enrichment. Such compositions are found in Late Archean/Early Proterozoic granulites and lower crustal xenoliths. We suggest that the unusual isotopic composition of the Valmaggia pipe reflects contamination of the mantle source of the pipe with a crustal component that is neither represented in the local Paleozoic crust nor in the isotopically anomalous hydrated mantle inferred as the source of the large-volume mafic underplate that formed the Mafic Complex. During post-collisional gravitational collapse of the Variscan Orogen, this source produced the alkaline, metal (Ni, Cu, PGE)- and volatile (H_2O , CO_2 , S)-rich mafic-ultramafic magma that formed the deep-crustal intrusion at Valmaggia. U/Pb dating of other chemically and geologically comparable pipes in the area shows that this process was active over at least 40 Ma. The Ivrea pipes illustrate how the lower continental crust can be fertilised with mantle-derived metals and volatiles, which are available for later remobilisation into upper-crustal ore systems. World-class mineral deposits along the margins of lithospheric blocks may thus be the result of both favourable crustal architecture (focussing of magmas and fluids) and localised volatile and metal enrichment of the lower crust related to mantle-derived hydrous metasomatism.

New magmatic oxybarometer using trace elements in zircon reveals oxidation states of Hadean and Eoarchean lithosphere in four cratons

R. LOUCKS AND M.L. FIORENTINI

Centre for Exploration Targeting, School of Earth Sciences, ARC Centre of Excellence for Core to Crust Fluid Systems (CCFS), University of Western Australia, 35 Stirling Hwy, Crawley WA6009, Australia

We derive a novel method for determining the oxygen fugacity of a magma as zircon crystallised, to a precision of ± 0.5 log unit fO_2 , using ratios of Ce, U, and Ti in zircon, without explicit determination of the ionic charge of any of them, and without independent determination of crystallisation temperature or pressure or parental melt composition. The method is applicable to detrital and xenocrystic zircons. Zircon/melt partition coefficients of Ce and U vary oppositely with fO_2 variation in the silicate melt. The Ce/U ratio in zircon also varies with the silicate melt's Ce/U element ratio. During mafic-to-felsic magmatic differentiation, Ce and U are incorporated mainly in calcium-dominated lattice sites of clinopyroxene, hornblende and apatite, all of which have a similar degree of preference for Ce over U. We employ the U/Ti ratio in silicate melts and in zircons as a magmatic differentiation index. Convergent- and divergent-plate-margin mafic-to-felsic differentiation series consistently follow the relation $\log (Ce/U) \approx -0.5 \log (U/Ti) + C'$ in silicate melts. That correlation permits thermodynamic derivation of the oxybarometry relation among those elements in zircon: $\log fO_2(\text{sample}) - \log fO_2(\text{FMQ}) = (4/2n+1) \log [(Ce/(U*Ti)^{0.5}) + C]$, wherein "FMQ" represents the reference buffer fayalite+magnetite+quartz, and "n" varies with the average valence of uranium in the zircon's parental silicate melt. We empirically calibrate this relation, using 862 analysed zircons in 76 natural populations having independent fO_2 constraints in the range FMQ-4.9 to FMQ+2.85, to obtain the least-squares fit: $\log fO_2(\text{sample}) - \log fO_2(\text{FMQ}) = 3.997 \log [Ce/(U*Ti)^{0.5}] + 2.272$, with a correlation coefficient $R = 0.941$ and standard deviation of 0.495 log unit fO_2 in calc-alkalic, tholeiitic, adakitic, and shoshonitic, metaluminous to moderately peraluminous and peralkaline melts. Thermodynamic assessment and empirical tests indicate that our formulation is insensitive to varying crystallisation temperature and pressure at lithospheric conditions. We use it to illuminate the Hadean "dark ages" (4.0-4.6 Ga), for which detrital and xenocrystic zircons are the principal record of magmatic processes during formation of the Earth's proto-continental lithosphere. We evaluate the oxidation states of magmas that produced Hadean and Eoarchean zircons in the Yilgarn, South China, Slave, and Wyoming cratons. Zircons in the 4375-3800 Ma age range from Australia's Yilgarn Craton cluster in the fO_2 range of modern mid-ocean-ridge magmas and Iceland and Yellowstone rhyolites, as do also three of four age bins of 3858-3200 Ma detrital zircons in the Wyoming Craton. More reducing conditions, $\sim 1-2$ log units lower fO_2 , are represented by 3970-3896 Ma zircons in the Wyoming Craton and all analysed Hadean igneous zircons (4121-4002 Ma) from the Cathaysia Block and from the Acasta Gneiss Complex. These more reduced suites imply derivation of parental mafic magmas or of re-melted mafic protoliths from lithospheric mantle domains substantially depleted in Fe^{3+} by prior episodes of basaltic/komatiitic melt extraction, and point to initiation by 4 Ga of chemically refractory, buoyant lithospheric mantle keels that shielded the base of proto-continental crust from ablative loss by asthenospheric mantle convection.

The continental lithosphere and the deep carbon cycle

S.F. FOLEY¹ AND T.P. FISCHER²

¹ARC Centre of Excellence for Core to Crust Fluid Systems (CCFS), Department of Earth and Planetary Sciences, Macquarie University, North Ryde, New South Wales 2109, Australia (stephen.foley@mq.edu.au)

²Department of Earth and Planetary Sciences, University of New Mexico, Albuquerque, New Mexico, U.S.A.

The generation of many continental alkaline magmas, including kimberlites, carbonatites, ultramafic lamprophyres, nephelinites and melilitites requires the presence of CO₂ or carbonates in the source region. These rocks are strongly associated with continental rifts, particularly those in proximity to cratons, where high concentrations of carbonatites occur. However, the origin of the large amounts of CO₂ needed to explain these occurrences remains largely unexplained. Here, we consider where these huge concentrations of carbon come from, and how they are reactivated to result in the generation of strongly alkaline, silica-undersaturated magmas.

In recent years, attempts to budget the deep carbon cycle have concentrated on the behaviour of carbon during release at the surface as CO₂ degassing through mid ocean ridges and ocean islands, and on the return of carbon to the mantle at subduction zones. However, these are modern-day budgets that neglect the effects of slow reorganisation of reservoirs through geological time since craton formation. The storage and re-release of carbon from the continental lithosphere, including rifts, has been overlooked or underestimated. Based on measurements of CO₂-release at volcanoes and along rift-bounding faults in two regions of the East African Rift, Lee et al [1] estimated that the whole East African Rift releases 19±9 Mt C per year, a figure 100-150 times higher than the estimation that led Kelemen and Manning [2] to ignore the continents in their summary of the deep carbon cycle. Much of the carbon in continental rifts is not degassed, but becomes stored near the surface in the form of carbonate-rich igneous rocks, so that Lee et al.'s [1] value may be an underestimate.

We have attempted to assess the time-integrated role of the continental lithosphere in the deep carbon cycle [3] by subdividing its history of formation and evolution into four stages, and mass-balancing the migration of carbon in its various forms (reduced and oxidised) through time. Stage one is the formation of the lithosphere in the late Archean: we chose to model this as accretion at subduction, which, assuming current subduction zone length, a convergence rate of 3cm/year, a 45° subduction angle and effective carbon release to a depth of 120km, results in <0.3 Mt C per km³. We realise that the mode of formation of craton lithosphere is debated, but alternative mechanisms are unlikely to change this value radically: it is insignificant compared with later metasomatic overprinting events. Stage two is the gradual degassing of the mantle over time, for which we used well-established mid-ocean ridge degassing models as a basis. Co-opting a value intermediate between the end-members of such models, restricting the addition of this carbon to the lower 5-10% of the lithosphere, and allowing for 50% convectational erosion of the lithosphere base, we calculate that 14-28 Mt C km⁻³ results, two orders of magnitude higher than that incorporated during lithosphere formation. Stage three is carbon enrichment caused by the partial melting of passing plumes. Based on studies of the episodism of alkaline magmatism in rifted cratons, we estimate that three such plumes have passed under most cratons since the end of the Archean. This would add a further 40-45 Mt C km⁻³. Together with the effects of gradual degassing, the lower cratonic lithosphere now contains a layer with 1.6-3.2 wt% CO₂. Stage four consists of the re-melting and focussing of this carbon into zones beneath rifts, which then contain 150-240 Mt C km⁻³. This is enough to feed 28-34 Mt C per year to the surface for the entire 40 million year lifespan of a continental rift – a value within a factor of two of that measured at the surface by Lee et al. [1]. The role of continental rifts during supercontinent breakup is greater, so that their effect on CO₂-degassing should be accentuated. We hypothesise that during these periods of Earth history, continental rifts became a climate factor.

REFERENCES:

- [1] Lee, H. et al. 2016. Massive and prolonged deep carbon emissions associated with continental rifting. *Nature Geoscience*, 9, 145-149.
- [2] Kelemen, P.B. and Manning, C.R. 2015. Reevaluating carbon fluxes in subduction zones, what goes down, mostly comes up. *Proceedings of the National Academy of Sciences*, 112, E3997-E4006.
- [3] Foley, S.F. and Fischer, T.P. 2017. The essential role of continental rifts and lithosphere in the deep carbon cycle. *Nature Geoscience*. In press, December 2017 issue.

Partitioning of nitrogen during partial melting of phlogopite-rich mantle assemblages

M.W. FÖRSTER¹, D. PRELEVIĆ², S. BUHRE² AND S.F. FOLEY¹

¹ARC Centre of Excellence for Core to Crust Fluid Systems (CCFS), Department of Earth and Planetary Sciences, Macquarie University, North Ryde, New South Wales 2109, Australia (michael.forster@hdr.mq.edu.au; stephen.foley@mq.edu.au)

²Institute of Geosciences, J.-J.-Becher-Weg 21, Johannes Gutenberg University, 55099 Mainz, Germany

Nitrogen, the most abundant element of Earth's atmosphere, is also an important constituent in high pressure fluids, melts and mineral phases. While nitrogen behaves highly incompatibly in anhydrous mantle rocks [1] and has low abundances in basalts (<10 ppm N), nitrogen-rich ultrapotassic magmas (~400 ppm N) indicate the presence of nitrogen-bearing lithologies [2]. The recycling of surficial nitrogen to mantle depths is thought to be associated with potassium-bearing silicates in subduction zones, whereby micas play an important role. Under reduced conditions, nitrogen is able to replace potassium in silicates such as phlogopite in the form of ammonium-NH₄⁺ [3].

We conducted experiments in piston-cylinder- and belt-apparatus at 2-5 GPa on clinopyroxene-bearing glimmerites (phlogopite >90 wt%) that are doped with 2 wt% N, as well on organic-rich marine sediments to examine the partitioning of nitrogen between phlogopite and melt during subduction and partial melting at various P-T conditions. Oxygen fugacity was controlled by the C-CO buffer. Samples were analysed with an electron probe microanalyzer (EPMA) using a 20 µm defocussed beam and calibrated for nitrogen on the synthetic NH₄-feldspar (buddingtonite).

The clinopyroxene-bearing glimmerites melted partially to generate silica-undersaturated (<45 wt% SiO₂) ultrapotassic melts. These melts were in equilibrium with orthopyroxene, clinopyroxene, phlogopite, and garnet, which formed the residual phases at a pressure range from 2-5 GPa. Melting of the marine sediments produced silica-oversaturated melts (55-65 wt% SiO₂) with clinopyroxene, garnet, and phengite as residual phases. All analysed glasses are potassic to ultrapotassic in composition and contain 0.2-3.0 wt% N, while phlogopites contain 0.1-0.7 wt% N. Furthermore, reaction experiments of sediment and dunite conducted at low temperature (<1000 °C) show the formation of a phlogopite-dominated alteration zone sandwiched between both lithologies, which indicates that the lithospheric mantle is strongly enriched in potassium and nitrogen during subduction.

Partition coefficients for nitrogen (N) and potassium (K) decrease with increasing pressure from 2-5 GPa. N partitions strongly to the liquid (N: 0.6-0.2) while K is more compatible in phlogopite (D_K: 1.8-1.0) and phengite (D_K: 2.3). Accordingly, partial melting of nitrogen-bearing metasomatic assemblages strongly partitions N into the melt. Thus, lamproites with up to 400 ppm N [2] tap a phlogopite-bearing source that contains between 80-240 ppm N. Since nitrogen would also be lost to a fluid phase, this has to be taken as a minimum estimate.

REFERENCES

- [1] Li, Y. et al. 2013. Nitrogen solubility in upper mantle minerals. *Earth and Planetary Science Letters*, 377, 311-323.
- [2] Jia, Y. et al. 2003. 15 N-enriched Gondwana lamproites, eastern India: crustal N in the mantle source. *Earth and Planetary Science Letters*, 215, 1, 43-56.
- [3] Johnson, B. and Goldblatt, C. 2015. The nitrogen budget of Earth. *Earth-Science Reviews*, 148, 150-173.

Nanoscale defects host isotopically-distinct Pb reservoirs in deformed Witwatersrand pyrite

D. FOUGEROUSE^{1,2}, S.M. REDDY^{1,2}, C.L. KIRKLAND¹, D.W. SAXEY^{2,3}, W.D.A. RICKARD^{2,3} AND R.M. HOUGH⁴

¹ARC Centre of Excellence for Core to Crust Fluid Systems (CCFS) and The Institute for Geoscience Research (TIGeR), Western Australian School of Mines, Curtin University, GPO Box U1987, Perth, WA 6845, Australia (denis.fougerouse@curtin.edu.au)

²Geoscience Atom Probe, Advanced Resource Characterisation Facility, John de Laeter Centre, Curtin University, GPO Box U1987, Perth, WA 6845, Australia

³Department of Physics and Astronomy, Curtin University, GPO Box U1987, Perth, WA 6845, Australia

⁴CSIRO Earth Sciences and Resource Engineering, 26 Dick Perry Avenue, Kensington, Perth, WA 6151, Australia

The modification of the trace element composition of minerals may take place by a range of different processes throughout the geological evolution of the host rock. One potentially important process is element migration along fast-diffusion pathways such as low and high-angle boundaries. However, it is often unclear if the localisation of trace elements in such boundaries represents a dynamic process of trace element segregation at the time of boundary formation or later diffusion along a static boundary. Pb is a potentially useful trace element for addressing this problem as it comprises temporally-evolving radiogenic isotopic components that can be used to distinguish between Pb incorporated at the time of growth and that introduced during recrystallisation or hydrothermal alteration. In this study, we have used atom probe microscopy to investigate the composition of deformation microstructures in detrital pyrite grains from the Witwatersrand gold province of South Africa.

Atom probe results from a high-angle (12°) boundary reveals a heterogeneous distribution of As, Co and Ni at the edges of the boundary with the 5 nm wide core of the boundary enriched in Sb, Bi and Pb. Pb enrichment is also seen in the region of a low-angle (2°) boundary, but in this case the enrichment has a clustered morphology centred on the intersection of two dislocations. The isotopic composition of this Pb cluster is consistent with a 3.0 Ga common Pb composition. However, the Pb isotopic value of the high-angle boundary indicates a 2.0 Ga radiogenic Pb component, consistent with the composition measured in the metamorphic pyrrhotite rim around the grain. These results indicate at least two distinct reservoirs of Pb within the pyrite; the first related to a component of Pb inherited during pyrite growth, the second associated with ingress of a more radiogenic Pb along the boundary during metamorphism. These results show the ability of deformation boundaries to behave as fast diffusion pathways long after they formed and highlight that the nanoscale analysis of Pb reservoirs can provide a temporal framework for understanding trace element mobility.

A showcase of analytical techniques: V metal in hibonite

S.E.M. GAIN¹, W.L. GRIFFIN¹, V. TOLEDO², M. SAUNDERS³, J.A. SHAW³ AND S.Y. O'REILLY¹

¹ARC Centre of Excellence for Core to Crust Fluid Systems (CCFS) and GEMOC, Earth and Planetary Sciences, Macquarie University, NSW 2109, Australia (sarah.gain@mq.edu.au)

²Shefa Yamim (A.T.M.) Ltd., Netanya 4210602, Israel

³Centre for Microscopy, Characterisation and Analysis, The University of Western Australia, WA 6009, Australia

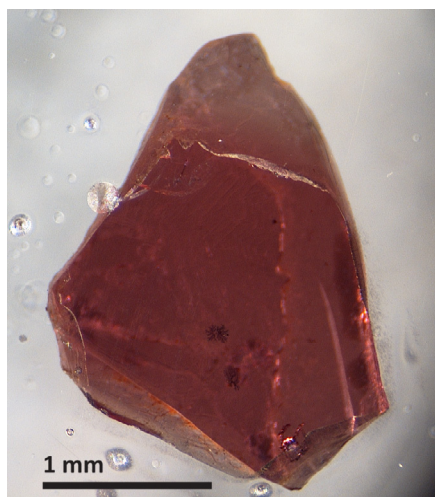


Figure 1. Stereo microscope image of hibonite with V^0 inclusions (dark aggregates).

The images reveal that the vanadium occurs both as rounded to drop-shaped inclusions, and as dendritic arrays of blobs and fibres that appear to have nucleated first on crystal faces, then continued to grow as the crystal face moved out into a surrounding melt/fluid. Pauses in crystallisation appear as planes cutting off the dendrites, and new nucleation points appear on these planes, growing further with the next pulse of crystallisation. These images reveal much about the growth environment, and the detailed morphology of dendritic crystallisation.

Hibonite ($\text{CaAl}_{12}\text{O}_{19}$) is one of the earliest phases to condense from the solar nebula. It also is found in high-temperature calc-silicate metamorphic rocks. We have found it intergrown with corundum, grossite (CaAl_4O_7), spinel and native vanadium in ejecta from Cretaceous volcanoes on Mt Carmel, Israel. The presence of V^0 (Fig. 1) implies very low oxygen fugacity, similar to nebular conditions.

Here we use this unusual material to illustrate a range of techniques for studying minerals and inclusions. The techniques we have used in this case study to analyse the V^0 inclusion in the hibonite include stereo microscopy (Fig. 1), backscattered electron (BSE) & energy dispersive X-ray spectroscopy (EDS) on a scanning electron microscope (SEM), focused ion beam (FIB), transmission electron microscopy (TEM), electron energy loss spectroscopy (EELS) and Micro-Computed Tomography (Fig. 2).

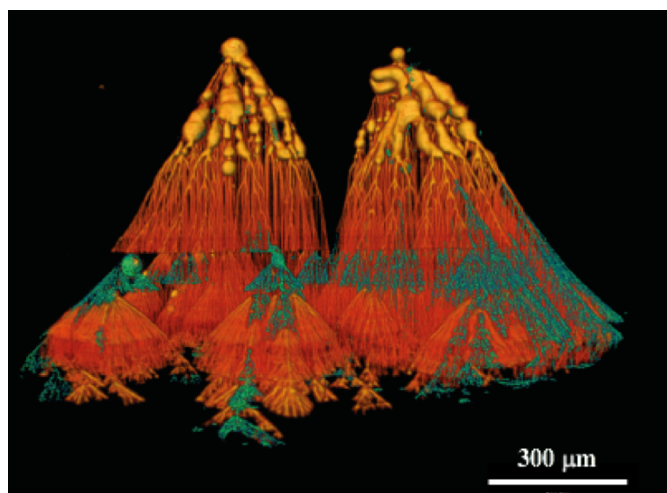


Figure 2. 3D-CT image of hibonite dendrites; crystal face is the lower surface.

Melting Earth's ancient mantle

N.J. GARDINER¹, T.E. JOHNSON¹, C.L. KIRKLAND¹, K. SZILAS² AND R.H. SMITHIES³

¹ARC Centre of Excellence for Core to Crust Fluid Systems (CCFS) and The Institute for Geoscience Research (TIGeR), Department of Applied Geology, Curtin University, GPO Box U1987, Perth WA 6845, Australia

²Department of Geosciences and Natural Resource Management, University of Copenhagen, Øster Voldgade 10, 1350 Copenhagen K, Denmark

³Geological Survey of Western Australia, 100 Plain Street, East Perth, WA 6004, Australia

The composition of the Hadean mantle remains contentious. Recent models suggest the mantle developed a superchondritic Sm/Nd ratio in the Early Hadean, and that this may have persisted through to the Eoarchaeon. We use a novel combination of phase equilibria and trace element modelling, to investigate melting of a primitive mantle composition. We show that melts with the Sm/Nd and Lu/Hf ratios of unaltered Eoarchaeon tholeiitic basalts from the Isua Supracrustal Belt, West Greenland, cannot be generated from chondritic mantle. In the preferred model, these basalts involve ~20 % melting of mantle with superchondritic Sm/Nd ratios of ~0.39. The elevated degree of mantle melting compared to modern MORB generation is consistent with a hotter upper mantle in the Early Archaean. The modelled Eoarchaeon mantle reservoir is more depleted than that calculated for the early Hadean, suggesting ongoing mantle depletion during the Hadean to Eoarchaeon. A non-chondritic mantle composition may be responsible for the decoupled Hf-Nd compositions measured in Archaean crustal rocks.

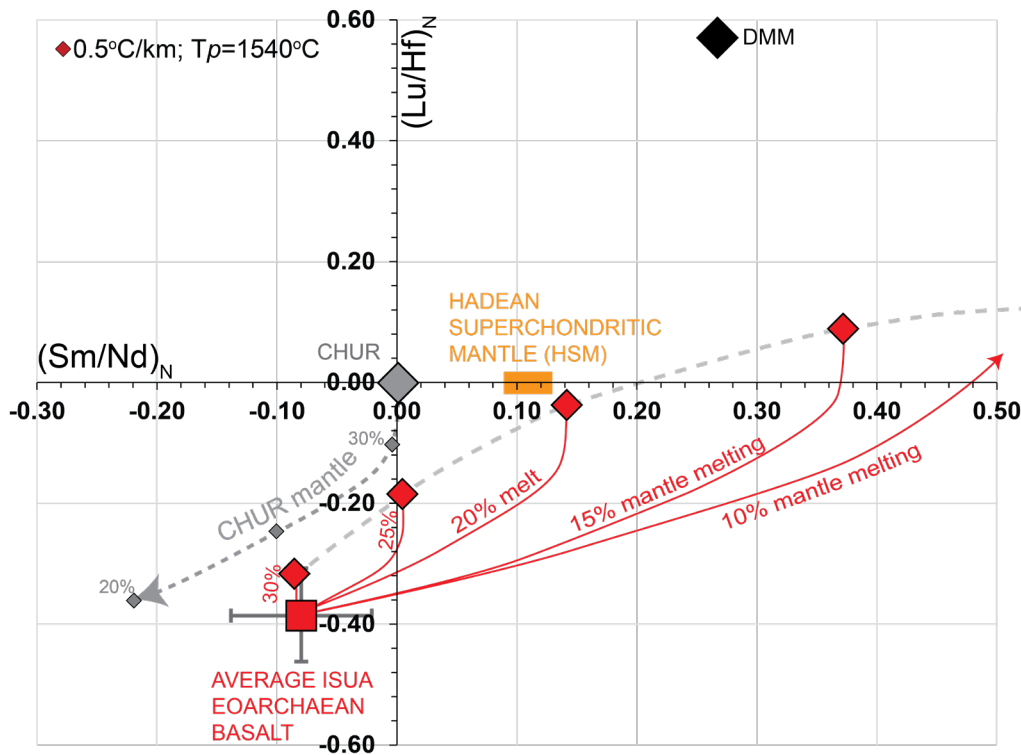


Figure 1. Melt modelling for Sm/Nd and Lu/Hf for the Eoarchaeon Earth System, modelling decompression melting of the primitive upper mantle (PUM). The melting curves (red lines) are anchored at the average measured Isua basalt (Sm/Nd)_N and (Lu/Hf)_N composition at different degrees of melting, allowing the calculation of the (Sm/Nd)_N and (Lu/Hf)_N compositions of mantle from which they were extracted as a function of melt degree.

Patterns of strain localisation: a numerical perspective

R.L. GARDNER¹, N.R. DACZKO¹ AND S. PIAZOLO^{1,2}

¹Australian Research Council Centre of Excellence for Core to Crust Fluid Systems (CCFS) and GEMOC, Department of Earth and Planetary Sciences, Macquarie University, Sydney, NSW 2109, Australia (robyn.gardner@mq.edu.au, nathan.daczko@mq.edu.au)

²School of Earth and Environment, University of Leeds, Leeds (s.piazolo@leeds.ac.uk)

Strain localisation fundamentally controls a material's rheological response to deformation, and there is well documented evidence of the major role that localisation plays in governing the development of important tectonic and economic structures. Shear zone initiation and development is, therefore, widely studied at all scales. However, speculation remains regarding the mechanisms and patterns of strain localisation, including the influence of the rheology and geometry of pre-existing heterogeneities, and the importance of weakening and strengthening processes.

We use the microdynamic modelling platform Elle to investigate the impact of the spatial distribution (i.e. the pre-deformation microstructure) and stress related evolution for a 20% weak phase on the bulk strength and strain localising behaviour of a material deformed in simple shear. The model is extended to simulate material weakening by allowing the strong phase to dynamically transition to weak, based on a stress threshold. Material strengthening is also simulated by allowing the weak phase to strengthen based on a time threshold. Systematic testing of the stress and time thresholds is undertaken.

Our results highlight that during simple shear, if dynamic weakening with or without strengthening feedbacks is present, strain is quickly localised into an interconnected weak layer (IWL), where an increasing proportion of weak material increases the interconnections between the IWLs, thereby increasing the anastomosing character of the shear zones. The results show the geometry of a shear zone can provide relative viscosity where it crosses a lithology boundary. Shear zones are wide and anastomosing compared with narrow and concentrated where viscosity is lower and higher, respectively.

We also establish the temporal patterns of shear zones are sensitive to the dominance of the weakening and strengthening process. Consequently, shear zones are dynamic in time and space within a single deformation event and therefore, the pattern of finite strain can be an incomplete representation of the evolution of a shear zone network.

Re-evaluation of the Yilgarn Craton's deep crustal structure

K. GESSNER¹, R.H. SMITHIES¹, Y. LU^{1,4}, C.L. KIRKLAND² AND H. YUAN^{1,3,4}

¹Geological Survey of Western Australia, 100 Plain Street, East Perth, WA 6004, Australia (Klaus.Gessner@dmirs.wa.gov.au)

²ARC Centre of Excellence for Core to Crust Fluid Systems (CCFS), Centre for Exploration Targeting – Curtin Node, John de Laeter Centre, Institute of Geoscience Research (TIGeR); Curtin University, WA 6045, Australia

³Australian Research Council Centre of Excellence for Core to Crust Fluid Systems (CCFS) and GEMOC, Department of Earth and Planetary Sciences, Macquarie University, Sydney, NSW 2109, Australia

⁴Australian Research Council Centre of Excellence for Core to Crust Fluid Systems (CCFS), The University of Western Australia, 35 Stirling Highway, Crawley, WA 6009, Australia (yongjun.lu@uwa.edu.au)

Major progress in the availability of high-quality and spatially extensive time constrained, geochemical and isotopic data and their integration with deep geophysical information allows unprecedented insights into the Yilgarn Craton, one of Earth's best studied segments of ancient continental crust. The spatial representation of new and expanded geochemical datasets reveal breaks and gradients in Nd isotope compositions and in trace element ratios that differ significantly from established interpretations of upper crustal structure from surface geological mapping and shallow level geophysical imaging.

The combination of isotopic ($^{143}\text{Nd}/^{144}\text{Nd}$ and $^{176}\text{Hf}/^{177}\text{Hf}$) and trace element ratios that reflect the degree of mantle contribution and the depth of melting in magmatic rocks (e.g. Eu/Eu^* , La/Yb and Sr/Y ratios), reveal information on the earliest deep structure of the craton. Specifically, these results suggest that the prominent NNW to NW-trending shear zones overprint an older, ENE to NE trending fabric that predates the segmentation of the Yilgarn Craton into tectonic domains. This large-scale ENE to NE trending fabric is also visible in long wavelength geophysical datasets, and is subparallel to the Yilgarn Craton's northern and southern Proterozoic margins.

The application of our combined imaging approach has the potential to re-evaluate other Archean cratons and the processes that shaped them. We speculate that this ENE to NE trending fabric represents the oldest known structural grain of the Yilgarn Craton and reflects early Earth geodynamic processes during craton formation.

This early fabric may also play a role in the localisation of previously reported structural elements, such as early faults with strong N-S movement components, E-trending basin transfers and local Au-mineralisation trends.

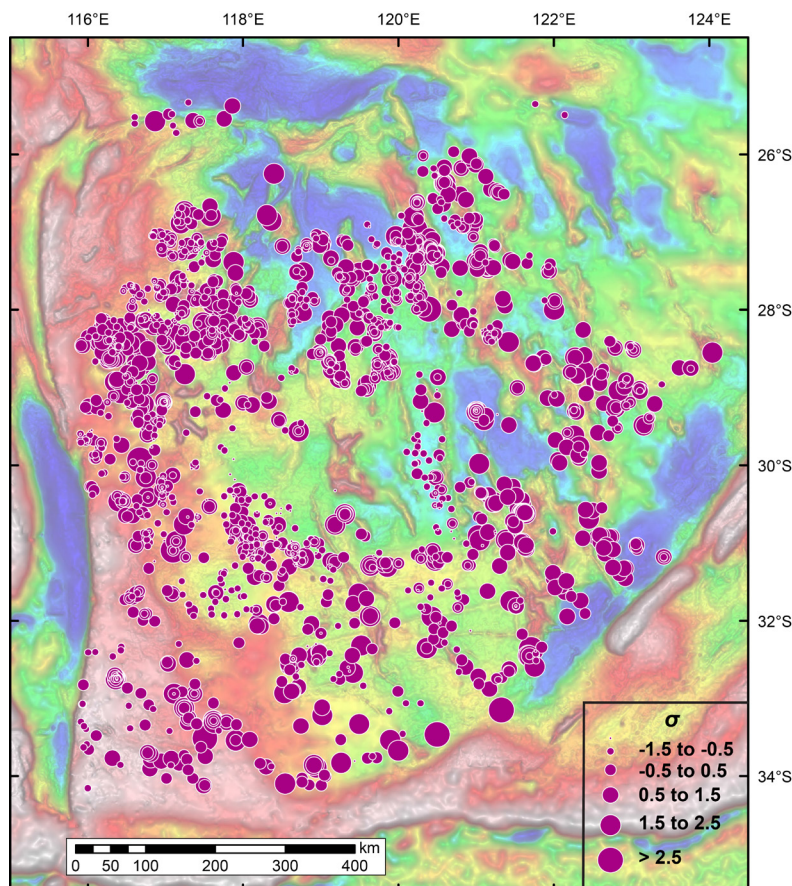


Figure 1. Whole-rock Eu/Eu^* values (range: $0 < x < 1.5$; graded in steps of $0.5x$ standard deviation σ) calculated from more than 2400 Neoproterozoic high and low Ca-type granites, show an ENE to NE trending spatial pattern across the Yilgarn Craton (background: gravity anomaly map).

Distinguishing hydration in shear zones by aqueous fluid versus silicate melt

H. GHATAK¹, N. DACZKO¹, S. PIAZOLO^{1,2} AND T. RAIMONDO³

¹Australian Research Council Centre of Excellence for Core to Crust Fluid Systems (CCFS) and GEMOC, Department of Earth and Planetary Sciences, Macquarie University, Sydney, NSW 2109, Australia (hindol.ghatak@hdr.mq.edu.au; nathan.daczko@mq.edu.au)

²School of Earth and Environment, University of Leeds, Leeds, England (S.Piazolo@leeds.ac.uk)

³School of Natural and Built Environments, University of South Australia, Adelaide, SA 5001, Australia

We distinguish the role of aqueous fluid versus silicate melt in hydration of dry granulite facies rocks within shear zones of the Alice Springs Orogeny (450-300 Ma), Central Australia. Meteoric water has been reported as the metasomatic fluid in the west of the orogen (Reynolds-Anmatjira Ranges), based on low $\delta^{18}\text{O}$ values in shear zones compared to wall rock. In contrast, in the east of the orogen (Strangways Range), field investigation identified syn-tectonic granitic dykes and lenses that retain igneous texture within the hydrous shear zones. Biotite selvages around the granitic dykes and lenses implicate silicate melt in hydration and metasomatism of these eastern shear zones. Microstructures indicative of the former presence of melt in the Strangways Range shear zones include felsic minerals that form films along grain boundaries or show low dihedral angles, and string of beads texture. While, these textures are lacking from the Reynolds-Anmatjira shear zones, hydration is indicated by muscovite pseudomorphs after K-feldspar, and increases in the mode of other hydrous minerals such as biotite and chlorite. Geochemical investigations using trace element, radiogenic isotope (Sr-Nd) and stable isotope ($\delta^{18}\text{O}$ - δD) analyses are presented for four transects across shear zones throughout the orogen. REE patterns in transects across the shear zones show limited REE metasomatism in the Reynolds-Anmatjira Ranges shear zones compared with significant REE metasomatism in the Strangways Range, consistent with the involvement of silicate melt during hydration and metasomatism in the Strangways Range.

Tracing mantle metasomatism using combined stable (S, O, N) and radiogenic (Sr, Nd, Hf) isotope geochemistry: case studies from mantle xenoliths of the Kimberley kimberlites

A. GIULIANI^{1,2}, D. PHILLIPS², R. MAAS³, J.D. WOODHEAD³, C. HARRIS⁴, M.L. FIORENTINI⁵, L.A.J. MARTIN⁶, J. FARQUHAR⁷, E. THOMASSOT^{8,9}, C. CHENG⁹ AND A. FITZPAYNE²

¹ARC Centre of Excellence for Core to Crust Fluid Systems (CCFS) and GEMOC, Department of Earth and Planetary Sciences, Macquarie University, Australia (andrea.giuliani@mq.edu.au; andrea.giuliani@unimelb.edu.au)

²KiDs (Kimberlites and Diamonds), School of Earth Sciences, The University of Melbourne, Australia

³Melbourne Isotope Geochemistry, School of Earth Sciences, The University of Melbourne, Australia

⁴Department of Geological Sciences, University of Cape Town, South Africa

⁵Centre for Exploration Targeting, ARC Centre of Excellence for Core to Crust Fluid Systems (CCFS), School of Earth and Environment, The University of Western Australia, Australia

⁶Centre for Microscopy, Characterisation and Analysis (CMCA), ARC Centre of Excellence for Core to Crust Fluid Systems (CCFS), School of Earth and Environment, The University of Western Australia, Australia

⁷Department of Geology and ESSIC, University of Maryland, College Park, USA

⁸Centre de Recherches Pétrographiques et Géochimiques, CNRS, Université de Lorraine, France

⁹Institute de Physique du Globe de Paris, France

Metasomatised mantle xenoliths entrained by kimberlite magmas during ascent through craton interiors provide ideal candidates to investigate the sources and compositions of mantle fluids. Here we document the results of a multi-isotope study of mantle xenoliths from the ~84 Ma Bultfontein Kimberlite (Kimberley, South Africa). The sample suite includes modally unmetasomatised harzburgites, phlogopite-rich peridotites hosting clinopyroxene and/or LIMA (lindsleyite-mathiasite) titanates, wehrlites, MARID rocks and a mantle polymict breccia (i.e. a failed kimberlite intrusion at mantle depths). These xenoliths equilibrated at variable P (~3.0 to 5.0 Gpa) and T conditions (~750 to 1150 °C), and experienced metasomatism at different times, between ~180 Ma (i.e. Karoo) and ~80-90 Ma (i.e. Cretaceous kimberlites).

The oxygen isotope composition of olivine grains is remarkably consistent among the examined samples, and overlaps with that of olivine in mantle peridotites worldwide ($\delta^{18}\text{O} = 5.18 \pm 0.14$, 1sd). Conversely, the $\delta^{18}\text{O}$ values of metasomatic clinopyroxene in the peridotite samples range between 4.4‰ and 5.2‰, below typical mantle values (5.57 ± 0.18 , 1sd). The $\delta^{34}\text{S}$ values of sulfide grains in four peridotites and the polymict breccia vary between ~-1 and -6‰. Phlogopite $\delta^{15}\text{N}$ compositions are between +4.4 and +6.2‰ (five peridotites, one MARID), which is significantly different from the mantle signature of -5 ± 2 ‰ inferred from studies of diamonds and oceanic basalts. Clinopyroxene in the two wehrlite samples exhibit similar values ($\epsilon\text{Nd}_{84\text{Ma}} = 3.2$ -3.7, $\epsilon\text{Hf}_{84\text{Ma}} = 2.0$ -2.1) in the range of southern African archetypal kimberlites. Conversely, metasomatic phases in the phlogopite-rich xenoliths, including two MARID samples, show a large compositional range from values ($\epsilon\text{Nd}_{84\text{Ma}} = -8$ to -13 , $\epsilon\text{Hf}_{84\text{Ma}} = -13$ to -17) typical of metasomatised lithospheric mantle magmas (e.g. lamproites, orangeites) to compositions below the Nd-Hf mantle array (i.e. $\Delta\epsilon\text{Hf}_{84\text{Ma}} = -10$ to -12 and $\epsilon\text{Nd}_{84\text{Ma}} = -3$ to -5), and similar to those of southern African transitional kimberlites.

The S isotope systematics are inconsistent with the metasomatic agent(s) that introduced sulfides into the Bultfontein mantle being sourced in the depleted asthenospheric mantle, whose $\delta^{34}\text{S}$ is ~-1.4‰, and require input from recycled crustal material, perhaps sulfide-bearing sediments. The interpretation that subducted material occurred in the source of the metasomatic fluids is strengthened by the O and N isotope data for clinopyroxene and phlogopite, respectively. Furthermore, sulfide S and phlogopite N isotope compositions are remarkably homogeneous across the sample suite despite the variable style, P-T conditions and age of metasomatism. This might indicate that metasomatic mantle fluids beneath Kimberley tapped a relatively homogeneous (sub-lithospheric?) source over a time-span extending from ~180 Ma to ~80-90 Ma. This view is at variance with the diverse range of recorded Sr-Nd-Hf compositions, which instead suggest contributions from different sources including the asthenospheric (see the wehrlites) and lithospheric mantle (see some of the phlogopite-rich xenoliths). This apparent contradiction could be reconciled if the Sr-Nd-Hf (and O) isotope compositions were affected by interaction with lithospheric wall rocks to a larger and more variable extent than the N-S isotope systems.

Olivine, kimberlites and the unavoidable contamination of carbonated melts in the deep Earth

A. GIULIANI^{1,2}, A. SOLTYS², E. LIM², H. FARR², D. PHILLIPS², K. GOEMANN³, S.F. FOLEY¹ AND W.L. GRIFFIN¹

¹ARC Centre of Excellence for Core to Crust Fluid Systems (CCFS) and GEMOC, Department of Earth and Planetary Sciences, Macquarie University, Australia (andrea.giuliani@mq.edu.au; andrea.giuliani@unimelb.edu.au)

²KiDs (Kimberlites and Diamonds), School of Earth Sciences, The University of Melbourne, Australia

³Central Science Laboratory, University of Tasmania, Tasmania, Australia

Recent advances in imaging and microanalytical techniques have shown that, in kimberlite rocks, olivine grains contain cores and rims with distinct compositions, regardless of their size and shape (i.e. macrocrysts and phenocrysts). The rims typically contain primary inclusions of groundmass phases (e.g. chromite, ilmenite), and exhibit homogeneous Mg# composition coupled with decreasing Ni and increasing Ca and Mn concentrations. These features are consistent with a magmatic origin for the rims. Conversely, the olivine cores host inclusions of typical mantle phases (e.g. clinopyroxene, garnet, Cr-spinel), which are not stable in kimberlite magmas. The cores show widely variable compositions extending from those of olivine in lithospheric mantle peridotites (i.e. Mg# ~ 91-94) to compositions richer in Fe. The olivine cores therefore derive from disaggregation of mantle wall rocks during kimberlite magma ascent.

The magmatic rims of olivine can be employed as proxies of the composition of kimberlite melts; whereas the xenocrystic cores can provide constraints on the composition of the lithospheric mantle traversed by kimberlite magmas. To understand the role, if any, of assimilation of lithospheric mantle material in the origin of kimberlites and other carbonate-rich magmas, we have examined the zoning (SEM-EDS imaging) and major-element compositions (electron microprobe (EMP) analyses) of olivine in archetypal kimberlites from South Africa, Botswana, Lesotho, Canada and Brazil, and compared these results with new and existing data for kimberlites, orangeites and ultramafic lamprophyres from South Africa, Canada, Russia and Greenland.

Olivine grains from the kimberlites examined in this study are typically zoned. The core is often partly resorbed, particularly when enriched in Fe. The compositional features of cores and rims are consistent with previous studies, e.g. variable core Mg# vs constant rim Mg#. Different kimberlite pipes from individual clusters (e.g. Kimberley in South Africa, Ekati in Canada) contain olivine with very similar compositional features (e.g. restricted range of rim Mg#). However, large compositional variations are evident for olivine grains from kimberlite clusters on the same craton and worldwide.

The most remarkable finding of this study is the linear correlation between the compositions of olivine cores and rims in kimberlites worldwide, which extends to South African orangeites and rocks from Brazil and Greenland with transitional features between kimberlites and ultramafic lamprophyres. The correlation between average core Mg# (or NiO concentrations) and average rim Mg# values of olivine in kimberlites is statistically significant ($R^2 = 0.85$), despite our dataset including samples from five continents and different carbonate-rich magma types. Conversely, olivine grains from the ultramafic lamprophyre (i.e. olivine melilitite and aillikite) samples included in this study plot outside this trend.

The correlation between Mg# of (xenocrystic) cores and magmatic rims suggests that the composition of wall rocks along the kimberlite magma conduit exerts a fundamental control on the composition of the olivine rims and, therefore, kimberlite magmas. This process also applies to other mantle-derived carbonate-rich magmas (e.g. orangeites) and might potentially affect the composition of any carbonated melt in the deep Earth.

Reconstructing the melt composition and evolution of the Bultfontein kimberlite (Kimberley, South Africa)

A. SOLTYS¹, A. GIULIANI^{1,2} AND D. PHILLIPS¹

¹KiDs (Kimberlites and Diamonds), School of Earth Sciences, The University of Melbourne, Australia

²ARC Centre of Excellence for Core to Crust Fluid Systems (CCFS) and GEMOC, Department of Earth and Planetary Sciences, Macquarie University, Australia (andrea.giuliani@mq.edu.au)

The compositions of kimberlite melts at depth and upon emplacement in the upper crust remain elusive. This can be attributed to the unquantified effects of multiple complex processes, such as alteration, assimilation, and xenocryst contamination. The inability to accurately constrain the composition and physical properties of kimberlite melts prevents a comprehensive understanding of their petrogenesis.

To improve constraints on the compositions of kimberlite melts, we have combined modal analysis including the discrimination of xenocrystic from magmatic phases, with mineral chemistry determinations to reconstruct a whole-rock composition. The accuracy of this whole-rock reconstruction process is validated by the similarity between reconstructed and measured whole-rock compositions. A series of corrections is then applied to account for the effects of post-emplacement alteration (dominantly serpentinisation), the inclusion and assimilation of mantle material, and pre-emplacement olivine crystallisation. This approach permits discernment of melt compositions at different stages of kimberlite evolution and is here applied to a sample of ‘fresh’ macrocrystic hypabyssal kimberlite (sample BK-1) from the Bultfontein mine (Kimberley, South Africa).

This primitive melt parental to the Bultfontein kimberlite is estimated to contain 20.5-21.5 wt% SiO₂, 21.6-24.4 wt% MgO, 22.9-25.4 wt% CaO, 1.6-1.9 wt% H₂O, 13.5-14.8 wt% CO₂, 2.5-3.9 wt% P₂O₅, 1.4-1.7 wt% TiO₂, 1.1-1.3 wt% Al₂O₃, and 0.8-0.9 wt% K₂O, and has a Mg# of 82.6-83.6. This composition is deficient in SiO₂, MgO and H₂O, but enriched in CaO and CO₂ compared with most previous estimates of primitive kimberlite melts. We suggested that the primitive melt parental to the Bultfontein kimberlite was a transitional silicate-carbonate melt, which was progressively enriched in SiO₂, MgO and to a lesser extent Al₂O₃ and Cr₂O₃ through the assimilation of lithospheric mantle material. Comparisons with experimentally produced low-degree melts of carbonated peridotite suggest that the Bultfontein kimberlite could have formed by ~0.5% melting of an asthenospheric lherzolite source at ~6.0-8.6 GPa (i.e. ~190-285 km) and ~1400-1500 °C.

The very low calculated content of Na₂O (≤0.1 wt%) in the parental melt is at variance with kimberlite derivation from low-degree melting of a clinopyroxene-bearing, lherzolite source. This, coupled with the relatively low H₂O concentration and H₂O/CO₂ ratio of the reconstructed melt, suggests that an alkali and volatile-rich fluid might be exsolved during melt ascent. Alternatively, provided that kimberlite melts evolve towards carbonate-dominated compositions via fractional crystallisation, an alkali-rich hydrous fluid might be released after emplacement in the upper crust and lost to the country rocks. We conclude that the Na₂O and H₂O concentrations in our reconstructed melt composition likely represent minimum values.

So what do you expect an orogenic belt to look like?

R.A. GLEN

Australian Research Council Centre of Excellence for Core to Crust Fluid Systems (CCFS) and GEMOC, Department of Earth and Planetary Sciences, Macquarie University, Sydney, NSW 2109, Australia (richard.glen@mq.edu.au)

Everyone has his or her pet idea of what an orogenic belt looks like. We know about orogenic belts (or orogens) that form by continent-continent collision. On the other side of the coin are non-collisional orogens. These are mainly called accretionary orogens, but non-collisional orogens also include non-accretionary orogens [1] that form without (significant) accretion of material from the lower to the upper plate. These are common in the eastern Australian Tasmanides, but are harder to understand and define. The Lachlan Orogen -- basement to CCFS and GEMOC and its cover of the Sydney Basin -- is the pre-eminent one.

The Lachlan Orogen

Rocks in the Lachlan Orogen range from Cambrian to Carboniferous, spanning almost 200 Ma. Almost every possible setting has been adduced for these rocks: from broadly accretionary, to collisional to collisional accretionary, to Turkic-style to extensional accretionary to largely intraplate backarc; to accretionary with multiple coeval subduction zones; to backarc after the upper Cambrian (references in [1]). To complicate things, the Lachlan Orogen lies east (outboard) of the Delamerian Orogen, another non-collisional orogen with a poorly understood/defined boundary and west (inboard) of the New England Orogen another really complex, long-lived orogen that was non-collisional (accretionary) in the mid Devonian to early Permian.

My reading of the Lachlan Orogen is: i) it fleetingly contained a continent-dipping plate boundary that rolled back east from the Delamerian Orogen into the New England Orogen from 515-503 Ma; ii) this rollback carried older MORB- and supra-subduction zone elements from near inboard settings to outboard ones in the New England Orogen; iii) from 503 Ma till Tasman Sea opening at ~100 Ma, the Lachlan Orogen lay behind a continent-dipping, convergent plate boundary located in the New England Orogen; iv) vast Ordovician turbidites were derived from East Antarctica [2] and deposited in two sub-basins either side of a basement block introduced at end of the Cambrian; v) the shapes of these rift sub-basins define the blocky rather than linear (and accreted) shape of the Lachlan Orogen; vi) classic S- and I- type granites of Chappell and White were emplaced into this extending backarc; vii) the absence of high-grade rocks reflects the lack of significant exhumation; viii) the Macquarie Volcanic Province is rift-related and not an arc, despite having supra-subduction zone arc-like chemistry; ix) major recycling of Ordovician detritus into Silurian and younger rocks precludes significant crustal growth.

Up to now, 3D models of the Lachlan Orogen and New England Orogen do not reflect these unusual features. They resemble more conventional orogens. So who has got things wrong? The surface mappers or the modellers, or is it even more complex? Can we set up projects that address this issue -- projects that involve targeted mapping tied into geochemistry, geochronology and seismic/modelling studies -- to make real sense of such a weird orogen that contains two world-class mineral provinces.

REFERENCES

- [1] Glen, R.A. et al. 2016. Different styles of modern and ancient non-collisional orogens and implications for crustal growth: a Gondwanaland perspective. *Canadian Journal of Earth Sciences*, 53, 1372-1415.
- [2] Glen, R.A. et al. 2017. East Antarctic sources of extensive Lower-Middle Ordovician turbidites in the Lachlan Orogen, southern Tasmanides, eastern Australia. *Australian Journal of Earth Sciences*, 64, 143-224.

Numerical geodynamic modelling of slab derived carbonate melting at upper mantle conditions

C.M. GONZALEZ, W. GORCZYK AND M.L. FIORENTINI

ARC Centre of Excellence in Core to Crust Fluid Systems (CCFS), University of Western Australia, 35 Stirling Highway, Crawley WA 6009, Australia (christopher.gonzalez@uwa.edu.au)

The mantle carbon cycle is an important, yet largely unconstrained and debated problem in the deep Earth volatile cycle. The uncertainty derives from two main causes: 1) The location of the carbonate melting P-T solidus (i.e. fO_2 and synthetic starting compositions) for subducting altered basalts and sediments and 2) the physical mechanisms by which carbon removal from the slab into the overlying mantle wedge occur. However, recent high pressure-temperature experiments, thermodynamic modelling, and geochemical observations over the last decade have reconciled these processes. Here, we couple, for the first time, experimentally produced solidi for carbonated basalts (MORB + CO_2) and sediments at pressures and temperatures relevant to upper mantle conditions, with the geodynamic modelling code I2VIS to elucidate subduction conditions at which carbonate melting commences beneath a subduction zone. This is accomplished through a robust thermomechanical and petrological modelling framework previously applied to decarbonation of subducting slabs and decarbonation within intracratonic settings. We find that the carbonated basaltic sections do indeed cross the carbonated basalt solidi during subduction and slab break-off of moderately aged oceanic lithosphere (60 Ma). What remains uncertain is the fate of the carbonated sediments, where when stagnated, have yet to sufficiently attain high enough temperatures to melt. Three implications arise from this work: 1) These models confirm the hypothesis that carbon is likely filtered out at upper mantle conditions suggesting a carbon increase in the upper mantle over time. 2) Carbonate melting in the mantle transition zone may be an important source component for organic carbon signatures of eclogitic diamonds. 3) The base of the subcontinental lithospheric mantle may be enriched by percolation of carbonatitic melts acting as a nucleation point for continental breakup.

Reconstructing the past 2500 years of volcanism and hazards of Kelut volcano, Indonesia

L.R. GOODE¹, H.K. HANDLEY¹ AND S.J. CRONIN²

¹ARC Centre of Excellence in Core to Crust Fluid Systems (CCFS), and GEMOC, Department of Earth and Planetary Sciences, Macquarie University, Sydney, NSW 2109, Australia (louise.goode@mq.edu.au; heather.handley@mq.edu.au)

²Department of the Environment, University of Auckland, Private Bag 92019, Auckland 1142, New Zealand (shane.cronin@auckland.ac.nz)

Investigations into the nature of surficial volcanic deposits are important for assessing and predicting future cataclysmic eruptive phenomena and cyclic behaviour at stratovolcanoes, in particular those with repeated, alternating plinian to dome-forming episodes. The volcanism of East Java, Indonesia is largely understudied compared to other Arc settings. Since little information is known about the prehistoric records of volcanism on Java, volcanoes with long eruptive histories, recent activity, and variations in eruptive styles are ideal to study in order to characterise the volcano. An example of such is Kelut volcano, Indonesia. Constructing detailed and combined records of volcanology, geochronology and geochemistry can provide insights into processes occurring prior to eruptions. These processes influence the style, magnitude, extent and duration of eruptions. It is important to build such records in order to understand how this volcano's past activity has varied over space and time. This assessment is vital to better mitigate against the devastating effects that large eruptions impinge on society. In order to do so, we will construct an understanding of Kelut's cyclic behaviour by combining evidence revealed by historical volcanological records, geochronology, and geochemical data.

Reactivation of an Archean craton margin - Albany-Fraser Orogen numerical case study

W. GORCZYK¹ AND C. SPAGGIARI²

¹ARC Centre of Excellence in Core to Crust Fluid Systems (CCFS), University of Western Australia, 35 Stirling Highway, Crawley, WA 6009, Australia (weronika.gorczyk@uwa.edu.au)

²Geological Survey of Western Australia, Department of Mines, Industry Regulation and Safety, Perth, WA 6004, Australia (Catherine.spaggiari@dmirs.wa.gov.au)

Lithospheric thinning and reactivation through extension and rifting, and implications for the destruction of craton margins have been addressed in several studies (e.g. North China Craton, NE-Atlantic, SW Greenland and West Iberia margins). Reactivated passive margins can be divided into two categories - volcanic and non-volcanic. Volcanic passive margins are distinct in origin and evolution from non-volcanic hyper-extended margins. Consequently, they should not be integrated into a single evolutionary process, and do not necessarily represent the ultimate stage of hyper-extension. Volcanic passive margins usually form in tectonic zones between cratonic nuclei, and may have been subjected to lengthy periods of divergence and convergence or strike-slip tectonics. Here we present a 2D numerical case study on the Albany-Fraser Orogen to provide insight into volcanic passive margin evolution.

The Albany-Fraser Orogen records Proterozoic modification of the southern and southeastern margin of the Archean Yilgarn Craton margin through coeval basin evolution and magmatism, which included variable additions of juvenile mantle material. Recent extensive geological mapping, geophysical, geochronological and geochemical analysis provide the necessary constraints for numerical studies to help establish best fit geodynamic scenarios for Albany-Fraser Orogen evolution.

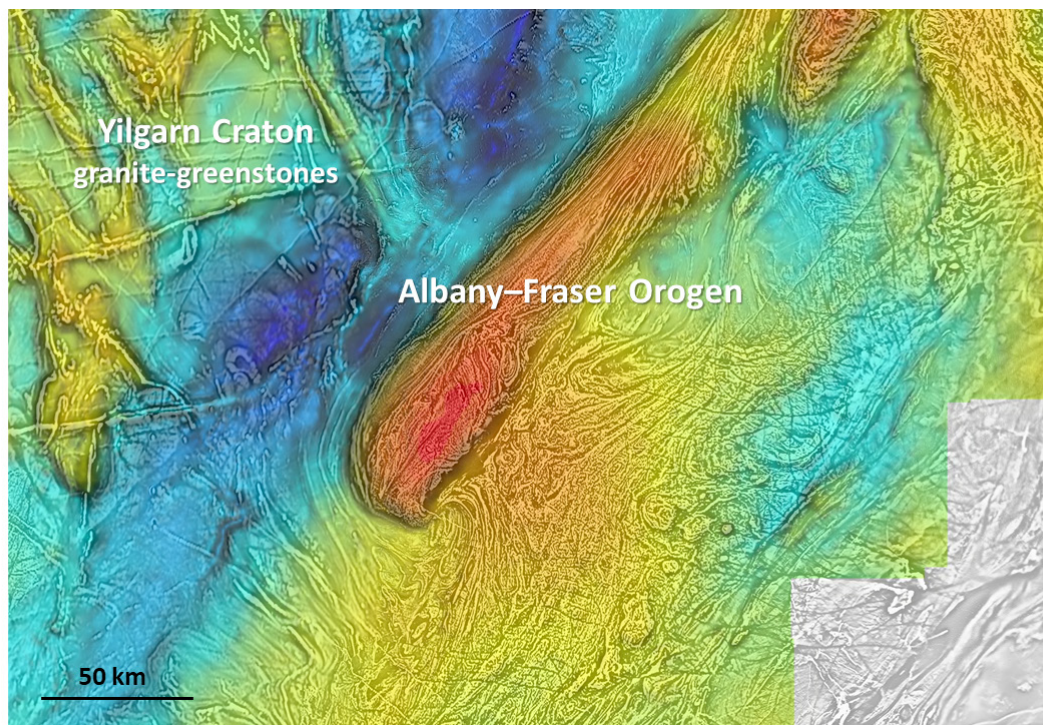


Figure 1. Gravity (colour) with IVD aeromagnetic (greyscale) draped image of the Yilgarn Craton and east Albany-Fraser Orogen interface. These data have facilitated GSWA mapping and sampling in the region.

Recrystallisation and “short-lived” lattice distortions along mantle fluid pathways

Y. GRÉAU¹, H. HENRY¹, T.D. MURPHY², J.-X. HUANG¹, W.L. GRIFFIN¹ AND S.Y. O'REILLY¹

¹Australian Research Council Centre of Excellence for Core to Crust Fluid Systems (CCFS) and GEMOC, Department of Earth and Planetary Sciences, Macquarie University, Sydney, NSW 2109, Australia (yoann.greau@mq.edu.au)

²Department of Earth and Planetary Sciences, Macquarie University, Sydney, NSW 2109, Australia

Mantle-derived xenoliths brought to the surface are often the witnesses of deep-seated processes that cannot be observed on outcropping ultramafic bodies because of preservation issues (e.g. metamorphic overprint, alteration) or simply due to sampling bias during emplacement. We present electron backscatter diffraction (EBSD) and *in situ* Sr isotopes data obtained on a composite eclogite xenolith from the Roberts Victor kimberlite, South Africa.

This rare sample consists, in one part, of a large megacrystic clinopyroxene (4 cm) associated with a small number of unaltered garnets. The second part is made of a more canonical bimineralic eclogite with garnets and clinopyroxenes displaying a “cloudy” appearance. Previous work [1] showed that the two domains are characterised by distinct major and trace element compositions, but also differ in terms of accessory minerals (none for megacrystic vs. calcite + sulfide + phlogopite + rutile).

In situ ⁸⁷Sr/⁸⁶Sr ratios of the clinopyroxenes were obtained using LA-MC-ICPMS techniques. The megacrystic clinopyroxene has a Depleted Mantle (DM) like ⁸⁷Sr/⁸⁶Sr ratio of 0.7025 ± 0.0004 (n=8). In contrast, the clinopyroxenes in the bimineralic eclogites have a more radiogenic ⁸⁷Sr/⁸⁶Sr ratio of 0.7074 ± 0.0005 (n=9), which can be ascribed to an enriched metasomatic fluid percolating through.

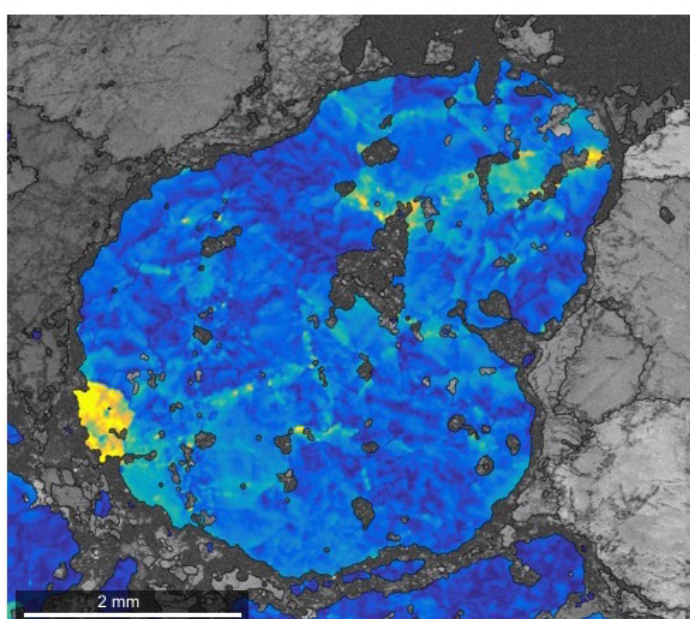


Figure 1. High resolution misorientation map of a garnet obtained by electron backscatter diffraction (EBSD) and revealing fine scale disruption of the crystal lattice.

EBSD analysis revealed a similar trend with a transition from a relatively undisturbed megacrystic domain to a rather complex bimineralic eclogite. In the latter, normalisation of lattice misorientation to the grain mean orientation highlights very unusual patterns in both garnet and cpx. These fine scale disruptions (10 μ m) of the lattice are pervasive and have not been described before. Quenching during the rapid ascent uniquely preserved these features, which can be seen as snapshots of recrystallisation during mantle metasomatism.

REFERENCES

- [1] Gréau, Y. et al. 2011. Type I eclogites from Roberts Victor kimberlites: products of extensive mantle metasomatism. *Geochimica et Cosmochimica Acta*, 75, 6927-6954.

Mystery mineral in a Jericho eclogite: Constraints on mantle metasomatism

S. GREENE^{1,2} D. JACOB¹ AND L.M. HEAMAN²

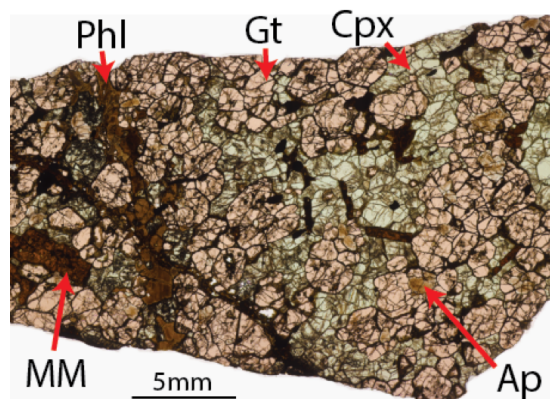
¹Australian Research Council Center of Excellence for Core to Crust Fluid Systems (CCFS) and Department of Earth and Planetary Sciences, Macquarie University, Sydney, NSW 2109, Australia (stephanie.nichols@hdr.mq.edu.au, dorrit.jacob@mq.edu.au)

²Department of Earth and Planetary Sciences, University of Alberta, Edmonton, T6G 2E3, Australia (lheaman@ualberta.ca)

A New Metasomatic Fingerprint

Metasomatic fluids are known to be important players in the evolution of the subcontinental lithospheric mantle, but the composition of these fluids are often poorly constrained. The discovery of an exotic mineral phase super-enriched in Th, LREE, and volatiles in a mantle eclogite from the Jericho kimberlite pipe, Nunavut, Canada provides a rare opportunity to derive a metasomatic fluid composition and examine the effects of this fluid on eclogite. This mystery mineral (MM), representing the result of modal metasomatism, is in equilibrium with surrounding clinopyroxene, garnet, and exsolved apatite. A “fingerprint” for this kind of metasomatism can thus be derived by looking at the trace element composition of clinopyroxene, where most incompatible trace elements are carried in bimineralic eclogite. Approximately 56% of eclogitic clinopyroxene (25/44 in a published and unpublished dataset), including in diamond-bearing eclogite, have trace element patterns similar to MM-associated clinopyroxene, suggesting that many Jericho eclogites have been affected by interaction with the MM-related fluid. Understanding the nature and effect of this metasomatism may thus be vital to understanding eclogite, diamond, and mantle evolution in the Northern Slave craton.

Figure 1. Thin section scan of the mystery mineral (MM)-bearing sample.



Super-reducing conditions in ancient and modern volcanic systems: implications for the carbon budget of the deep lithosphere

W.L. GRIFFIN¹, S.E.M. GAIN¹, J. HUANG¹, Y. GREAU¹, V. TOLEDO² AND S.Y. O'REILLY¹

¹Australian Research Council Centre of Excellence for Core to Crust Fluid Systems (CCFS) and GEMOC, Department of Earth and Planetary Sciences, Macquarie University, Sydney, NSW 2109, Australia (bill.griffin@mq.edu.au)

²Shefa Yamim (A.T.M.) Ltd., Netanya 4210602, Israel

Estimates of the oxygen fugacity (fO_2) of the cratonic subcontinental lithospheric mantle (SCLM) range from above the quartz-fayalite-magnetite (QFM) buffer to a bit above the iron-wustite (IW) buffer, and generally decrease with depth. While several lines of evidence suggest that the sublithospheric mantle may be constrained by the IW buffer (the presence of metallic Fe), there also is evidence that at least localised volumes of significantly lower fO_2 must exist within the SCLM, and perhaps within the deeper mantle.

Aggregates of hopper-formed crystals of Ti-rich corundum are abundant in Upper Cretaceous basaltic pyroclastic rocks (vent breccias, tuffs) exposed on Mt Carmel near Haifa, Israel. Melt pockets trapped within and between corundum crystals contain mineral assemblages (SiC (moissanite), TiC, Fe-Ti-Zr silicides/phosphides and native V) that require $P \geq 1$ GPa, $T = 1500$ - 1150 °C and extremely low fO_2 (ΔIW -10 to -12) (Griffin et al., 2016). Mineral parageneses suggest that the corundum and the low- fO_2 assemblages developed through interaction of basaltic magmas with mantle-derived (CH_4+H_2) at high fluid/melt ratios.

Similar mineral assemblages (+ diamond) occur in the “ophiolitic” peridotites of the Yarlong-Zangbo and Bangong-Nujiang suture zones (southern Tibet) and the Polar Urals. In each case, as in the Mt Carmel example, most of the more highly reduced phases, including nitrides, silicides and carbides, are found as inclusions in grains of Ti-rich corundum. The main difference between the “ophiolitic” and Israeli occurrences is that some carbon in the former occurs as diamond (in breccias of amorphous carbon). We therefore have suggested that the “ophiolitic” occurrences reflect crystallisation in late-magmatic systems related to the rapid emplacement of the host peridotites to shallow depths. Similar processes probably are occurring today beneath the Kamchatka volcanic arc, where mafic pyroclastic volcanic rocks carry diamond, SiC and Ti-rich corundum.

The streaming of low- fO_2 fluids from the deep upper mantle thus may accompany many types of deep-seated volcanism, especially in tectonic situations (continental-collision zones, deep subduction zones, major transform faults) that allow the rapid ascent and focussing of deep-seated magmas. If the fO_2 of the deep upper mantle is controlled by the IW buffer, then C-O-H fluids will be dominated by CH_4+H_2 , like those trapped in metal-bearing Type II diamonds (Smith et al. 2016). The rapid transport of such fluids to shallower depths as components of deep-seated magmas (including kimberlites) is thus inferred to produce local, perhaps transient, volumes of low- fO_2 assemblages.

SiC is a key indicator for these processes; it is widespread in Siberian kimberlites, and is reported from S. African kimberlites. In both cratons SiC occurs as inclusions in diamond, and we have separated SiC from Roberts Victor eclogites, apparently associated with the metasomatism that generated diamonds in these rocks. The most common inclusion in SiC from all of these localities is silicon metal, with morphologies suggesting trapping as a liquid, which subsequently commonly exsolved $FeSi_2$ and related phases; these are high-temperature phases (1400-1500 °C) and clearly are not related to late serpentinisation. The extremely low fO_2 required for the formation of SiC strongly suggests the presence of H_2 , which could be generated by the partial oxidation of CH_4 and the deposition of diamond (i.e. $SiO_2 + 3CH_4 \rightarrow SiC + C + 3H_2 + CO_2$). The isotopically light carbon ($\delta^{13}C = -25$ to -33) of the SiC in the Mt Carmel samples (and kimberlitic SiC worldwide) is similar to that in the Tibetan diamonds and some Transition-Zone diamonds, and may reflect the composition of methane in the deep upper mantle.

Redox melting in the presence of abundant CH_4+H_2 , rather than simply carbon, may be more efficient; it may also involve the desilication of wall rocks and their melts, and the production of Al-rich lithologies such as corundum eclogites with negative Eu anomalies. We suggest that all of these processes would accompany the arrival at the SCLM of kimberlites or other melts generated in the Transition Zone, and may have contributed significantly to the carbon budget of the lower lithosphere through time. The recognition that CH_4+H_2 may accompany melts rising from a deeper, metal-saturated mantle also suggests an explanation for the zones of high conductivity that mark the tracks of mantle-derived magmatic systems (from kimberlites to Bushvelds). The oxidation of CH_4 in rising fluids could propagate networks of microveinlets of amorphous carbon (even if later recrystallised to other forms), which might provide the fine-scale connectivity of conductive material implied by the striking MT images now becoming more widely available.

Apatite as tracer for the evolution of porphyry systems: A case study from the Macquarie Arc

J. HAMMERLI¹, T. KEMP², M. FIORENTINI¹ AND P. BLEVIN³

¹ARC Centre of Excellence for Core to Crust Fluid Systems (CCFS), Centre for Exploration Targeting, School of Earth Sciences, The University of Western Australia (Johannes.hammerli@uwa.edu.au)

²School of Earth Sciences, The University of Western Australia

³Geological Survey of South Australia

The evolution of the mineralised Macquarie Arc

In this study, we investigate porphyry systems of the Macquarie Arc (NSW), which led to mineralisation over an extended time period. The general compositions of the different porphyry systems vary from alkaline and shoshonitic to calc-alkaline. Here, we aim to characterise and understand the evolution of fertile melts responsible for Cu-Au mineralisation between ~468 Ma and ~435 Ma and the lifetime of the arc. Trace element analyses of apatite, their Nd isotope signatures, combined with whole-rock geochemistry, allow detailed insights into the geochemistry and metal loads of the mineralised and “barren” porphyry systems of the Macquarie Arc.

The Nd isotope signature of apatite shows a clear trend towards less radiogenic melt components in younger porphyries, implying input of older crustal material during the evolution of the arc. The homogeneous apatite populations in terms of their Nd isotope signatures rule out late-stage interaction of externally derived magma with crystallising porphyry bodies.

An important discovery is that trace elements in apatite from mineralised and seemingly “barren” intrusions all plot in the same “mineralised” field in the apatite discrimination diagram by Mao et al. (2016)[1]. Together with other geochemical tracers, not used in the discrimination diagram in Fig. 1, there are several more signs pointing towards the fertility of igneous suites, which have previously been classified as “barren” systems.

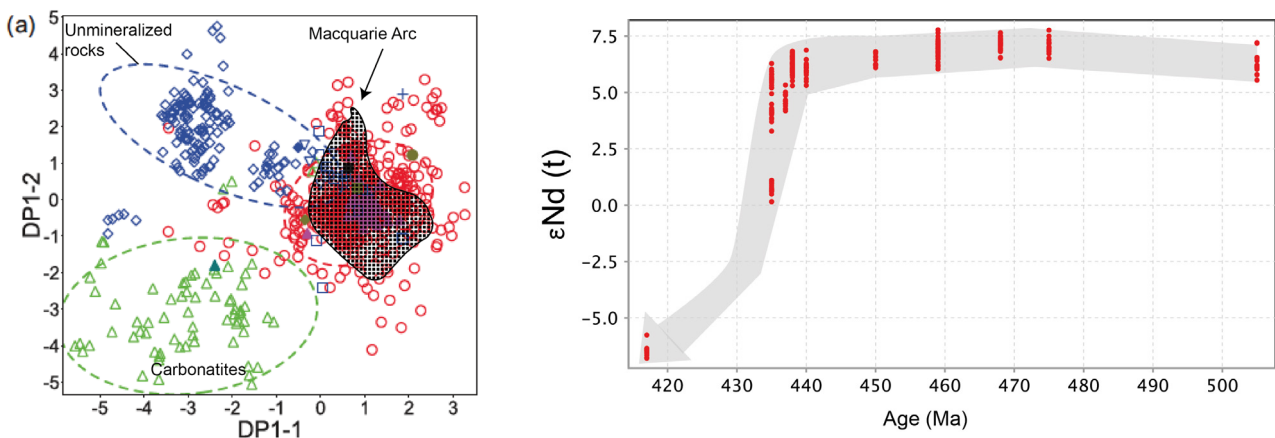


Figure 1. Left: Discrimination plot for apatite from mineralised rocks (red) and barren systems (blue) (1). All samples from the Macquarie Arc (shaded field) plot well within the “mineralised” field. Right: $\epsilon\text{Nd}(t)$ in apatite vs. emplacement age of porphyry systems. At ~440 Ma a significant change in ϵNd can be observed, indicating substantial melting of crustal material.

The development of *in situ* sulfur isotope analysis in apatite is near completion and preliminary results of some key samples will be discussed as well as the potential of quantifying sulfur isotopes in apatite in general.

REFERENCES

- [1] Mao, M. et al. 2016. Apatite trace element compositions: A robust new tool for mineral exploration. *Economic Geology*, 111, 1187-1222. doi:10.2113/econgeo.111.5.1187

Petrologic characterisation of granite before conductivity experiment

K. HAN¹ AND S.M. CLARK¹

¹Australian Research Council Centre of Excellence for Core to Crust Fluid Systems (CCFS) and GEMOC, Department of Earth and Planetary Sciences, Macquarie University, Sydney, NSW 2109, Australia (kui.han@hdr.mq.edu.au, simon.clark@mq.edu.au)

Two natural granite samples and two constitutionally consistent samples created from pure phases were compared to investigate the relationship between electrical conductivity of the bulk rock and its component minerals as well as the other factors such as grain size, grain boundaries and foliation. Fundamental petrologic characteristics, consequently, coupled with water content in and between mineral grains, were determined before electrical conductivity measurements [1]. Although varying compositions are presented in the two bulk granites, the major constitutional minerals are quartz, plagioclase and K-feldspar. The combined results of microscope observations, XRF and XRD, reveal compositions of 40% quartz, 20.7% plagioclase, 35.2% k-feldspar and 36.9% quartz, 44.5% plagioclase, 16.5% k-feldspar for the two natural granites. Minor minerals such as biotite, amphibole and muscovite are found in both samples using optical microscopy, and water is enclosed in both quartz and orthoclase crystals. Thermogravimetric analysis (TGA) shows three main stages, from room temperature to around 450 °C, 450 °C to 650 °C, and above 650 °C, presumably indicating the loss of absorbed water on the mineral surface, water inclusions and crystal lattice water, with a total amount of 0.8362% wt. EBSD was applied to interpret the crystallographic preferred orientation that might affect electrical conductivity via diffusion of ions in different directions, and demonstrates a random orientation of the major minerals for both granites (Fig. 1). The potential relationship should simulate and predict the electrical conductivity of rocks in the deep Earth.

GOF

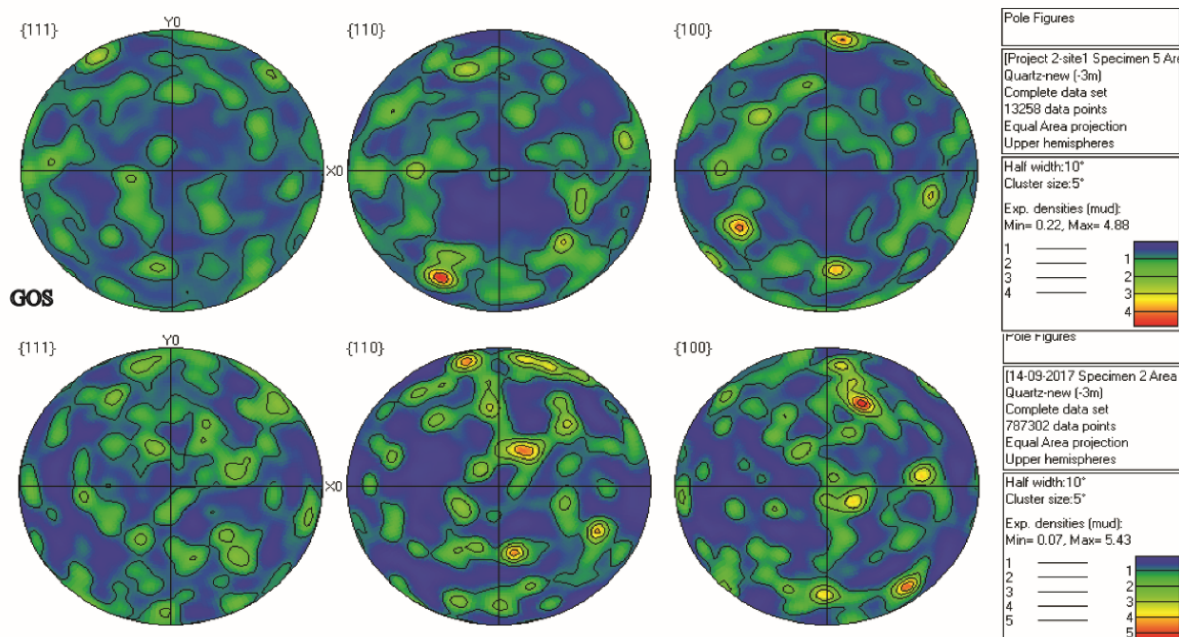


Figure 1. Pole figures of quartz.

REFERENCES

- [1] Yoshino, T. 2010. Laboratory electrical conductivity measurement of mantle minerals. *Surveys in Geophysics* 31, 2, 163-206.

New petrogenetic model for the adakitic magmatism of Patagonia and the Austral Volcanic Zone

G.J. HENRIQUEZ^{1,2}, R.R. LOUCKS^{1,2} AND M.L. FIORENTINI^{1,2}

¹Centre for Exploration Targeting, School of Earth Sciences, The University of Western Australia, Crawley, WA 6009, Australia (gonzalo.henriquez@research.uwa.edu.au; robert.loucks@uwa.edu.au; marco.fiorentini@uwa.edu.au)

²Australian Research Council Centre of Excellence for Core to Crust Fluid Systems (CCFS), The University of Western Australia, Crawley, WA 6009, Australia

Motivation of Research

The “Adakites” from the Patagonian Cordillera and the Austral Volcanic Zone (AVZ) in the southwest margin of South America, are believed to be among the few true slab-melts on Earth. Their steep REE patterns have been interpreted as implying a substantial role of restite garnet and petrogenesis by partial melting of eclogite in the subducting plate (e.g. [1]; [2]), by analogy with the alleged slab-melting origin of compositionally similar “adakites” on Adak Island in the central Aleutian arc [3]. These are distinguished from ordinary calc-alkalic arc andesites and dacites by steeper REE patterns with low concentrations of HREE and Y, and high values of Mg#, Cr, Ni, and Sr for their SiO₂ contents mainly in the range 56-63 wt%. However, an alternative interpretation of “adakite” petrogenesis in Adak due to hydrous magmatic differentiation at high-pressure and temperature can be proposed based on: 1) subsequent descriptions of xenolith suites; 2) finding of a seismically active slab-mantle interface to depths of at least 270 km under the central Aleutians, which means that slab temperature is less than 650 °C under the volcanic front [4], too cool to be melted; and 3) along-arc variations of tectonic stress. This project aims to explore this alternative non-eclogitic petrogenetic interpretation without slab melting in the Plio-Holocene volcanic centres from the AVZ, as well as to the mid-Miocene Patagonian “adakites”.

Why Patagonia?

The western margin of Patagonia has experienced the subduction of the Chile Rise since ~22 Ma. As a result, a series of adakitic igneous complexes are related with the northward-propagating compressive deformation wave, which seems to be associated with the young, warm and buoyant southern part of the Nazca Plate subducted. On the other hand, all six Holocene volcanic centres of the Andean AVZ (49–54°S), associated with subduction of the Antarctic Plate under the South American and Scotia Plates, have erupted exclusively adakitic andesites and dacites [1]. These two scenarios integrated in one particular tectonic setting, makes Patagonia a perfect location to understand the processes involved in the genesis of the adakitic magmas.

Sampling Scope and Analytical Techniques

This research project aims to integrate both whole-rock geochemistry and U-Pb dating and trace elements (including REE) from zircons by LA-ICP-MS analyses (*in situ* and detrital) from Patagonian igneous centres. Zircon Cathodoluminescence images will be used to search unzoned cores textures, which could imply deep and slow crystallisation of the plutonic rocks. Additionally, we will perform Al-in-hornblende (EPMA) barometry on hornblende phenocrysts in host rock and plutonic enclaves.

To date, rocks and stream sediments were taken from 5 mid-Miocene igneous centres, during March 2017 at Patagonia (Chile and Argentina). Zircon mineral separation and geochemical sample preparation have already been undertaken at UWA. Field work to sample 2 adakitic volcanoes from the AVZ is planned for February to March 2018. Preliminary results of ~2000 zircon LA-ICP-MS analyses (*in situ* and stream sediments materials), in addition to 15 whole-rock geochemistry analyses, are expected in December 2017.

REFERENCES

- [1] Stern, C.R. and Kilian, R. 1996. Role of the subducted slab, mantle wedge and continental crust in the generation of adakites from the Andean Austral Volcanic Zone. *Contributions to Mineralogy and Petrology*, 123, 263-281.
- [2] Ramos, V. et al. 2004. Las adakitas de la cordillera Patagónica: Nuevas evidencias geoquímicas y geocronológicas. *Revista de la Asociación Geológica Argentina*, 59, 4, 693-706.
- [3] Kay, R.W. 1978. Aleutian magnesian andesites: melts from subducted Pacific Ocean crust. *Journal of Volcanology and Geothermal Research*, 4, 117-132.
- [4] Gorbatov, A. and Kostoglodov, V. 1997. Maximum depth of seismicity and thermal parameter of the subducting slab: general empirical relation and its application. *Tectonophysics*, 277, 165-187.

The seismicity of subduction zones: Switch of fast-velocity direction from trench-normal to trench-parallel is assisted by layered-pyroxenite domains

H. HENRY^{1,2}, B. OLIVEIRA BRAVO¹, R. TILHAC^{1,2}, W.L. GRIFFIN¹, S.Y. O'REILLY¹ AND G. CEULENEER²

¹ARC Centre of Excellence for Core to Crust Fluid Systems (CCFS) and GEMOC, Department of Earth and Planetary Sciences, Macquarie University, Sydney NSW 2109, Australia

²Géosciences Environnement Toulouse (GET), CNRS, CNES, IRD, Université Toulouse III, 14 avenue E. Belin, 31400 Toulouse, France

Seismic waves provide information on the interior of the Earth in the form of delayed or quicker arrival time relative to a standard Earth model. The travel time of seismic waves reflects a complex combination of variations in temperature, mineralogy, melt and fluid content all along the wave trajectory. Previous studies showed that the measured seismic wave anisotropy in the Earth mantle may be related to (1) the lattice preferred orientation of the minerals [1] and (2) transposed lithological heterogeneities (i.e. layering [2]), both developing during solid-state flow. The volumetric dominance of olivine in the upper mantle focussed the interpretation of seismic anisotropy on this mineral. In mantle material, pyroxenes are being widely observed in xenoliths, ophiolites and abyssal peridotites, sometimes in proportions not negligible, and so far their influence on the seismic signal in pyroxene-rich domains is still unclear.

Here we show that pyroxenite layering in a supra subduction zones upper mantle [3] explains some seismic observations. When compared to a peridotitic and pyroxenite-poor supra subduction upper mantle, our model predicts a small decrease in Vp and Vs maximum anisotropy. P- and S2-waves are slowed in the lineation direction and P-waves accelerated at 90° to the lineation in the foliation plane. In the volcanic front, where large volumes of pyroxenites are expected, the abrupt 90° change in the fast velocity direction is attributed to a change in olivine slip direction [4]. Our model suggests that layered pyroxenite will contribute to the sharpness of the transition. Additionally, the combination of (1) a surface wave velocity decrease in both P-waves and Vs2 and (2) an isotropically slowed Vs1 could be used as indicators for a pyroxenite-rich layered region in the upper mantle. Our results could be a starting point to investigate how different percentages of pyroxenites and fabrics will influence the seismic signal coming from the Earth's upper mantle.

REFERENCE

- [1] Nicolas, A. and Christensen, N.I. 1987. Composition, structure and dynamics of the lithosphere-asthenosphere system. American Geophysical Union Geodynamics Series, 16, 111-123.
- [2] Schoenberg, M. and Muir, F. 1989. A calculus for finely layered anisotropic media. Geophysics 54, 581-589.
- [3] Tilhac, R. et al. 2016. Primitive arc magmatism and delamination: Petrology and geochemistry of pyroxenites from the Cabo Ortegal Complex, Spain. Journal of Petrology, 57, 1921-1954.
- [4] Jung, H. and Karato, S.-I. 2001. Water-induced fabric transitions in olivine. Science, 293, 1460-1463.

Moissanite in volcanic systems: Super-reduced conditions in the mantle

J.-X. HUANG¹, W.L. GRIFFIN¹, T. MURPHY¹, S.E.M. GAIN¹, V. TOLEDO² AND S.Y. O'REILLY¹

¹ARC Centre of Excellence for Core to Crust Fluid Systems (CCFS), Macquarie University, Australia
(jinxiang.huang@mq.edu.au)

²Shefa Yamim (A.T.M.) Ltd., Netanya 4210602, Israel

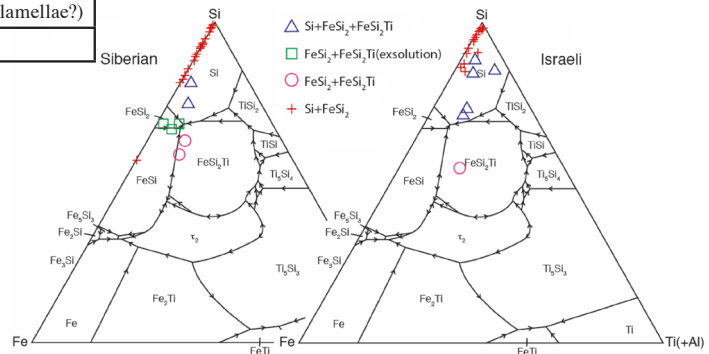
The oxidation state, commonly described by the oxygen fugacity (fO_2) of the system relative to various buffer reactions, is a critical parameter in Earth processes. The fO_2 of the lithospheric mantle up to 7 GPa ranges from $\Delta QFM+1$ to $\Delta QFM-5$, normally higher than the Iron-Wustite (IW) oxygen buffer. However, many reduced phases such as Fe, Si, Ni, Cr metals and alloys have been found in peridotite xenoliths and ophiolitic chromitites and associated peridotites, indicating that the redox state of the mantle is not homogeneous and some volumes are more reduced than others, at least locally. How does this occur?

Moissanite (SiC) is a characteristic reduced mineral in the lithosphere and deeper mantle, which is stable only at $fO_2 < \Delta IW-5$. It has been reported as diamond inclusions from cratons, as xenocrysts from kimberlites and lamproites, as coexisting minerals in carbonados, impact melt rocks, xenolithic carbonatites and eclogites, serpentinites and eclogites in orogenic belts. In this work, SiC from Siberian kimberlites and an Israeli volcanic systems were studied to investigate their growth environments and to evaluate the redox state of the local mantle.

Siberian SiC is from heavy-mineral separates from Mir, Aikhal and Udachnaya kimberlites. The Israeli SiC is from Cretaceous pyroclastic rocks on Mt Carmel and associated alluvial deposits, which is associated with corundum, Fe balls, and native V etc. Most SiC grains are fractured; only few preserve some well-formed crystallographic faces. Siberian SiC samples have a wide colour range, from colourless to blue to green, many colourless, while most Israeli ones are blue to green.

Locality	Siberia	Israel
1	Si+ FeSi ₂	Si+FeSi ₂ (Al)
2	FeSi ₂ + FeSi ₂ Ti (lamellae)	/
3	FeSi ₂ + FeSi ₂ Ti (crystal)	FeSi ₂ + FeSi ₂ Ti (crystal)
4	Si+ FeSi ₂ + FeSi ₂ Ti (lamellae)	Si+ FeSi ₂ (Al)+ FeSi ₂ Ti (lamellae?)
5	/	Si+ FeSi ₂ Al ₃ +CaSi ₂ Al ₂

Figure 1. Bulk compositions of melt inclusions in Siberian and Israeli SiC samples plotted in Si-Fe-Ti (+Al) liquidus projection.



An important feature of the studied SiC is that it contains melt inclusions, which generally consist of two or more phases (Table 1). In samples from both localities, a Si+FeSi₂ assemblage in melt inclusions is the most common type. Other assemblages include FeSi₂+ FeSi₂Ti (crystal) and Si+ FeSi₂+ FeSi₂Ti. Inclusions with FeSi₂+ FeSi₂Ti (lamellae) are only found in Siberian

samples and Israeli samples have Si+ FeSi₂Al₃+CaSi₂Al₂. The bulk compositions of inclusions were calculated and plotted in the Si-Fe-Ti diagram. Israeli SiC inclusions normally have trace amounts of Al, while Siberian ones do not, which is consistent with the mineral associations in those two volcanic systems. The Israeli volcanic system has a large amount of corundum, while corundum is yet to be found in the Siberian kimberlites.

It is well accepted that melt inclusions are small amounts of melt trapped within a crystal during its original growth from that melt, or during subsequent healing of fractures in the presence of melt. It is less likely that the inclusions in this work are related to secondary processes, simply because the secondary melt would have to be very reduced, otherwise SiC would be oxidised; furthermore, the chemical compositions of the melts are similar to the ones from which SiC can crystallise. Although SiC has 50 atomic percent of C, SiC can crystallise from a Si melt even when C is less than 6 percent at low T. If Fe is present in the Si melt, the growth is even easier and quicker. As reflected in the mineralogy of the inclusions, Fe was present in this Si-C melt.

The reduced Fe-Si-C-(Al) melt may be one product of the evolution of basaltic melts in the mantle. When CH_4+H_2 from the deep mantle fluxes into the melt, it becomes more and more reduced with the change of chemical compositions, as some phases would crystallise at certain reduced conditions. At the same time, some melts will become immiscible and separate from each other. During the eruption of the magma, the reduced phases together with reduced melts and normal oxidised magma are brought to the Earth's surface and quenched.

Insights into diamond formation from polycrystalline diamond aggregates

D.E. JACOB¹, R.A. STERN², J. CHAPMAN³, T. STACHEL² AND S. PIAZOLO¹

¹Australian Research Council Centre of Excellence for Core to Crust Fluid Systems (CCFS), Department of Earth and Planetary Sciences, Macquarie University, Sydney, NSW 2109, Australia (dorrit.jacob@mq.edu.au)

²CCIM, University of Alberta, Edmonton, Canada (rstern@ualberta.ca)

³Gemetrix Pty Ltd, Perth, Australia (john@gemetrix.com.au)

Polycrystalline diamond aggregates (diamondites) are produced by rapid crystal nucleation caused by extreme carbon supersaturation in mantle fluids. They may form episodically and under variable chemical conditions, providing snapshots of diamond formation in the Earth's mantle. Diamondites, thus, represent an extreme end member of diamond formation mechanisms, while forming via the same processes and ingredients as the gem-sized diamonds.

We present results on a large suite of diamondites from the Venetia mine (South Africa), comprising a complete characterisation of the diamonds and their silicate inclusions and intergrowths. The highlighted characteristic of this sample suite is its heterogeneity in all aspects, from affiliated silicate to diamond composition and texture of the diamond aggregates. The diamond grains in the samples are intergrown with silicates (garnets, clinopyroxenes, phlogopites) comprising a websteritic-eclogitic and a peridotitic-pyroxenitic suite of minerals.

Diamonds, regardless of their affiliation based on their silicate phases, overlap in carbon and nitrogen composition and have $\delta^{13}\text{C}$ values between -28 and -8 ‰, $\delta^{15}\text{N}$ values of 0.8 to 16.3 ‰ and nitrogen contents of

4 to 2329 ppm. The entire range of carbon and nitrogen variability of the suite is also reflected in some individual samples. Cathodoluminescence imaging (Fig. 1) visualises different zones in the samples that can be interpreted as different growth events with differing nitrogen contents and $\delta^{15}\text{N}$ decoupled from $\delta^{13}\text{C}$ values, in line with the variability of nitrogen aggregation states. Electron backscatter diffraction analyses identify an original texture of randomly intergrown diamond grains that is partly changed by deformation and newly grown smaller diamond grains. The large overall variability suggests episodic formation of diamondite with nitrogen from crustal sources.

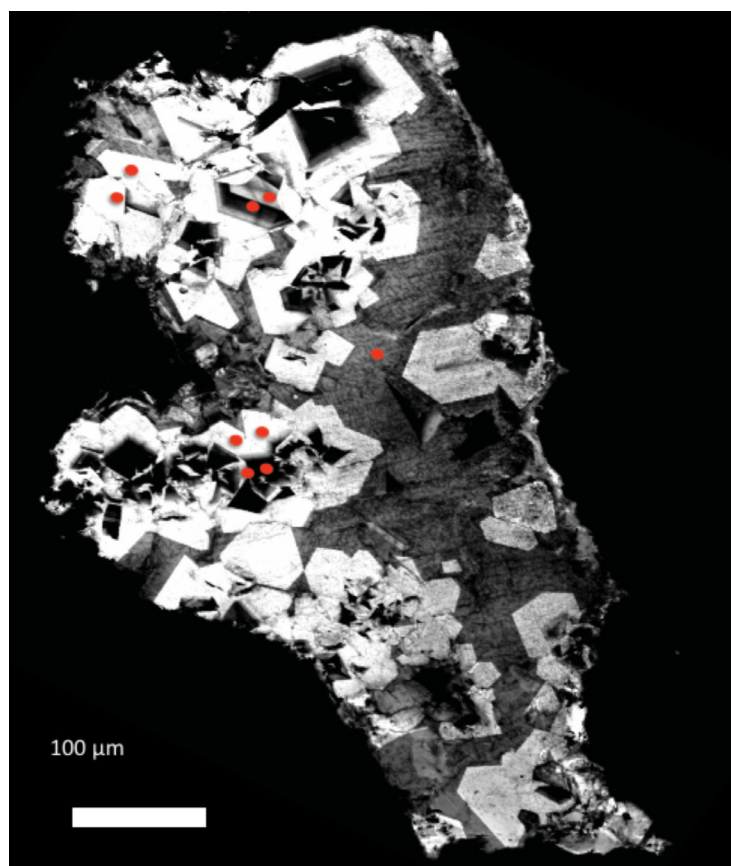


Figure 1. Cathodoluminescence image of a diamondite fragment showing growth zonation. (SIMS spots indicated in red).

Gold pathways in El Indio Belt: Preliminary zircon U-Pb and O-isotopes analyses

C. JARA¹, J. MILLER², M. FIORENTINI¹, H. JEON¹, M. FANNING³ AND D. WINOCUR⁴

¹Centre for Exploration Targeting (CET) and ARC Centre of Excellence in Core to Crust Fluid Systems (CCFS), University of Western Australia, 35 Stirling Highway, Crawley, Australia (constanza.jarabarra@research.uwa.edu.au)

²CSIRO - Kensington, Australian Resources Research Centre (ARRC), 26 Dick Perry Ave, Kensington WA 6152

³Australian National University, Research School of Earth Sciences, 142 Mills Rd, Acton ACT 0200

⁴Universidad de Buenos Aires, Buenos Aires, Argentina

Project Scope

This study tests the Mineral System concept hypothesis in one of the most highly Au-endowed provinces of the Andes Cordillera: the El Indio Belt (EIB, Chile-Argentina 29° 00'–30° 30' S), which holds >45 Moz Au mainly hosted in Miocene world-class epithermal systems (Pascua-Lama, El Indio, Veladero, and Alturas). By means of the integration of currently available data with new structural and zircon analyses, it intends to define: 1) the trans-lithospheric architecture that acted as the magma/fluids pathway, linking the fertile metal source with the deposit's location; 2) the architecture's geodynamic evolution related to metallogenic events.

El Indio Belt Geology

The EIB is associated with a long-lived subduction zone. It comprises of Permian-Triassic pyroclasts and granites intruding Carboniferous-Devonian metasediments, segmented by Triassic to Jurassic sedimentary basins. During the Cenozoic, a volcanic arc developed over this basement, evolving among different compression and extensional regimes according to variations in the subduction vector and subducting oceanic slab features [2]. Mineralisation is linked to the final, localised stages of volcanic arc magmatism, associated with strong compression due to the subduction of an inactive ridge. Location of the deposits is hypothesised to be linked to trans-lithospheric structures that cut across the volcanic arc. Currently, the EIB is located in an inactive volcanic segment of the Andes, over a flat slab.

U-Pb and O-isotope Zircon Analyses

O-isotope and Lu-Hf analysis are expected to yield clues on first-order variations in the basement and Cenozoic magmas along the EIB, highlighting the location of big, deep-seated structures. Both the Permian-Triassic granitic basement and Cenozoic intrusives or *in-situ* domes were sampled for zircon analyses in Chile and Argentina. Zircon grains were obtained following the conventional methods of density, magnetic and heavy liquids separation, mounted in epoxy resin mounts and imaged, including CL. U-Pb SHRIMP-II geochronology in zircon was performed at Curtin University and at ANU. Subsequent O-isotope analyses were carried out using CAMECA IMS-1280 at CMCA, UWA.

Preliminary results are compared with the mantle reservoir values of Valley et al. (2005) [1] of $5.3 \pm 0.6\text{‰}$ $\delta^{18}\text{O}$ (2σ). There is a marked difference between Permian-Triassic basement and Cenozoic $\delta^{18}\text{O}$ values. Basement samples have higher $\delta^{18}\text{O}$, between mantle and evolved crust values, and the oldest inherited cores of all samples show a much higher supracrustal component. The Cenozoic magmatic events show a variation from the Eocene, with $\delta^{18}\text{O}$ close to 6.0‰ , indicating both a mantle and evolved crust component in the magmas in a probably compressive regime, towards mantle-like $\delta^{18}\text{O}$ during the Oligocene to Miocene, preliminarily indicating almost no evolved crustal component in these later magmas. Only in Argentina do they show a higher $\delta^{18}\text{O}$ value of $6\text{--}7\text{‰}$, probably indicating a higher crustal involvement in the eastern area of the EIB, where the crust may be thicker and influenced by older Carboniferous-Devonian basement. Slightly higher $\delta^{18}\text{O}$ values are locally seen in late Miocene dome and dyke samples, possibly pointing towards a longer residence time inside the crust or further interaction with meteoric waters. These samples also show the biggest data spread, with one $\delta^{18}\text{O}$ value below the mantle reservoir values.

Metallogenic implications of these preliminary observations are not yet clear, and they need to be thoroughly assessed in light of petrography and geological context, complemented with Lu-Hf isotopic analyses and whole-rock geochemistry. First-order variations are preliminarily observed between the E and W domains of the EIB, although further analyses are needed to assess the existence of a N-S variation along the belt.

REFERENCES

- [1] Valley, et al. 2005. 4.4 billion years of crustal maturation: oxygen isotope ratios of magmatic zircon. *Contributions to Mineralogy and Petrology*, 150, 561-580.
- [2] Winocur, D.A. 2010. *Geología y estructura del Valle del Cura y el sector central del Norte Chico*, PhD Thesis, University of Buenos Aires, Argentina.

Good data from bad numbers: Visualising temporal and spatial patterns of isotope disturbance

C.L. KIRKLAND, N.J. GARDINER, F. ABELLO AND M. DANIŠÍK

Department of Applied Geology, Curtin University, GPO Box U1987, Perth WA 6845, Australia, ARC Centre of Excellence for Core to Crust Fluid Systems (CCFS) and The Institute for Geoscience Research (TIGeR).

The zircon U-Pb system is a powerful geochronometer, however disturbance to this system can be widely diagnosed on U-Pb concordia diagrams where it is typically interpreted as a consequence of radiogenic-Pb loss. Pb is incompatible in zircon, but is generated by radioactive decay of U in the grain, a process that leads to some degree of radiation damage in the crystal lattice. As a result, Pb is only loosely bound to the zircon crystal lattice, whence U was tightly bound. Hence radiogenic Pb is, in comparison to U, readily mobile, particularly at the margins of the crystal and along any fractures. In many cases, removal of radiogenic-Pb is not complete, and Discordia regressions on concordia diagrams provide a means to track both the original age of crystallisation of the rock and the timing of isotopic disturbance. In this talk I will present a new approach to determine the most pervasive time of U-Pb disturbance in a sample. This new statistical approach, the Concordant-Discordant Comparison (CDC) test, evaluates the similarity between a sample's concordant age structure and a modelled age structure, from discordant analyses, over a wide range of potential disturbance times. The closest similarity in concordant and discordant age populations as derived from a specified time of elemental mobility, is interpreted as the best estimate for the time of U-Pb disturbance. The CDC test is appropriate for magmatic as well as detrital samples, and yields dates that can be spatially interpolated to produce regional maps (Fig. 1) that define spatial domains of temporally similar U-Pb disturbance. A range of case studies using the CDC test will be presented including examples from North Greenland and the Eastern Goldfields Superterrane of the Yilgarn Craton, Western Australia. The CDC test typically captures information on the timing of fluid-rock interaction and has been used to date a wide range of events including mineralisation and dyke emplacement. CDC modelling of discordant U-Pb zircon analyses may provide a means to recognise the distal footprint of otherwise difficult to date tectonothermal events and extract useful information from often discarded analyses.

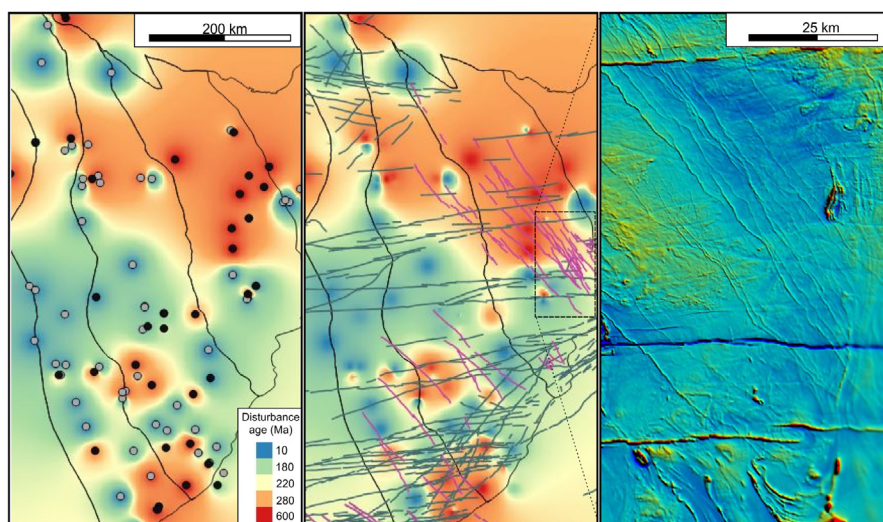


Figure 1. Spatial interpolation of the best estimates of the time of U-Pb disturbance. Left: sample locations. Centre: overlay of the location of east-west dykes (green) and northwest-southeast dykes (purple). Right: aeromagnetic image of an enlargement of a section of the Eastern Goldfields Superterrane intruded by northwest-southeast dykes that correlate with a ~ 600 Ma U-Pb zircon disturbance.

Mantle control of the geodynamo: paleomagnetic update

U. KIRSCHER AND R. MITCHELL

Earth Dynamics Research Group, ARC Centre of Excellence for Core to Crust Fluid Systems (CCFS) and The Institute for Geoscience Research (TIGeR), Department of Applied Geology, Curtin University, GPO Box U1987, WA 6845, Australia (Uwe.Kirsch@curtin.edu.au)

It is broadly accepted that the heat flux through the core-mantle boundary (CMB) is a crucial influencing parameter for the geodynamo [1]. This relationship, however, has mostly been utilised by the geodynamo community in terms of improving simulations related to secular cooling, inner core nucleation, and driving mechanisms for the geodynamo [2,3]. Here we present preliminary results, which tackle potential implications deduced from paleomagnetic field characteristics, for the history of the mantle. On one hand, we present new paleomagnetic data from recent magnetic field reversals, where we re-establish the old idea that the geometry of field reversals is linked to CMB heat flow related to large low shear velocity provinces (LLSVPs) in the lowermost mantle. By doing this further back in time, it may be possible to evaluate if these LLSVPs are spatially fixed or more dynamic features. On the other hand, we suggest that the strength of the magnetic field is largely underutilised in deciphering the long term evolution of the Earth. We propose an approach, where variability of the magnetic field strength is accepted to be inherent and we treat the magnetic signal as a composite effect of several mechanisms leading to cyclic behaviour. Accordingly, we performed a time series analysis on fluctuations in magnetic field strength over the past 3.5 billion years (Gyr) using absolute paleointensity estimates obtained from the most recently compiled paleointensity database. This yields the presence of multiple significant cycles that range across three orders of magnitude in duration. After subtraction of the most significant raw cycles obtained by bandpass filters, a linear decrease as well as the previously statistically detected step change at ~1.4 Gyr [4] are remarkably apparent. Comparison of one of the most prominent cycles with the simulated CMB heat flux for the last 500 Ma [5] yields a high degree of similarity and leads us to propose a direct cause and effect relationship between the supercontinent cycle, the CMB heat flow and the strength of the magnetic field. We furthermore point out that our parameterisation of the magnetic field strength incorporates several observed features such as the Paleoproterozoic dipole low [6] and emphasises that the inner core nucleation is masked and barely visible by the cyclic behaviour related to other mechanisms of the magnetic field.

REFERENCES

- [1] Olson, P. 2016. Mantle control of the geodynamo: consequences of top-down regulation. *Geochemistry, Geophysics, Geosystems*, 17, 1935-1956.
- [2] Driscoll, P. and Olson, P. 2011. Superchron cycles driven by variable core heat flow. *Geophysical Research Letters*, 38, L09304.
- [3] Takahashi, F. et al. 2008. Effects of thermally heterogeneous structure in the lowermost mantle on the geomagnetic field strength. *Earth and Planetary Science Letters*, 272, 738-746.
- [4] Mitchell, R. et al. Did Earth's first supercontinent form the inner core? Submitted.
- [5] Zhang, N. and Zhong, S. 2011. Heat flux at the Earth's surface and core-mantle boundary since Pangea formation and their implications for the geomagnetic superchrons. *Earth and Planetary Science Letters*, 306, 3-4, 205-216.
- [6] Valet, J.-P. et al. 2014. The intensity of the geomagnetic field from 2.4 Ga old Indian dykes. *Geochemistry, Geophysics, Geosystems*, 15, 2426-2437.

Volatile pathways through the lithosphere: The MIF-S tracer

C. LAFLAMME, M.L. FIORENTINI, N. THÉBAUD, D. SUGIONO, S. CARUSO AND V. SELVARAJA

Australian Research Council Centre of Excellence for Core to Crust Fluid Systems (CCFS) and Centre for Exploration Targeting, School of Earth Sciences, University of Western Australia, Perth, WA 6009, Australia
(crystal.laflamme@uwa.edu.au)

The anomalous sulfur isotopic signature $\Delta^{33}\text{S}_0 \neq 0\text{‰}$ that occurs in a restricted range of sulfur-bearing rock types throughout the geological record has been used to assess the surficial nature of the biological and atmospheric and hydrological sulfur cycle through time. It is widely accepted that $\Delta^{33}\text{S}_0$ anomalies ($\Delta^{33}\text{S}_0 > \pm 0.2\text{‰}$) were formed in the Archean eon, largely through mass independent fractionation of sulfur (MIF-S) in an oxygen-poor atmosphere, and imparted to the Archean supracrustal rock record (as MIF- S_0). Here, we harness the indelible MIF- S_0 signature to trace sulfur pathways to mineral systems where the signature is recycled as MIF- S_1 . Through this recycling process, the original MIF- S_0 signal ($\Delta^{33}\text{S}_0 \neq 0\text{‰}$) may be diluted by mixing between sulfur reservoirs to such an extent as to yield near-zero values ($\Delta^{33}\text{S}_1 = 0 \pm 0.5\text{‰}$). In such cases, interpretation of the geological significance of such isotopic signatures may be compromised as it is known that mass dependent fractionation of sulfur (MDF-S, recorded as $\delta^{34}\text{S}$) can yield small $\Delta^{33}\text{S}$ values ($\pm 0.2\text{‰}$), often owing to geobiological reactions involving sulfur.

In this study, we reassess the quantification of $\Delta^{33}\text{S}$ due to MDF-S from the traditionally accepted $0 \pm 0.2\text{‰}$ value to demonstrate that its magnitude is not constant, but rather directly linked to the degree of $\delta^{34}\text{S}$ fractionation. We then apply this knowledge to the Waroonga Archean orogenic gold deposit in which gold-bearing arsenopyrite yields $\Delta^{33}\text{S}_1 = +0.3\text{‰}$. Our results indicate that sulfur, the complexing ligand for gold transport, was sourced at least partially from the Archean sediment record. When these spatially- and temporally-constrained measurements are combined with detailed chemical maps of arsenopyrite, we demonstrate that the Archean sediment reservoir was likely devolatilised at depth. Ore deposits (leaving aside their economic significance) are loci where mass and energy concentrative processes take place, being the ideal natural laboratories to study volatile pathways. The outcomes from these studies have the potential to greatly enhance the application of

MIF- S_1 ($\Delta^{33}\text{S}_1$) as a powerful tracer of sulfur pathways through the lithosphere.

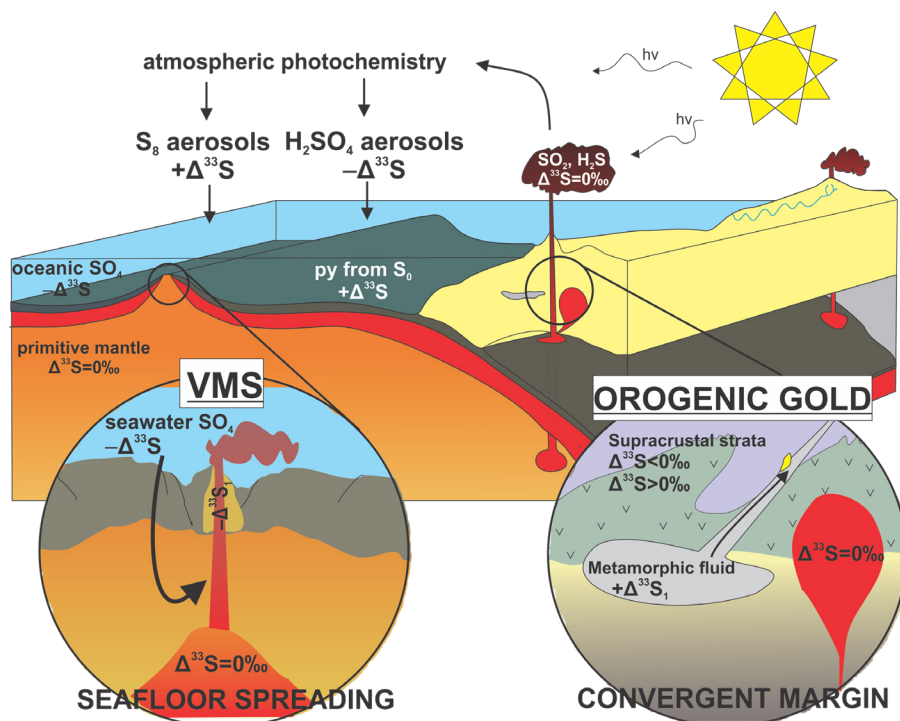


Figure 1. Sulfur cycling on the continental scale after Farquhar and Wing (2003). Insets to schematically demonstrate how sulfur can be traced (as $\Delta^{33}\text{S}$) through the lithosphere to mineral systems.

Dating early silicate differentiation on Mars using new developed ^{92}Nb - ^{92}Zr chronometer

Y.-J. LAI^{1,2} AND M. SCHÖNBÄCHLER¹

¹Institute of Geochemistry and Petrology, ETH Zürich, 8092 Zürich, Switzerland

²Macquarie University GeoAnalytical, Earth and Planetary Sciences, Macquarie University, Sydney, NSW 2109, Australia (yi-jen.lai@mq.edu.au)

^{92}Nb - ^{92}Zr short-lived radiogenic isotope system

Short-lived decay systems are powerful tools to date early planetary differentiation. One of these systems is ^{92}Nb , which decays to ^{92}Zr with a half live of 37 Myr. This system has great potential to date early silicate differentiation and core segregation of planets owing to Nb-Zr fractionation during these processes. Moreover, the Nb-Zr chronometer provides important, complementary information to the short-lived ^{146}Sm - ^{142}Nd (half-life ~ 103 Myr) and ^{182}Hf - ^{182}W (half-life ~ 8.9 Myr) chronometer regarding planetary differentiation. The obtained Nb-Zr ages, however, critically depend on the initial $^{92}\text{Nb}/^{93}\text{Nb}$ ratio of our solar system, which has been controversial [e.g. 6, 7]. Our recent results from basaltic achondrites, mesosiderites and calcium aluminium rich inclusions (CAIs) significantly improved the estimate for the initial ^{92}Nb abundance of our solar system and demonstrated the homogeneous distribution of Nb and Zr isotopes in the solar system [3, 4, 5]. Here, we applied the Nb-Zr chronometer to constrain early silicate differentiation on Mars to complement previous evidence from the ^{182}Hf - ^{182}W and ^{146}Sm - ^{142}Nd decay systems.

Method

High-precision Zr isotope data of eight Martian meteorites (four depleted and enriched basaltic shergottites, the orthopyroxenite ALH84001, two nakhlites, and one chassignite) were obtained. The Zr isotope ratios were measured on a Neptune Plus MC-ICPMS at ETH Zürich. The average $\epsilon^{92}\text{Zr}$ value, and associated external precision (2SE) of this technique for the USGS basalt BHVO-2 is 0.01 ± 0.02 ($n = 74$) during the course of this study. To improve the analytical uncertainty (< 3 ppm), the samples were analysed at least 5 times when sufficient material was available.

Results and Discussion

The analysed Martian samples exhibit well-resolved variations in $^{142}\text{Nd}/^{144}\text{Nd}$ and $^{182}\text{W}/^{183}\text{W}$, which indicate that the source of the shergottite reservoir formed at ~ 4525 Ma [2]. Nevertheless, all shergottites, nakhlites and chassignite show $\epsilon^{92}\text{Zr}$ values identical to the terrestrial basalt BHVO-2 and chondrites. The exception is orthopyroxenite, ALH84001, which yields a slightly positive $\epsilon^{92}\text{Zr}$ value relative to chondrites and terrestrial samples. This indicates that the formation of early enriched silicate reservoirs on Mars occurred within the first ~ 50 Myr, which is in agreement with the conclusion obtained from with previous Sm-Nd data [1]. We further constrain that the Martian magma ocean most likely had a depth of 900 to 1350 km.

REFERENCES

- [1] Debaille, V. et al. 2009. Early Martian mantle overturn inferred from isotopic composition of nakhlite meteorites, *Nature Geoscience*, 2, 8, 548-552.
- [2] Foley, C.N. et al. 2005. The early differentiation history of Mars from ^{182}W - ^{142}Nd isotope systematics in the SNC meteorites. *Geochimica et Cosmochimica Acta*, 69, 4557-4571.
- [3] Haba, M.K. et al. 2017. Rutile and zircons of mesosiderites: combined niobium-zirconium and uranium-lead chronometry and the initial abundance of niobium-92 in the solar system. LPSC abstract, 1739.
- [4] Iizuka, T. et al. 2016. The initial abundance and distribution of ^{92}Nb in the Solar System. *Earth and Planetary Science Letters*, 439, 172-181.
- [5] Lai, Y.-J. et al. 2017. The Abundance of ^{92}Nb in the Early Solar System. Goldschmidt abstract.
- [6] Münker, C. et al. 2000. ^{92}Nb - ^{92}Zr and the early differentiation history of planetary bodies. *Science* 28, 1538-1542.
- [7] Schönbächler, M. et al. 2002. Niobium-zirconium chronometry and early solar system development. *Science*, 295, 1705-1708.

REE³⁺ luminescence hyperspectral mapping for the quantitative visualisation of trace-element distributions in zircon?

C. LENZ^{1,2}, E. BELOUSOVA¹, C. CHANMUANG² AND D. JACOBS¹

¹Australian Research Council Centre of Excellence for Core to Crust Fluid Systems (CCFS) and GEMOC, Department of Earth and Planetary Sciences, Macquarie University, Sydney, NSW 2109, Australia (christoph.lenz@mq.edu.au)

²Institut für Mineralogie und Kristallographie, Universität Wien, 1090 Wien, Austria

Here, we present first results of a study which aims at developing laser-induced photoluminescence spectroscopy of REEs for a (semi-)quantitative visualisation of their distribution in zircon. The intensity of luminescence emissions of trace elements in steady-state spectra of minerals basically depends on the presence and concentration of certain luminescence centres in the material. Because of the latter, semi-quantitative REE distribution patterns may be easily produced using a confocal spectrometer system with a spatial resolution of few μm and software-controlled x-y mapping stage [2]. Hyperspectral PL maps show that emission intensities as caused by traces of Dy³⁺ in zircon correlate closely with its concentration (Fig. 1). Quantitative data or concentration ratios of REEs in zircon give valuable genetic implications on its geological history [1]. Photoluminescence intensity maps produced are found to be more sensitive to minute changes in element concentrations than panchromatic CL images that are typically used to unravel the primary formation and post-growth geological history of accessory minerals. Potential effects which may bias the luminescence yield, are discussed; e.g. crystal orientation, radiation damage accumulation, concentration quenching.

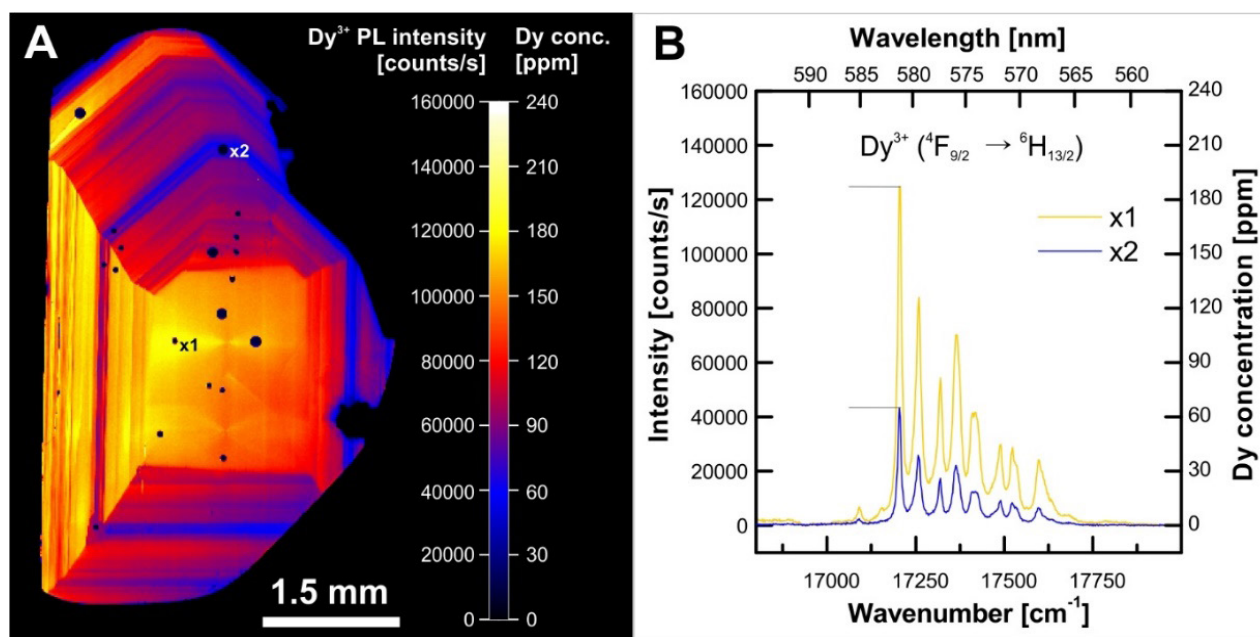


Figure 1. Photoluminescence hyperspectral map of a zircon crystal from DakLak, Vietnam acquired with a Horiba LabRam Evolution Raman spectrometer (A). The PL intensity of Dy³⁺ (B) have been found to strongly correlate with its trace element concentration as measured with LA-ICP-MS (various laser-ablation points are visible in the map as dark spots).

Acknowledgments

We gratefully acknowledge the support from ARC CCFS at Macquarie University, Sydney for the use of analytical instrumentation and financial support of C.L. by the Austrian Science Fund (FWF) project J3662-N19. We thank Andreas Wagner (Vienna) for extensive sample preparation.

REFERENCES

- [1] Belousova, E. et al. 2002. Igneous zircon: trace element composition as an indicator of source rock type. *Contributions to Mineralogy and Petrology*, 143, 602-622.
- [2] Lenz, C. et al. 2015. Laser-induced REE³⁺ photoluminescence of selected accessory minerals - An "advantageous artefact" in Raman spectroscopy. *Chemical Geology*, 415, 1-16.

Quantification of radiation damage in accessory minerals using REE³⁺ photoluminescence spectroscopy

C. LENZ^{1,2}, G.R. LUMPKIN², G.J. THOROGOOD², M. IONESCU² AND R. AUGHTERSON²

¹Australian Research Council Centre of Excellence for Core to Crust Fluid Systems (CCFS) and GEMOC, Department of Earth and Planetary Sciences, Macquarie University, Sydney, NSW 2109, Australia (christoph.lenz@mq.edu.au)

²Nuclear Fuel Cycle Research, Australian Nuclear Science and Technology Organisation, NSW 2234, Australia

Many accessory minerals, i.e. zircon, incorporate variable amounts of actinides, whose radioactive decay creates structural disorder, in their crystal structure. The generally increased susceptibility of radiation-damaged zircon to chemical alteration or aqueous leaching is of enormous importance, as these processes may for instance bias results of chemical and isotopic age determinations [1, 3]. Effects of radiation damage accumulation on the photoluminescence of zircon have been documented recently [2]. Here, we present a new concept based on the luminescence emission of REE³⁺, which aims at direct determination of the amorphous fraction from a single PL measurement using state-of-the-art confocal spectrometers with spatial resolution in the μm -range. Careful investigation of PL spectra from self-irradiated zircon samples from Sri Lanka as well as artificially irradiated analogous, polycrystalline ceramics (heavy-ion Au irradiation with energies up to 35 MeV) revealed that the detected luminescence emission of e.g. Dy³⁺ in zircon is basically a superposition of emissions from Dy ions in various, structurally different sites. We found that the relative integrated area of a fitted model spectra from an amorphous reference sample in relation to the full integrated area of the luminescence emission obtained gives a good estimate of the amorphous fraction present in the probed sample volume (Fig. 1a). This opens up the possibility to investigate the accumulation of radiation damage in zircon single crystals (Fig. 1b) in detail and gives rise to direct comparisons with damage accumulation in heavy ion irradiation experiments (Fig. 1c).

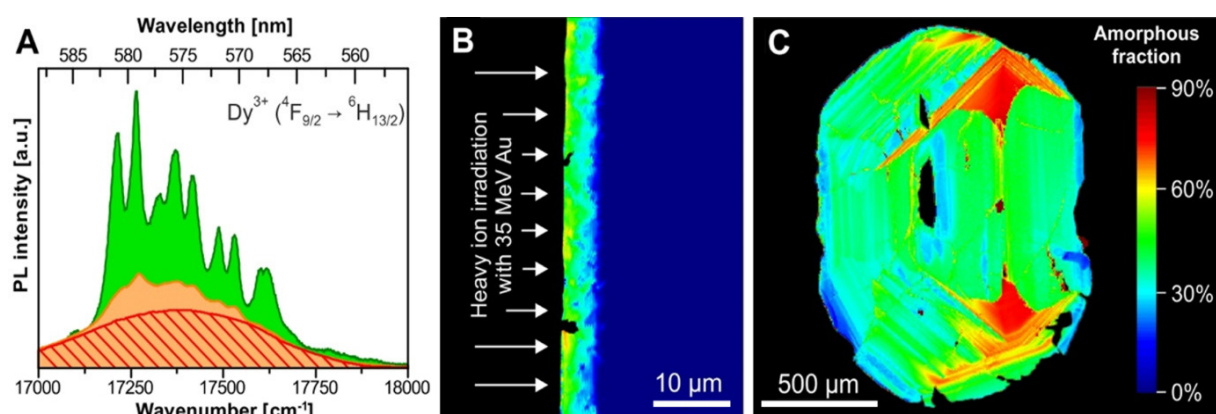


Figure 1. Use of PL spectra of Dy³⁺ to quantify radiation damage in zircon. (A) PL spectra of mildly (green) and strongly (ochre) radiation damaged zircon, normalised to an “amorphous” model spectrum (red). The integrated area of the amorphous model in relation to that of the observed spectrum may be used as an estimate for the amorphous fraction (e.g. 75% for the ochre and 40% for the green spectrum). (B) Colour-coded, hyperspectral PL map of a cross-section of an Au-irradiated ZrSiO₄ ceramic pellet. (C) Colour-coded, hyperspectral PL map of a zircon single-crystal from Plešovice, Czech Republic (Sláma et al. 2008). High concentrations of U and Th result in high damage accumulation over geological periods of time.

ACKNOWLEDGMENTS

C.L. gratefully acknowledges the use of instrumentation within an honorary associate agreement with the ARC CCFS at Macquarie University, Sydney. Ion accelerators at ANSTO are supported through NCRIS. Financial support of C.L. by the Austrian Science Fund (FWF) project J3662-N19 is kindly acknowledged.

REFERENCES

- [1] Kuiper, Y.D. 2005. Isotopic age constraints from electron microprobe U-Th-Pb dates, using a three-dimensional concordia diagram. *American Mineralogist*, 90, 586-591.
- [2] Lenz, C. et al. 2015. A photoluminescence study of REE³⁺ emissions in radiation-damaged zircon. *American Mineralogist*, 100, 1123-1133.
- [3] Zamyatin, D. et al. 2017. Alteration and chemical U-Th-total Pb dating of heterogeneous high-uranium zircon from a pegmatite from the Aduiskii Massif, Middle Urals, Russia. *Mineralogy and Petrology*, 11, 4, 475-497.

Thermal history of Proterozoic NE Australia: Insights into Nuna assembly and breakup

J. Li¹, A. POURTEAU¹, F. JOURDAN², S. VOLANTE¹, A. NORDSVAN¹ AND Z.-X. Li¹

¹Earth Dynamics Research Group, ARC Centre of Excellence in Core to Crust Fluid Systems (CCFS), and The Institute for Geoscience Research (TIGeR), Department of Applied Geology, Curtin University, Perth WA 6845, Australia (jiangyu.li@postgrad.curtin.edu.au, amaury.pourteau@curtin.edu.au, sylvia.volante@postgrad.curtin.edu.au, adam.nordsvan@postgrad.curtin.edu.au, Z.Li@curtin.edu.au)

²Western Australian Argon Isotope Facility, The Institute for Geoscience Research (TIGeR), Department of Applied Geology, Curtin University, GPO Box U1987, Perth WA 6845, Australia (F.Jourdan@exchange.curtin.edu)

The palaeogeographic configuration of the Paleo- to Mesoproterozoic supercontinent Nuna has been developed over the last 30 years. Multiple scenarios have been proposed based on geological analyses and palaeomagnetism. However, debate remains on the exact timing of Nuna assembly and breakup, and spatial relationships between different continents. Most Nuna reconstructions have NE Australia connected with NW Laurentia, but detailed studies on the Proterozoic crustal evolution and tectonic regime of NE Australia are still needed in order to test such reconstructions and to better understand the tectonic processes involved.

In NE Australia, Proterozoic rocks outcrop in two main inliers (the Mt. Isa and Georgetown inliers). The Mt. Isa Inlier is characterised by a protracted tectonic history consisting of two orogenic events (the Barramundi Orogeny, 1.87 - 1.84 Ga, and the Isan Orogeny, 1.6 - 1.52 Ga) associated with varying grades of metamorphism. East of the Mt. Isa Inlier, the Georgetown Inlier consists of sediments deposited simultaneously with that in the Mt. Isa Inlier and underwent orogenesis at ca. 1.6 Ga (the Jana Orogeny). The ca. 1.6 Ga Proterozoic orogenesis in NE Australia has been correlated with the Racklan Orogeny in NW Canada (Laurentia). However, whilst the orogenesis in Australia occurred over a period of ~60 Ma years, the Racklan Orogeny was short lived in comparison.

Some thermochronological work have previously been conducted in NE Australia. For the Mt Isa Inlier, mica K-Ar measurements [1] on granites yielded a cluster age of 1450-1400 Ma, which has been interpreted as representing a “metamorphic discontinuity”. More recent ⁴⁰Ar/³⁹Ar studies [2, 3] revealed a regional thermal cooling after magmatism during 1440-1390 Ma, and a reheating thermal event by dyke intrusions at 1260-1000 Ma. However, no older metamorphic record has been recognised by such analyses in Mt Isa. For the Georgetown Inlier, five ⁴⁰Ar/³⁹Ar analyses yielded Palaeozoic ages only. Therefore, a more systematic and precise thermochronological investigation remain to be done in order to delineate distinct Proterozoic tectonic events.

In this study, 26 samples, including granites and metamorphic rocks (e.g. amphibolite, migmatite, biotite gneiss, mica schist and metabasalt) have been collected along a W-E corridor across the Mt Isa and Georgetown Inliers. For ⁴⁰Ar/³⁹Ar analysis, multiple samples of hornblende (13), biotite (7) and muscovite (6) grains have been picked and sent for irradiation. We will utilise high-temperature thermochronology methods which offer a range of closure temperatures (from 300 to 700 °C), to reconstruct the uplift and exhumation history of the inliers, hopefully covering both syn- and post-orogenic events. The expected results will provide new insights into the assembly and breakup processes of the supercontinent Nuna, and the tectonic evolution of NE Australia in the Paleoproterozoic.

REFERENCE

- [1] Richards, J.R. et al. 1963. Potassium - argon ages on micas from the Precambrian region of northwestern Queensland. *Journal of the Geological Society of Australia*, 10, 299-312.
- [2] Spikings, R.A. et al. 2001. Post- orogenic (<1500 Ma) thermal history of the Proterozoic Eastern Fold Belt, Mount Isa Inlier, Australia. *Precambrian Research*, 109, 103-144.
- [3] Spikings, R.A. et al. 2002. Post-orogenic (<1500 Ma) thermal history of the Palaeo-Mesoproterozoic, Mt Isa Province, NE Australia. *Tectonophysics*, 349, 327-365.

Decoding Earth's rhythm: Modulation of supercontinent cycles by longer superocean cycles

Z.X. LI¹, R.N. MITCHELL¹, C.J. SPENCER¹, R. ERNST², S. PISAREVSKY¹ AND J.B. MURPHY^{1,3}

¹Earth Dynamics Research Group, ARC Centre of Excellence for Core to Crust Fluid Systems (CCFS), The Institute for Geoscience Research (TIGeR), Department of Applied Geology, Curtin University, GPO Box U1987, WA 6845, Australia (Z.Li@exchange.curtin.edu.au)

²Department of Earth Sciences, Carleton University, Ottawa, K1S 5B6 Canada

³Department of Earth Sciences, P.O. Box 5000, St. Francis Xavier University, Antigonish, N.S. B2G 2W5

The ca. 600 Ma supercontinent cycle is commonly considered the longest cycle of the Earth system. However, global zircon Hf isotopic signatures, seawater Sr isotope ratios, and occurrences of certain mineral deposits, suggest the existence of a cycle twice the duration of the supercontinent cycle. Here we demonstrate that the superocean surrounding supercontinent, along with the circum-supercontinent subduction girdle, survive every second supercontinent cycle since 2 Ga, as supported by global paleogeographic history and time variation of passive margin and orogenic records that exhibit two periodic signals at 500-700 and 1000-1500 million years. We propose that supercontinents assemble alternately through dominantly extraversion (the previous supercontinent turned inside-out through the destruction of the Panthalassa-type superocean) after a more complete breakup, and dominantly introversion (survival of the superocean) after an incomplete breakup of the previous supercontinent, giving rise to the two harmonic supercycles. Coexistence of the two supercycles may reflect an oscillatory feedback system between supercontinent assembly tectonics and mantle thermal state and structure.

FIB-SEM study of a silicate melt inclusion in upper mantle lherzolite

N. LIPTAI^{1,2}, M. BERKESI², L.E. ARADI², L. PATKÓ², S.Y. O'REILLY¹, W.L. GRIFFIN¹ AND C. SZABÓ²

¹Australian Research Council Centre of Excellence for Core to Crust Fluid Systems (CCFS) and GEMOC, Department of Earth and Planetary Sciences, Macquarie University, Sydney, NSW 2109, Australia (nora.liptai@hdr.mq.edu.au)

²Lithosphere Fluid Research Laboratory, Department of Petrology and Geochemistry, Institute of Geography and Earth Sciences, Eötvös University, Budapest, 1117, Hungary

The application of focused ion beam (FIB) coupled scanning electron microscope (SEM) has recently become a valuable tool in studying very small, μm -scale, geological samples such as silicate melt inclusions (SMIs) hosted in mineral constituents of mantle rocks. The analysis of the modal and geochemical composition of these inclusions can provide insight into the properties of melts percolating in the upper mantle and reacting with the peridotite wall-rock resulting in a variety of metasomatic processes.

In the Carpathian-Pannonian region, upper mantle peridotite xenoliths are brought to the surface by young alkali basalts at five localities, one of which is the Nógrád-Gömör Volcanic Field in the northern edge of the Pannonian Basin. The peridotite xenoliths of this locality can be divided into a lherzolitic and a wehrlitic series, the latter considered to be the product of metasomatic reaction between wall-rock and a mafic silicate melt [1]. While it has recently been found that part of the lherzolites were also affected by this metasomatic event [2], SMIs related to this reaction have never been previously studied due to their scarcity in lherzolites.

One of the metasomatised xenoliths however, contains clinopyroxenes hosting primary, partly crystallised, multiphase SMIs, which are 10-20 μm in diameter with negative crystal shape. Several of these SMIs were analysed using different techniques, including phase determination and mapping with Raman spectroscopy, and

slicing the inclusions using FIB-SEM to acquire a 3D-map of the structure and volume proportion of the constituent phases. Besides the dominant glass phase, crystallised daughter minerals, such as amphibole, mica, apatite, spinel and sulfide appear as well (Fig. 1).

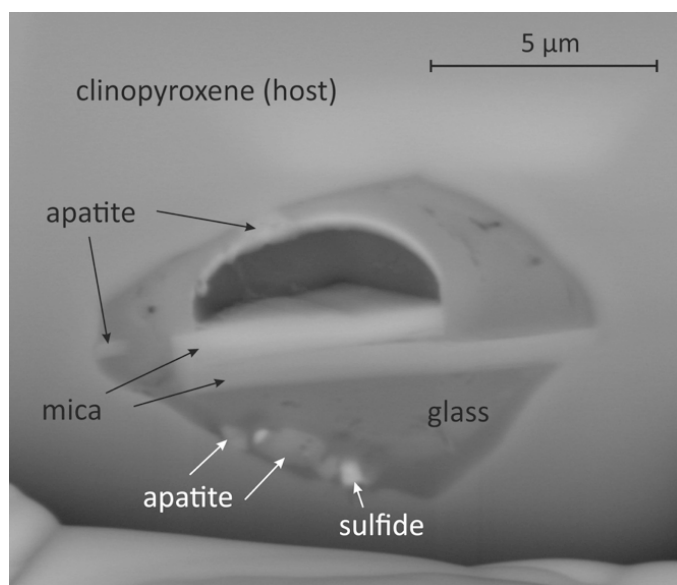


Figure 1. Back-scattered electron image of an SMI slice with the observable daughter phases.

All SMIs contain a bubble, composed mainly of CO_2 , occasionally with small sulfate crystals (anhydrite, barite) or mica at the contact of the bubble and the glass, indicating their possible reaction. Major element composition analyses of the daughter phases revealed the SMIs to be rich in Fe and Ti, which is a characteristic feature of the metasomatising melt related to wehrlite formation [1]. Therefore, it is inferred that the

inclusions were trapped from a basaltic melt of the same intraplate origin, which is also responsible for the metasomatic signature in the mineral constituents of the lherzolite.

REFERENCES

- [1] Patkó, L. et al. 2013. Wehrlitization processes within the upper mantle beneath the Northern Pannonian Basin (Hungary). *Mineralogical Magazine*, 77, 1934.
- [2] Liptai, N. et al. 2017. Multiple metasomatism beneath the Nógrád-Gömör Volcanic Field (Northern Pannonian Basin) revealed by upper mantle peridotite xenoliths. *Journal of Petrology*, 58, 1107-1144.

Deformation and tectonic evolution of the upper mantle in the northern Pannonian Basin

N. LIPTAI^{1,2}, K. HIDAS³, L. PATKÓ², S.Y. O'REILLY¹, W.L. GRIFFIN¹, N.J. PEARSON¹ AND C. SZABÓ²

¹Australian Research Council Centre of Excellence for Core to Crust Fluid Systems (CCFS) and GEMOC, Department of Earth and Planetary Sciences, Macquarie University, Sydney, NSW 2109, Australia (nora.liptai@hdr.mq.edu.au)

²Lithosphere Fluid Research Lab, Institute of Geography and Earth Sciences, Eötvös University, 1/C Pázmány Péter sétány, Budapest, 1117, Hungary

³Institutio Andaluz de Ciencias de la Tierra, CSIC & UGR, Avenida de las Palmeras 4, E-18100 Armilla (Granada), Spain

The Carpathian-Pannonian region is a young back-arc basin with a complex Neogene tectonic evolution, mainly characterised by extension and asthenosphere uplift during the Miocene associated with subduction and slab rollback in the Eastern Carpathians. Post-extensional alkali basalts have sampled the upper mantle at five occurrences. One of these is the Nógrád-Gömör Volcanic Field (NGVF), located in the northernmost part of the Pannonian Basin. This study is the first to explore the deformation history and seismic characteristics inferred from mantle-derived xenoliths for comparison with results from other parts of the Carpathian-Pannonian region.

A representative set of approximately 50 xenoliths has been analysed using electron backscatter diffraction to characterise their microstructural properties and crystal preferred orientations (CPO) of their major minerals, olivine and pyroxenes. Olivine textures include all three of the most abundant CPO-types, although orthorhombic and [010]-fibre are dominant over [100]-fibre symmetries. The CPO-types show no clear correlation with equilibrium temperatures, grain size or fabric strength, suggesting a mixed effect of different deformation regimes. Coarser grained xenoliths generally have higher equilibrium temperatures and J-indices (an indicator for the strength of fabric) compared with samples of smaller grain size. This suggests that the former group represents a deeper mantle domain with stronger preferred orientation, whereas the latter represents a shallower region characterised by more dispersed CPOs indicating dynamic recrystallisation. In most of the xenoliths, grain growth of olivine, where not pinned by other phases, as well as a lower degree of intragranular deformation (e.g. subgrain boundaries) in larger grains, suggests the effect of post-kinematic annealing. This annealing is inferred to result from mafic melts percolating through the upper mantle of the NGVF and causing multiple different metasomatic events [1].

Seismic anisotropy calculations reveal a maximum of 5% S-wave anisotropy under the NGVF in a direction which falls in the plane of foliation, but is perpendicular to the lineation. Geophysical data show NW-SE directions for the fast-polarised S-wave in the vicinity of the NGVF, consistent with the recent compressional tectonic regime in the Carpathian-Pannonian region. Calculations for the thickness of the anisotropic layer (minimum 125 km; method of [2]) suggests a significant contribution from the sublithospheric mantle.

REFERENCES

- [1] Liptai, N. et al. 2017. Multiple metasomatism beneath the Nógrád-Gömör Volcanic Field (Northern Pannonian Basin) revealed by upper mantle peridotite xenoliths. *Journal of Petrology*, 58, 1107-1144.
- [2] Baptiste, V. and Tommasi, A. 2014. Petrophysical constraints on the seismic properties of the Kaapvaal craton mantle root. *Solid Earth Discuss.* 5, 963-1005.

Palaeomagnetism of the Boonadgin Dyke Suite, Yilgarn Craton: Implications for the assembly of the Western Australian Craton and possible connection with India

Y. LIU, Z.X. LI, S.A. PISAREVSKY, U. KIRSCHER, R. MITCHELL AND J.C. STARK

Earth Dynamics Research Group, ARC Centre of Excellence for Core to Crust Fluid Systems (CCFS) and The Institute for Geoscience Research (TIGeR), Department of Applied Geology, Curtin University, GPO Box U1987, WA 6845, Australia (yebo.liu@postgrad.curtin.edu.au)

We report a high-quality palaeopole from the recently identified ca. 1.89 Ga Boonadgin dyke swarm [1] in the Yilgarn Craton, Western Australia. This pole is based on ten dykes and its primary nature is supported by a positive baked contact test and a positive reversal test. The Boonadgin pole reveals that the Yilgarn Craton was near the equator at ca. 1.89 Ga. Meanwhile, a paleopole from the ca. 1.88 Ga Dharwar dykes of South India, supported by a positive baked-contact test [2], puts India at a similar paleolatitude. The Boonadgin dyke swarm can be interpreted to represent an arm of a radiating dyke swarm that shared the same plume centre with coeval mafic dykes in the Dharwar and Bastar cratons of southern India. We therefore propose that the West Australian Craton (WAC, consisting of the Yilgarn and Pilbara cratons) and South Indian Block (SIB, consisting of the Dharwar, Bastar and Singhbhum cratons) were connected ca. 1.89 Ga (Fig. 1).

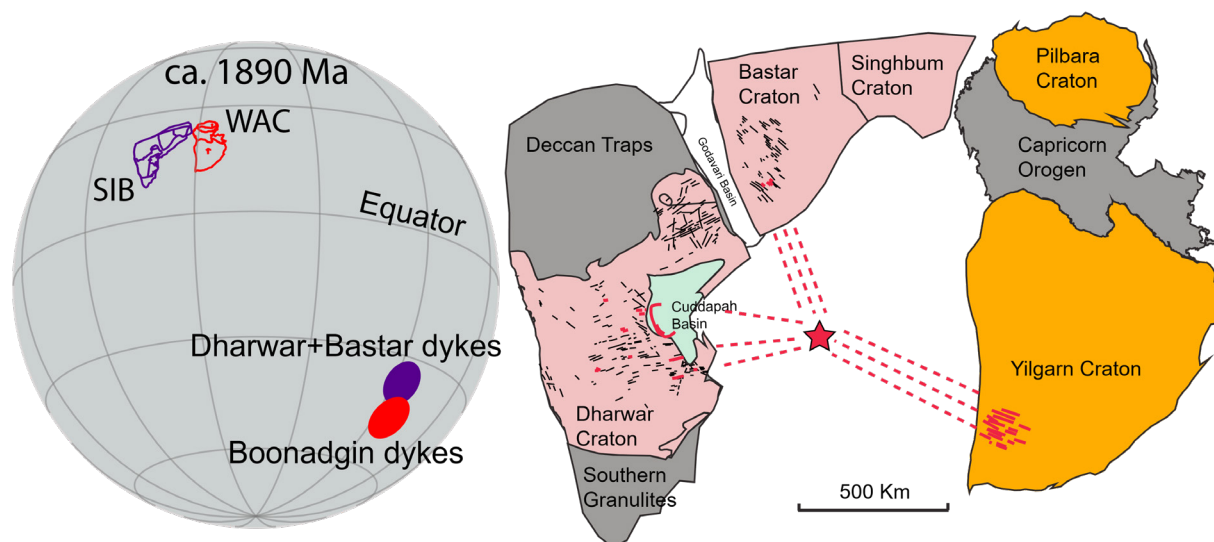


Figure 1. Possible configuration of the WAC and SIB at ca. 1.89 Ga reconstructed in SIB coordinates. Coeval paleopoles are plotted on the left-hand side and colour coded with the respective cratons. More detailed reconstructions are shown on the right side. Red star denotes possible location of a mantle plume.

Paleomagnetic investigations yielded a series of reliable palaeopoles from the pervasive ca. 1.89 Ga magmatism found on most Precambrian cratons. Based on available high-quality poles, we propose the most up-to-date ca. 1.89 Ga palaeogeography [3] of all cratons, in which the WAC is placed northwest of proto-Laurentia during the assembly of the supercontinent Nuna.

REFERENCES

- [1] Stark, J.C. et al. 2017. Newly identified 1.89 Ga mafic dyke suite in the Archean Yilgarn Craton, Western Australia suggests a connection with India. *Precambrian Research*, submitted.
- [2] Belica, M.E. et al. 2014. Paleoproterozoic mafic dyke swarms from the Dharwar craton; paleomagnetic poles for India from 2.37 to 1.88 Ga and rethinking the Columbia supercontinent. *Precambrian Research*, 244, 100-122.
- [3] Liu, Y. et al. 2017. Palaeomagnetism of the 1.89 Ga Boonadgin dykes of the Yilgarn Craton: Possible connection with India. *Precambrian Research*, submitted.

The effect of C-O-H fluids on partial melting of eclogite and lherzolite under reducing conditions

Z. LIU^{1,2}, A. ROHRBACH¹, S. KLIMME¹ AND S. FOLEY²

¹Institut für Mineralogie, Westfälische Wilhelms-Universität Münster, Münster, Germany (zairong.liu@hdr.mq.edu.au)

²Australian Research Council Centre of Excellence for Core to Crust Fluid Systems (CCFS) and GEMOC, Department of Earth and Planetary Sciences, Macquarie University, Sydney, NSW 2109, Australia

C-O-H fluids are well known to cause partial melting of eclogite and peridotite, producing melts at much lower temperatures than in dry conditions, and thus causing heterogeneities in the Earth's mantle [1]. At high pressure and low oxygen fugacity conditions, C-O-H fluids consist mostly of $\text{H}_2\text{O} + \text{CH}_4$ [2]. However, under these reducing conditions, the effect of the C-O-H fluids on the melting process of eclogite and lherzolite is not well constrained.

In this work, we performed high pressure experiments to investigate how C-O-H fluid would affect the melting of eclogite and lherzolite at different redox conditions. The experiments at 2 GPa and 6 GPa were performed with piston cylinder and multi-anvil apparatus, respectively, over a temperature range between 900 – 1500 °C. Under oxidising conditions, both eclogite and lherzolite starting compositions contained about 5 wt% H_2O ; while at reducing conditions (with an oxygen fugacity of around IW-0.4) the identical compositions contained 5 wt% COH fluids (1 wt% H_2O and 4 wt% CH_4).

The solidus temperature is bracketed by subsolidus experiments with no melt present, and experiments containing small amounts of melt. The mineral and melt phases are detected with electron microprobe analysis (EMPA) in Münster University. The result show that:

- (1) under reducing conditions, the solidus temperature of eclogite with C-O-H fluids is about 200 °C lower than that of lherzolite with the same C-O-H fluids;
- (2) Solidus temperatures under reducing conditions for both eclogite with C-O-H fluids and lherzolite with C-O-H fluids are 100 °C higher than those for the same system with H_2O alone in the more oxidising experiments;
- (3) For eclogite with C-O-H fluids under reducing conditions, the temperature of garnet out is lower than clinopyroxene.
- (4) For both eclogite with 5 wt% H_2O and eclogite with 5 wt% COH fluids, as the temperature increases, SiO_2 content in the melt increases at first and then decreases after the appearance of orthopyroxene;
- (5) For lherzolite with C-O-H fluids, at 6 GPa, a remarkable amount of graphite occurs at high temperature. It is not clarified yet whether the appearance of graphite is related to Fe-loss due to the use of Pt capsule or not.

Further comprehensive analysis is continuing, including characterisation of the melt compositions. The results will be applied to predict the effect of reducing redox conditions on the partial melting of eclogite and lherzolite in the presence of C-O-H fluids.

REFERENCES

- [1] Litasov, K.D. et al. 2014. Melting and subsolidus phase relations in peridotite and eclogite systems with reduced C-O-H fluid at 3-16 GPa. *Earth and Planetary Science Letters*, 391, 87-99.
- [2] Frost, D.J. and C.A. McCammon. 2008. The redox state of Earth's mantle. *Annual Review of Earth and Planetary Sciences*, 36, 389-420.

Garnet websterite xenoliths from Western Victoria: Tracing a deep lithospheric event

J.G. LU^{1,2}, W.L. GRIFFIN¹, S.Y. O'REILLY¹, Q. XIONG^{1,2}, J.X. HUANG¹ AND J.P. ZHENG²

¹Australian Research Council Centre of Excellence for Core to Crust Fluid Systems (CCFS) and GEMOC, Department of Earth and Planetary Sciences, Macquarie University, Sydney, NSW 2109, Australia (jianggu.lu@mq.edu.au)

²State Key Laboratory of Geological Processes and Mineral Resources, School of Earth Sciences, China University of Geosciences, Wuhan 430074, China

Pyroxenite and its associated melts can act as metasomatic agents to modify the lithospheric mantle and provide important information about mantle heterogeneity. New major- and trace-element and Sr-Nd-Hf isotopic compositions of minerals from garnet websterites captured by basanite tuffs in Bullenmerri and Gnotuk maars, southeastern Australia, were combined with the detailed petrographic study [1] to constrain their sources and genesis, and the dynamic evolution of the upper mantle.

Most garnet websterites show high contents of MgO and Cr₂O₃, relatively flat LREE patterns ((La/Nd)_n=0.77-2.22) and OIB-like Sr-Nd-Hf isotopic compositions (⁸⁷Sr/⁸⁶Sr=0.70386-0.70657; εNd=-0.60-4.37; εHf=0.91-17.9) in whole-rock samples and clinopyroxene. Some of the samples show subduction-related signatures with strong enrichment in LILE and LREE and negative anomalies in HFSE, as well as high ⁸⁷Sr/⁸⁶Sr (up to 0.708) and decoupled Hf-Nd (εNd=-3.94; εHf=9.42) isotopic compositions. The data suggest that the garnet pyroxenites record partial melting of the convective mantle wedge and represent the crystallisation products of the earliest recognised episodes of infiltration by mafic melts into the lithospheric mantle in this region. The Hf model ages and Sm-Nd mineral isochrons suggest that these pyroxenites probably formed in a Paleozoic accretionary orogen and re-equilibrated at ~40 Ma before being entrained by the host basanite.

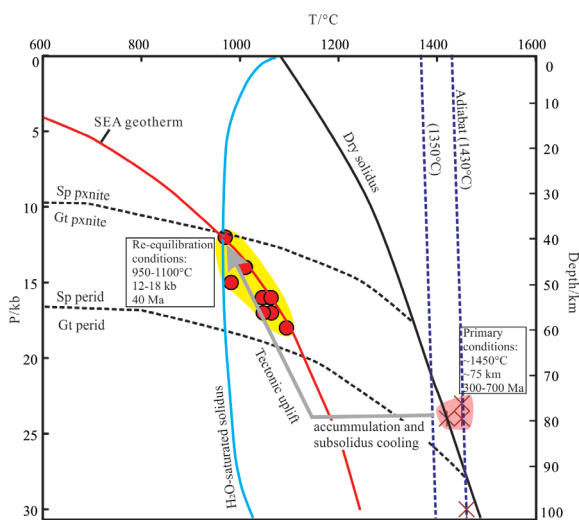


Figure 1. *P-T-t* path showing the likely formation conditions of cumulates in a convective mantle wedge (pink area) and the final re-equilibration of garnet websterites (yellow area) from Lakes Bullenmerri and Gnotuk.

The combined evidence reveals a two-step process (Fig. 1). During Paleozoic time, continued subduction of the proto-Pacific plate triggered melting of the convective mantle wedge beneath southeastern Australia and generated hydrous tholeiitic melts that crystallised clinopyroxene-dominated pyroxenites at ~1420-1450 °C and ~75 km. The pyroxenites then cooled to the ambient geotherm, as shown by extensive exsolution and recrystallisation of garnet and orthopyroxene (± ilmenite) from clinopyroxene megacrysts. They were then uplifted to depths of 40-60 km and equilibrated at ~970-1100 °C at

~40 Ma during back-arc lithospheric extension. The timing of these mantle events coincides with tectonic events recorded in the overlying crust.

REFERENCES

- [1] Lu, J.G. et al. 2017. The crust-mantle and lithosphere-asthenosphere boundaries: Insights from xenoliths, orogenic deep sections, and geophysical studies. Geological Society of America Special Publication, 526, 27-48.

Porphyry Cu fertility in the Tibetan Plateau

Y.-J. LU^{1,2}, Z.-Q. HOU³, Z.-M. YANG³, L.A. PARRA-AVILA², M. FIORENTINI², T.C. McCUAIG^{2,4} AND R.R. LOUCKS²

¹Geological Survey of Western Australia, 100 Plain Street, East Perth, WA 6004, Australia (yongjun.lu@dmirs.wa.gov.au)

²Australian Research Council Centre of Excellence for Core to Crust Fluid Systems (CCFS), The University of Western Australia, 35 Stirling Highway, Crawley, WA 6009, Australia

³Institute of Geology, Chinese Academy of Geological Sciences, Beijing 100037, PR China

⁴BHP, 125 St Georges Terrace, Perth WA 6000 Australia

Cenozoic porphyry Cu deposits in the Tibetan Plateau are the archetypal porphyry systems developed in continental collision zones. Understanding the temporal and spatial distribution of these deposits will help unravel the genesis of porphyry deposits in collision zones and exploration targeting of porphyry deposits in similar orogenic belts.

Zircon Lu-Hf isotopic mapping results using 652 zircon samples in the Tibetan Plateau are presented in Figure 1. They demonstrate that the majority of porphyry Cu deposits are associated with isotopically juvenile domains along the terrane-bounding Indus-Yarlung and Jinsha suture zones (Fig. 1). Such isotopic mapping can narrow the search space from over 2500 km scale to ~500 km scale.

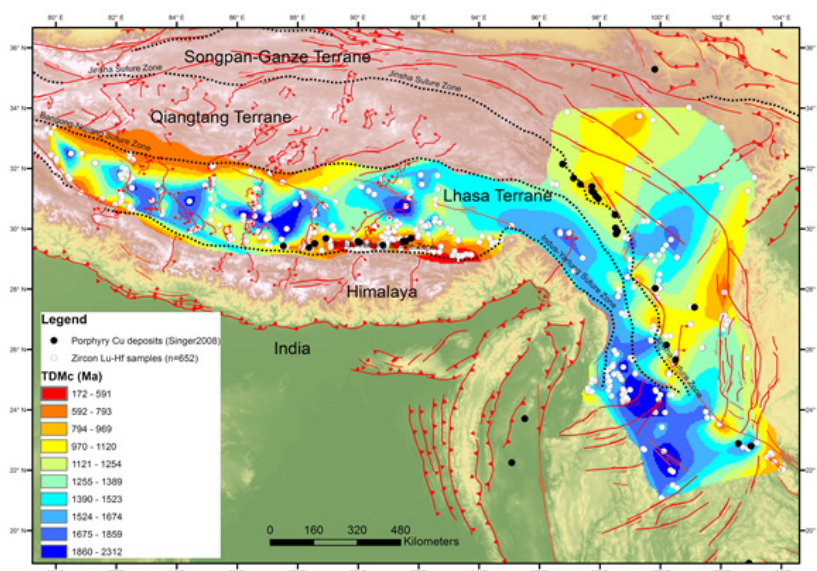


Figure 1. Contour map of zircon two-stage depleted mantle model ages (TDMc) for granitoid and felsic volcanic rocks in the Tibetan Plateau.

Whole-rock geochemical mapping using c. 1200 samples across the Lhasa Terrane show that all porphyry Cu deposits occur in domains of high $10000 \cdot (\text{Eu}/\text{Eu}^*)/\text{Y}$ (>800). Thus, the $(\text{Eu}/\text{Eu}^*)/\text{Y}$ ratio is the best whole-rock fertility indicator, and is interpreted to indicate extremely high magmatic water content which induces early and prolific hornblende fractionation and suppresses early plagioclase crystallisation.

Zircon U-Pb and trace-element data were obtained from 66 igneous samples of Jurassic to Miocene age (181-11 Ma) in the eastern Gangdese belt. Both xenocrystic and magmatic zircons show systematic compositional evolution from Jurassic to Miocene. From c. 200 Ma to c. 55 Ma, zircon Eu/Eu^* (0.1-0.4), $10000 \cdot (\text{Eu}/\text{Eu}^*)/\text{Y}$ (0.1-10), and $(\text{Ce}/\text{Nd})/\text{Y}$ (0.001-0.05) ratios remain broadly similar. However, these zircon trace element ratios increase rapidly after c. 55 Ma and culminate at c. 13 Ma with Eu/Eu^* , $10000 \cdot (\text{Eu}/\text{Eu}^*)/\text{Y}$, and $(\text{Ce}/\text{Nd})/\text{Y}$ ratios up to 1, 70, and 2, respectively. Similar temporal trends are also observed for whole-rock Sr/Y , La/Yb , and $(\text{Eu}/\text{Eu}^*)/\text{Y}$ ratios, although whole-rock Eu/Eu^* ratios appear to be similar throughout the Jurassic-Miocene period. In addition, Cretaceous samples show juvenile Hf-O isotopic signatures, whereas Eocene-Miocene intrusions show increasing zircon $\delta^{18}\text{O}$ values and decreasing epsilon Hf values, suggesting increasing amounts of supracrustal materials were incorporated in magma genesis after c. 55 Ma.

Exploration is a scale reduction process. Zircon Lu-Hf isotopic mapping is powerful in identifying juvenile crust domains which are preferable for porphyry Cu formation. All porphyry Cu deposits in the Lhasa Terrane are characterised by distinctly high whole-rock $10000 \cdot (\text{Eu}/\text{Eu}^*)/\text{Y}$ ratios (>800), which is the best fertility indicator. The combined isotopic mapping and whole-rock $10\,000 \cdot (\text{Eu}/\text{Eu}^*)/\text{Y}$ ratio mapping can help focus exploration on prospective areas.

Zircon composition as a fertility indicator of Archean granites

Y.-J. LU^{1,2} AND H. SMITHIES¹

¹Geological Survey of Western Australia, 100 Plain Street, East Perth, WA 6004, Australia (yongjun.lu@dmirs.wa.gov.au)

²Australian Research Council Centre of Excellence for Core to Crust Fluid Systems (CCFS), The University of Western Australia, 35 Stirling Highway, Crawley, WA 6009, Australia (yongjun.lu@uwa.edu.au)

Porphyry Cu deposits are major sources of Cu and Mo. They range in age from Archean to modern, but most are Jurassic and younger. Porphyry deposits in Precambrian terranes are rare, and the reasons for this remain unclear. Nevertheless, several porphyry-type deposits occur in the Abitibi and Opatoca greenstone belts in the Superior Craton, suggesting that the potential for porphyry deposits in Archean cratons has not been fully recognised.

Lu et al. (2016) [1] proposed that zircon compositions can be an excellent pathfinder for porphyry Cu deposits. The best fertility indicators are zircon Eu/Eu^* (>0.3) and $10,000 \cdot (\text{Eu}/\text{Eu}^*)/\text{Y}$ (>1) ratios, whereas $(\text{Ce}/\text{Nd})/\text{Y}$ (>0.01) and Dy/Yb (<0.3) ratios are moderately useful. These distinct zircon trace element ratios are interpreted to reflect a specific differentiation trend, e.g. suppression of plagioclase fractionation and enhanced early amphibole fractionation as a result of high magmatic water content, which is a prerequisite for magmatic-hydrothermal (porphyry) ore formation.

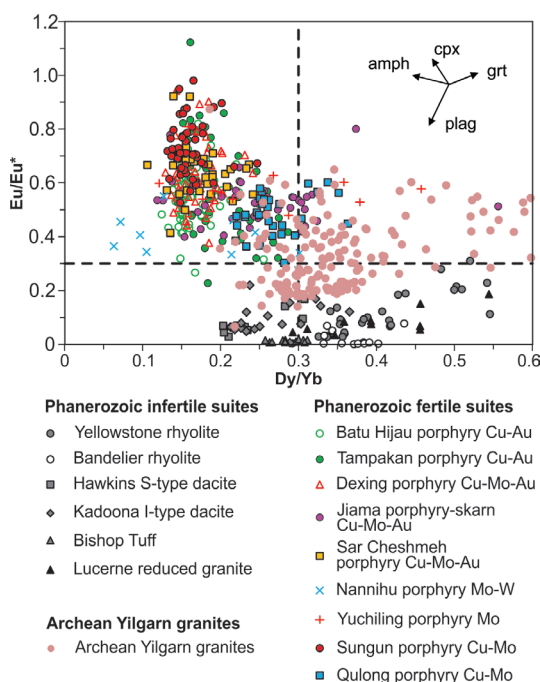


Figure 1. Eu/Eu^* vs Dy/Yb plot for zircons from Archean Yilgarn granites and Phanerozoic infertile and fertile suites.

We test the above zircon fertility indicators in Archean granites across the Yilgarn Craton in Western Australia. The studied granites range in age from c. 2930 Ma to c. 2640 Ma, and from high-Al TTG to potassic granite. These Archean granites lie transitionally between Phanerozoic infertile and fertile granite suites, as defined in Lu et al. (2016), on Eu/Eu^* vs $(\text{Ce}/\text{Nd})/\text{Y}$ and $(\text{Eu}/\text{Eu}^*)/\text{Y}$ vs $(\text{Ce}/\text{Nd})/\text{Y}$ plots. On a Eu/Eu^* vs Dy/Yb plot, Yilgarn Archean granites have distinctly higher Dy/Yb ratios (>0.3), and define a positive trend, which contrast with the negative trend for Phanerozoic fertile suites (Fig. 1). This indicates that Archean granite compositional evolution was strongly influenced by garnet (source retention) whereas Phanerozoic fertile suites are strongly influenced by amphibole fractionation. This in turn suggests that Archean granite magmas are typically relatively dry compared to Phanerozoic fertile suites, and is consistent with the absence of amphibole phenocrysts in most granites in the Yilgarn Craton.

The systematic difference in zircon chemistry between Archean granites and Phanerozoic fertile and infertile suites suggests that different processes were involved in forming Archean granites. We argue that Archean granites were mainly formed through lower- or infracrustal partial melting of mafic crust in the garnet stability field, whereas Phanerozoic fertile suites were formed by intracrustal amphibole-dominated fractionation of mafic magmas. Granites formed by the former process have lower potential for porphyry Cu mineralisation due to insufficient water and the lack of build-up of copper and sulfur in the melt. Further data is needed from mineralised Archean granites to determine whether they have different genesis from those unmineralised Archean granites.

REFERENCES

[1] Lu, Y.J. et al. 2016. Zircon compositions as a pathfinder for porphyry Cu \pm Mo \pm Au deposits. Society of Economic Geologists Special Publication No. 19, 329-347.

Imaging the SW Yilgarn basement through granite geochemistry

R.H. SMITHIES¹, Y.-J. LU^{1,2}, K. GESSNER^{1,2}, D.C. CHAMPION³ AND M.T.D. WINGATE¹

¹Geological Survey of Western Australia, 100 Plain Street, East Perth, WA 6004, Australia

²ARC Centre of Excellence for Core to Crust Fluid Systems (CCFS) (yongjun.lu@dmirs.wa.gov.au)

³Geoscience Australia, GPO Box 378, Canberra, ACT 2601, Australia

Compared to other parts of the Yilgarn Craton, the Archean geological evolution of the South West Terrane is poorly understood. We have compiled a new dataset of ~250 new whole-rock geochemical analyses of granitic rocks to better constrain the geological evolution of this region. Of particular interest is whether these data provide insight into the origins of a lower-crustal density anomaly that follows the southern and western margins of the South West Terrane (Fig. 1) and has been attributed to remnant eclogite residuum from Archean crustal differentiation. In addition, we aim to test the (craton-wide) assumption that basement terranes (i.e. granite source regions) parallel the late north-northwest structural trend of the Yilgarn Craton.

Extraction of felsic magma, leaving a dense crustal residuum of garnet-rich, or eclogitic mineralogy imparts distinctively high Sr/Y, La/Yb, Nb/Ta characteristics on those magmas. In our dataset, variation in such melting-pressure proxies shows no spatial relationship with the high density (gravity) anomaly identified in the lower crust of the southern and western parts of the region. Therefore, this anomaly does not appear to be directly related to Archean felsic magmatism.

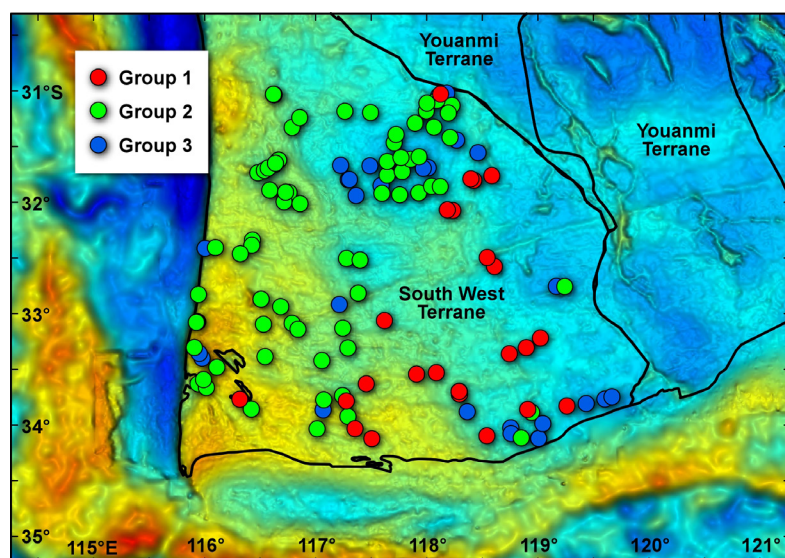


Figure 1. Gravity image of the southwestern part of the Yilgarn Craton showing the distribution of new granite samples.

Rather, felsic magmas showing evidence of garnet-present, and potentially rutile-present, melting occupy only the southeastern part of the region. We have simplified the dataset into three groups. Group 1 comprises granitic rocks of dominantly high-Ca composition, with low K_2O/Na_2O (avg. 0.6) high Sr (388 ppm), Sr/Y (avg. 72), La/Yb (avg. 86) and Nb/Ta (avg. 22), reflecting true high Al-TTG derived through high-pressure

melting of a sodic, mafic source. Group 2 comprises high- and low-Ca granitic rocks, with a wide compositional range, but generally higher K_2O/Na_2O (avg. 1.0) and lower Sr (241 ppm), Sr/Y (avg. 16), La/Yb (avg. 44) and Nb/Ta (avg. 11), reflecting lower-pressure melting of a less homogeneous source. Group 3 also comprises high- and low-Ca granitic rocks (dominantly low-Ca). Their compositions are mainly similar to Group 2, but lie within the upper range of Group 2 in terms of K_2O/Na_2O (avg. 1.16) and La/Yb (avg. 71), within the lower range in terms of Sr (227 ppm) and Sr/Y (avg. 14), but have distinctly higher Nb/Ta (avg. 25) and typically higher Dy/Yb, perhaps reflecting melting, over a range of pressures, of an inhomogeneous, hornblende-rich source that locally included high Al-TTG components from which high La/Yb and Nb/Ta signals were inherited.

The geographical distribution of these three groups defines northeast trends that truncate the north-northwest trends that characterise the more obvious structural trend of the Yilgarn Craton, including terrane boundaries. We suggest that these trends in granite composition reflect similar trends in basement source domains, i.e. northeast-trending belts of either compositionally distinct crust or of crust undergoing melting at specific conditions, or both. Preliminary data further suggest that these northeast basement trends may not be confined to the South West Terrane, but may extend across the entire craton. The idea that the Yilgarn Craton evolved through processes leading to northeast domainal trends that were later overprinted by (intra-cratonic?) north-northwest trends deserves further consideration.

Multi-observable probabilistic inversions for the physical state and water content of the continental lithosphere

M.C. MANASSERO¹, J.C. AFONSO¹, F.I. ZYSERMAN², M. ROSAS-CARBAJAL³, S. THIEL⁴ AND S.M. CLARK⁵

¹Australian Research Council Centre of Excellence for Core to Crust Fluid Systems (CCFS) and GEMOC, Department of Earth and Planetary Sciences, Macquarie University, Sydney, NSW 2109, Australia (constanza.manassero@hdr.mq.edu.au, juan.afonso@mq.edu.au)

²CONICET - Facultad de Ciencias Astronomicas y Geofisicas, Universidad Nacional de La Plata, Argentina (zyserman@fcaglp.unlp.edu.ar)

³Institut de Physique du Globe de Paris, Sorbonne Paris Cité, CNRS UMR-7154, Université Paris Diderot, Paris CEDEX 05, France (rosas@ipgp.fr)

⁴University of Adelaide, South Australia, Australia (Stephan.Thiel@sa.gov.au)

⁵Department of Earth and Planetary Sciences, Macquarie University, North Ryde, NSW 2109, Australia (simon.clark@mq.edu.au)

Multi-observable probabilistic inversion [e.g. 1, 2] for the compositional and thermal structure of the lithosphere is providing a new picture of the complex physicochemical interactions between plates and the underlying convecting upper mantle. Of particular importance is the inversion of magnetotelluric (MT) data, as it provides complementary information on the temperature and water content that other observables cannot constrain. MT holds, therefore, great potential for understanding and imaging the complex fluid-rock interactions responsible for mineralisation events due to its sensitivity to water and other volatiles.

In order to implement MT data into multi-observable probabilistic inversions for 3D imaging of deep thermochemical anomalies and fluid pathways in the Earth, we first need to solve the problem of computational efficiency in solving Maxwell's equations in 3D. For this, we will combine state-of-the-art probabilistic inversion methods with advanced algebraic decomposition techniques such as reduced basis [3] to obtain fast, yet accurate, solutions to the 3D MT problem. Firstly, we have compared the results and efficiency of different forward MT codes, being the finite element (FE) code max3d [4] our preferred MT forward solver. We have also modified the FE processing of max3d in order to make it compatible with reduced basis methods.

Further work includes the resolution of the adjoint problem in MT and application of reduced basis methods with the aim of constructing the first conceptual and numerical platform capable of jointly inverting 3D MT, seismic, and gravity data in a probabilistic manner.

REFERENCES

- [1] Afonso, J.C. et.al. 2013. 3-D multi-observable probabilistic inversion for the compositional and thermal structure of the lithosphere and upper mantle. II: General methodology and resolution analysis. *Journal of Geophysical Research*, 118, 1650-1676.
- [2] Afonso, J.C. 2013. *Journal of Geophysical Research*, 118, 2586-2617.
- [3] Quarteroni A. et al. 2011. Manzoni, Certified reduced basis approximation for parametrized PDE and applications. *Journal of Mathematics in Industry*, 1, 3. <https://doi.org/10.1186/2190-5983-1-3>.
- [4] Zyserman, F. and Santos, J. 2000. Parallel finite element algorithm with domain decomposition for three-dimensional magnetotelluric modelling. *Journal of Applied Geophysics*, 44, 337-352.

An Australian source for Pacific-Gondwanan zircons: Implications for the assembly of northeastern Gondwana

E.L. MARTIN¹, W.J. COLLINS¹ AND C.L. KIRKLAND²

¹Earth Dynamics Research Group, ARC Centre of Excellence for Core to Crust Fluid Systems (CCFS) and The Institute for Geoscience Research (TIGeR), Department of Applied Geology, Curtin University, Perth, WA 6845, Australia (erin.l.martin@postgrad.curtin.edu.au; william.collins@curtin.edu.au)

²Centre for Exploration Targeting-Curtin Node, ARC Centre of Excellence for Core to Crust Fluid Systems (CCFS) and The Institute for Geoscience Research (TIGeR), Department of Applied Geology, Curtin University, GPO Box U1987, Perth WA 6845, Australia (c.kirkland@curtin.edu.au)

Detrital zircons in Neoproterozoic-Paleozoic basins of the Pacific-Gondwana region contain a distinctive 700-500 Ma population conventionally considered to be derived from Antarctica. However, the 700-600 Ma age component of the population predates major peripheral orogenesis (Terra Australis orogen), which began at ca. 580 Ma, and the highly evolved $\epsilon\text{Hf}(t)$ -in-zircon values (to -40) require an Archean source, which is not proximal to the Terra Australis active margin. To assess the provenance of Pacific-Gondwanan zircons, we analysed zircons from granites of the Paterson orogen, then compared these with compiled zircon U-Pb and Lu-Hf data from the Terra Australis margin of Australia and Antarctica.

The late Neoproterozoic Paterson and Petermann orogens have traditionally been treated separately, yet are linked via the Anketell gravity ridge, and have coeval 600-530 deformation histories. We consider the Paterson-Petermann orogenic belt as a transcontinental system, with a length of >2000 km, and width of at least 500 km including ca. 560 Ma thrust systems of the King Leopold orogen. We argue that Lu-Hf zircon data from the Paterson-Petermann orogen, along with magmatism, metamorphism and regional deformation indicate that it was a continuous late Neoproterozoic magmatic belt associated with south-dipping subduction. Convergence

began at least by ca. 680 Ma, but terminated in the Paterson-Petermann orogen at 550-530 Ma when the North Australian Craton collided with Gondwana.

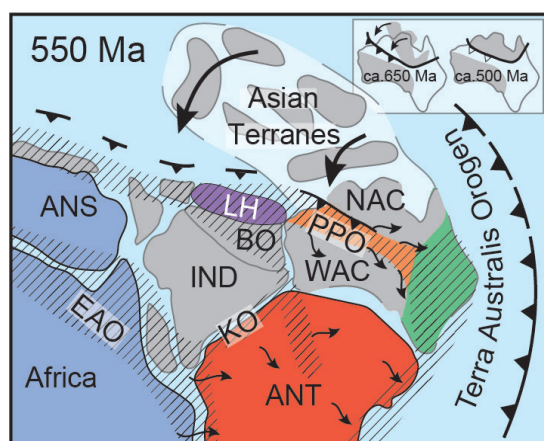


Figure 1. 550 Ma reconstruction of NE Gondwana.

Based on similar $\epsilon\text{Hf}(t)$ arrays defined by Neoproterozoic granites in Western Australia and detrital zircon populations from the surrounding basins, we suggest that Pacific-Gondwanan zircon grains were partially derived from the >2000-km-long, late Neoproterozoic Paterson-Petermann orogen, which sutured northern and southern Australia at 550-530 Ma. The rising Paterson-Petermann orogen distributed a vast swathe of sediment eastward into evolving early Cambrian backarc basins of the Tasmanides. Following

inversion of these Tasmanide basins during the ~500 Ma Delamerian-Ross orogen of Australia and Antarctica, detrital zircons were recycled into adjacent, outboard, basins.

We propose the North Australian Craton was a crustal block connected to now-dispersed southeast Asian terranes during the Neoproterozoic. The Himalayan-style Paterson-Petermann orogen was responsible for amalgamating Southeast Asian terranes into northeast Gondwana, thereby constraining the paleogeography of the northern Gondwanan margin at the Precambrian-Cambrian boundary. Remarkable isotopic similarity of zircon grains with the Lhasa terrane of Tibet suggests that the Paterson-Petermann orogen was the eastern sector of the developing circum-Gondwana subduction system from ca. 700 Ma (Fig. 1).

Isotopic record of the lawsonite-bearing HP-rocks from Port Macquarie (Australia)

L.A.J. MARTIN AND A. GALTIER

Australian Research Council Centre of Excellence for Core to Crust Fluid Systems (CCFS) and Centre for Microscopy, Characterisation and Analysis, The University of Western Australia (Laure.martin@uwa.edu.au)

The Rocky Beach Melange (RBM), located at Port Macquarie, is part of the New England Orogen, which shapes the east coast of Australia. The RBM is composed of heterogeneous tectonic blocks of variable size, embedded in a serpentinite matrix and recording HP-LT conditions [1]. The blocks are mostly composed of metabasites recording lawsonite-bearing blueschist and eclogite facies mineralogies. The aim of this study is to unravel the fluid-rock interactions recorded in these complex rocks using isotopic tracers (O and S) in pyrite and lawsonite.

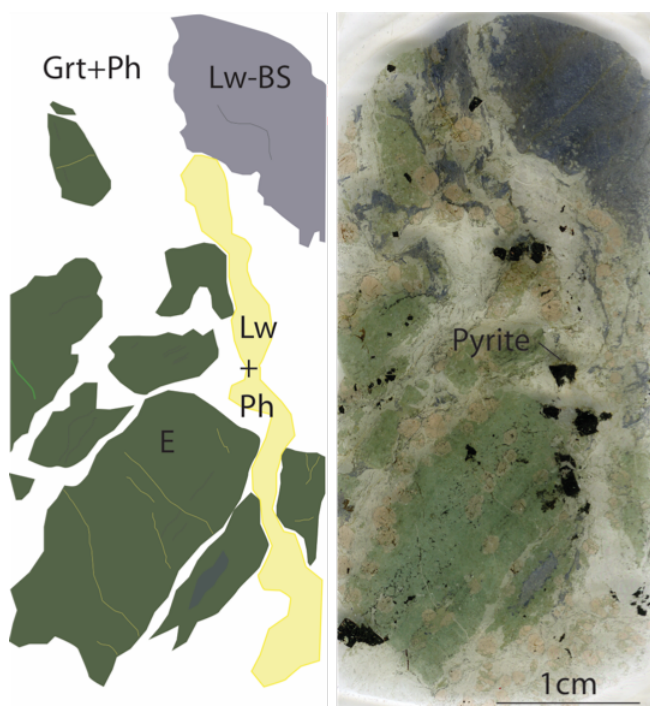


Figure 1. Example of lawsonite eclogite from Port Macquarie.

Oxygen isotope analyses were performed by SIMS in lawsonite crystals from three blueschist and one eclogite-facies sample. In three samples, lawsonite crystals show the same $\delta^{18}\text{O}$ with values at $\sim 10\text{‰}$. Sample LMPM10 is a strongly deformed blueschist with small lawsonite crystals that are characterised by the lowest $\delta^{18}\text{O}$ ($7.7 \pm 0.5\text{‰}$). In all samples, lawsonite crystals are homogeneous in O isotopes composition. When present, garnet shows cores characterised by $\delta^{18}\text{O}$ values at $\sim 10\text{‰}$, consistent with lawsonite composition of the same sample. A slight decrease is observed on the rims of the garnet with $\delta^{18}\text{O}$ at $\sim 8\text{‰}$.

Pyrite crystals show different internal textures from sample to sample. In blueschist LMPM10, pyrite porphyroclasts characterised by an oscillatory zoning for Ni and Co, show positive $\delta^{34}\text{S} \sim 1\text{‰}$. In an additional metasomatic sample, unzoned pyrite

porphyroblasts with inclusions of metamorphic silicates such as phengite show $\delta^{34}\text{S} \sim -7.2\text{‰}$. In eclogite samples, pyrite crystals show complex internal texture and zoning for Ni, As and Co. $\delta^{34}\text{S}$ varies from -8‰ in the cores to -5‰ in the rims.

By combining textural and chemical data, the origin of the isotopic composition recorded in the three minerals will be discussed in terms of geodynamic context, fluid source and metamorphic conditions.

REFERENCES

[1] Och, D. et al. 2003. Blueschist and eclogite in tectonic mélange, Port Macquarie, NSW, Australia. *Mineralogical Magazine*, 67, 609-624.

SIMS development and application to geoscience and environmental sciences

L.A.J. MARTIN, M. KILBURN, P. GUAGLIARDO AND H. JEON

Australian Research Council Centre of Excellence for Core to Crust Fluid Systems (CCFS) and Centre for Microscopy, Characterisation and Analysis, The University of Western Australia (Laure.martin@uwa.edu.au)

Secondary Ion Mass Spectrometers are instruments designed to analyse the isotopic or elemental composition of the surface of solid materials. Large geometry SIMS, such as the Cameca 1280, are usually dedicated to precise isotopic analyses, routinely performed at the 10 to 20 μm scale, whereas the nanoSIMS is mostly used to image materials at the submicron scale. Although based on the same principle, the sputtering of the surface sample by primary ions, both instruments have very different applications.

Quantitative analysis of stable isotopes in minerals is the method of choice to trace fluid-mineral interactions and help understanding a wide range of processes involved in subduction zones, crustal evolution, ore deposit formation... Stable isotopes can also be used for thermometry and help unravelling temperature of mineral formation in different contexts from biogenic minerals to quartz cement during diagenesis. S isotopes are used to trace and understand Early Earth processes. In contrast, nanoSIMS images are rarely quantitative, but provide invaluable information of the relative concentration of elements or isotopes in samples typically imaged at the 50x50 μm scale. The shape of zonations and the textural repartition of elements help to understand the processes forming minerals or those modifying their composition. In this presentation, I will show several examples of application of SIMS techniques applied to geoscience or environmental sciences.

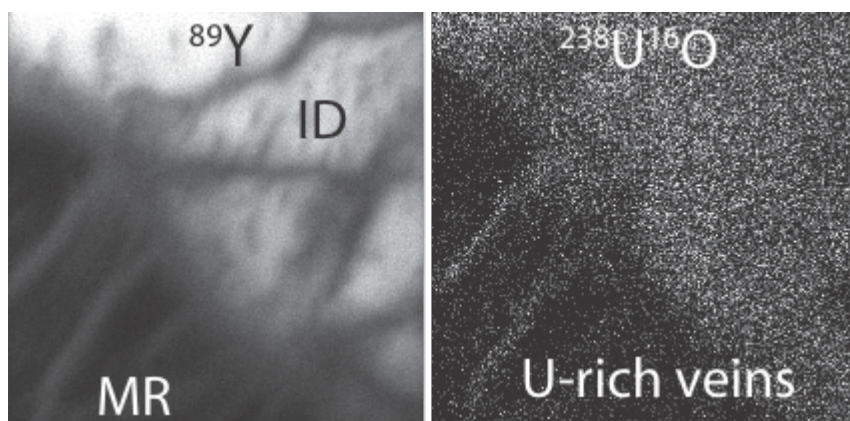


Figure 1. Example of nanoSIMS image (50x50 μm) showing U mobility in inherited (ID) and metamorphic rims (MR) of titanite crystals.

Microstructural indicators of channelled melt flow through the lower crust

U. MEEK¹, N. DACZKO¹ AND S. PIAZOLO^{1,2}

¹Australian Research Council Centre of Excellence for Core to Crust Fluid Systems (CCFS) and GEMOC, Department of Earth and Planetary Sciences, Macquarie University, Sydney, NSW 2109, Australia (uvana.meek@students.mq.edu.au; nathan.daczko@mq.edu.au)

²School of Earth and Environment, University of Leeds, Leeds, UK (s.piazolo@leeds.ac.uk)

Here we report and interpret microstructural features of a lower crustal mass transfer zone. The mass transfer zone is characterised by a 30-40 m wide hornblende unit which cuts granulite facies gabbroic gneiss. Field observations argue against an igneous cumulate origin for hornblende, instead previous work shows that the gabbroic gneiss has been fluxed by a hydrous gabbroic melt that caused extensive melt-rock interaction [1].

In the conceptual model of these zones, the host rock (in this case, two-pyroxene-pargasite gabbroic gneiss) is modified by flux of externally-derived melt, causing reaction-replacement. The migrating melt invokes dissolution of host rock phases that are out of equilibrium with the fluxing melt (in this study, plagioclase + pyroxene), enhancing porosity and permeability and therefore melt flow. New phases crystallise from the migrating melt (in this study, mainly hornblende ± clinozoisite and garnet). As a result, this body represents an “imposter cumulate”.

This study focusses on recognising microstructural indicators with which it is possible to differentiate between an igneous cumulate body and an “imposter cumulate” in lower crustal systems. The microstructural features are described and characterised using thin section microscopy (optical and SEM), along with EBSD mapping of key features. The contact character of ultramafic versus host rock is the most important feature identified. At a microstructural (1-10 µm) scale, the replacement involves dissolution and precipitation of phases. The key texture involves partially dissolved phases that have irregular grain boundaries, as the new precipitating phase replaces them. Other features of channelled melt flow through the lower crust may include (i) the presence of local microstructures typical of the former presence of melt (namely low dihedral angles along grain boundaries that are pseudomorphs of former melt, melt pockets, local pegmatitic domains), and (ii) a high modal abundance of one (or two) phases as a reaction product from melt.

Utilising these indicators, along with careful field analysis, will help to identify melt transfer zones that so far have been largely under-recognised.

REFERENCES

[1] Daczko, N.R. et al. 2016. Hornblende delineates zones of mass transfer through the lower crust. *Scientific Reports*, 6, 31369, doi:10.1038/srep31369, 1-6. [<http://www.nature.com/articles/srep31369>]

Evidence of trace element mobility in zircon-reidite interface

S.D. MONTALVO^{1,2}, S.M. REDDY^{1,2}, D.W. SAXEY^{1,3}, W.D.A. RICKARD^{1,3} AND D. FOUGEROUSE^{1,2}

¹Geoscience Atom Probe, Advanced Resource Characterisation Facility, Curtin University, Perth, Australia (s.montalvo@postgrad.curtin.edu.au, S.Reddy@curtin.edu.au, denis.fougerouse@curtin.edu.au)

²CCFS and Department of Applied Geology, Western Australian School of Mines, Curtin University, Perth, Australia

³Department of Physics and Astronomy, Curtin University, Perth, Australia (david.saxe@curtin.edu.au, W.Rickard@curtin.edu.au)

The mineral zircon (ZrSiO_4) is an important mineral for geochronological and geochemical analysis. The incorporation of radioactive elements during crystal growth, combined with its physical robustness, makes zircon an ideal mineral for radiometric dating and for the preservation of other significant geochemical information over billions of years. However, the chemical composition of zircon can be modified by several processes, which may affect the reliability of the geochemical data acquired.

In a hypervelocity impact event, the temperatures and pressures generated by the shock waves exceed the values produced by endogenic processes. This process can modify the trace elements distribution in zircon grains located in target rocks, ultimately disturbing the geochemical data and the reliability of zircon as a geochronometer. Under such conditions, the shocked zircon can form lamellae of the high-pressure polymorph reidite. The shock-induced phase transformation of zircon to reidite lamellae has previously been proposed to be of a diffusionless-driven displacive manner. However, using atom probe microscopy in conjunction with electron backscatter diffraction (EBSD), transmission kikuchi diffraction (TKD), time-of-flight secondary ion mass spectrometry (ToF-SIMS), and transmission electron microscopy (TEM), we found segregation of trace elements along zircon-reidite interfaces (Fig. 1) in shocked zircon derived from the Stac Fada impact site in Scotland. Our results are not consistent with the sole martensitic mechanism operating during reidite formation. We propose that high-pressure transformation to reidite requires an additional short range diffusion-driven component to explain the local compositional variation found at the nanoscale.

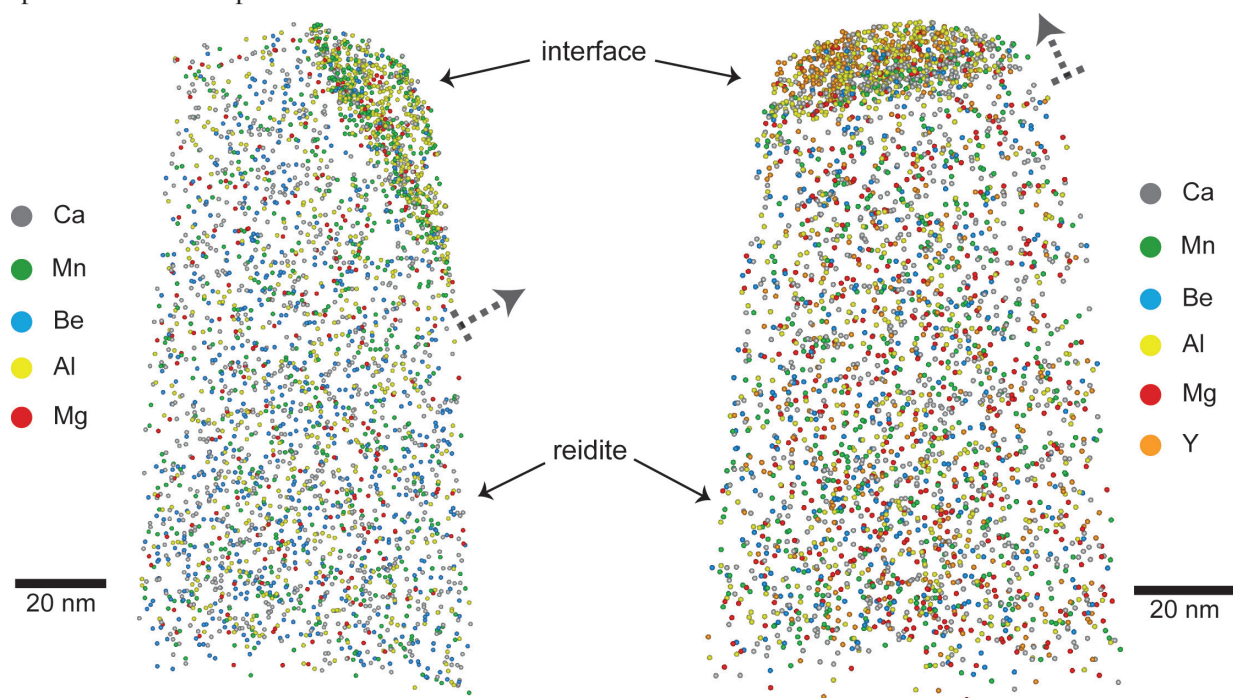


Figure 1. Atom probe 3D reconstruction of two needles. Each sphere represents a Ca, Mn, Be, Al, Mg or Y atom. The interface between reidite and zircon (located at the top of each needle) displays an enrichment of trace elements with respect to the rest of the reidite.

Microstructural and microchemical evidence for deep crustal melt-rock interaction in mass transfer zones, Finero Complex, Ivrea Verbano Zone, Italy

J.K. MUNNIKHUIS¹, N. DACZKO¹, S. PIAZOLO² AND A. LANGONE³

¹Australian Research Council Centre of Excellence for Core to Crust Fluid Systems (CCFS) and GEMOC, Department of Earth and Planetary Sciences, Macquarie University, Sydney, NSW 2109, Australia (Jonathan.Munnikhuis@mq.edu.au; Nathan.Dazcko@mq.edu.au)

²School of Earth and Environment, Institute of Geophysics and Tectonics, University of Leeds, Leeds, LS2 9JT, United Kingdom, (S.Piazolo@leeds.ac.uk)

³C.N.R. - Istituto di Geoscienze e Georisorse, U.O.S. di Pavia, Via Ferrata 1, Pavia, Italy (Langone@crystal.unipv.it)

Understanding deep melt pathways

The deep crustal section of the Ivrea-Verbano Zone (IVZ, western Alps) has been the study of numerous structural, geophysical and geochemical studies which have attempted to better understand lower crustal processes ($P = 10 - 12$ kbar) and the magmatic and tectonic evolution of the area. The Finero Complex, in the northern IVZ, is characterised by the occurrence of a pervasively metasomatised mantle unit comprising of 8 km² of phlogopite-bearing ultramafic rocks called the Phlogopite-Peridotite [1]. This unit is surrounded by a nested suite of mafic-ultramafic intrusions which forms a pseudo-antiformal structure with the Phlogopite-Peridotite at the core. The core is surrounded by a 100 m thick unit of interlayered garnet gabbros and hornblendites (called the Layered Internal Zone), a 600 m thick cumulus amphibole peridotite, and a 450 m thick garnet gabbro. The Finero Complex is bordered by the Insubric line to the N-NW and the metasedimentary Kinzingite unit to the S-SE. Contacts between the Phlogopite-Peridotite and units within the mafic complex are consistently characterised by dm-scale mylonitic shear zones. The hydrous metasomatism in peridotite and structural features at the margins of peridotite are absent from the other mafic complexes of the central and southern IVZ (Balmuccia and Baldissero), suggesting that the Finero Complex experienced a more complex geodynamic evolution involving extensive metasomatism. During the first year of my PhD (2017), I will collect new microstructural and microgeochemical data from the peridotites and gabbroic units of the Finero Complex. The aims include to understand (i) metasomatic processes involving melt-rock interaction at upper mantle and deep crustal conditions, (ii) the relationship of different types of metasomatism in different units, (iii) the age of igneous protoliths and timing of metasomatism throughout the complex, and (iv) the formation of high variance assemblages exposed in the Layered Internal Zone. Preliminary results suggest that the microstructures and microgeochemical data can be explained by a model of both widely distributed and channelled diffuse porous melt flow which occurred through the peridotite and along the deforming boundaries with the other lower crustal units. By gaining a better understanding of the reaction and deformation textures formed by the interaction between silicate melts and previously established frameworks of protoliths, similar areas of mass transfer can be recognised in the field.

REFERENCES

[1] Siena, F. and Coltori, M. 1989. The petrogenesis of a hydrated mafic - ultramafic complex and the role of amphibole fractionation at Finero (Italian Western Alps). *Neues Jahrbuch für Mineralogie*, 6, 255-274.

Stabilising a craton: The 3.1 Ga Mpuluzi Batholith, Swaziland and South Africa

R.C. MURPHY, W.L. GRIFFIN, N.J. PEARSON AND S.Y. O'REILLY

Australian Research Council Centre of Excellence for Core to Crust Fluid Systems (CCFS) and GEMOC, Department of Earth and Planetary Sciences, Macquarie University, Sydney, NSW 2109, Australia (rosanna.murphy@mq.edu.au)

The Barberton Greenstone Belt (BGB) and Ancient Gneiss Complex (AGC), located in the eastern part of the Kaapvaal Craton (Swaziland and adjacent South Africa), represent some of the best-preserved and most-studied Early- to Mid-Archaean (3.6–3.2 Ga) crustal remnants. The extensively-studied granite-greenstone belt is surrounded and overlain by several large granitoid bodies (Mpuluzi, Piggs Peak, Nelspruit, and Heerenveen batholiths), all emplaced at ~3.1 Ga, which coincides with the end of TTG magmatism and regional metamorphism in the area. This study focuses on the Mpuluzi batholith as a case study to constrain the prevailing conditions at 3.1 Ga that led to the generation and emplacement of these granitoids, and subsequent cratonisation.

The granitoids were emplaced as extensive, km-thick sheets and extend over more than 10,000 km². Zircon U-Pb ages vary from ~3.16 to ~3.09 Ga; the presence of inherited cores in some grains suggests the involvement of an older crustal component (~3.5 Ga) in the magma generation. This is confirmed by the Hf isotopic data, which show clear indications of mixing between an older crustal component and juvenile material. The Hf isotopic data also provide a good estimate of the age of extraction of the inherited component, with one sample showing a well-defined evolution trend back to ~4.1 Ga. The Hf data also suggest that the juvenile material may have been extracted from the mantle very close to the time of emplacement of the batholith, with the mixing trend intersecting the depleted mantle line in some samples.

Whole-rock Sr and Nd isotopic data yield tight isochrons for both systems (MSWD <1), and calculated isochron ages are within error of each other, and of the U-Pb ages (Sr: 3113 ± 84 Ma; Nd: 3027 ± 520 Ma). The close agreement between ages from the three isotopic systems strongly suggests that the whole mass formed and cooled together.

The isotopic evidence for mixing between an older crustal component and juvenile material suggests that the mantle may have both provided the heat for melting and contributed material to the magma itself. The variation within the batholith thus represents variable proportions of mixing between these components, and perhaps also a build-up of heat over time. These 3.1 Ga granitoids therefore represent the final stage in the cratonisation of the region; this could represent the “draining” of fusible material from the lower crust, increasing its rigidity and limiting further tectonism.

Potential field methods to model a Devonian granitic intrusion in Marulan

T.B. NIMALSIRI¹ AND M. LACKIE²

¹Australian Research Council Centre of Excellence for Core to Crust Fluid Systems (CCFS) and GEMOC, Department of Earth and Planetary Sciences, Macquarie University, Sydney, NSW 2109, Australia (thusitha.nimalsiri@hdr.mq.edu.au)

²Department of Earth and Planetary Sciences, Macquarie University, Sydney, NSW 2109, Australia (mark.lackie@mq.edu.au)

Potential field methods play a pivotal role in understanding regional geological structures. The total magnetic intensity (TMI) map of New South Wales shows a distinct positive anomaly related to the Marulan granite. This rock formation, along with other Devonian intrusive bodies in the area, is collectively identified as the Marulan Supersuite [1] which includes granites, granodiorites and tonalites, and is bordered by Devonian volcano-sedimentary deposits. In this study we aim to understand the structure of the Supersuite and to develop a 3D model to represent its formation within the sedimentary terrain. For that, the TMI data will be analysed in detail along with existing and collected gravity data. Further, rock sampling will be carried out to provide petrophysical data for the models.

So far, petrophysical sampling has been carried out in the Marulan area, collecting rocks from both the Supersuite and the neighbouring formations. The calculated density of the sampled intrusives ranged from 2.66 to 2.87 gcm⁻³ and that of the sedimentary rocks from 2.59 to 2.63 gcm⁻³. The Supersuite rocks recorded a range of magnetic susceptibility values from 0.005 to 0.027 SI and markedly low values (<0.0001 SI) were shown by the sedimentary rocks. However, some ignimbrite samples also showed relatively high susceptibility values.

The initial gravity survey was conducted in the southern Marulan area. Compared to the existing Geoscience Australia (GA) data, a tighter sampling interval, 500 m near identified boundaries and 1000 m in other areas, was maintained during the acquisition. A good precision was attained by recording 6 Hz data for 60 seconds at a station. Location of stations with precise elevations were logged in order to be used in gravity reduction. A reference station from the national Fundamental Gravity Network was measured to tie the collected data to the national grid. The collected data was tied and reduced followed by gridding along with the GA data to produce the Spherical Cap Bouguer anomaly map. Profile lines were synthesised in preferred directions to analyse the gravity anomaly.

Synthetic profiles, nearly normal to the anomalies, were designed on the TMI map to carry out detailed magnetic modelling of the Supersuite. Models were initially created with simple tabular bodies, to be modified later with more detailed structures.

Initial assessment of gravity data revealed that the signal of the Marulan Supersuite is overshadowed by a much larger and deeper feature in the terrain, although the residual anomaly of some southern profiles still retain some signal due to the suite. On the contrary, the TMI map depicts the Supersuite more reliably, where the intrusions mapped on the surface overlap with sharp magnetic peaks. These peaks are modelled by a series of shallow and thin tabular bodies, whereas the broad magnetic anomaly to the west of the sharp peaks are matched with deeper, thicker bodies.

The variation of density and susceptibility within the formation may be accounted for by extensive weathering. Analysis of drill core samples for the same properties could provide more accurate data for currently weathered surface samples. Models created by detailed magnetic processing will be used in gravity modelling to see if the near surface suite response can be incorporated with the deeper gravity signal.

REFERENCES

- [1] Glen, R. 2005. The Tasmanides of eastern Australia. Geological Society, London, Special Publications, 246, 1, 23-96.

Origin and significance of the Turee Creek Group Clotted Microbialite

B.J. NOMCHONG^{1,2} AND M.J. VAN KRANENDONK^{1,2}

¹Australian Research Council Centre of Excellence for Core to Crust Fluid Systems (CCFS), Department of Earth and Planetary Sciences, Macquarie University, Sydney, NSW 2109, Australia (b.nomchong@unsw.edu.au)

²Australian Centre for Astrobiology and PANGAEA Research Centre, School of Biological, Earth and Environmental Sciences, University of New South Wales, Kensington, NSW 2052, Australia (m.vankranendonk@unsw.edu.au)

The Turee Creek Group Clotted Microbialite

Microbialites comprise the earliest lifeforms preserved in the geological record, with the oldest examples being 3.7 Ga stromatolites from Greenland [1]. Through time, microbialites evolved with increasing morphological and biological complexity, with major evolutionary milestones coinciding with the Great Oxidation Event (GOE) at c. 2.45-2.32 Ga [2]. Researchers recently described a new dolomite microbialite reef from the 2.4 Ga Turee Creek Group (TCG), WA, that displays complex microbialite morphologies including thick units of massively clotted, thrombolite-like microbialite [3]. It has since been revealed that this TCG clotted microbialite represents a diverse suite of both biogenic and abiogenic carbonate textures, the classification of which is the subject of this research.

To classify the various clotted carbonate textures, we studied their field relationships (e.g. association with adjacent lithologies/stromatolites) and microtexture in thin section. Samples that display preserved marine cements and co-occur with well-laminated stromatolites are more primary whereas those that have been partially silicified or co-occur with recrystallised stromatolites are less primary. Raman spectroscopy was used to detect preserved kerogen and confirm the biogenicity of some clotted microbialite types.

Results and Discussion

Four main types of clotted carbonate were identified, including three primary biogenic textures. These include: a unique clotted microbial aggregate that formed during periodic high energy events; massive beds of clotted microbialite that grade through wrinkly microbial mats into stromatolites; the oldest described true thrombolites (Fig. 1); and multiple diagenetic carbonate textures, including recrystallised microbial mats and recrystallised clotted microbialite.



Figure 1. 2.4 Ga thrombolites in the TCG pre-date any previously described occurrences.

Our research confirms that new expressions of clotted microbial growth, including the earliest described occurrence of thrombolites in the rock record, coincided with the GOE. This presents the question; was this increase in microbial complexity driven by global environmental change? Future research will address this question by aiming to characterise the environmental conditions during the deposition of the TCG carbonate and its diverse microbialite assemblage using a range of both new and established geochemical analyses.

REFERENCES

- [1] Nutman, A.P. et al. 2016. Rapid emergence of life shown by discovery of 3,700-million-year-old microbial structures. *Nature*, 537, 535-538.
- [2] Schirmer, B.E. et al. 2013. Evolution of multicellularity coincided with increased diversification of cyanobacteria and the Great Oxidation Event. *Proceedings of the National Academy of Sciences*, 110, 1791-1796.
- [3] Barlow, E. et al. 2016. Lithostratigraphic analysis of a new stromatolite-thrombolite reef from across the rise of atmospheric oxygen in the Paleoproterozoic Turee Creek Group, Western Australia. *Geobiology*, 14, 317-343.

Laurentian provenance of the NE Australian Paleoproterozoic Georgetown Inlier — Implications for Nuna amalgamation

A.R. NORDSVAN¹, B.J. COLLINS¹, Z.X. LI¹, C.J. SPENCER¹, A. POURTEAU¹, P.G. BETTS², I.W. WITHNALL² AND S. VOLANTE¹

¹Earth Dynamics Research Group, ARC Centre of Excellence for Core to Crust Fluid Systems (CCFS) and The Institute for Geoscience Research (TIGeR), Department of Applied Geology, Curtin University, GPO Box U1987, WA 6845, Australia (adam.nordsvan@postgrad.curtin.edu.au)

²School of Earth, Atmosphere and Environment, Monash University, Clayton Campus, VIC 3800, Australia

³Geological Survey of Queensland, Department of Natural Resources and Mines, PO Box 15216, City East, QLD 4002, Australia

Reconstructions based on paleomagnetic data for the Paleo- to Mesoproterozoic supercontinent Nuna suggest a connection between NE Australia and NW Laurentia throughout its development. However, whilst similarities in tectonic evolution between the two regions have been discussed in broad terms, the timing and nature of this proposed connection has not yet been tested in the most eastern Proterozoic block, the Georgetown Inlier.

The Georgetown Inlier consists of the lower Etheridge, the upper Etheridge, the Langlovale and the Inorunie groups. Sediments of the lower Etheridge Group range from offshore mudstone to wave and tidally influenced lower shoreface and wave dominated upper shoreface facies deposited during the sag phase of a passive margin or intracontinental rift. Sedimentation was followed by the eruption of the tholeiitic Deadhorse Metabasalt (ca. 1665 Ma) and emplacement of tholeiitic Cobbold Metadolerite sills and dykes. A deepening of the basin occurred simultaneously with the mafic magmatism, resulting in deposition of the overlying offshore mudstones of the uppermost part of the lower Etheridge Group and the upper Etheridge Group. Unconformably overlying the Etheridge Group, basal sediments of the Langlovale Group were deposited in fluvial environments that deepen up-sequence to submarine fan facies. To evaluate the palaeogeographic connection between NE Australia and NW Laurentia throughout Nuna we use new and existing detrital zircon data from the Georgetown Inlier sedimentary groups.

Detrital zircon age spectra from sedimentary strata within the Inlier show two distinct changes in sedimentary provenance: (1) The lowermost units (depositional age of ca. 1700–1650 Ma) have detrital zircon age spectra that strongly resemble Laurentian magmatic ages and detrital zircon age spectra of the similar-aged Wernecke Supergroup of northwest Laurentia; (2) Sediments deposited from ca. 1650 to 1610 Ma show a unimodal proximal signature, and (3) sediments deposited post-1550 Ma have zircon age spectra similar to the Mt. Isa Inlier of the North Australian Craton (NAC). Along with new paleocurrent measurements, the detrital age data challenge current models that suggest the Georgetown Inlier was part of Australia before ca. 1700 Ma. Rather, we argue it was a continental ribbon rifted from west Laurentia during slab-rollback at approximately 1690 Ma, by 1650 Ma the Georgetown Inlier had completely rifted from Laurentia and, at ca. 1600 Ma, was colliding with Australia during Nuna amalgamation.

Numerical modelling of Multi-Phase Multi-Component Reactive Transport in the Earth's interior

B. OLIVEIRA¹, J.C. AFONSO^{1,2}, S. ZLOTNIK³ AND R. TILHAC¹

¹Australian Research Council Centre of Excellence for Core to Crust Fluid Systems (CCFS) and GEMOC, Department of Earth and Planetary Sciences, Macquarie University, Sydney, NSW 2109, Australia (benat.oliveira-bravo@mq.edu.au)

²Centre for Earth Evolution and Dynamics, Department of Geosciences, University of Oslo, Oslo, Norway

³Laboratori de Calcul Numeric, Escola Tecnica Superior d'Enginyers de Camins, Canals i Ports, Universitat Politecnica de Catalunya, Barcelona, Spain

We present a conceptual and numerical approach to model processes in the Earth's interior that involve multiple phases simultaneously interacting thermally, mechanically and chemically [1]. This approach is truly multiphase in the sense that each dynamic phase (i.e. melt/solid) is explicitly modelled with an individual set of mass, momentum, energy and chemical mass balance equations coupled via interfacial interaction terms. It is also truly multi-component in the sense that the compositions of the system and its constituting minerals are expressed by a full set of major elements, rather than proxies (i.e. oxides). In contrast to previous approaches, these chemical components evolve, react with, and partition into, different phases with different physical properties according to an internally consistent thermodynamic model. This enables a thermodynamically consistent coupling of the governing set of balance equations. Interfacial processes such as surface tension and/or surface energy contributions to the dynamics and energetics of the system are also taken into account.

Our model describes the dynamic evolution and non-linear feedbacks of complex geochemical processes governed by Multi-Phase Multi-Component Reactive Transport (MPMCRT), such as melt generation, migration and differentiation. This novel approach provides a flexible platform to track changes in the chemical compositions and physical properties of the lithospheric mantle through time, over different spatial and temporal scales. In particular, we compute major- and trace-element reactive transport with diffusion-controlled trace-element re-equilibration associated with melt migration, metasomatism and metamorphism processes. Several numerical examples including melt percolation, partial melting and crystallisation, are presented to illustrate the behaviour of the system as well as to highlight the benefits and limitations of the model.

REFERENCES

[1] Oliveira, B. et al. 2017. Numerical modelling of Multi-Phase Multi-Component Reactive Transport in the Earth's interior, *Geophysical Journal International*, ggx399, <https://doi.org/10.1093/gji/ggx399>.

Geodynamic processes during heroic collisions: the power of integrating geochemical, microstructural and geodynamic information

S.Y. O'REILLY¹, W.L. GRIFFIN¹, Q. XIONG¹, J.C. AFONSO¹, T. SATSUKAWA^{1,2}, J.X. HUANG¹, G. BEGG^{1,3}

AND THE TARDIS TEAM

¹Australian Research Council Centre of Excellence for Core to Crust Fluid Systems (CCFS) and GEMOC, Department of Earth and Planetary Sciences, Macquarie University, Sydney, NSW 2109, Australia

²Department of Geophysics, Kyoto University, Kyoto 606-8502, Japan

³Minerals Targeting International PL, 17 Prowse St, West Perth, Western Australia 6005, Australia

Some regions of Tibet are proving to be an excellent analogue for understanding very large-scale collision events, including those characterising some of the tectonism within the Tasmanides of eastern Australia.

Large peridotite massifs scattered along the 1500 km length of the Yarlung–Zangbo Suture Zone (southern Tibet, China), the major suture between Asia and Greater India, provide an outstanding natural laboratory to track multiple lithosphere evolution events throughout the complex history of this major collisional tectonic terrane. The massifs reveal: a sequence of repetitive docking of distinct lithospheric mantle domains over at least 250 My [1]; repeated metasomatic and magmatic episodes that can be distinguished with detailed geochronology; mineral phases that indicate metamorphism under the conditions of the Mantle Transition Zone (MTZ); others that require a super-reducing environment over a range of depths; and microstructural analysis of chromites with fine-grained inclusions of olivine (inverted wadsleyite), diopside and silica that provide the first evidence for deformation by dislocation creep in the MTZ, an important consideration for interpreting seismic signals [2, 3].

Re-Os-isotope data suggest that the subducted mantle consisted of previously depleted subcontinental lithosphere, dragged down by a younger subducting oceanic slab. Thermomechanical modelling shows that roll-back of a (much later) subducting slab would produce a high-velocity channelised upwelling that could exhume the buoyant harzburgites (and their chromites) from the Transition Zone in <10 Myr. This rapid upwelling, which may explain some characteristics of the diamonds, appears to have brought some massifs to the surface in forearc or back-arc basins, where they provided a basement for oceanic crust. This model can reconcile many apparently contradictory petrological and geological datasets. It also defines an important, previously unrecognised, geodynamic process that may have operated along other large suture zones such as the Urals.

These nano- to micro-scale to global observations using geochronology, geochemistry, mineral microstructures and geodynamic modelling are starting to fill in the huge 4D sudoku that is the complex evolution and deep architecture of such large-scale (heroic) collision events. This may allow us to identify analogous ancient events lurking in the geological record.

REFERENCES

- [1] Xiong, Q. et al. 2016. Two-layered oceanic lithospheric mantle in a Tibetan ophiolite produced by episodic subduction of Tethyan slabs. *Geochemistry, Geophysics, Geosystems*, 18, 3, 1189-1213.
- [2] Griffin et al., 2016. Transition zone metamorphism of Tibetan ophiolitic peridotites and its tectonic implications. *Journal of Petrology*, 57, 655-684.
- [3] Satsukawa et al. 2015. Messengers from the deep: Fossil wadsleyite-chromite microstructures from the Mantle Transition Zone. *Scientific Reports* 5, 16484. doi: 10.1038/srep16484

High-resolution microanalytical methods for the investigation of bivalve shell ultrastructures – Relevance for paleoclimate reconstructions

L.M. OTTER¹, M.R. KILBURN², R. WIRTH³, S. BUHRE⁴, K. EDER⁵, S.J. MOODY⁵ AND D.E. JACOB¹

¹Australian Research Council Centre of Excellence for Core to Crust Fluid Systems (CCFS) and GEMOC, Department of Earth and Planetary Sciences, Macquarie University, Sydney, NSW 2109, Australia (laura.otter@hdr.mq.edu.au)

²Centre for Microscopy, Characterization and Analysis, The University of Western Australia, Western Australia, Australia

³GeoForschungsZentrum Potsdam, Telegrafenberg C120, Potsdam, Germany

⁴Institute for Geosciences of the Johannes Gutenberg-University Mainz, J.-J.-Becher Weg 21, Mainz, Germany

⁵Australian Centre for Microscopy and Microanalysis, The University of Sydney, NSW, Australia

The understanding of recent shell biomineralisation, especially beyond the sub-micron range, is essential for our understanding of fossil shells used for paleoclimate reconstructions. Therefore, this study focusses on the high-resolution microanalytical investigation of various types of recent (non-fossil) bivalve shell ultrastructures.

Bivalve shells are nanocomposite materials consisting of crystalline calcium carbonate phases that are embedded within an organic scaffold. These two building blocks are arranged into a highly hierarchically structured architecture with different arrangements. A detailed understanding of recent shell architecture is critical to correctly decipher a vast amount of paleo proxies for e.g. salinity, seawater temperature, and pH in fossil shells.

Although shell-building processes are still not fully understood, attention has moved away from classical ion-by-ion crystallisation models to non-classical crystallisation pathways that are based largely on colloid attachment and transformation processes where individual crystals form via nano-granular amorphous calcium carbonate (ACC) precursor phases with subsequent transformation to their final aragonitic or calcitic states. Based on these principles, it is necessary to establish detailed growth models for recent shell ultrastructure types to understand their different spatial and temporal growth dynamics and to thoroughly understand which impact environmental parameters have on their metabolic activity and net calcification rates. In addition, the study of recent shell ultrastructures enables the investigation of metastable phases, such as amorphous calcium carbonate (ACC) that are otherwise lost in fossil material by postdepositional modifications.

Snapshots of sub-micron growth are visualised through pulsed strontium labelling experiments conducted at the Macquarie Seawater Facility. Living bivalves were transferred several times between elevated Sr and normal ambient seawater conditions with durations varying between 1 and 12 days and 6 to 12 days for labelled and normal conditions, respectively. After the termination of aquaculture experiments animals were sacrificed, shells cleaned from organic tissue and prepared for analyses by sectioning and polishing.

We applied stepwise spatially-downscaled microbeam analyses with (1) quantitative wavelength dispersive X-ray spectrometry (WDX) for geochemical data acquisition using an Electron Probe Micro Analyzer (EPMA), (2) Field-Emission Gun Scanning Electron Microscopes (FEG-SEM) for high magnification photomicrographs and Electron Backscatter Diffraction (EBSD), (3) Micro-Raman Spectroscopy for phase-related and crystallographic information, (5) qualitative high resolution NanoSIMS isotopic mapping, as well as (6) Atom Probe Tomography (APT) that yields sub-micrometer geochemical and position-sensitive data. This combined multi-analytical approach with combined visual, geochemical, and crystallographic information together with the known schedule for Sr-labelling meets the demands of high spatially resolved analysis of the hierarchical bio-composite materials and allows us to unravel the shell architectures of nacreprismatic, composite prismatic, and crossed-lamellar ultrastructures of the studied species.

Magmatic fertility of porphyry Cu-Au deposits: Insights from zircon morphology, trace element and Hf-O isotopes

L.A. PARRA-AVILA¹, M.L. FIORENTINI¹, R. LOUCKS¹ AND Y. LU^{1,2}

¹ARC Centre of Excellence for Core to Crust Fluid Systems (CCFS), Centre for Exploration Targeting, School of Earth Sciences, The University of Western Australia, 35 Stirling Highway, Perth, WA 6009, Australia (luis.parraavila@uwa.edu.au)

²Geological Survey of Western Australia, East Perth, WA 6004, Australia

Porphyry Cu-Au deposits have a relatively well defined geodynamic framework and are recognised as a valuable source of Cu and other elements such as Au and Ag [1]. Due to the limited success in finding new large to giant deposits it is important to keep refining the understanding of the geologic processes and factors that lead to their formation. Zircon compositions are powerful in unravelling the petrogenesis and magmatic fertility evolution of Cu-ore-forming magmas [2], which are hydrous magmas in continental and island arcs [3].

Zircons were obtained from pre, syn- and post- ore stage samples from the Tampakan (Philippines) and Batu Hijau (Indonesia) porphyry Cu-Au systems. Tampakan and Batu Hijau sit along subduction zones in island arc settings in Southeast Asia. Such zircons produced a comprehensive database of *in-situ* analyses for O, U-Pb, and Lu-Hf isotopes as well as trace-element compositions.

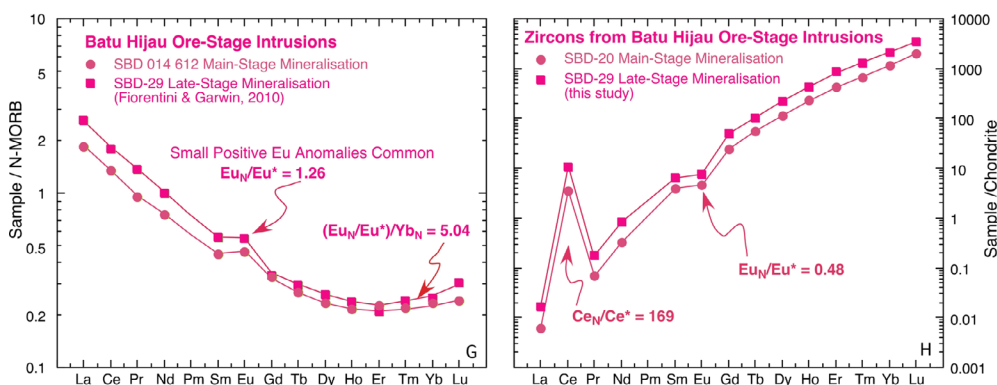


Figure 1. Distinctive features of typical whole-rock and zircon REE patterns of copper-ore-productive felsic igneous suites emanating from subduction-metasomatised mantle at Plio-Pleistocene convergent plate margins.

Zircon trace-element data display typical features of felsic arc magmas parental to major magmatic-hydrothermal copper ore deposits such as steep, hook-shaped REE patterns with a minimum around Er and absence of a significant negative Eu anomaly (Fig. 1). Pre- and post-ore-stage samples, although not mineralised, also display the same characteristics, suggesting the systems that generate such deposits become fertile around 5 Ma prior to mineralisation, and remained fertile for ca. 3 Ma after mineralisation. This means other factors on top of magma fertility played a role in leading to mineralisation. Regarding O-isotopes, the *in-situ* zircon data reflect no involvement of supracrustal materials as shown by mantle-like zircon $\delta^{18}\text{O}$ values ranging between 4.47 and 6.00 ‰. Morphologically, syn-ore zircons from the two studied deposits are characterised by unzoned cores surrounded by thin, oscillatory zoned rims. We interpret these zircon textural characteristics to reflect two-stage magma emplacement. The unzoned cores are indicative of crystallisation within a long-lived, deep, hot magma chamber and the thin, zoned rims suggest a relatively short residence time in the shallow crust, which prevents the loss of Cu metals.

REFERENCES

- [1] Sillitoe, R.H. 2010. Porphyry copper systems. *Economic Geology*, 105, 3-41.
- [2] Lu, Y.J. et al. 2016. Zircon compositions as a pathfinder for porphyry Cu \pm Mo \pm Au deposits. *Society of Economic Geologists Special Publication No. 19*, 329-347.
- [3] Loucks, R.R. 2014. Distinctive composition of copper-ore-forming arc magmas. *Australian Journal of Earth Sciences*, 61, 5-16.

Neutron imaging to measure grain boundary proton diffusion in forsterite

S. PATABENDIGEDARA^{1,2}, F.F. SALVEMINI² AND S. CLARK^{1,2}

¹Australian Research Council Centre of Excellence for Core to Crust Fluid Systems (CCFS) and GEMOC, Department of Earth and Planetary Sciences, Macquarie University, Sydney, NSW 2109, Australia
(sarith-kumara.samaya-manthr@hdr.mq.edu.au)

²Australian Centre for Neutron Scattering, ANSTO, Lucas Heights NSW, Australia

During the past decade, various laboratories have been undertaking the difficult measurements needed to derive proton conduction in mantle minerals as a function of temperature and water content. They have used different formalisms to fit their laboratory observations [1, 2]. The mechanism of hydrogen diffusion in those minerals was described by Demouchy (2010) and Demouchy and Casanova (2016) using a defect model in crystalline materials. This concept is well-known and well documented in the material science community [3] where the effects of in-grain and grain boundary diffusion are separated using the bricklayer model and other associated derivatives of this model [4]. Separation of the two components of the proton conductivity in olivine will substantially improve current proton conduction models. However, measuring the grain boundary proton conduction is not easy. Demouchy (2010) was the first, and to date there has only been experimental work on hydrogen grain boundary diffusion in olivine. Demouchy used FTIR measurements on hydrogen sensors (a large olivine grain compared to fine grained olivine matrix) to calculate the grain boundary hydrogen diffusion rate in a forsterite polycrystalline matrix.

The sensitivity of this technique is questionable due to Demouchy having cut and polished the sample. Therefore, we propose to use the neutron tomography technique to directly image water transport through a polycrystalline matrix [5].

We have already completed a test measurement on the DINGO neutron tomography facility at the Australian Centre for Neutron Scattering. One anhydrous and one hydrous synthetic forsterite sample (cylinder) were imaged for direct comparison. The sample was hydrated at 2 GPa and 1000 °C. Figure 1 shows a reconstructed image of the neutron tomography of both samples. The anhydrous reference sample shows a low neutron attenuation (rendered in blue colour in the tomogram). The neutron attenuation coefficient has increased in the treated sample due to the diffusion of hydrogen through the olivine cylinder (rendered in green in the tomogram). The annealing time used in this experiment allowed hydrogen to diffuse completely through the sample. We are now preparing to conduct a range of experiments with various annealing times and temperatures to obtain the diffusion rate. The preliminary study has proved the capability of neutron tomography for mapping the diffusion of hydrogen through mantle minerals.

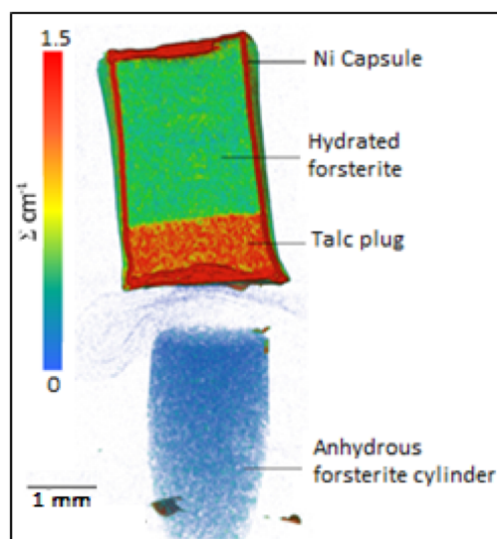


Figure 1. 2D section of the neutron tomography of the hydrated (top) and the anhydrous (bottom) samples. The tomographic models are rendered in false colours and a scale bar is reported at the bottom to show the correlation between colour and total neutron attenuation coefficient.

REFERENCES

- [1] Katsura, T. et al. 2009. Electrical conductivity of the major upper mantle minerals: a review. *Russian Geology and Geophysics*, 50, 12, 1139-1145.
- [2] Yoshino, T. et al. 2009. The effect of water on the electrical conductivity of olivine aggregates and its implications for the electrical structure of the upper mantle. *Earth and Planetary Science Letters*, 288, 1, 291-300.
- [3] Nowick, A.S. 2012. *Diffusion in solids: recent developments*. Elsevier.
- [4] Tuller, H.L., Ionic conduction in nanocrystalline materials. *Solid State Ionics*, 2000. 131, 1, 143-157.
- [5] Sakaguchi, H. et al. 2003. Analysis of hydrogen distribution in hydrogen storage alloy using neutron radiography. *Journal of alloys and compounds*, 354, 1, 208-215.

The Earliest history of the Earth and the Moon, the zircon geochronological evidence

R.T. PIDGEON, A.A. NEMCHIN AND M.L. GRANGE

ARC Centre of Excellence for Core to Crust Fluid Systems (CCFS) and The Institute for Geoscience Research (TIGeR), Department of Applied Geology, Curtin University, GPO Box U1987, Perth WA 6845, Australia
(r.pidgeon@curtin.edu.au; A.Nemchin@curtin.edu.au; M.Grange@curtin.edu.au)

The early record of Earth history, from the time of formation about 4.56 Ga ago to the formation of the first rocks at about 4.0 Ga, has been lost except for the occurrence of > 4.0 Ga detrital zircons in quartzites from the Archean Yilgarn Craton of Western Australia [1, 2]. As the only remaining fragments of early Earth history these zircons are extremely precious and have been intensively studied using numerous techniques to try to extract as much information as possible about their source rocks and processes active in the Hadean period of Earth history. Peaks in the U-Pb geochronological record in the Jack Hills, Mt Narryer and Maynard Hills zircons are found to vary between samples, indicating a heterogeneous Hadean source region, with zircon-bearing source rock ages up to at least 4.37 Ga, the oldest zircon found on Earth. Another potential source of information on the Hadean history of the Earth is the Moon. It has been proposed that the Moon formed from the ejecta from the impact of a Mars-sized body with the proto Earth at about 4.51 Ga [3]. The surface of the newly formed Moon is thought to have been molten, forming a magma ocean which, on cooling and solidifying, preserved its subsequent Hadean history. This could, in many ways, mirror the early history of the Earth. The early Moon history was dominated by a multitude of impacting bodies and rocks returned by the Apollo missions from the lunar highlands are commonly impact breccias. Zircons have been identified and studied from samples of these breccias and lunar regolith and also from lunar meteorites [4, 5]. The lunar zircon geochronological record extends from 4.42 Ga to 3.90 Ga and there are a number of age peaks that point to major events on the Moon. Is there any commonality in the history of the two bodies as recorded by their zircon geochronology? In the extended presentation we will consider the detailed zircon geochronological evidence from the two bodies and draw conclusions on their comparative histories.

REFERENCES

- [1] Froude, D.O. et al. 1983. Ion microprobe identification of 4,100-4,200 Myr-old terrestrial zircons. *Nature*, 304, 616-618.
- [2] Compston, W. and Pidgeon, R.T. 1986. Jack Hills, evidence of more very old detrital zircons in Western Australia. *Nature* 321, 766-769.
- [3] Elkins-Tanton, L.T. et al. 2011. The lunar magma ocean: Reconciling the solidification process with lunar petrology and geochronology. *Earth and Planetary Science Letters*, 304, 326-336.
- [4] Nemchin, A.A. et al. 2008. SIMS U-Pb study of zircon from Apollo 14 and 17 breccias: Implications for the evolution of lunar KREEP. *Geochimica et Cosmochimica Acta*, 72, 668-689.
- [5] Liu, D. et al. 2012. Comparative zircon U-Pb geochronology of impact melt breccias from Apollo 12 and lunar meteorite SaU 169, and implications for the age of the Imbrium impact. *Earth and Planetary Science Letters*, 319-320, 277-286.

Crustal structure of Western Capricorn Orogen (WA) inferred from 3-D Magnetotelluric imaging

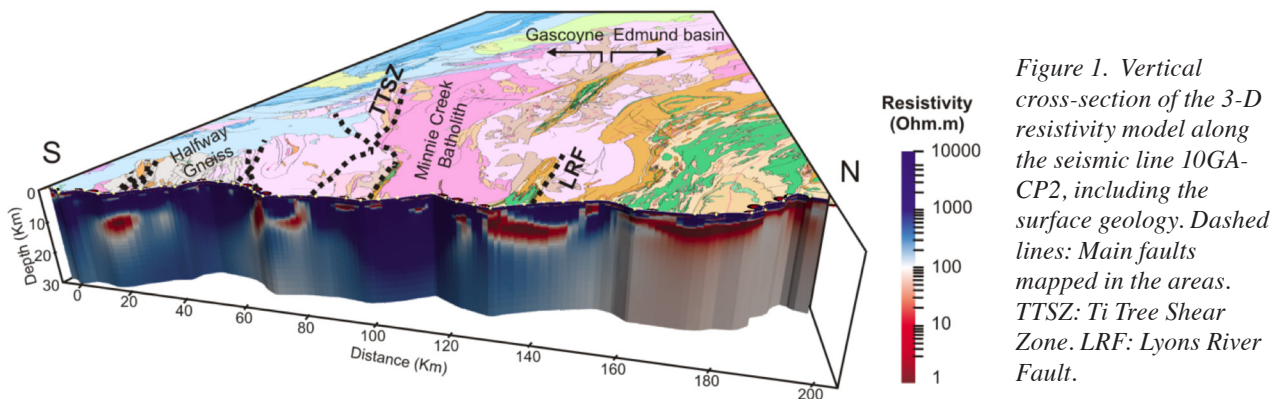
P. PIÑA-VARAS AND M. DENTITH

Centre for Exploration Targeting, School of Earth Sciences, The University of Western Australia, 35 Stirling Highway, Crawley, Western Australia 6009 (perla.pinavaras@uwa.edu.au)

In April 2010, deep reflection-seismic data were collected along three different transects across the western part of the Capricorn Orogen (Western Australia), in order to better understand the depth and shape of the numerous granitic batholiths mapped in the area, as well as the overall architecture of the Edmund and Collier Basins. In October of the same year, an extensive magnetotelluric (MT) survey was conducted along the same transects, where both broadband (BBMT) and long period (LMT) MT sites were collected. Data were inverted using 2-D algorithms, although data analysis reveals the area to be complex and geoelectrically 3-D in some regions and for some period ranges [1].

Now, 3-D inversion models (Fig. 1) have been performed by using the BBMT sites collected along the three seismic lines (2010 survey). This approach allows us to include the whole dataset in the inversion process. To perform the previous resistivity models, those data affected by 3-D effects, and consequently in disagreement with the 2-D assumption, were not included in the inversion process. Thus, the 3-D inversion models are able to resolve new structures, but also provide a more accurate imaging of the geometry of the structures resolved in both 2-D and 3-D resistivity models.

Joint interpretation of the 3-D resistivity models and the deep reflection-seismic sections is providing new and valuable information to better understand the crustal structures across the Western Capricorn Orogen.



REFERENCES

- [1] Johnson, S. et al. 2011. Capricorn Orogen Seismic and Magnetotelluric (MT) Workshop 2011: Extended abstracts. Geological Survey of Western Australia Report (Vol. 2011/5).

Paleoarchean lower crust in western China: Eoarchean growth of the continental crust

X. PING^{1,2}, J. ZHENG¹, W.L. GRIFFIN², H. DAI¹, S.Y. O'REILLY², Q. XIONG^{1,2}, H. TANG¹ AND Y. SU¹

¹School of Earth Sciences, State Key Laboratory of Geological Processes and Mineral Resources, China University of Geosciences, Wuhan 430074, China (xianquan.ping@mq.edu.au)

²Australian Research Council Centre of Excellence for Core to Crust Fluid Systems (CCFS) and GEMOC, Department of Earth and Planetary Sciences, Macquarie University, NSW 2109, Australia

Amazing Discovery

How has the continental crust of the early Earth evolved? Most of our knowledge comes from surface exposures. Although early Archean rocks are relatively scarce around the world [1], they are keys to revealing the early evolution of continents on Earth. In China, these rocks are distributed in its eastern part, represented by ~3.8 Ga TTG gneisses in the Anshan area [2] from the North China Craton and ~3.45 Ga TTG gneisses in the Kongling area [3] from the South China Craton. However, deep-seated xenoliths in volcanic rocks can provide more information about the early evolution of continental crust, even when early Archean rocks are absent on the surface. The ~3.65 Ga felsic granulite xenoliths have been reported in the Xinyang area in the southern margin of the eastern North China Craton [4], where the oldest age of the surface rocks is ~2.85 Ga.

So far, the oldest exposures in the western North China Craton are 2.5-2.7 Ga TTG gneisses [5], and therefore the early evolution of continental crust in the western part is still unclear. Here we report U-Pb ages and Hf-isotope analyses of zircons from mafic granulite xenoliths from the Langshan area, western China. The data reveal Early Archean (≥ 3.5 Ga) lower crust beneath the younger (<2.7 Ga) surface rocks in the western part of the craton, and suggest that the part (Western Block) is a discrete block with a Paleoarchean nucleus different from the eastern part of the craton (Eastern Block).

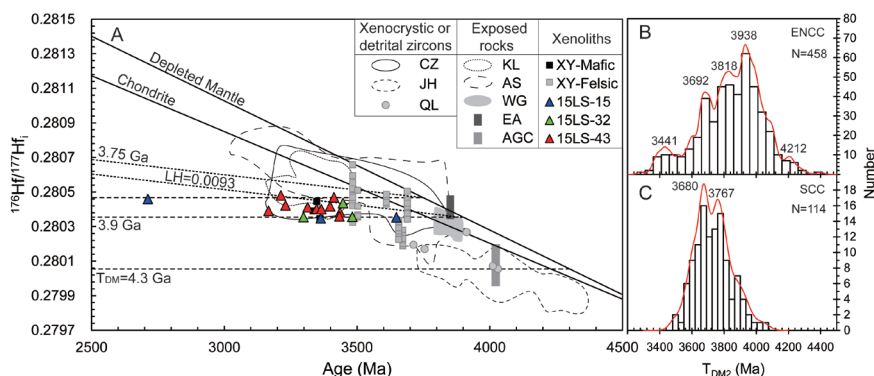


Figure 1. U-Pb age vs initial $^{176}\text{Hf}/^{177}\text{Hf}$ ratio of zircons from the Langshan mafic granulite xenoliths (A), histograms of two-stage Hf model ages (T_{DM2}) of zircons in early Archean rocks/xenoliths from the Eastern Block of the North China Craton (ENCC) (B) and South China Craton (SCC) (C). Data sources: the coloured triangles are from this study, while the others from Literatures.

The calculation of T_{DM2} refers to $^{176}\text{Lu}/^{177}\text{Hf} = 0.0093$ based on data from [6]. Abbreviations: LH, $^{176}\text{Lu}/^{177}\text{Hf}$; XY-Mafic, Xinyang mafic granulite xenolith; XY-Felsic, Xinyang felsic granulite xenolith; KL, Kongling area; AS, Anshan area; CZ, Caozhuang area; QL, North Qinling orogenic belt; JH, Jack Hills; EA, East Antarctica; AGC, Acasta Gneiss Complex; WG, Western Greenland.

Hf model ages of the zircons indicate extraction of the protoliths of the mafic granulite xenoliths from the mantle at ca 3.75-3.91 Ga. Integrating these observations with published data, we find that the continental crust in China evolved through a series of Eoarchean accretion events at 3.94 Ga, 3.82 Ga, 3.77 Ga and 3.69-3.68 Ga (Fig. 1). Since the exposed upper continental crust in at least some cratons is underlain by early Archean crust, estimates of crustal growth rates through time will need revision.

REFERENCES

- [1] Condie, K. 2007. The distribution of Paleoarchean Crust, in van Kranendonk, M.J. Smithies, R.H. and Bennett, V.C. eds., *Earth's Oldest Rocks. Developments in Precambrian Geology*, 15, London, Elsevier, 9-18.
- [2] Liu, D.Y. et al. 1992. Remnants of 3800 Ma crust in Chinese part of the Sino-Korean craton. *Geology*, 20, 339-342.
- [3] Guo, J.L. et al. 2014. 3.45 Ga granitic gneisses from the Yangtze Craton, South China: Implications for Early Archean crustal growth. *Precambrian Research*, 242, 82-95.
- [4] Zheng, J.P. et al. 2004. 3.6 Ga lower crust in central China: new evidence on the assembly of the North China Craton. *Geology*, 32, 229-232.
- [5] Zhai, M.G. 2015. *Precambrian Geology of China*. Berlin, Springer, p. 1-389.
- [6] Vervoort, J.D. and Patchett, P.J. 1996. Behavior of hafnium and neodymium isotopes in the crust: constraints from Precambrian crustally derived granites. *Geochimica et Cosmochimica Acta*, 60, 3717-3733.

The composition of melts in the incipient melt regime

Z. PINTÉR¹, S.F. FOLEY¹, G.M. YAXLEY² AND T. RUSHMER¹

¹Australian Research Council Centre of Excellence for Core to Crust Fluid Systems (CCFS) and GEMOC, Department of Earth and Planetary Sciences, Macquarie University, Sydney, NSW 2109, Australia (laura.otter@hdr.mq.edu.au)

²Research School of Earth Sciences, The Australian National University, Australian Capital Territory 0200, Australia (greg.yaxley@anu.edu.au)

The composition of mantle-derived magmas suggests a remarkable variety in the abundances of volatiles of the upper mantle. Volatile components, like H- and C-species (H_2O , CO_2 , CH_4 , H_2), generally depress the melting point of mantle considerably [1]. However we have little knowledge about these first, incipient melts.

The incipient melts exist in a large temperature range ($\sim 300^\circ\text{C}$) in the upper mantle, but the chemical compositions of these melts are poorly constrained, and therefore the effect of volatiles on the various melt proportions could change the behaviour of melt significantly. The nature of these incipient melts is also strongly dependent on oxygen fugacity [2], which controls the abundance of H- and C-species in the melt (carbonatitic, carbonate-bearing or hydrous silicate melt character).

Nature provides us with limited samples of primitive mantle-derived melts, which have mostly suffered fractionation or weathering processes. Therefore it's necessary to simplify the picture for studying the primitive melts. Experimental petrology provides better insights into the incipient melting regime in mantle conditions. My project consists of a systematic study to determine the chemistry of incipient melts with various volatile compositions, considering the effects of temperature and pressure in the incipient melt regime, using piston cylinder apparatus.

REFERENCES

- [1] Green, D.H. 2015. Experimental petrology of peridotites, including effects of water and carbon on melting in the Earth's upper mantle. *Physics and Chemistry of Minerals*, 42, 95-122.
- [2] Foley, S.F. 2011. A reappraisal of redox melting in the Earth's Mantle as a function of tectonic setting and time. *Journal of Petrology*, 52, 1363-1391.

Global paleogeography at 2.0-1.6 Ga

S.A. PISAREVSKY, Z.X. LI, Y. LIU, U. KIRSCHER AND R. MITCHELL

Earth Dynamics Research Group, ARC Centre of Excellence for Core to Crust Fluid Systems (CCFS) and The Institute for Geoscience Research (TIGeR), Department of Applied Geology, Curtin University, GPO Box U1987, WA 6845, Australia (Sergei.Pisarevskiy@curtin.edu.au)

The 2.0-1.6 Ga time interval in Earth's history was marked by worldwide orogenic events [1]. These events were associated with the assembly of the Laurentia (the cratonic part of North America), Baltica, Siberia, Australia, North China, and Kalahari cratons [2, 3, 4, 5], and accretionary growth of others [6]. In particular, the Statherian period (1.8-1.6 Ga) [7] was characterised by the final assembly of possibly the first supercontinent Nuna. Recent 1.9-1.8 Ga paleogeographic reconstructions based on new paleomagnetic data demonstrate that Nuna, and even its building blocks such as Laurentia, did not assemble before 1.86-1.87 Ga [8, 9]. The Wyoming Craton joined Laurentia only by ~1.72 Ga [10]. The three segments of Baltica (the cratonic part of Europe) - Fennoscandia, Sarmatia and Volgo-Uralia - did not amalgamate into a single entity until 1.8-1.75 Ga [13]. There are several lines of evidence suggesting that the final assembly of Nuna occurred during the ~1.6 Ga collision of Australia with Laurentia [11, 12]. Three segments of Baltica (cratonic part of Europe) - Fennoscandia, Sarmatia and Volgo-Uralia - did not amalgamate into a single entity until 1.8-1.75 Ga [13]. A recent detailed study of the Svecofennian orogeny in Fennoscandia [13] does not support the SAMBA model, and instead suggests that Amazonia was not connected to Baltica. The paleopositions of India and Kalahari in relation to Nuna are uncertain.

Here we present a new global paleogeographic animation for the 2.0-1.6 Ga interval. This model is based on 76 new high-quality paleomagnetic poles from cratons Superior, Slave, Rae, Fennoscandia, Volgo-Sarmatia, North and West Australia, Amazonia Siberia and North China, including several new poles produced by the Curtin team. In making this animation, we also utilised recent geological models for cratonic assemblies and other geological constraints such as using the Large Igneous Provinces barcode to match across cratons.

REFERENCES

- [1] Zhao, G. et al. 2009. The Xiong'er volcanic belt at the southern margin of the North China Craton: Petrographic and geochemical evidence for its outboard position in the Paleo-Mesoproterozoic Columbia Supercontinent. *Gondwana Research*, 16, 170-181.
- [2] Hoffman, P.F. 1988. United plates of America, the birth of a craton: early Proterozoic assembly and growth of Laurentia. *Annual Review of Earth and Planetary Sciences*, 16, 543-603.
- [3] Pisarevsky, S.A. et al. 2008. Proterozoic Siberia: a promontory of Rodinia. *Precambrian Research*, 160, 66-76.
- [4] Cawood, P.A. and Korsch, R.J. 2008. Assembling Australia: Proterozoic building of a continent. *Precambrian Research*, 166, 1-38.
- [5] Hanson, R.E. et al. 2011. Paleomagnetic and geochronological evidence for large-scale post-1.88 Ga displacement between the Zimbabwe and Kaapvaal cratons along the Limpopo belt. *Geology* 39, 487-490.
- [6] Brito Neves, B.B. 2011. The Paleoproterozoic in the South-American continent: diversity in the geologic time. *Journal of South American Earth Sciences*, 32, 270-286.
- [7] Nance, R.D. and Murphy, J.B. 2013. Origins of the supercontinent cycle. *Geoscience Frontiers*, 4, 439-448.
- [8] Buchan, K.L. et al. 2016. Paleo- magnetism of ca. 2.13-2.11 Ga Indin and ca. 1.885 Ga Ghost dyke swarms of the Slave craton: Implications for the Slave craton APW path and relative drift of Slave, Superior and Siberian cratons in the Paleoproterozoic. *Precambrian Research*, 275, 151-175.
- [9] Klein, R. et al. 2016. A late Paleoproterozoic key pole for the Fennoscandian Shield: A paleomagnetic study of the Keuruu diabase dykes, Central Finland. *Precambrian Research*, 286, 379-397.
- [10] Kilian, T.M. et al. 2016. Wyoming on the run -toward final Paleoproterozoic assembly of Laurentia. *Geology*, 44, 863-866.
- [11] Betts, P.G. and Giles, D. 2006. The 1800-1100 Ma tectonic evolution of Australia. *Precambrian Research*, 144, 92-125.
- [12] Pisarevsky, S.A. et al. 2014. Mesoproterozoic paleogeography: supercontinent and beyond. *Precambrian Research*, 244, 207-225.
- [13] Bogdanova, S.V. et al. 2013. Trans-Baltic Palaeoproterozoic correlations towards there construction of supercontinent Columbia/Nuna. *Precambrian Research*, 259, 5-33.

Permian magmatism in an early Andean metallogenic belt, Cordillera Frontal, Argentina

G.H. POOLE^{1,2}, S.G. HAGEMANN², A.I.S. KEMP², M.L. FIORENTINI^{1,2} AND E.O. ZAPPETTINI³

¹Australian Research Council Centre of Excellence for Core to Crust Fluid Systems (CCFS), The University of Western Australia, 35 Stirling Highway, Crawley, WA 6009, Australia (gregory.poole@research.uwa.edu.au, marco.fiorentini@uwa.edu.au)

²Centre for Exploration Targeting, School of Earth Sciences, University of Western Australia, Crawley, Western Australia 6009, Australia (steffen.hagemann@uwa.edu.au, tony.kemp@uwa.edu.au)

³Servicio Geológico Minero Argentino (SEGEMAR), Argentina, Av. General Paz 5445 (colectora), Parque Tecnológico Miguelete, Edificio 25 San Martín (B1650 WAB), Provincia de Buenos Aires, Argentina (eduardo.zappettini@segemar.gov.ar)

The Andean margin has experienced continuous subduction processes for over 300 million years and is the case study location for modern “Cordillera-type arc” subduction systems. Across this protracted period of evolution, epochs of porphyry Cu-Au-Mo and epithermal Au-Ag systems have occurred in well constrained metallogenic belts. Certain epochs, such as the Miocene-early Pliocene and middle Eocene-early Oligocene, are well endowed with metals and tend to form in more recent times. During the early history of the Andes, lesser known and sometimes thought of as unfavourable or infertile belts occurred, one being a Permian belt consisting of several porphyry and epithermal systems located in the Cordillera Frontal, Argentina. This belt developed promptly after the initial onset of subduction and is thought to be genetically related to the extensive volcanic Choiyoi Group, a period of arc relaxation that produced copious amounts of felsic volcanism covering most of the Andes between 26° and 42°S. This study collected igneous material related to eleven mineral occurrences located within this Permian belt, however the effects of hydrothermal alteration, exposure and burial reduces the possible information we can obtain from such samples. However, resistive minerals like zircon can withhold crucial information on the absolute age, magma source, fertility and composition to decipher the metallogenic history of an early Andean porphyry and epithermal belt.

Nuna final assembly nailed by crustal thickening at 1600 Ma in NE Australia and NW Laurentia

A. POURTEAU¹, M. SMIT², S. VOLANTE¹, A. NORDSVAN¹, J. LI¹, W.J. COLLINS¹ AND Z.X. LI¹

¹Earth Dynamics Research Group, ARC Centre of Excellence for Core to Crust Fluid Systems (CCFS), The Institute for Geoscience Research (TIGeR), Department of Applied Geology, Curtin University, GPO Box U1987, WA 6845, Australia (amaury.pourteau@curtin.edu.au)

²Pacific Centre for Isotope and Geochemical Research, Department of Earth, Ocean & Atmospheric Sciences, University of British Columbia, 2020–2207 Main Mall (EOS South Rm. 363), Vancouver, British Columbia, V6T 1Z4, Canada

Widespread 2.1–1.8 Ga orogens between Archean–Palaeoproterozoic crustal blocks worldwide record the preliminary assembly of the supercontinent Nuna; however, complete amalgamation did not occur until the juxtaposition of Laurentia to Australia and Antarctica some time before 1540 Ma [1]. Orogenic events between 1650–1540 Ma in eastern Australia have been ascribed to collision with western Laurentia, as suggested by the palaeomagnetic record. However, the record of crustal thickening associated with this final event of Nuna assembly has remained elusive.

Proterozoic inliers in NE Australia are characterised by ca. 100–300 Myr of sedimentation and volcanism in a continental back-arc setting followed by deformation and metamorphism between <1650 and 1540 Ma (Isan Orogeny and equivalents), and late to post-orogenic magmatism until ca. 1500 Ma. The metamorphic record of this orogeny is dominated by a low-*P*, high-*T* imprint and the production of both I-type and S-type granites. Several of the metamorphic domains, especially in the Mt. Isa Inlier, followed counter-clockwise *P*–*T* paths with prograde andalusite, peak sillimanite, and retrograde kyanite. Other regions, like the easternmost Mt. Isa Inlier and the central Georgetown Inlier, evolved along clockwise *P*–*T* paths, with an early medium-*P*/*T* stage and a subsequent thermal pulse. Whereas the high-*T* phase and associated magmatism is constrained between 1585 and 1540 Ma depending on regions, the timing of the early, medium-*P*/*T* stages has been largely unknown.

Here, we report Lu–Hf MC-ICPMS analyses of garnet and *P*–*T* estimates based on equilibrium phase diagrams for medium-grade metapelitic samples from the Robertson River area (central Georgetown Inlier) and the Snake Creek Anticline (easternmost Mt. Isa Inlier). Three-point Lu–Hf isochrons give a 1599.4 ± 3.7 Ma date for a garnet–staurolite schist from the Robertson River, and a 1606.6 ± 2.8 Ma date for a garnet phyllite and a 1605.5 ± 3.8 Ma date for a garnet–staurolite–andalusite schist from the Snake Creek Anticline. Conditions for garnet growth are estimated at ~0.6 GPa and from 530 to 560°C in the Robertson River, and at ~0.4 GPa and from 530–600°C in the Snake Creek Anticline. However, the presence of prograde kyanite in the Snake Creek Anticline [2] suggests higher *P* in places.

Our results, the first precise age estimates for crustal thickening associated with the final assembly of Nuna, show coeval prograde metamorphism in the easternmost Mt. Isa and central Georgetown inliers at ca. 1600 Ma. Given the N-Laurentian affinity of the Georgetown sedimentary rocks [3] and the seismically-imaged crustal imbrication of the region, we regard the Georgetown Inlier as part of an exotic continental domain that was accreted to the Mt. Isa continental back-arc basin at 1605–1600 Ma, consolidating the North Australian craton. Contemporaneous medium-*P*/*T* metamorphism occurred during the 1610–1600 Ma Racklan Orogeny in NW Laurentia. We therefore interpret the coeval prograde medium-*P*/*T* metamorphic events at 1610–1600 Ma in NE Australia and NW Laurentia, as well as subsequent low-*P*/high-*T* events (1590–1550 Ma), as results of crustal thickening associated with the assembly of Nuna, and subsequent post-collisional processes, respectively, therefore for the first time nailing the final assembly of the supercontinent Nuna.

REFERENCES

- [1] Pisarevski et al. 2014. Mesoproterozoic paleogeography: Supercontinent and beyond. *Precambrian Research*, 224, 207–225.
- [2] Rubenach et al. 2008. Age constraints on the tectonothermal evolution of the Selwyn Zone, Eastern Fold Belt, Mount Isa Inlier. *Precambrian Research*, 163, 81–107.
- [3] Nordsvan et al. 2017. Laurentian crust in NE Australia: A critical tie-point during the assembly of the supercontinent Nuna. (under review).

A reference global lithospheric and upper mantle model for gravity and integrated studies

F. SALAJEGHEH AND J.C. AFONSO

Australian Research Council Centre of Excellence for Core to Crust Fluid Systems (CCFS) and GEMOC, Department of Earth and Planetary Sciences, Macquarie University, Sydney, NSW 2109, Australia (farshad.salajegheh@mq.edu.au)

The ever-increasing interest in the generation of high-resolution models of the lithosphere's thermochemical state by industry and academia has stimulated the development of joint inversions of multiple geophysical data sets. These types of inversions are computationally expensive and rely on efficient algorithms to solve the forward problems. Potential field data (e.g. gravity, geoid and GOCE gravity gradients data) is of particular interest given their complementary sensitivities to both crustal and deep lithospheric structure, as well as to bulk composition when jointly inverted with seismic data. When the inversion is performed in 3D Cartesian geometry, very efficient solvers exist, and this why most implementations of multi-observable probabilistic inversions rely on such geometry. This, however, precludes the application of the inversion method to large-scale domains (e.g. continental or global studies).

For the forward calculation in 3D spherical coordinates, we have implemented the prism approximation for calculating tesseroids' gravity signals (Fig. 1). This removes numerical problems (singularities) at elevations close to the tesseroid's surface. However, a series of coordinate transformations is required to connect the local rectangular prism to the global spherical coordinates.

We have applied a linearised Quasi-Newton algorithm to jointly invert free-air gravity, geoid anomalies, topography and gravity gradients data. We obtain variations in Moho depth, average crustal density, average asthenosphere density (all *in situ*) and LAB depth for the entire globe. This method is able to provide, in a relatively efficient way, a simplified global lithospheric model, which can be subsequently used to model edge effects in regional studies or to serve as a reference model for high-resolution inversions. In this study, we

propose a parallel computation procedure that allows us to obtain fast and reliable solutions of the joint inversion in the presence of large multi-observable datasets at global scale and present a global lithospheric model by inverting gravity anomalies, gravity gradients, geoid anomalies and absolute elevation.

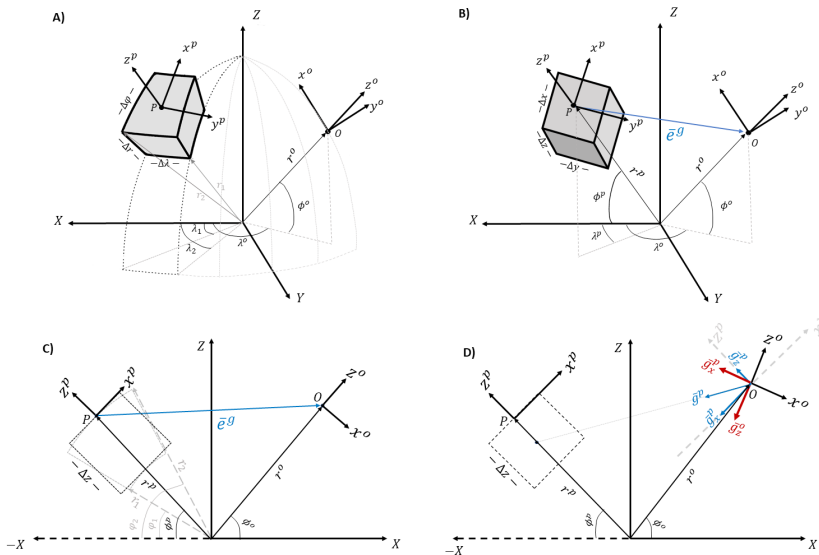


Figure 1. A-B) Geometry of a tesseroid replaced by a rectangular prism with mass equivalence and identical vertical extension. C-D) Transformation of the local edge system of the prism in the reference system of the computation point.

REFERENCES

- [1] Wild-Pfeiffer, F. 2008. A comparison of different mass elements for use in gravity gradiometry. *Journal of Geodesy*, 82, 637-653.
- [2] Tarantola, A. 2005. *Inverse Problem Theory and Model Parameter Estimation*. Society for Industrial and Applied Mathematics. Philadelphia.

Identifying open-system behaviour in Sm/Nd and U/Pb data in titanite

E. SCIBIORSKI^{1,2,3}, C. KIRKLAND⁴, A. KEMP³, E. TOHVER³, N. EVANS⁵ AND M. FIORENTINI^{1,2}

¹ARC Centre of Excellence in Core to Crust Fluid Systems (CCFS), University of Western Australia, 35 Stirling Highway, Crawley, WA 6009, Australia (elisabeth.scibiorski@research.uwa.edu.au)

²Centre for Exploration Targeting, University of Western Australia, 35 Stirling Highway, Crawley, WA 6009, Australia

³School of Earth Sciences, University of Western Australia, 35 Stirling Highway, Crawley, WA 6009, Australia

⁴Australian Research Council Centre of Excellence for Core to Crust Fluid Systems (CCFS) and Department of Applied Geology, Curtin University, Kent Street, Bentley, WA 6102, Australia

⁵John de Laeter Centre, The Institute for Geoscience Research, Department of Applied Geology, Curtin University, Kent Street, Bentley, WA 6102, Australia

Titanite is a valuable chronometer as it occurs in a wide variety of geological settings, and may record multiple stages of high-grade metamorphism and fluid mobility. Although titanite is most commonly used for U/Pb geochronology, Sm/Nd data may be used to obtain the Nd isotope composition at the time of titanite growth. In these cases, the U/Pb isotope system provides valuable context for the interpretation of titanite Sm/Nd data.

Here, we use three titanite-bearing samples from the Mesoproterozoic Albany-Fraser Orogen of Western Australia to investigate the behaviour of the U/Pb and Sm/Nd isotopic systems in titanite. We used LA-SS-ICPMS to analyse the U/Pb, Sm/Nd and trace element composition of titanite *in situ* in thin section. The samples were selected to encompass a range of processes, from a simple system with a single titanite population, to a more complicated case showing evidence of open-system behaviour.

Chondrite-normalised REE abundance patterns discriminate between multiple populations of titanite in each sample. These populations correlate with distinct BSE microstructures and petrographic context, as well as the behaviour of the U/Pb and Sm/Nd isotope systems.

In one sample, a single compositional population of titanite yields a homogenous cluster of U/Pb data. Similarly, the Sm/Nd data define a single isochron with low dispersion in $^{147}\text{Sm}/^{144}\text{Nd}$ values. This suggests that titanite in this sample remained a closed system following crystallisation.

In a second sample, two compositional populations of titanite were subjected to age resetting during metamorphism, and yielded a single U/Pb age. The two titanite populations differ slightly in Sm/Nd characteristics, primarily in $^{147}\text{Sm}/^{144}\text{Nd}$ and ϵNd values, but define a single isochron line, suggesting a single Sm/Nd reservoir for titanite in this sample. Therefore, differences in the Sm and Nd content may be a product of titanite recrystallisation during metamorphism.

In the third sample, the U/Pb data are distributed along a mixing line between radiogenic and common (non-radiogenic) Pb. Analyses of titanite with a high proportion of radiogenic lead define an isochron in Sm/Nd space, whereas titanite analyses that contain a high proportion of common lead are discordant, and plot below the isochron. This suggests that the incorporation of common lead into the titanite was accompanied by open system behaviour in Sm/Nd.

A small, unextractable partial melt fraction as the cause for Earth's weak asthenosphere

K. SELWAY¹, J.P. O'DONNELL², C. CONRAD³ AND M. SMIRNOV³

¹Australian Research Council Centre of Excellence for Core to Crust Fluid Systems (CCFS) and GEMOC, Department of Earth and Planetary Sciences, Macquarie University, Sydney, NSW 2109, Australia

²School of Earth and Environment, University of Leeds, UK

³Centre for Earth Evolution and Dynamics (CEED), University of Oslo, Norway

⁴Division of Geosciences and Environmental Engineering, Luleå Technical University, Sweden

The cause for the changes in viscosity and physical properties between the lithosphere and asthenosphere is still debated. The two main possibilities are that the asthenosphere contains a small amount of partial melt or a small amount of hydrogen in its constituent minerals. We combine recent magnetotelluric, seismic and experimental data to show that the geophysical properties of old oceanic asthenosphere cannot universally be explained by hydrogen, but are consistent with the presence of $\sim 0.1\%$ partial melt. This interpretation relies on magnetotelluric data from the ~ 130 Ma north-west Pacific lithosphere and the ~ 70 Ma central Pacific lithosphere. MT data from the lithosphere beneath Svalbard suggest the presence of an even larger melt fraction, presumably due to the effects of the proximal Mid-Atlantic Ridge. The presence of an extensive partial melt fraction in the oceanic asthenosphere is also supported by a recent compilation of seamount data, which shows that significant volumes of seamounts are erupted on oceanic lithosphere older than 60 Ma.

The estimate of $\sim 0.1\%$ partial melt in old oceanic asthenosphere corresponds with the volume of unextractable melt expected to remain in the asthenosphere after melting at mid-ocean ridges. We suggest that this melt fraction is essentially trapped in the asthenosphere as it convects away from a mid-ocean ridge (Fig. 1). Asthenospheric viscosities calculated from this melt fraction reproduce the predicted viscosity drop between the lithosphere and asthenosphere. This unextractable partial melt fraction may be the primary driver of the different rheological characteristics of the lithosphere and asthenosphere. Solidus temperature calculations (Fig. 1) show that the oceanic lithosphere-asthenosphere boundary lies at the approximate temperature where this unextractable partial melt volume crystallises; this may be a primary definition of this boundary. These results enable more accurate links to be made between geophysical data and models of mantle volcanism, volatile contents, and viscosity, with implications for geodynamic and glacial isostatic adjustment models.

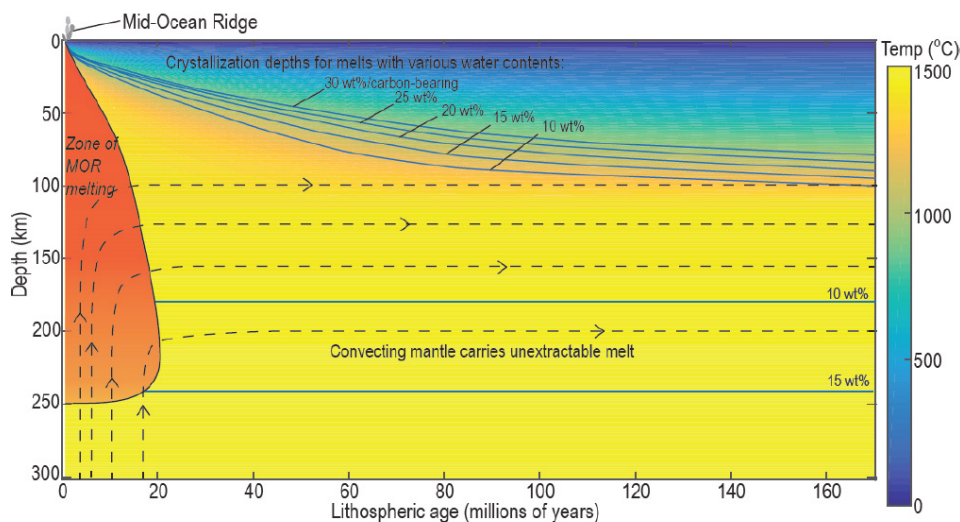


Figure 1. Distribution of partial melt in the oceanic upper mantle. Melting occurs beneath the mid-ocean ridge (MOR), denoted schematically by the red shaded region. As the upper mantle ages, it convects away from the MOR (black dashed lines) and carries with it an unextractable melt fraction of $\sim 0.1\%$. This unextractable melt will remain in the upper mantle until the temperature drops enough that the melt crystallises. The blue lines show the depths at which melt containing 10–30 wt % water, which is within the expected range for upper mantle melt compositions, will crystallise for a typical upper mantle geotherm (52). Such melts will crystallise at the approximate depth of the lithosphere-asthenosphere boundary, possibly explaining the contrasts in strength, seismic velocities and electrical resistivities across this boundary.

Variations in regional stresses, geometry and shape of low strengths zones controls the periodic Alice Springs Orogeny

D. SILVA¹, S. PIAZOLO², N. DACZKO¹, T. RAIMONDO³, G. HOUSEMAN⁴ AND L. EVANS⁵

¹ARC Centre of Excellence for Core to Crust Fluid Systems (CCFS) and GEMOC, Department of Earth and Planetary Sciences, Macquarie University, Sydney, NSW 2109, Australia (David.barbosa-da-silva@hdr.mq.edu.au)

²School of Earth and Environment, University of Leeds, Leeds, LS2 9JT, United Kingdom

³School of Natural and Built Environments, University of South Australia, Adelaide, SA 5001, Australia

⁴Institute of Geophysics and Tectonics, University of Leeds, Leeds, LS2 9JT, United Kingdom

⁵School of Earth Sciences, University of Melbourne, Carlton, VIC 3053, Australia

The intracontinental Alice Springs Orogeny (ASO), central Australia, is a long lasting polyphase orogeny spanning a period from 450 Ma to 300 Ma. Due to the periodic nature of ASO orogenesis, numerical modelling using the software Basil was performed to model the deformation in the ASO. The model used as parameters the lithospheric stress propagation from N-S and E-W, representing the possible Gondwana-Laurussia amalgamation and the periodic extensional and compressional movement of paleo-Pacific subduction system, respectively. Additionally, a weaker rheological crustal element representing the Larapinta rift was added to understand the tectonic implication of a submersive wedge in the ASO deformation. We conclude that a combination of compressional or extensional movement of the paleo-Pacific plate, added to a soft rift system in the west, best represents the deformation in ASO.

Phosphogenesis in the immediate aftermath of the Great Oxygenation Event: Evidence from the Turee Creek Group, Western Australia

G.G. SOARES^{1,2}, E. BELOUSOVA¹, S.N. THOMSON³ AND M. VAN KRAANENDONK^{1,2}

¹Australian Research Council Centre of Excellence for Core to Crust Fluid Systems (CCFS) and GEMOC, Department of Earth and Planetary Sciences, Macquarie University, Sydney, NSW 2109, Australia (g.soares@unsw.edu.au)

²The Australian Centre for Astrobiology (ACA) and Pangea Centre of Research, School of Biological Earth and Environmental Science, UNSW, Sydney, NSW 2052, Australia

³Department of Geosciences, University of Arizona, Gould-Simpson Building, Tucson, AZ 85721-0077, USA

The influence of atmospheric oxygen on biological evolution is not well constrained due to the lack of well-preserved fossiliferous units surrounding the Great Oxidation Event (GOE). The ~2.4 Ga stromatolite-thrombolite carbonate reef complex, in the Turee Creek Group of Western Australia, coincides with the GOE and demonstrates microbial complexity not seen in older stromatolitic reefs [1]. Our research presents centimetric microbial mat fragments and millimetric organic-rich peloids that contain apatite granules and euhedral apatite crystals. These demonstrate a direct correlation between the presence of oxygen, evidenced by phosphorous rich stromatolites, and increased microbial complexity within the stromatolite-thrombolite reef.

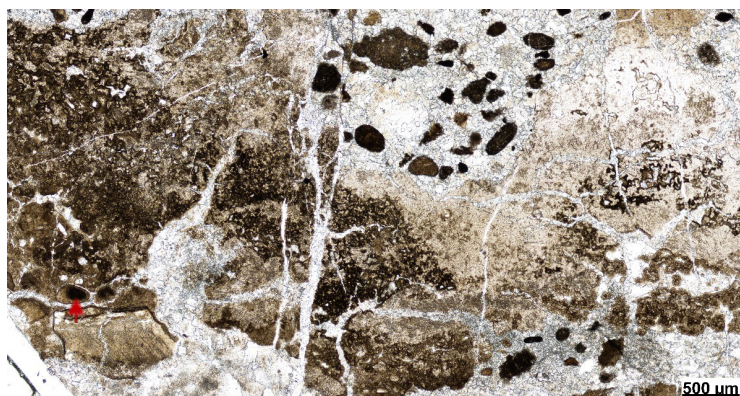


Figure 1. Petrographic image in PPL of fossilised microbial mat fragment, surrounded by smaller rounded peloids.

Petrographic examination of the mat fragments reveals complex internal textures interpreted as primary features (Fig. 1). Significant components of the mats include: abundant fine apatite granules; rounded clumps of silica; disseminated kerogen; and kerogenous, apatite- and quartz crystal bearing peloids (red arrow

Fig. 1). Peloids of the same composition also occur in the fine intercolumn dolomitic sediment, some of which also contain clay minerals.

The ripped-up, phosphorous-rich microbial mat clasts are interpreted to represent fragments of a peritidal phosphorite deposit, enriched in phosphate through microbial activity in a thin, oxygenated zone of a shallow marine basin. The kerogenous apatite- and quartz-crystal-bearing peloids likely formed within the mat, via degradation of organic material, resulting in the authigenic precipitation and accumulation of apatite granules. The clay-bearing peloids are interpreted to represent peloids that have been affected by Paleoproterozoic surficial weathering and then re-sedimented and captured both in the mats and in the intercolumn sediment. Euhedral apatite crystals that line the insides of peloids were dated as 2104 ± 70 Ma and 1987 ± 26 Ma, using two different methods. This age of c. 2.0 Ga is interpreted to represent the time of metamorphic fluid circulation in the reef complex during regional orogenesis and provides a new minimum age of the reef. These results establish oxygen as present in the shallow water of the stromatolite-thrombolite reef, illustrating that atmospheric change may have influenced biological evolution.

REFERENCES

[1] Barlow, E. et al. 2016. Lithostratigraphic analysis of a new stromatolite-thrombolite reef from across the rise of atmospheric oxygen in the Paleoproterozoic Turee Creek Group, Western Australia. *Geobiology*, 14, 317-343. doi:10.1111/gbi.12175.

Geology and genesis of Fe-Ni-Cu-(PGE) mineralisation in the Black Label Hybrid Zone of the 2.7 Ga Black Thor Intrusive Complex, McFaulds Lake greenstone Belt, Ontario, Canada

C.S. SPATH III^{1,2}, C.M. LESHER², N. FARHANGI² AND M.G. HOULÉ^{3,2}

¹Centre for Exploration Targeting and the ARC Centre of Excellence for Core to Crust Fluid Systems (CCFS), School of Earth Science, University of Western Australia, 35 Stirling Highway, Crawley, WA, 6009, Australia

²Mineral Exploration Research Centre, Laurentian University, 935 Ramsey Lake Road, Sudbury, Ontario, P3E 2C6 (cspath@laurentian.ca)

³Geological Survey of Canada, 490 rue de la Couronne, Québec City, Québec, G1K 9A9

The 2.7 Ga Black Thor Intrusive Complex (BTIC) is a >5 km long, ~1.5 km thick, >1 km wide (open at depth) layered intrusion that has been rotated to a sub-vertical orientation and is composed of dunite, lherzolite, olivine websterite, websterite, and chromitite overlain by lesser gabbro and anorthosite. All lithologies have been metamorphosed to lower greenschist facies, but most contain well-preserved igneous textures, which contain relict igneous chromite, pyroxene, and olivine. After emplacement, but before complete crystallisation, a petrogenetically-related Late Websterite Intrusion (LWI) reactivated the feeder conduit invading the lower and central part of the BTIC, including the Black Label Chromitite Zone (BLCZ) and Black Thor Chromitite Zone (BTCZ). Field and petrographic examination shows that the LWI magma disaggregated and partially assimilated parts of the BLCZ producing marginal zones of heterogeneous, interfingering hybrid LWI matrix with variably sized (<2 m, rarely > 5 m) lherzolite/dunite/chromitite inclusions and chromite/olivine xenocrysts defined as the Black Label Hybrid Zone (BLHZ). The BLHZ contains 5-20% patchy disseminated to patchy net-textured Fe-Ni-Cu-(PGE) sulfide mineralisation that is spatially restricted to the hybrid zones with no sulfide in adjacent inclusion-poor LWI or in unbrecciated BLCZ. Sulfide preferentially wets olivine relative to pyroxene with interfacial angles ranging 20-55°, mainly 25-35° (olivine) and 75-95° (pyroxene). The low interfacial angles for olivine suggest a relatively high fO_2 within the system. Although the BTIC contains basal concentrations of Fe-Ni-Cu-(PGE) sulfides (e.g. AT-12, AT-12 Extension, and Contact Zone, and the larger Eagle's Nest deposit), only the most fractionated interstitial phases of the LWI contain minor Fe-Ni-Cu-(PGE) sulfides (i.e. it was not saturated in sulfide on emplacement). The BLCZ contains anomalous PGE-Cu-Ni, but only a small amount of sulfides. The relatively high (normal) PGE contents of the mineralisation in the BLHZ indicates that the LWI magma had not previously segregated sulfides. The restriction of sulfide mineralisation to the BLHZ indicates that it formed during partial melting and assimilation of the BLCZ by the LWI (i.e. Fe-Ni-Cu-(PGE) sulfides were generated by decreasing sulfide solubility when the more evolved LWI magma incorporated cumulate rocks generated by the more primitive phase of the magma that formed the BTIC). Although there have been many models proposed for the generation of Fe-Ni-Cu-(PGE) sulfides by magma mixing and magma contamination by country rocks, this appears to be one of the first examples of mineralisation generated by contamination of a magma by cognate xenoliths and xenocrysts.

The recognition of former melt flux through high-strain zones

C.A. STUART¹, S. PIAZOLO^{1,2} AND N.R. DACZKO¹

¹ARC Centre of Excellence for Core to Crust Fluid Systems (CCFS) and GEMOC, Department of Earth and Planetary Sciences, Macquarie University, Sydney, NSW, 2109, Australia (catherine.stuart@students.mq.edu.au; nathan.daczko@mq.edu.au)

²School of Earth and Environment, University of Leeds, Leeds, UK (s.piazolo@leeds.ac.uk)

High-strain zones are potential pathways of melt migration through the crust. However, the identification of melt-present high-strain deformation is commonly limited to cases where the interpreted volume of melt ‘frozen’ within the high-strain zone is high (> 10 %). In this contribution, we examine high-strain zones in the Pembroke Granulite, an otherwise low-strain outcrop of volcanic arc lower crust exposed in Fiordland, New Zealand. These high-strain zones display compositional banding, flaser-shaped mineral grains, and closely spaced foliation planes indicative of high-strain deformation. Rare segregations of leucocratic material and coarse-grained peritectic garnet grains suggest deformation was synchronous with partial melting. High-strain zones lack typical mylonite microstructures and instead display typical equilibrium microstructures, such as straight grain boundaries, 120° triple junctions, and subhedral grain shapes. We identify five key microstructures indicative of the former presence of melt within the high-strain zones: (1) small dihedral angles of interstitial phases; (2) extremely elongate interstitial grains; (3) small aggregates of quartz grains with xenomorphic plagioclase grains connected in three dimensions; (4) fine-grained, K-feldspar bearing, multiphase aggregates with or without augite rims; and (5) mm- to cm-scale felsic dykelets. We propose that microstructures indicative of the former presence of melt, such as the five identified above, may be used as a tool for recognising rocks formed during melt-present high-strain deformation.

Multiple sulfur isotopes approach to interpret the source, development and precipitation of hydrothermal fluids in Archean orogenic gold deposits

D. SUGIONO, C.K. LAFLAMME, N. THEBAUD AND M.L. FIORENTINI

ARC Centre of Excellence in Core to Crust Fluid Systems (CCFS), University of Western Australia, 35 Stirling Highway, Crawley, WA 6009, Australia (dennis.sugiono@research.uwa.edu.au)

Mass independent fractionation ($\Delta^{33}\text{S}$) as applied to orogenic gold deposits has enabled new interpretation of source reservoirs of sulfur. Since gold in the Archean orogenic gold deposits is mainly transported by sulfur ligand complexes, the addition of $\Delta^{33}\text{S}$ adds new possibilities in interpreting $\delta^{34}\text{S}$ values due to mixing of sulfur reservoirs versus changes in fluid thermochemistry. *In situ* sulfur isotope analysis using Secondary Ion Mass Spectrometry (SIMS) has enabled us to analyse micron scale analyses for small sulfides and even different zonation within a single sulfide grain. The micro-scale analysis within texturally-constrained sulfide minerals can be used to better understand the source, evolution of the hydrothermal fluids and possibly the precipitation mechanics of the sulfides in relation to gold deposition (Fig. 1). Recent studies have revealed that Archean orogenic gold deposits source some of the sulfur from the Archean sedimentary rock record and that precipitation mechanics of gold is complex.

The Kanowna Belle deposit in the Kalgoorlie Terrane is a large 6.4 Moz Archaean orogenic gold deposit that lies near to the Fitzroy fault and is hosted within different stratigraphic and intrusive units of the Norsemen-Wiluna granite-greenstone belt. Multiple phases of veining and gold deposition with different alteration assemblages are observed in this deposit. There is also some debate regarding lithological controls on the gold mineralisation. Multiple sulfur isotopes will be used in conjunction with the lithology, structural correlation and vein paragenesis to understand the fluid evolution in the deposit. This will have bearing on our understanding of the fluids and mechanics of the formation of the first bloom of Archean orogenic gold deposits.

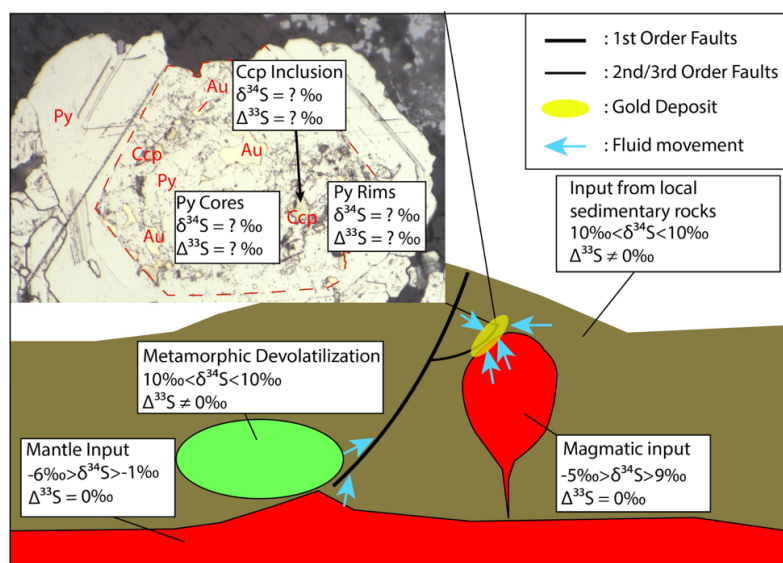


Figure 1. A model of Archean orogenic gold and their sulfur reservoirs. Different mechanisms of sulfur precipitation will influence different sulfur isotopic values on each growth zone.

The protracted and polyphased formation of the Agnew Gold Camp (Yilgarn Craton, Western Australia)

N. THÉBAUD^{1,2}, D. SUGIONO^{1,2}, C. LAFLAMME^{1,2}, J. MILLER³, L. FISHER³, F. VOUTÉ², S. TESSALINA⁴, I. SONNTAG³ AND M. FIORENTINI^{1,2}

¹ARC Centre of Excellence in Core to Crust Fluid Systems (CCFS), University of Western Australia, 35 Stirling Highway, Crawley, WA 6009, Australia (nicolas.thebaud@uwa.edu.au)

²Centre for Exploration Targeting, School of Earth Sciences Robert Street Building, M006, The University of Western Australia, 35 Stirling Hwy, Crawley, WA, 6009, Australia

³CSIRO Australian Resources Research Centre 26 Dick Perry Ave., Kensington 6151 Western Australia

⁴John de Laeter Centre, Curtin University, Building 301, Bentley 6845 Western Australia

The Archean orogenic gold class deposits have common characteristics and a similarity in gold mineralisation ages that provides evidence for a single late tectonic gold mineralisation event [1]. Although valid for a large majority of deposits in the Yilgarn, this model does not, however, account for certain atypical gold deposits. In the world-class Agnew Gold Camp (Yilgarn Craton, Western Australia) structural and paragenetic relationships, combined with a compilation of geochronology and multiple sulfur isotopes, indicate that mineralisation developed during a two stage process involving different fluid sources. The initial event dated at c. 2660 Ma is related to the onset of folding during Kalgoorlie Orogenesis and presents characteristics compatible with magmatic intrusion related mineralisation. A second event dated at c. 2630 Ma presents a mineral and metal inventory typical of Archean orogenic-like gold mineralisation, and developed at a later stage of orogenic process. Measurements of $\delta^{34}\text{S}$ and $\Delta^{33}\text{S}$ from spatially constrained samples from the two distinct mineralising events in the Agnew Gold Camp further ascertain contrasting fluid composition and/or reservoirs (Fig. 1). Combined with geochronological data obtained on the poly-magmatic Lawlers granitic dome, our study points towards a polyphased mineralisation process accompanied by the progressive magmatic emplacement of the Lawlers granitic dome; a mineralisation process involving early mineralisation of magmatic affinity followed

by a late mineralisation process involving Archean sedimentary sulfur reservoir in Au-bearing hydrothermal solution. We propose that the change in source reservoir for sulfur in hydrothermal fluids may be the result of a regional change in tectonic regime from compressive to transcurrent, allowing fluids to be first sourced from non-MIF-S-bearing magmas followed later by MIF-S-bearing metamorphic fluids.

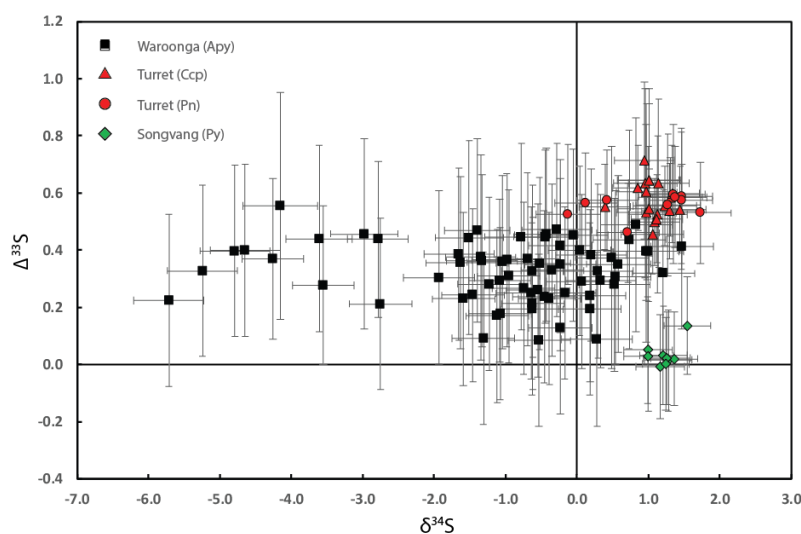


Figure 1. $\delta^{34}\text{S}/\Delta^{33}\text{S}$ plot for the Agnew Gold Camp including gold related sulfides from Songvang, Waroonga and Turret.

REFERENCES

- [1] Groves, D.I. et al. 1998. Orogenic gold deposits: a proposed classification in the context of their crustal distribution and relationship to other gold deposit types, *Ore Geology Reviews*, 13, 7-27.

Initial investigation of the gold occurrences in the Nuuk district, West Greenland

L. PIRES¹, N. THÉBAUD^{1,2}, J. KOLB^{1,2,3}, M. FIORENTINI^{1,2} AND C. LAFLAMME^{1,2}

¹Centre for Exploration Targeting, University of Western Australia, 35 Stirling Highway, Crawley, 6009 WA, Australia (nicolas.thebaud@uwa.edu.au)

²ARC Centre of Excellence for Core to Crust Fluid Systems (CCFS), University of Western Australia

³Karlsruhe Institute of Technology Institute for Applied Geosciences Geochemistry and Economic Geology Group Adenauerring 20b D - 76131 Karlsruhe Germany

The North Atlantic craton of southwestern Greenland hosts orogenic gold occurrences, although, to date, none are in production. The lack of economic gold deposits may find its origin in the fact that most of the considered Archean rocks are metamorphosed to the granulite and upper amphibolite facies metamorphic grades ($T \geq 550^\circ\text{C}$) [1]. Accordingly the Nuuk area represents a unique natural laboratory to investigate the nature and potential for mineralisation of high grade metamorphic terranes. Hydrothermal gold mineralisation and the metamorphic evolution in the Archean high metamorphic Nuuk area (Fig. 1), have recently been investigated by research programs of the Geological Survey of Denmark and Greenland (GEUS) and a basic understanding of the regional geological control and hydrothermal mineral assemblages has been established (e.g. [1]). Contrasted models have been proposed to explain gold occurrences including: (1) early syn-volcanic mineralising event later remobilised during the orogenic processes (e.g. [2]) and (2) orogenic gold mineralisation at early to syn- peak-metamorphic conditions [1].

Petrographic analyses of samples collected in the Nuuk peninsula, Sadelø island and Bjørneøen greenstone belts (Fig. 1) combined with wavelength-dispersive spectrometry (WDS) analysis of tourmaline and multiple sulfur isotopes analysis of sulfide phases using secondary ion mass spectrometry (SIMS) will enable us to further investigate the nature of the mineralisation in the region. Preliminary mineral paragenesis suggest that the gold mineralisation is associated with base metal mineralisation (Pb, Mo, Cu, Zn) as well as mineral species atypical to the orogenic mineralisation including barite and large amount of tourmaline from the schorl-dravite solution

series. This study proposes that the investigated gold occurrences are related to a volcanogenic exhalative environment. Sulfur isotope analysis point towards a dominant mantle derived source of S with $\Delta^{33}\text{S} \approx 0$ and an average $\delta^{34}\text{S} \approx 2.7\text{‰}$ suggesting mixing between a mantle source and sulfur derived from sulfates in a submarine environment. Collectively the preliminary analysis of the mineralisation of the Nuuk goldfields point toward a syn-genetic mineralisation process related to volcanogenic exhalative environment that was then metamorphosed during the ca. 2.65-2.58 Ga Kapisilik orogeny.

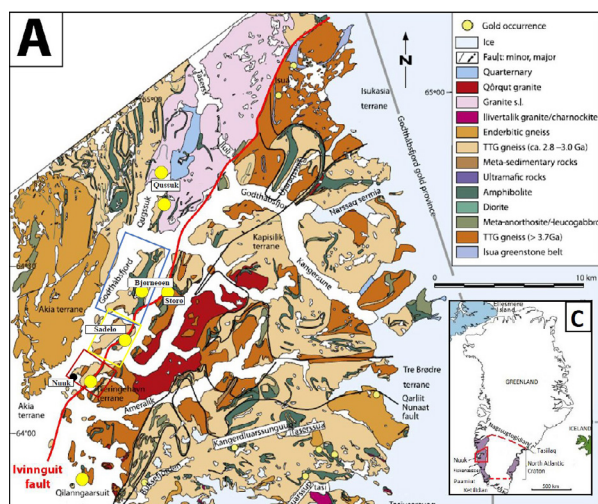


Figure 1. Geological map of the Nuuk district, West Greenland after Kolb et al., 2013.

REFERENCES

- [1] Kolb, J. et al. 2013. Gold occurrences of the Archean North Atlantic craton, southwestern Greenland: a comprehensive genetic model. *Ore Geology Reviews*, 54, 29-58.
- [2] Knudsen, C. et al. 2007. Gold-hosting supracrustal rocks on Storø, southern West Greenland: lithologies and geological environment. *Geological Survey of Denmark and Greenland Bulletin*, 13, 41-44.

Cadomian reworking of ancient SCLM during incipient arc magmatism? (Cabo Ortegal Complex, Spain)

R. TILHAC^{1,2}, W.L. GRIFFIN¹, S.Y. O'REILLY¹, G. CEULENEER², B.F. SCHAEFER¹, H. HENRY^{1,2} AND M. GREGOIRE^{1,2}

¹Australian Research Council Centre of Excellence for Core to Crust Fluid Systems (CCFS) and GEMOC, Department of Earth and Planetary Sciences, Macquarie University, Sydney, NSW 2109, Australia (romain.tilhac@mq.edu.au)

²Géosciences Environnement Toulouse (GET), CNRS, CNES, IRD, Université Toulouse III, France

An isotopic perspective on pyroxenite petrogenesis

Pyroxenites exposed in orogenic peridotite massifs are valuable to investigate the diversity of petrogenetic processes occurring in the supra-subduction mantle. However, the source of their parental melts and their age are commonly obscured by metasomatism and metamorphism. Here we report Sr-, Nd-, Hf- and Os-isotope compositions for a set of primitive pyroxenites from the Variscan Cabo Ortegal Complex, Spain, where a robust tectonothermal, petrological and geochemical background exists [1]. These pyroxenites, associated with dunite, formed by melt/harzburgite interaction following the intrusion of picritic and/or boninitic melts at shallow levels of a sub-arc mantle domain (Fig. 1). Our isotopic data yield age-corrected $^{87}\text{Sr}/^{86}\text{Sr} = 0.7037\text{--}0.7045$ and $\epsilon_{\text{Nd}} = 0.3\text{--}7.5$, equivalent to the mixing of depleted MORB mantle (DMM) and enriched mantle components (EM I and/or II) [2]. Combined with strikingly unradiogenic age-corrected Hf-isotope compositions ($\epsilon_{\text{Hf}} = -205\text{--}41$), we interpret this mixing as the contribution of an old and metasomatised mantle domain (e.g. SCLM), acquired either in the melt source, or during peridotite replacement.

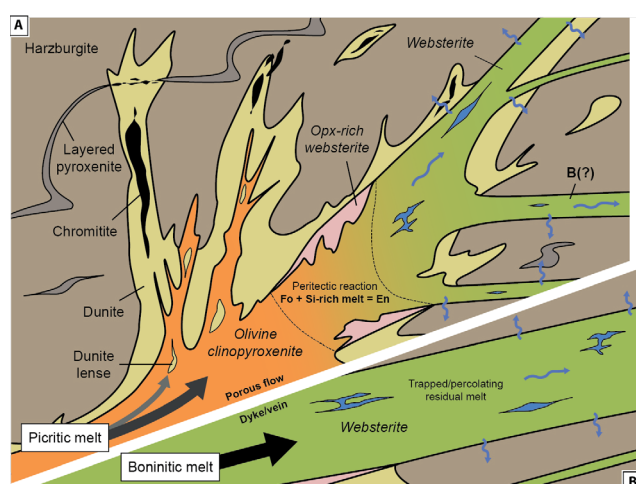


Figure 1. Petrogenetic model for the magmatic episode of the formation of Cabo Ortegal pyroxenites in a sub-arc mantle domain. Scenario A corresponds to the intrusion of picritic melts differentiated into boninitic compositions during melt-rock interaction, forming a sequence of olivine clinopyroxenites to (opx-rich) websterites, while scenario B envisages that websterites crystallised from boninitic melts migrating through dykes and veins (these alternatives are not mutually exclusive). Blue arrows illustrate the potential amphibolitisation that occurred during late-magmatic migration of residual melts.

In addition, isotopic disequilibrium between clinopyroxene and amphibole suggests that two phases of amphibolitisation probably occurred, potentially including the migration of residual melts

during the main magmatic episode (Fig. 1). Most internal and external Nd isochron ages (421–592 Ma), and second-stage Nd model ages (502–762 Ma) specify that this episode occurred in Ordovician to Neoproterozoic (Cadomian?) times [2], in good agreement with Os model ages (τ_{MA}), Re-depletion ages (τ_{RD}) and isochron ages (588–950 Ma). We thus suggest that Cabo Ortegal pyroxenites recorded incipient arc magmatism re-working a northern margin of Gondwana, or pre-Gondwanan continental blocks. Relatively young Rb–Sr and Sm–Nd internal isochrons suggest that previous ages reported at *ca* 390 Ma record a late metamorphic event corresponding to the exhumation of the Cabo Ortegal mantle from granulite- to amphibolite-facies conditions in a subduction channel. This occurred following the breakdown of garnet and upon the addition of volatiles, which led to the remobilisation of Re that produced a wide range of Os-isotope compositions ($^{187}\text{Os}/^{188}\text{Os} = 0.16\text{--}1.44$). As a consequence, correlations between amphibole content, LREE enrichment and $^{187}\text{Re}/^{188}\text{Os}$ are now observed.

REFERENCES

- [1] Tilhac, R. et al. 2016. Primitive arc magmatism and delamination: petrology and geochemistry of pyroxenites from the Cabo Ortegal Complex, Spain. *Journal of Petrology*, 57, 1921–1954.
- [2] Tilhac, R. et al. 2017. Sources and timing of pyroxenite formation in the sub-arc mantle: case study of the Cabo Ortegal Complex, Spain. *Earth and Planetary Science Letters*, 474, 490–502.

Mantle in a bleb

I. TRETIAKOVA^{1,2}, M. FIORENTINI¹, V. MALKOVETS² AND L. MARTIN^{1,3}

¹ARC Centre of Excellence in Core to Crust Fluid Systems (CCFS), University of Western Australia, 35 Stirling Highway, Crawley, WA 6009, Australia (irina.tretiakova@uwa.edu.au)

²Institute of Geology and Mineralogy SB RAS, 3 Koptuyg ave, Novosibirsk, 630090, Russia

³Centre for Microscopy, Characterisation and Analysis, University of Western Australia, 35 Stirling Hwy, Crawley, 6009, WA

Sulfide inclusions in mantle silicate minerals from kimberlites have been widely used for geochronological and geochemical studies to constrain the mantle reservoirs that sourced these magmas. Commonly, composition of these inclusions corresponds to monosulfide (MSS) or intermediate solid solution (ISS), with varying Fe, Ni and Cu contents. Sulfide inclusions generally contain high concentrations of platinum-group elements, including Os, which makes them suitable for Re-Os geochronology [1, 2, 3, 4]. In order to better constrain the evolution of the lithospheric mantle of the Siberian Craton, thirty-eight sulfide inclusions hosted in olivine grains with clear mantle derivation (Mg# - from 90 to 93) have been selected from the heavy mineral concentrate of crushed harzburgite-dunite xenoliths from the Udachnaya pipe, Yakutia, Russia.

Inclusions range from 50 to 250 μm in size. The majority (n=31) of sulfide inclusions are rounded isometric or slightly elongated. However, four show negative crystal shape controlled by the enclosing olivine and the other three are isometric, but with uneven irregular edges. The high Mg# and undisturbed composition of the host olivine clearly indicates the mantle origin of inclusions. Reflected light optical microscopy revealed complex internal textures. Most of the sulfide inclusions demonstrate three distinct mineral phases: (i) exsolutions of Fe- and Ni-rich MSS in the central part of inclusion; (ii) pentlandite forming rim or flame-like textures protruding into MSS; (iii) chalcopyrite rim. Back-scattered electron imaging revealed small bright particles in the inner and outer parts of some inclusions, which were later distinguished as platinum-group minerals (PGMs) of different composition.

Imaging using nanoSIMS (CMCA at UWA, Perth) shows variations in PGM morphology, composition and localisation: two types of PGMs were recognised. The first type comprises relatively osmium-poor and iridium-rich needle-like particles located in the central parts of inclusions. They are generally oriented along the exsolution structures of MSS. The second type comprises osmium-rich small globules localised in pentlandite-chalcopyrite rims. The occurrence of two types of PGMs within a single sulfide inclusion was observed in at least 8 out of 31 studied samples.

Sulfur isotopic compositions of pentlandite rims and MSS cores have been studied using Cameca 1280 SIMS (CMCA at UWA, Perth). In general, across all studied inclusions both main mineral phases (pyrrhotite and pentlandite) demonstrate similar range of $\delta^{34}\text{S}$ values: from -0.5 to +3.5‰ and from +0.2 to +3.0‰, respectively. However, comparison of $\delta^{34}\text{S}$ of pentlandite and pyrrhotite within a single inclusion reveals a difference of up to 3‰. Such difference could not be explained by isotopic fractionation between sulfide phases crystallised from the same melt [5]. Moreover, a wide range of Re-Os model ages calculated for those inclusions (TRD from 0.47 to 3.49 Ga) could reflect mixing of the melts/fluids with different isotopic composition.

Occurrence of two PGM generations and the clear isotopic disequilibrium of the sulfides in the blebs hosted within a single inclusion suggest that these sulfides formed at different times and/or different parts of the mantle. The complex nature of these blebs reflects the chemical and isotopic heterogeneity of the lithospheric mantle of the Siberian Craton, which recorded and stored multiple metasomatic events over a long time.

REFERENCES

- [1] Alard, O. et al. 2002. New insights into the Re-Os systematics of subcontinental lithospheric mantle from *in situ* analysis of sulphides. *Earth and Planetary Science Letters*, 203, 651-663.
- [2] Griffin, W.L. et al. 2002. Cr-pyrope garnets in the lithospheric mantle 2. Compositional populations and their distribution in time and space. *Geochemistry Geophysics Geosystems*, 3, 12, 1073, doi:10.1029/2002GC000298, 2002.
- [3] Harvey, J. et al. 2010. Unravelling the effects of melt depletion and secondary infiltration on mantle Re-Os isotopes beneath the French Massif Central. *Geochimica et Cosmochimica Acta*, 74, 293-320.
- [4] Pearson, N.J. et al. 2002. *In situ* measurement of Re-Os isotopes in mantle sulfides by laser ablation multicollector-inductively coupled plasma mass spectrometry: analytical methods and preliminary results. *Geochimica et Cosmochimica Acta*, 66, 1037-1050.
- [5] LaFlamme, C. et al. 2016. *In situ* multiple sulfur isotope analysis by SIMS of pyrite, chalcopyrite, pyrrhotite, and pentlandite to refine magmatic ore genetic models. *Chemical Geology*, 444, 1-15.

CCFS Flagship Program 4: Advances in understanding the Atmospheric, Environmental and Biological co-evolution of Earth

M.J. VAN KRANENDONK

ARC Centre of Excellence in Core to Crust Fluid Systems (CCFS), Australian Centre for Astrobiology, and School of Biological, Earth, and Environmental Sciences, University of New South Wales, Kensington, NSW 2052 Australia (m.vankranendonk@unsw.edu.au)

Earth is a system of linked shells that have evolved through distinct stages over its 4.56 billion-year history. Physical shells include the core, mantle, crust, hydrosphere, and atmosphere. The biosphere spans the outermost three physical shells and interacts with, and influences, the mantle.

Stage 1 was rapid accretion, forming the Earth and Moon by c. 4.5 Ga. Cooling of the magma ocean and condensation of the atmosphere occurred by 4.4-4.2 Ga, respectively, producing a crust whose remnants are preserved only as detrital and inherited zircons. Intense bombardment ceased by c. 3.9 Ga. Modelling suggests that the early crust was a thick, dominantly basaltic, stagnant lid, with limited internal differentiation. This provided the first stable habitats for life. Currently, favoured models suggest an origin of life in deep sea (warm, alkaline) hydrothermal vents, *but a recent groundswell from disparate scientific fields suggests an origin of life in anoxic hot springs, on land.*

Stage 2: Perhaps as early as 3.9 Ga, *but certainly by 3.7 Ga*, life had successfully colonised the anoxic, Fe-rich oceans. *By 3.5 Ga, it was already diverse, occupied a variety of niche spaces, and was perhaps voluminous.* This accompanied a geodynamic transition from a stagnant lid to an early form of plate tectonics that formed crust via a combination of shallow subduction and mantle plumes and continued to 3.2 Ga.

Stage 3: Secular cooling from radioactive decay and conductive heat loss, combined with global, deep subduction of cold oceanic lithosphere cooled the mantle such that *by 3.2 Ga, modern-style plate tectonics had commenced.* *This led to the onset of the supercontinent cycle* and the deposition of the first thick continental clastic successions. *Life had colonised the shorelines and fluvial-lacustrine waterways* and had evolved oxygenic photosynthesis. Combined, these factors produced the first pulse of free atmospheric oxygen, which led to continental glaciations by 2.9 Ga, as well as to biogenic precipitation of the largest gold deposits.

Stage 4: Reheating of the mantle (by core conduction) at 2.8 Ga kick-started the Late Archean Superevent, a global period of voluminous, dominantly basaltic, successions now preserved in greenstone belts around the world. Continuing until ~2.42 Ga, this unprecedented volcanism belched out reducing gasses, leading to a return of anoxic conditions and the largest range in S-MIF anomalies. Whiffs of oxygen accompanied the global precipitation of banded iron-formation in the latter part of this stage, derived from rusting of the seas as a result of the oxygen produced by a globally dispersed cyanobacterial community thriving on widespread, stable coastal platforms. The formation of supercontinent Superia/Sclavia at the end of this stage was accompanied by chaos in the biosphere, as evidenced by the largest negative C- and Fe-isotopic anomalies in Earth history.

The aftermath of the Late Archean Superevent led to a global shutdown of magmatism and possible return to stagnant lid geodynamics from 2.42-2.22 Ga. The decreased volcanic gas emissions, combined with the increased cyanobacterial activity, combined to effect the Great Oxygenation Event. *The biological response to oxygenation of the atmosphere was swift, resulting in significant diversification and, perhaps, the rise of eukaryotes at this time.*

Stage 5: At 2.22 Ga, the mantle engine restarted, leading to a temporary return of Archean-like granite-greenstone crust formation, the re-appearance of iron-formations, and a large positive C-isotopic excursion of carbonates (the Lomagundi-Jatuli event). The formation of supercontinent Columbia/Nuna at c. 1.8 Ga was accompanied, or closely followed by, another (local) glaciation.

Columbia/Nuna remained fused until ~1.5-1.3 Ga and trapped mantle-derived melts that were emplaced into the crust in the form of large anorthosite-mangerite complexes. The stable land surfaces were colonised by eukaryotes and newly developed fungi.

Stage 6: A final Precambrian stage witnessed *the largest orogenic event in Earth history* during formation of Supercontinent Rodinia via the 1.3-0.9 Ga Grenvillian orogeny. This led to widespread uplift, weathering, and deposition of clastic sediments, and mantle cooling as reflected by the Snowball Earth glaciations. The associated rise in atmospheric oxygen led to the proliferation of eukaryotes and evolutionary development of, first, the Ediacaran fauna, and then the hard-bodied fauna of the Cambrian explosion.

Trace element nanoclusters in rutile and their geological significance

R. VERBERNE^{1,2,3}, S.M. REDDY^{1,2,3}, D.W. SAXEY^{3,4}, D. FOUGEROUSE^{1,2,3}, W.D.A. RICKARD^{3,4}, D. PLAVSA¹ AND A. AGANGI¹

¹Department of Applied Geology, The Institute for Geoscience Research (TIGeR), Western Australian School of Mines, Curtin University, GPO Box U1987, Perth, WA 6845, Australia (rick.verberne@postgrad.curtin.edu.au)

²ARC Centre of Excellence for Core to Crust Fluid Systems (CCFS), Department of Applied Geology, Curtin University, GPO Box U1987, Perth WA 6845, Australia

³Geoscience Atom Probe, Advanced Resource Characterisation Facility, John de Laeter Centre, Curtin University, GPO Box U1987, Perth, WA 6845, Australia

⁴Department of Physics and Astronomy, Curtin University, GPO Box U1987, Perth, WA 6845, Australia

Rutile is a common accessory mineral present in a wide range of rocks. The geochemical analysis of trace elements in rutile is routinely used to extract information on the nature and timing of geological events. However, there is a gap of knowledge about the incorporation and mobility of these trace elements which are thought to be controlled by nanoscale processes. To address this gap of knowledge we have used atom probe microscopy and correlated microscopy (EDS, EBSD, LA-ICP-MS, FIB-SEM with ToF-SIMS) to characterise the nanoscale distribution of trace elements in rutile sourced from the Moogie Metamorphics (Capricorn orogeny, Western Australia). Atom probe specimens were prepared by standard site-specific FIB-SEM preparation techniques and analysed with the Cameca LEAP 4000X-HR housed at the Geoscience Atom Probe Facility (Curtin University). The instrument was operated in laser-assisted mode, using a UV-laser, a pulse rate of 200 kHz, a laser power of 30-70 pJ, base temperatures ranging from 40-60 K and a 0.8% automated detection rate.

Characterisation of rutile prior to atom probe microscopy indicates the rutile is undeformed and homogeneous on the μm -scale. LA-ICP-MS shows concordant U-Pb age indicating crystallisation around 1874.5 ± 4.8 Ma.

The reconstructed atom probe data reveals clusters of trace elements within the TiO_2 matrix dominated by Pb and enriched in the common trace elements found in rutile with the exception of Nb.

The cluster may have formed by a range of mechanisms including annealing, demixing and phase exsolution or be inherited during growth. The Pb isotopic composition and major element chemistry of the clusters are consistent with the clusters having formed during metamorphism. The atom probe data suggests that similarly to zircon [1, 2], Pb may be trapped in point defects, such as vacancies, Frenkel-defects or impurities, as the onset of cluster formation. The LA-ICP-MS data is concordant and did not record Pb loss at the scale of the analytical spot indicating that Pb and trace elements were mobile at the submicron scale only.

REFERENCES

- [1] Peterman, E.M. et al. 2016. Nanogeochronology of discordant zircon measured by atom probe microscopy of Pb-enriched dislocation loops. *Science Advances*, 2, 9, e1601318.
- [2] Valley, J.W. et al. 2015. Presidential address. Nano- and micro-geochronology in Hadean and Archean zircons by atom-probe tomography and SIMS: New tools for old minerals. *American Mineralogist*, 100, 7, 1355-1377.

Investigating trace elements as indicators of the mode of origin of orthopyroxene in mantle rocks

M. VETER AND S.F. FOLEY

Australian Research Council Centre of Excellence for Core to Crust Fluid Systems (CCFS) and GEMOC, Department of Earth and Planetary Sciences, Macquarie University, Sydney, NSW 2109, Australia (marina.veter@mq.edu.au; stephen.foley@mq.edu.au)

Orthopyroxene is the second most abundant silicate mineral after olivine in the Earth's lithospheric mantle and, hence, bears great potential in recording information about reactions that have occurred in the mantle. Clinopyroxene and garnet are traditionally preferred for the analysis of trace elements due to the higher abundances of most trace elements than in olivine or orthopyroxene. However, clinopyroxene and garnet are frequently introduced later during mantle metasomatism and so cannot provide information about earlier stages of development and modification witnessed by orthopyroxene and olivine.

In highly depleted peridotites that have experienced >25% partial melting, clinopyroxene is the first phase to be completely consumed leaving behind an ol-opx-gt/sp residue, whereas orthopyroxene can persist in the residue until ~40% partial melting. Because of this, orthopyroxene is the main trace element repository for many trace elements [1]. Recent studies of trace element examinations of orthopyroxenes in such highly depleted peridotites have provided useful insights into depletion, enrichment and equilibration processes of the lithospheric mantle [1] or have contributed to geodynamic reconstructions [2].

The aim of this study is a systematic geochemical investigation and comparison of trace elements in orthopyroxenes from a variety of cratonic and non-cratonic, opx-rich peridotites from different geodynamic settings. Our approach is to gather precise EPMA and LA-ICP-MS measurements to thoroughly characterise the minor and trace element concentrations. These data promise to be successful in determining depletion and enrichment events as well as giving indication for tectonic environments.

Samples are being selected to enable investigation of orthopyroxenes that may have formed by a variety of processes, ranging from residues after depletion to reactions of lithospheric peridotites that have reacted with silica-rich, silica-poor or potentially also carbonate-bearing mantle melts or fluids. These include cratonic peridotites that occur as xenoliths in kimberlites in southern Africa and the North Atlantic craton (Kimberley; Zero, Kuruman, Greenland), and xenoliths from the continental lithospheric mantle brought to the surface by basalts away from the cratons (Dzhilinda and Vitim in Siberia [3]; Lambert-Amery rift region of eastern Antarctica [4]).

Massif peridotites samples from Ronda (Spain) allow more spatial context, enabling orthopyroxenes at differing distances to pyroxenitic veins to be analysed, so that the migration of trace elements during metasomatism can be characterised. In later stages of the project, orthopyroxenes from layered igneous intrusions may be included in the study.

REFERENCES

- [1] Scott, J.M. et al. 2016. Mantle depletion and metasomatism recorded in orthopyroxene in highly depleted peridotites. *Chemical Geology*, 441, 280-291.
- [2] Jean, M.M. and Shervais, J.W. 2017. The distribution of fluid mobile and other incompatible trace elements in orthopyroxene from mantle wedge peridotites. *Chemical Geology*, 457, 118-130.
- [3] Glaser, S.M. et al. 1999. Trace element enrichment by melt infiltration in garnet- and spinel peridotite xenoliths from the Vitim volcanic field, Transbaikalia, eastern Siberia. *Lithos*, 48, 263-285.
- [4] Foley, S.F. et al. 2006. Evidence from Antarctic mantle peridotite xenoliths for changes in mineralogy, geochemistry and geothermal gradients beneath a developing rift. *Geochimica et Cosmochimica Acta*, 70, 3096-3120.

Tectono-metamorphic Evolution of the Georgetown Inlier (NE Australia) and Implications for the Assembly of Nuna

S. VOLANTE, A. POURTEAU, Z.-X. LI AND W.J. COLLINS

Department of Applied Geology, Earth-Dynamics Research Group, ARC Centre of Excellence for Core to Crust Fluid Systems (CCFS) and The Institute for Geoscience Research (TIGeR), Perth, WA 6845, Australia
(silvia.volante@postgrad.curtin.edu.au)

Recent tectonic reconstructions for the Proterozoic supercontinent Nuna (1.8 to 1.5 Ga) suggest connections between eastern Australia and western Laurentia [1]. The Georgetown Inlier (NE Australia) is crucial for testing such links. Although regional-scale metamorphic imprints of ca. 1600 to 1550 Ma have been ascribed to continental collision between NE Australia and NW Laurentia during Nuna assembly [1], the central and eastern domains of the Inlier record low- to medium-*P*/high-*T* metamorphic imprints associated with partial melting (in the east) and emplacement of S-type granites, which are not characteristic features of crustal thickening that are generally associated with regional medium *T/P* gradients.

The central domain of the Georgetown Inlier preserves poly-deformed and metamorphosed sedimentary and mafic rocks [2]. Three progressive deformation events (D1, D2, D3) have been described, during which successive generations of planar fabrics developed (S1, S2, S3). Conflicting interpretations amongst previous work in the region [3, 4] reflect the critical lack of geochronological constraints on minerals which are part of equilibrium microstructures of specific metamorphic stages.

In this study, we apply a multi-scale analytical approach that combines petro-structural field mapping with microstructural analysis, *P–T* estimation, and geochronology (U–Pb in monazite and zircon; Lu–Hf in garnet) in order to reconstruct multi-point pressure–temperature–deformation–time (*P–T–d–t*) paths for different sectors of the Georgetown Inlier.

Preliminary multi-scale structural analysis has revealed successive tectono-metamorphic and magmatic events: during D1, a compositional layering S1(Ms+Bt+Qz) was developed, which is generally parallel to S2 and therefore difficult to be differentiated from the overprinting fabric. However, the two fabrics are readily distinguishable in the hinges of F2 folds and in Q-domains of the S2 differentiate crenulation cleavage. During D2, a pervasive foliation S2 developed in metapelite, amphibolite, calc-silicate, and granite which is parallel to pegmatitic dykes. S2 is the axial planar fabric of tight to isoclinal F2 folds, and is associated with a pervasive mineral lineation (L2). Different mineral assemblages (Bt+Ms+Qz±Grt±Clt; Bt+Ms+Grt+St+Qz; Bt+Ms+And+Qz±Grt; Bt+Ms+Sil+Qz±Grt±Fsp) define successive stages of the S2 evolution [5] throughout the central Georgetown Inlier, suggesting that the progressive development of S2 occurred at different *P–T* conditions. During D3, open, upright E–W trending F3 mesoscopic folds superimposed on S2, developing a crenulation cleavage (S3). Type 2 fold interference pattern resulted from the superposition of F2 and F3 folds, at least in the southern part of the central region of the Georgetown Inlier.

Our first results suggest that the central domain of the Georgetown Inlier is a single tectono-metamorphic unit, recording different *P–T* conditions in adjacent sectors of the same tectonic domain. Further interpretations on the significance of these petro-structural observations will depend on forthcoming geochronological analysis on monazite, zircon and garnet.

REFERENCES

- [1] Betts, P. et al. 2015. Australia and Nuna. Geological Society, Special Publications, 424, 47-81.
- [2] Black, L. P. et al. 1979. Geochronology of discrete structural-metamorphic events in a multiply deformed Precambrian terrain. *Tectonophysics*, 54, 103-137.
- [3] Cihan, M. et al 2006. Time constraints on deformation and metamorphism from EPMA dating of monazite in the Proterozoic Robertson River Metamorphics, NE Australia. *Precambrian Research*, 145, 1-23.
- [4] Hills, Q. 2003. The deformational and metamorphic history of the Georgetown Inlier, North Queensland: implications for the 1.7 to 1.5 Ga tectonic evolution of northeastern Proterozoic Australia. PhD Thesis, pp. 212.
- [5] Bell, T.H. and Rubenach, M.J. 1983. Sequential porphyroblast growth and crenulation cleavage development during progressive deformation. *Tectonophysics*, 92, 171-194.

Quantitative trace element mapping of multiple sulfide phases from the Fraser Zone, Albany-Fraser Orogen

A. WALKER¹, K. EVANS², C. KIRKLAND³ AND N. EVANS⁴

¹ARC Centre of Excellence for Core to Crust Fluid Systems (CCFS) and The Institute for Geoscience Research (TIGeR), Department of Applied Geology, Curtin University, GPO Box U1987, Perth WA 6845, Australia (alexander.t.walker@postgrad.curtin.edu.au)

²Department of Applied Geology, Curtin University, GPO Box U1987, Perth WA 6845, Australia (k.evans@curtin.edu.au)

³ARC Centre of Excellence for Core to Crust Fluid Systems (CCFS) and The Institute for Geoscience Research (TIGeR), Department of Applied Geology, Curtin University, GPO Box U1987, Perth WA 6845, Australia (c.kirkland@curtin.edu.au)

⁴Department of Applied Geology, Curtin University, GPO Box U1987, Perth WA 6845, Australia (noreen.evans@curtin.edu.au)

The proterozoic Albany-Fraser orogen, a tectonically complex orogenic belt hosting reworked Archaean material on the margin of the Yilgarn Craton, comprises multiple lithotectonic zones each potentially hosting distinctive mineral systems. The Fraser Zone in particular, characterised as a mid-deep crustal hot zone formed by mantle upwelling, is prospective for magmatic nickel sulfide mineralisation. Samples of mineralised igneous and metasedimentary material from the Octagonal prospect within the Fraser Zone were imaged via TIMA (TESCAN Integrated Mineral Analyser) analysis; these images were then used to select locations of samples to be analysed via laser ablation ICPMS.

By combining laser mapping and TIMA techniques, it is possible to not only generate quantitative trace element data for multiple sulfide phases, but to visualise that data in contour maps that can be overlaid on TIMA mineral maps of the analysed areas. The synthesised data can be used to aid recognition of the trace element signature and textural characteristics of processes that formed and redistributed elements in the rocks. Bi and Ag are seen to be concentrated along the margins of pentlandite grains; primarily where pentlandite is in contact with magnetite grains in the case of Ag, and where pentlandite contacts chalcopyrite for Bi. Mn, present in low (up to c. 100 ppm) concentrations throughout material in the two samples of sulfide breccias analysed, appears strongly concentrated within late magnetite and serpentine veins cross-cutting sulfides; suggesting possible remobilisation of Mn from sulfides into serpentine during the high temperature metamorphism that has modified Fraser Zone geology.

The data presented in this study have implications for the distribution and redistribution of elements, including Ag, Pb, Mn, Bi, Se, Te, that may be considered for use as indicators of mineralisation and alteration, particularly in sulfide minerals that have undergone high temperature amphibolite-granulite grade metamorphism. Elements such as Mn may be remobilised into later alteration features such as infilled cracks and veins, or potentially into other sulfide phases.

Crustal structures of southern California revealed by adjoint tomography of ambient seismic noise

K. WANG¹, Y. YANG¹ AND Q. LIU²

¹Australian Research Council Centre of Excellence for Core to Crust Fluid Systems (CCFS) and GEMOC, Department of Earth and Planetary Sciences, Macquarie University, Sydney, NSW 2109, Australia (kai.wang@mq.edu.au)

²Department of Earth Science, University of Toronto, Toronto, Canada

We construct a new shear-wave velocity (V_s) model for the crust of southern California by adjoint tomography based on Rayleigh-wave Empirical Green's functions (EGFs) at 5-50 s period from Z-Z component ambient noise cross-correlation functions. The initial model of our adjoint tomography is the isotropic V_s model M16 from Tape et al. [2009], which was generated by three-component body and surface waves at 2-30 s period from local earthquake data. Synthetic Green's functions (SGFs) from M16 show a good agreement with the EGFs from ambient noise at 5-50 s and 10-50 s period bands, but have an average 2.12 s time advance at 20-50 s band. By minimising the traveltimes differences between the EGFs and SGFs using gradient-based algorithm, the V_s model is refined successively, and the total misfits is reduced from the initial 1.75 to 0.33 at convergence after five iterations. The final V_s model fits EGF waveforms better than the initial model at all the three period bands with reduced variances in time misfits.

Our new V_s model reveals several new features in the mid- and lower-crust, including: (1) the mean V_s speed of lower crust is slowed down by about 6%; (2) the V_s speed in the Los Angeles Basin and Central Transverse Range is higher (up to +4%) than the initial model throughout the crust; (3) beneath the westernmost Peninsular Range Batholith (PRB) and Sierra Nevada Batholith (SNB), we observe higher V_s in the lower crust; (4) an enhanced shallow high-velocity zone in the mid-crust is observed beneath Salton Trough Basin. Our updated model also shows refined lateral velocity gradient across PRB, SNB, San Andreas Fault (SAF), which helps define the west-east compositional boundary between PRB and SNB, as well as the dip angle and the depth extent of SAF.

Our study demonstrates the feasibility of applying adjoint tomography to ambient noise data in southern California, which is complementary in coverage to the earthquake data used in previous studies. The numerical spectral-element solver used in adjoint tomography provides accurate structure sensitivity kernels through 3D model iterations, and hence generate more robust images than those by traditional ambient noise tomography based on analytical methods.

REFERENCE

- [1] Tape, C. et al. 2009. Adjoint tomography of the southern California crust. *Science*, 325, 988-992.
- [2] Tape, C. et al. 2010. Seismic tomography of the southern California crust based on spectral-element and adjoint methods. *Geophysical Journal International*, 180, 433-462.

Manganese-rich garnets pre-concentrate heavy rare earth elements during prograde subduction metamorphism

Y. WANG^{1,2} AND S.F. FOLEY²

¹State Key Laboratory of Isotope Geochemistry, Guangzhou Institute of Geochemistry, Chinese Academy of Sciences, Guangzhou 510640, China

²ARC Centre of Excellence for Core to Crust Fluid Systems (CCFS)/GEMOC; Department of Earth and Planetary Sciences, Macquarie University, NSW 2109, Australia (yu.wang33@students.mq.edu.au)

Metamorphic Mn-rich garnets have been widely recognised in greenschists and blueschists, mostly exhibiting strong elemental zoning. Here we report on a natural Mn-rich garnet bearing blueschist from the Tavşanlı Zone, Turkey, and a series of melting experiments conducted on the same sample to show that Mn-rich garnets play a significant role in the concentration of trace elements during prograde metamorphism. Mn-rich and Mn-poor almandine garnets show distinct behaviour in terms of REE distribution patterns, especially for heavy rare earth elements (HREE). Partition coefficients between garnet and melt from the experiments indicates that HREE are much more compatible in Mn-rich garnet ($D_{\text{garnet/melt}}^{100-1000}$) with positive HREE slopes ($D_{\text{Lu}} \gg D_{\text{Dy}}$) and concentrations over two orders of magnitude higher than in Mn-poor garnets, which have much lower D_{HREE} (~ 10) with negative slopes ($D_{\text{Lu}} < D_{\text{Dy}}$). Mn-rich garnets possibly originated from widespread Mn-rich sediment on the seafloor (e.g. Mn-nodules and Mn-coatings), and may be effective pre-concentrators of HREE during prograde metamorphism, localising these elements and influencing their later redistribution in higher-grade phases. This may prove to be a useful indicator for the reconstruction of prograde paths, seeing further back in time than inclusions in peak metamorphic assemblages.

Flagship Project 6: 2017 results

S.A. WILDE, R. GE AND X.-C. WANG

ARC Centre of Excellence for Core to Crust Fluid Systems (CCFS) and The Institute for Geoscience Research (TiGeR), Department of Applied Geology, Curtin University, GPO Box U1987, Perth WA 6845, Australia
(s.wilde@curtin.edu.au; rongfeng.ge@curtin.edu.au; x.wang3@curtin.edu.au)

Study focussed on three main areas: Jack Hills, Labrador and China. For Jack Hills, the paper on the CO₂ and graphite inclusions in zircon with Martina Menneken was published [1] and the paper by former Curtin PhD student Qian Wang on details of her traverse through the metasedimentary belt is now in revision for Gondwana Research. Rongfeng Ge continued with his post-doctoral studies investigating the oldest zircons from the W74 site at Jack Hills. Careful selection of grains has led to the identification of several old crystals that show minimal effects related to later geological processes - including identification of the oldest grain on Earth. He visited the NordSIM facility in Stockholm and, applying ion imaging techniques, was able to establish that this latter grain had in fact undergone Pb* (radiogenic lead) redistribution and that its 'real' age was probably closer to 4277 Ma. This highlights an ever-growing problem in micro-beam geochronology whereby even concordant ages may not reflect the timing of actual geological events.

The Saglek Bay area of Labrador was revisited in July-August, with fieldwork concentrated in areas identified as potential sites for ancient gneisses. Transport was mainly via zodiac to coastal sites, although the weather was not good overall. Together with Monika Kusiak and Daniel Dunkley from CCFS, and Monika's PhD student Anna Salacinska, we have submitted two papers for publication, based on the work undertaken in the 2015 field season. A total of 133 new specimens have been collected and work will commence on these once they have been forwarded from Canada. Papers published recently indicate the growing importance of this area, with zircon U-Pb ages > 3.95 Ga reported [2]. The site where Komiya et al (2015) reported these ancient ages was visited and samples collected for future analysis.

Work in the North China Craton consisted of testing a range of TTG gneisses from Anshan, the oldest rocks in China, for ¹⁴²Nd anomalies. Given the range in ages from 3.8-3.0 Ga it was anticipated that there might be evidence for a gradual diminution of any anomaly. This turned out not to be the case, but several samples showed positive ¹⁴²Nd anomalies up to +9.2 ppm relative to the modern accessible Earth. Anshan is now yet another area where there is evidence that early mantle reservoirs have survived mantle mixing for considerable periods of geological time [3].

Work continued on the Tarim Craton in northern China that formed the focus of Rongfeng Ge's PhD at Curtin/Nanjing, with the manuscript providing evidence for 3.7 Ga rocks in the north-east of the craton being submitted for publication.

Other research not directly related to the early Earth included work in the Central Asian Orogenic Belt (CAOB) and in Tibet, with several papers published in 2017.

REFERENCES

- [1] Menneken, M. et al. 2017. CO₂ fluid inclusion in Jack Hills zircons. *Contributions to Mineralogy and Petrology*, 172, 66, 18p.
- [2] Komiya, T. et al. 2015. Geology of the Eoarchean, >3.95 Ga, Nulliak supracrustal rocks in the Saglek Block, northern Labrador, Canada: The oldest geological evidence for plate tectonics. *Tectonophysics*, 662, 40-66.
- [3] Li, C.F. et al. 2017. Differentiation of the early silicate Earth as recorded by ¹⁴²Nd - ¹⁴³Nd in 3.8-3.0 Ga rocks from the Anshan Complex, North China Craton. *Precambrian Research*, 301, 86-101.

Mountain building in central and western Tien Shan Orogen: Insight from surface wave tomography

S. WU, Y. YANG AND K. WANG

ARC Centre of Excellence for Core to Crust Fluid Systems (CCFS)/GEMOC, Department of Earth and Planetary Sciences, Macquarie University, North Ryde, NSW 2109, Australia (shucheng.wu@hdr.mq.edu.au)

The Tien Shan orogeny, situated in central Asia about 2000 km away from the collision boundary between Indian plate and Eurasian plate, is one of the highest, youngest, and most active intercontinental mountain belts on the earth. Although many studies have been carried out to investigate the dynamic processes of the Tien Shan orogeny, its tectonic rejuvenation and uplift mechanism still remain elusive. Some researchers believe that the mountain building of Tien Shan is ascribed to the shortening of the crust accompanied by a similar style in the lithospheric upper mantle, caused by the collision of the Indian plate with the Eurasian plate [1, 2]. Other researchers suggest that small-scale convection is active beneath the Tien Shan and the upwelling of the upper mantle is responsible for the rapid uplift of the Mountains based on the observations of the low-velocity anomalies [3] in the upper mantle. A high-resolution model of crust and mantle beneath Tien Shan is critical to discriminate among the competing models for the mountain building.

In this study, we collect and process seismic data recorded by several seismic arrays in the central and western Tien Shan region to generate surface wave dispersion curves at 6-140 s period using ambient noise tomography (ANT) and two-plane surface wave tomography (TPWT) methods. Using these dispersion curves, we construct a high-resolution 3-D image of shear wave velocity (V_s) in the crust and upper mantle up to ~300 km depth. Our current model constrained only by surface waves shows that, under the Tien Shan orogenic belt, a strong low S-wave velocity anomaly exists in the uppermost mantle down to the depth of ~200 km, supporting the model that the hot upper mantle is upwelling under the Tien Shan orogenic belt, which may be responsible for the mountain building. To the west of central Tien Shan across the Talas-Fergana fault, low S-wave velocity anomalies in the upper mantle become much weaker and finally disappear beneath the Fergana basin, while in the east of the Tien Shan Orogen, the low-velocity mantles sandwich a high velocity zone underneath Lake Issyk-Kul. Beneath the Fergana and Tarim basins, high S-wave velocities are found in the lowermost crust and upper mantle. These high velocities may indicate stable craton-like structures under these two basins.

REFERENCES

- [1] Molnar, P. and Tapponnier, P. 1975. Cenozoic tectonics of Asia: effects of a continental collision. *Science*, 189, 4201, 419-426.
- [2] England, P. and Houseman, G. 1986. Finite strain calculations of continental deformation: 2. Comparison with the India-Asia collision zone. *Journal of Geophysical Research: Solid Earth*, 91, B3, 3664-3676.
- [3] Roecker, S.W. et al. 1993. Three-dimensional elastic wave velocity structure of the western and central Tien Shan. *Journal of Geophysical Research: Solid Earth*, 98, B9, 15779-15795.

Apatite trace-element compositions: An indicator for exploring covered post-collisional porphyry Cu±Au deposits?

B. XU^{1,2*}, W.L. GRIFFIN², E.A. BELOUSOVA², S.Y. O'REILLY² AND Z.-Q. HOU³

¹Australian Research Council Centre of Excellence for Core to Crust Fluid Systems (CCFS) and GEMOC, Department of Earth and Planetary Sciences, Macquarie University, Sydney, NSW 2109, Australia (bo.xu2@hdr.mq.edu.au)

²State Key Laboratory of Geological Processes and Mineral Resources, China University of Geosciences, Beijing

³Institute of Geology, Chinese Academy of Geological Sciences, Beijing 100037, China

Apatite may be a useful indicator mineral for ore systems. The present study uses a large integrated dataset of LA-ICPMS trace-element analyses and electron probe major-element analyses of apatite and fertile granite-porphyry magmatic suites, in order to identify any distinctive apatite signatures diagnostic of the metallogenic fertility of their parent magma in post-collisional environments. We focus on three large post-collisional metallogenic belts, including the Arasbaran porphyry copper belt in northwestern Iran, the Gangdese belt in southern Tibet and the Sanjiang orogen in Yunnan province, China. Apatite grains were selected from representative intrusions from porphyry-skarn Cu±Au systems (Sungun and Masjed Daghi, Arasbaran belt; Qulong and Jiama, Gangdese belt; Beiya and Machangqing, Sanjiang orogeny). The barren suites are defined as magmatic rocks that lack alteration and mineralisation at any grade. They were collected from the Yare, Zhada, Renduo granite and Namuqie porphyries (west Gangdese), Linzhi and Sangri granites (eastern Tibet) and the Binchuan porphyries (west Yunnan). In total, we collected 473 analyses with 588 spots from standards, in order to ensure the quality of our dataset.

The results show that apatites from ore-bearing and barren rocks are fluorapatite ($F > 3\%$). The fertility indicators are apatite $(Ce/Pb)_N$ and V, as well as S and Cl ratios, and apatite $(La/Sm)_N$ and Th/U ratios are also useful. In detail, apatites from fertile magmatic suites have collectively higher $(Ce/Pb)_N$ ratios (715-2026), V contents (4.13-29.38 ppm), $(La/Sm)_N$ (>1.2), and Th/U (0.17-3.65) ratios than apatites from barren rocks. Moreover, apatites from porphyry systems are enriched in sulfur and chlorine. In fertile suites, apatite $(Eu/Eu^*)/Y$ ratios are also positively correlated with Sr/Y ratios, but this correlation is lacking in the infertile suites. These distinctive ratios in the fertile suites could be interpreted as reflecting higher volatile contents, such as sulfur, chlorine and possibly, water content in mineralised rocks, which may induce hornblende fractionation and suppress early plagioclase crystallisation. The higher concentrations of incompatible elements in fertile magmatic suites also indicates the mineralised porphyries experienced high activities of fluid and/or melt. Analysing the trace-element compositions of apatite from an area with little geologic information could efficiently and cheaply discriminate whether the drainage source area is dominated by unprospective granitoids or by prospective porphyries, and therefore could help focus exploration on prospective areas.

Finite- frequency P wave tomography of the upper mantle beneath Capricorn Orogen and adjacent areas

X.B. XU¹, L. ZHAO^{1,2}, H.Y. YUAN^{3,4,5*}, S.P. JOHNSON⁴, M. DENTITH⁵, R. MURDIE⁴, K. GESSNER⁴, F.J. KORHONEN⁴ AND P. PIÑA-VARAS⁵

¹State key Laboratory of Lithospheric Evolution, Institute of Geology and Geophysics, Chinese Academy of Science, Beijing 100029, China (xuxiaobing@mail.iggcas.ac.cn)

²CAS Centre for Excellence in Tibetan Plateau Earth Sciences, Beijing, China (zhaoliang@mail.iggcas.ac.cn)

³ARC Centre of Excellence for Core to Crust Fluid Systems (CCFS), Department of Earth and Planetary Sciences, Macquarie University, New South Wales 2109, Australia (huaiyu.yuan@gmail.com)

⁴Geological Survey of Western Australia, Mineral House, 100 Plain Street, East Perth, Western Australia 6004, Australia

⁵Centre for Exploration Targeting, University of Western Australia, 35 Stirling Highway, Crawley, Perth, Western Australia 6009, Australia (michael.dentith@uwa.edu.au)

The Proterozoic Capricorn Orogen located in central Western Australia, recorded the assembly of the Archean Pilbara and Yilgarn Cratons to form the West Australia Craton during two stages of Paleoproterozoic Orogenies. To better understand the associated early tectonic evolution, we applied a finite-frequency P wave tomography technique to obtain the 3D body-wave velocity model of the upper mantle of this region. The P wave relative travel-time residuals were picked by applying a multichannel cross-correlation technique to the waveforms collected at 8 permanent and 57 broadband seismic stations of the Capricorn Orogen Passive-source Array. Overall a dataset including 6788 P wave travel-time data was obtained from 344 teleseismic events (distance range from 20 to 98 degrees, magnitude from Mw5.0 to Mw8.0). Preliminary results show an excellent spatial correlation with the geologic structure in this region, but also reveal intriguing features in the orogenic lithosphere that may shed light onto the regional tectonics. The Capricorn Orogen is imaged clearly as a significant low-velocity zone extending downward to ~250 km, likely reflecting the effects of punctuated lithospheric reworking and reactivation during the over-a-billion-years of cratonisation of West Australia Craton. The Glenburgh Terrane is underlain by a high-velocity anomaly with ~200 km thickness, consistent with an Archean megablock origin of the Glenburgh Terrane. The Pilbara Craton is characterised by high-velocity anomalies downward to 300 km, but with alternating low-velocity anomalies inside. The amplitude of the high-velocity is substantially lower compared with the Yilgarn Craton. To the northeast of the Pilbara Craton, a slow velocity anomaly is found beneath the Paterson Orogen. The most intriguing feature of the model is the high-velocity slab-like anomalies that extend northwards to over 200 km depth beneath the Capricorn Orogen, favouring the operation of a 2.0 Ga Paleoproterozoic subduction during the final assembly of the West Australian Craton.

REFERENCES

- [1] Cawood, P.A. and Korsch, R.J. 2008. Assembling Australia: Proterozoic building of a continent. *Precambrian Research*, 166, 1-35.
- [2] Dahlen, F.A. et al. 2000. Fréchet kernels for finite-frequency traveltimes-I. Theory. *Geophysical Journal International*, 141, 157-174.
- [3] Hung, S. et al. 2000. Fréchet kernels for finite-frequency traveltimes-II, Examples. *Geophysical Journal International*, 141, 175-203.
- [4] Sheppard, S. et al. 2007. Grenvillian-aged orogenesis in the Palaeoproterozoic Gascoyne Complex, Western Australia: 1030-950 Ma reworking of the Proterozoic Capricorn Orogen. *Journal of Metamorphic Geology*, 25, 477-494.
- [5] Reading, A.M. et al. 2012. Seismic structure of the crust and uppermost mantle of the Capricorn and Paterson Orogens and adjacent cratons, Western Australia, from passive seismic transects. *Precambrian Research*, 196, 295-308.
- [6] Vandecar, J.C. and Crosson R.S. 1990. Determination of teleseismic relative phase arrival Times using multi-channel cross-correlation and least-squares. *Bulletin of the Seismological Society of America*, 80, 150-169.

Indication from finite-frequency tomography beneath North China Craton: the heterogeneity of Craton destruction

X.B. XU¹, L. ZHAO^{1,2}, K. WANG¹ AND J.F. YANG¹

¹State Key Laboratory of Lithospheric Evolution, Institute of Geology and Geophysics, Chinese Academy of Sciences, Beijing, China (xuxiaobing@mail.iggcas.ac.cn)

²CAS Centre for Excellence in Tibetan Plateau Earth Sciences, Beijing, China (zhaoliang@mail.iggcas.ac.cn)

Using a multi-frequency joint inversion tomographic technique, we constructed new 3D P and S velocity models of the North China Craton (NCC) upper mantle with high resolution. Our research was based on previous work in the region, but was augmented by a much denser station coverage in the western NCC. The new data set is composed of 65629 P- and 447050 S-wave travel time residuals in multiple frequency bands, measured from 793 teleseismic events recorded by 738 permanent stations of the upgrade China National Seismic Network and 685 broadband stations of 10 temporary arrays in the region. The new P and S models provide several salient features from which we draw possible inferences on the regional tectonics. High-velocity anomalies are observed in the mantle transition zone (MTZ), with great morphological heterogeneities suggesting the buckling and/or fragmentation of the subducted Pacific slab. Some of the slab materials may be inferred from the high velocity anomalies visible below 660 km discontinuity, which further sink into the lower mantle. The velocity structure of the eastern NCC is dominated by small-scale lateral heterogeneities. At shallow depth, the high-velocity anomalies beneath the southern part of the eastern NCC and the Yanshan region likely represent the remnant cratonic lithosphere, which may suggest the craton destruction of the NCC is spatially non-uniform. A high-velocity anomaly is also observed in the Sulu Orogen, which is seemingly associated with the Tanlu Fault. The northern boundary of this anomaly spatially coincides with the Yantai-Qingdao-Wulian Fault, and it is likely a remnant of the Yangtze cratonic lithosphere subducting northwestwards. Significant low-velocity anomalies imaged beneath the central NCC exhibit a spatial discordance between its northern and southern parts, in which the northern low-velocity anomaly extends downwards to the top of MTZ with a lateral NW-SE trend, while the southern one extends downwards only to ~200-300 km. Slow-velocity anomalies are present beneath the Phanerozoic orogenic belt surrounding the NCC, the Paleoproterozoic Trans-North China Orogen and the Tanlu Fault. This feature not only shows the excellent spatial correlation with the orogens at surface, but also exhibits a consistent vertical continuity between 60 and 250 km depth. This intriguing feature suggests that the collisional orogenic belts are the inherited weak zones, which may play an important role in the craton destruction. Combining the multidisciplinary results in this area, we suggest that the spatial heterogeneities associated with the NCC craton destruction most likely result from a combined effect of the spatially non-uniform distribution of the wet upwellings triggered by the subducted Pacific slab and the pre-existing weak zones in the cratonic lithosphere.

REFERENCES

- [1] Chen, L. 2010. Concordant structural variations from the surface to the base of the upper mantle in the North China Craton and its tectonic implications. *Lithos*, 120, 1, 96-115.
- [2] Yang, J.F. et al. 2017. Slab-triggered wet upwellings produce large volumes of melt: Insights into the destruction of the North China Craton, *Tectonophysics*. <https://doi.org/10.1016/j.tecto.2017.04.009>
- [3] Zhao, L. et al. 2012. High-resolution body wave tomography models of the upper mantle beneath eastern China and the adjacent areas. *Geochemistry, Geophysics, Geosystems*, 13, Q06007.
- [4] Zhu, R.X. et al. 2017. Craton destruction and related resources. *International Journal of Earth Sciences*, 106, 7, 2233-2257.

The origin and mantle dynamics of Quaternary intra-plate volcanism in Northeast China from joint inversion of surface and body waves

Y. YANG¹, Z. GUO^{1,2}, K. WANG¹, Y. TANG³, Y.J. CHEN^{2,4}, S.-H. HUNG⁵

¹ARC Centre of Excellence for Core to Crust Fluid Systems (CCFS), GEMOC ARC National Key Centre, Department of Earth and Planetary Sciences, Macquarie University, Sydney, New South Wales, Australia

²School of Oceanography, South University of Science and Technology of China, Shenzhen, China.

³State Key Laboratory of Petroleum Resource and Prospecting, and Unconventional Natural Gas Institute, China University of Petroleum, Beijing 102249, China.

⁴Institute of Theoretical and Applied Geophysics, School of Earth and Space Sciences, Peking University, Beijing, China.

⁵Department of Geosciences, National Taiwan University, Taipei, Taiwan

We present a high-resolution 3-D model of NE China (NEC) by joint inversion of body- and surface- waves. This joint inversion significantly improves the resolution at shallow depths compared with body-wave tomography alone and provides seismic evidence for the origin of Quaternary intraplate volcanism. Mantle upwelling beneath the Changbaishan volcano originates from the uppermost lower mantle, reaches to ~60 km in the upper mantle, and spreads at the base of the lithosphere, with its head ~5 times larger than the rising tail in the lower upper mantle. It causes partial melting at shallow depths < 200 km, where the strongest velocity reduction occurs (4%-6%). However, low velocities beneath volcanoes in Halaha and Abaga are confined to depths shallower than 150 km, suggesting that magmatism in the Xinmeng belt is more likely caused by localised asthenospheric upwelling at shallow depths rather than from a common deep source. A small-scale sublithospheric convection cell may control the spatial and temporal distribution of Quaternary magmatism in NEC, that is, the upwelling beneath the Changbaishan triggers the downwelling beneath the southern Songliao basin, where the high velocity is imaged extending to ~300 km. The downwelling may further induce localised upwelling at surrounding areas, such as the Halaha and Abaga volcanos. Thanks to constraints from both surface- and body- waves, we can estimate the size of the convection cell more precisely. It is located between 42°N and 45°N, spreads ~500 km in W-E direction, measured from the distance between centres of downwelling and upwelling, and extends vertically to ~300 km.

Long-travelled sediments from India to Australia in the assembled Gondwana

W. YAO, Z.-X. LI, C. SPENCER AND E. MARTIN

Earth Dynamics Research Group, ARC Centre of Excellence for Core to Crust Fluid Systems (CCFS) and The Institute for Geoscience Research (TIGeR), Department of Applied Geology, WASM, Curtin University, Perth, Australia (weihua.yao@curtin.edu.au)

Previous studies of the late Neoproterozoic to early Paleozoic sedimentary strata in the Centralian Superbasins of Australia revealed their sedimentary sources as being the local Paterson-Petermann Orogen and Musgrave Inliers. This occurred during the assembly of Gondwana, based on the prevailing 700-500 Ma and 1.2-1.0 Ga zircon age populations and Hf isotope affinities of these sedimentary rocks with that of the magmatic suppliers in the Petermann orogen and Musgrave Inliers (e.g. [1, 2]).

Investigations into the Cambrian strata of the Ord basin in northern Australia, however, reveal a provenance affinity which is different from the Australian suppliers. The prevailing 980-930 Ma zircon population with dominant positive epsilon Hf values from the Ord Basin Cambrian sediments indicates an Indian Himalaya source which features matching zircon ages and Hf signals (e.g. [3]). Furthermore, the northeastern-directed paleocurrents in the Cambrian coastal marine environments of the Ord Basin agree with the possibility of the Cambrian detritus travelling along the northeastern Gondwana shoreline from Indian Himalaya to the Australian Ord Basin. This work demonstrates that, during the assembly of Gondwana, Australian basins not only received local sediments, but also caught detritus that travelled for thousands of kilometres from the Indian Himalaya.

REFERENCES

- [1] Maidment, D.W. et al. 2007. Testing long-term patterns of basin sedimentation by detrital zircon geochronology, Centralian Superbasin, Australia. *Basin Research*, 19, 335-360.
- [2] Martin, E.L. et al. 2017. An Australian source for Pacific-Gondwanan zircons: Implications for the assembly of northeast Gondwana. *Geology* (in-press).
- [3] Yao, W.H. et al. 2014. From Rodinia to Gondwanaland: a tale of detrital zircon provenance analyses from the southern Nanhua basin, South China. *American Journal of Science*, 314, 278-313.

Crustal structure of the Capricorn Orogen of Western Australia and its role in Paleoproterozoic craton assembly and reworking: a high-density passive seismic receiver function study

H. YUAN^{1,2,3}, S.P. JOHNSON², M. DENTITH³, R. MURDIE², K. GESSNER², F.J. KORHONEN² AND P. PIÑA-VARAS³

¹ARC Centre of Excellence for Core to Crust Fluid Systems (CCFS), Department of Earth and Planetary Sciences, Macquarie University, New South Wales 2109, Australia (huaiyu.yuan@gmail.com)

²Geological Survey of Western Australia, Mineral House, 100 Plain Street, East Perth, Western Australia 6004, Australia

³Centre for Exploration Targeting, University of Western Australia, 35 Stirling Highway, Crawley, Perth, Western Australia 6009, Australia

The Capricorn Orogen records the punctuated Paleoproterozoic amalgamation of the Western Australian Craton. Regional geological, geochemical, and geophysical studies revealed a prolonged tectonic history in craton assembly and subsequent intraplate reworking, which significantly re-shaped the orogenic crust. In this study, a high-density seismic receiver function study targeted the Glenburgh Terrane, an exotic late-Archean to Paleoproterozoic crustal block in the core of the orogen. Prominent Moho and intracrustal discontinuities are present, replicating the overall trend and depth range interpreted from a previous deep crustal seismic reflection survey. Low V_p/V_s ratios (~ 1.70) are mapped terrane-wide, indicating a felsic bulk crustal composition. However, significant lateral variations in the seismic signal are present across the terrane, showing a relatively thin crust (<40 km) with small V_p/V_s ratios (~ 1.70) in the centre of the terrane, compared to thickened crust (>40 km) with elevated V_p/V_s ratios (>1.76) along the margin. Within the shallow crust, a fast-velocity intraplate is present indicating significant modification of the crust during post-cratonisation magmatic differentiation processes. Based on existing age, isotopic, chemical and conductivity data, and the absolute shear wave velocity data presented here, the Glenburgh Terrane is interpreted as an Archean microcontinent that was significantly modified during Paleoproterozoic orogenesis. This is supported by the presence of significant seismic variations across the terrane boundary. The crust of the Glenburgh Terrane has preserved a unique seismic signature which was inherited from processes associated with crust formation in the Archean and significant reworking processes in the Paleoproterozoic. These results illustrate that multi-disciplinary datasets provide complementary resolution and texture information allowing for tighter constraints on Proterozoic cratonisation processes.

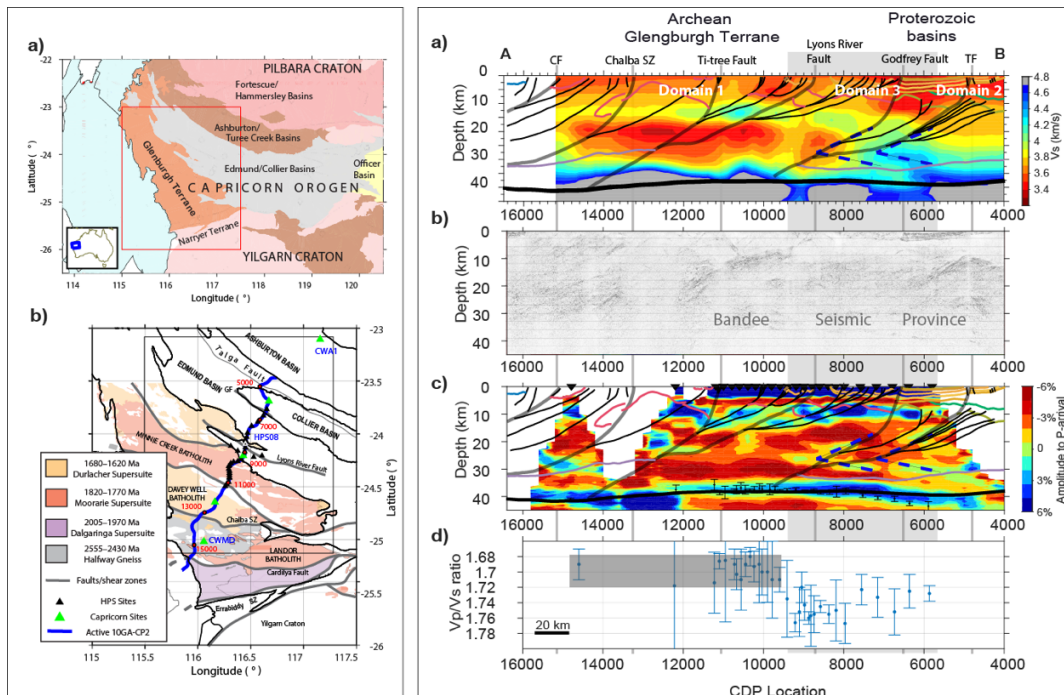


Figure 1. (a) Tectonic setting of the Capricorn Orogen, and (b) the close view of the Glenburgh Terrane. (Left panel)

Figure 2. Comparison between (a) the annotated velocity model with the active-source interpretations (b) the migrated active source image without

the interpretations. (c) receiver function common-conversion-point with the active-source interpretations. (d) V_p/V_s ratios and errors from receiver function H-k technique. (Right panel)

Thermochemical structures of the Dabie Orogenic Belt constrained from geophysical data

A. ZHANG^{1,3}, Z. GUO², J.C. AFONSO³, Y. YANG³, B. YANG⁴ AND Y. XU⁴

¹Institute of Geophysics and Geomatics, China University of Geosciences (Wuhan), 388 Lumo Road, Wuhan, China, 430074 (anqi.zhang5676@foxmail.com)

²Department of Ocean Science and Engineering, Southern University of Science and Technology, Shenzhen, China, 518055

³ARC Centre of Excellence for Core to Crust Fluid Systems (CCFS), Department of Earth and Planetary Sciences, Macquarie University, Sydney, New South Wales, Australia (juan.afonso@mq.edu.au; yingjie.yang@mq.edu.au)

⁴School of Earth Sciences, Zhejiang University, 38 Zheda Road, Hangzhou, China, 310027

The Dabie Orogen is a key component of the Central China Orogenic Belt. It was formed by continent-continent collision between the North China and Yangtze Cratons in the Middle-to-Late Triassic and began collapsing at the middle of the Early Cretaceous. Voluminous geochemical and geophysical data suggested that the mountain-root removal might have occurred in the Dabie region, which induced mantle upwelling, lower crust delamination and post-collision magmatism. These complex evolution processes have led to some controversial interpretations at present. Here, we jointly inverted the multi-observable geophysical data (i.e. Rayleigh wave dispersion curves, surface heat flow, geoid height and absolute elevation) by using a probabilistic inversion method to present an integrated thermochemical model of composition, bulk density and temperature beneath the Dabie Orogenic Belt and surroundings. Our models reveal that the lithospheric mantle has elevated temperature, but relatively lower density (thus larger buoyancy) beneath eastern Dabie, indicating a hotter asthenospheric upwelling. The lithospheric mantle under the Tongbai mountains, however, shows lower temperature, but relatively higher density. These consistent results demonstrate a deeper lithospheric root persisting underneath the Tongbai mountains and that a strong orogenic collapse only occurred in the eastern Dabie. The inverted lithospheric composition agrees well with a refertilised mantle with lower value of Mg# beneath North China Craton indicating its intense degree of lithospheric destruction. Finally, we estimate the water content based on the thermochemical model and electrical conductivity structures of two magnetotelluric (MT) profiles. We suggest that the orogenic belt (i.e. Dabie mountains and Tongbai mountains) shows a hotter and dryer lithospheric mantle, whereas the lithospheric mantle beneath the Jiangnan Basin of the Yangtze Craton and the Hehuai Basin of the North China Craton are cooler and wetter. This is also a feasible way to identify the water content effect on electrical conductivity by removing the background effect of temperature.

Melt segregation during ascent of buoyant diapirs in subduction zones

N. ZHANG

Earth Dynamics Research Group, ARC Centre of Excellence for Core to Crust Fluid Systems (CCFS), Department of Applied Geology, Curtin University, GPO Box U1987, Perth, WA 6845, Australia (nan.zhang@curtin.edu.au)

Cold, low-density diapirs arising from hydrated mantle and/or subducted sediments on the top of subducting slabs may transport key chemical signatures from the slab to the shallow source region of arc magmas. These chemical signatures are strongly influenced by the melting of this buoyant material during its ascent. However, to date there have been relatively few quantitative models to constrain melting and melt segregation in an ascending diapir.

Here, we use a two-phase Darcy-Stokes-energy model to investigate thermal evolution, melting, and melt segregation in a buoyant diapir during ascent through the mantle wedge. Using a simplified 2-D circular geometry we investigate diapir evolution in three scenarios with increasing complexity. First, we consider a case without melting in which the thermal evolution of the diapir is controlled solely by thermal diffusion during ascent. Our results show that for most cases (e.g. diapir radius ≤ 3.7 km and diapir initiation depths of ~ 75 km) thermal diffusion times are smaller than the ascent time—implying that the diapir will thermally equilibrate with the mantle wedge. Secondly, we parameterise melting within the diapir, but without melt segregation, and add the effect of latent heat to the thermal evolution of the diapir. Latent heat significantly buffers heating of the diapir. For a diapir with a radius of ~ 3.7 km, conductive heating from the outside is slowed $\sim 30\%$. Finally, we investigate numerical simulations that include melt segregation within the diapir. Melting initiates at the boundaries of the diapir as the cold interior warms in response to thermal equilibration with the hot mantle wedge. This forms a zone of high porosity and high permeability around the margin of the diapir. As the diapir continues to warm and ascend, new melts are focused into this rim and migrate upward, accumulating near the top of the diapir. The rim thus acts like an annulus melt channel, isolating the central part of diapir from the hot exterior and leading to even slower heating rates compared to cases without melt segregation.

These model results suggest that the melting and melt migration in an ascending diapir will segregate the interior from the outer rim, and may generate strong chemical gradients across the diapir.

Modelling melt extraction in long term planetary evolution

S. ZHANG AND C. O'NEILL

Australian Research Council Centre of Excellence for Core to Crust Fluid Systems (CCFS) and GEMOC, Department of Earth and Planetary Sciences, Macquarie University, Sydney, NSW 2109, Australia (siqu.zhang@mq.edu.au; craig.oneill@mq.edu.au)

A new melt extraction model

In the early-stage evolution of Earth and other planetary bodies, the mantle is very hot and melt processes much stronger than present-day. These intensive melt processes are not only very effective at cooling the planet, but are also an important mechanism of planetary resurfacing. Therefore, understanding the melt processes of an early-stage planet is crucial when studying planetary evolution.

Melt generation and migration can be modelled using McKenzie equations in reasonable detail. However, this method requires large computational power and a very small time step for the simulation. It is suitable for modelling localised features over a short time scale, but not very practical for global scale models examining the long-term evolution of a planetary body. Additionally, melt extraction is usually ignored or oversimplified in this method through simply removing the melt and then placing it onto the surface.

In this study, we developed a one dimensional statistical approach to treat melt generation and migration in 2D/3D mantle convection models. In this approach, the composition of the mantle is tracked, with melt extraction altering the residual composition, making it depleted and therefore more difficult to generate subsequent melts. As well as this, not all melts erupt onto the surface. The melt is emplaced at the level of neutral buoyancy if this is reached prior to the melt reaching the surface. Given that the density structure is far more complicated in the field than in simplified models, a perturbation is added to the density column and a Monte Carlo approach is used to counter this effect.

This new tool allows us to study the long-term evolution of the Earth and other planetary bodies in far more detail, providing a better understanding of their thermal history and the surface features we observe at present-day.

Mantle input's influence on mineralisation of the giant porphyry Cu–Au–Mo deposits

Y.C. ZHENG^{1,2}, L. WANG¹, Z.S. YANG³, B. XU^{1,2} AND Z.Q. HOU⁴

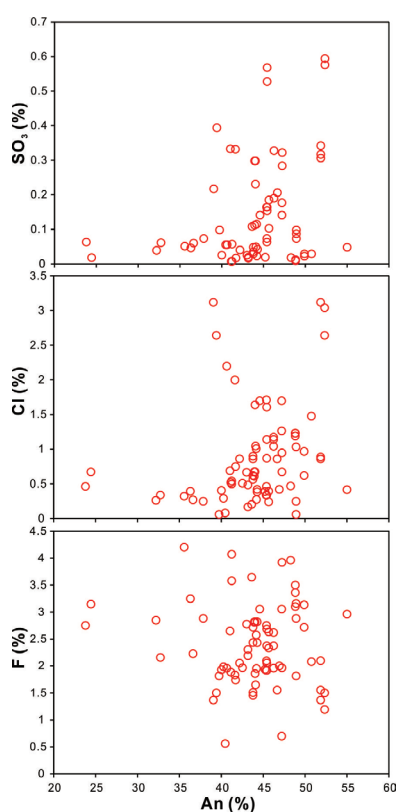
¹School of Earth Sciences and Resources, China University of Geosciences, Beijing 100083, PR China (zhengyuanchuan@gmail.com)

²Australian Research Council Centre of Excellence for Core to Crust Fluid Systems (CCFS) and GEMOC, Department of Earth and Planetary Sciences, Macquarie University, Sydney, NSW 2109, Australia (yuanchuan.zheng@mq.edu.au)

³Institute of Mineral Resources, Chinese Academy of Geological Sciences, Beijing, 100037, PR China (yangzhusen@vip.sina.com)

⁴Institute of Geology, Chinese Academy of Geological Sciences, Beijing, 100037, PR China (houzengqian@126.com)

Porphyry Cu–(Au–Mo) deposits (PCDs) are the world's largest source of copper and molybdenum, and an important source of gold. Individual deposits are often very large (Cu up to 203 Mt; Au up to 3000 t), making giant PCDs prime targets for modern research and mineral exploration. However, the source regions of fluids, sulfur and metals for PCDs remain controversial. It is generally believed that fluids, sulfur and metals exsolved directly from the hosting intermediate to felsic porphyries, while others suggest these ore-forming materials were mainly derived from coeval mafic magmas. Apatite [Ca₅(PO₄)₃(F,OH,Cl)] contains large amounts of volatile components (F, OH and Cl) and a small amount of S. Thus, apatite can be used to track the S, Cl, and F evolution of a PCD system (Streck and Dilles, 1998).



The Tethyan Belt is one of three major PCD metallogenic belts on Earth. Within this belt sits the giant porphyry Cu–Au deposit Saindak, located in Pakistan, which developed at 22 Ma. This deposit is composed of three mining districts, each district centred around multiple stocks with small diameters of less than 1 km. These stocks are mainly composed of tonalite and granodiorite, and intruded by diorite dikes. Both tonalite and granodiorite contain large amounts of high-Mg dioritic enclaves (MgO up to 7.3 wt%). These enclaves show typical igneous textures, acicular apatites, and crystallisation ages identical to those of the host rocks, indicating that they are of magmatic origin. These enclaves should represent the product of injection of mafic magmas into the ore-forming intermediate porphyries, making the giant Saindak PCD an ideal place to verify whether the injection of mafic magmas will introduce volatiles (S, Cl, F), metals and fluids to the PCDs.

Figure 1. Contents of SO₃, Cl and F in apatite vs An number of the host plagioclase.

The ore-forming granodiorite contains abundant apatite, but only grains hosted in plagioclase have been used here. These apatite grains are euhedral and very small, commonly less than 10 μm and 50 μm in width and length, respectively. We conducted EMPA both on the apatite grains and their hosting plagioclase. The EMPA data indicate that the apatite grains contain SO₃, Cl and F varying from 0.01 to 0.59 wt%, 0.06 to 3.12 wt%, and 0.56 to 4.20 wt%, respectively. The plagioclase is dominated by labradorite

to andesine, with minor oligoclase (An=12–58 %). As shown in Figure 1, apatites hosted in high An number plagioclase commonly have higher contents of SO₃ and Cl, which might indicate that mafic magmas have released considerable amounts of S and Cl into the felsic rocks, which is then available for PCD mineralisation. However, F content of apatite vs An number of hosting plagioclase shows a reverse trend, indicating that F should be mainly enriched in felsic porphyries.

REFERENCE

[1] Streck, M.J. and Dilles, J.H. 1998. Sulfur evolution of oxidised arc magmas as recorded in apatite from a porphyry copper batholith. *Geology*, 26, 523–526.

Presenting Author Index - Oral Presentations

Afonso, Juan Carlos	3	Lenz, Christoph	55
Barlow, Erica	5	Li, Zheng-Xiang	58
Baumgartner, Raphael	6	Liptai, Nora	60
Belousova, Elena	8	Liu, Zairong	62
Caruso, Stefano	10	Lu, Yongjun	66
Castillo Oliver, Montgarri	12	Martin, Laure	70
Chen, Chunfei	13	Montalvo Delgado, Stephanie	72
Clark, Simon	16	Nomchong, Brendan	76
Daczko, Nathan	17	Oliveira, Beñat	78
Denyszyn, Steven	18	Suzanne, O'Reilly	79
Dering, Gregory	19	Pidgeon, Robert	83
Djokic, Tara	20	Piña-varas, Pirla	84
Etheridge, Michael	21	Pisarevskiy, Sergei	87
Fiorentini, Marco	23, 24, 25	Poole, Gregory	88
Foley, Stephen	26	Pourteau, Amaury	89
Förster, Michael	27	Soares, Georgia	94
Fougerouse, Denis	28	Sugiono, Dennis	97
Gardiner, Nicholas	30	Thebaud, Nicolas	98
Gardner, Robyn	31	Tilhac, Romain	100
Gessner, Klaus	32	Tretiakova, Irina	101
Giuliani, Andrea	35	Van Kranendonk, Martin	102
Glen, Richard	37	Verberne, Rick	103
Gonzalez, Christopher	38	Volante, Silvia	105
Gorczyk, Weronika	40	Wang, Kai	107
Gréau, Yoann	41	Wilde, Simon	109
Griffin, William	43	Wu, Shucheng	110
Hämmerli, Johannes	44	Xu, Bo	111
Henriquez, Gonzalo	46	Xu, Xiaobing	112
Henry, Hadrien	47	Yang, Yingjie	114
Huang, Jinxiang	48	Yao, Weihua	115
Jacob, Dorrit	49	Yuan, Huaiyu	116
Jara, Constanza	50	Zhang, Anqi	117
Kirkland, Christopher	51		
Kirscher, Uwe	52		
LaFlamme, Crystal	53		

Presenting Author Index - Poster Presentations

Alard, Olivier	4	Scibiorski, Elisabeth	91
Baumgartner, Raphael	7	Selway, Katherine	92
Bennett, Jason	9	Silva, David	93
Caruso, Stefano	11	Spath III, Charles	95
Chen, Ying	14	Stuart, Catherine	96
Choi, Eunjoo	15	Thebaud, Nicolas	99
Farmer, Michael	22	Veter, Marina	104
Gain, Sarah	29	Walker, Alexander	106
Ghatak, Hindol	33	Wang, Yu	108
Giuliani, Andrea	34, 36	Xu, Xiaobing	113
Goode, Louise	39	Zhang, Nan	118
Greene, Stephanie	42	Zhang, Siqi	119
Han, Kui	45	Zheng, Yuanchuan	120
Lai, Yi-Jen	54		
Lenz, Christoph	56		
Li, Jiangyu	57		
Liptai, Nora	59		
Liu, Yebo	61		
Lu, Jianggu	63		
Lu, Yongjun	64, 65		
Manassero, Maria	67		
Martin, Erin	68		
Martin, Laure	69		
Meek, Uvana	71		
Munnikhuis, Jonathan	73		
Murphy, Rosanna	74		
Nimalsiri, Thusitha	75		
Nordsvan, Adam	77		
Otter, Laura	80		
Parra Avila, Luis	81		
Patabendi Gedara, Sarath	82		
Ping, Xianquan	85		
Pintér, Zsanett	86		
Salajegheh, Farshad	90		



Australian Government
Australian Research Council



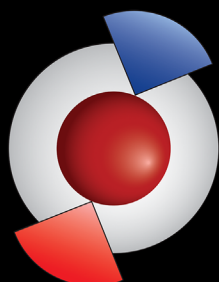
MACQUARIE
University



Curtin University



THE UNIVERSITY OF
WESTERN
AUSTRALIA



**ARC Centre of Excellence
for Core to Crust
Fluid Systems**

**2017
CCFS Whole-of-Centre Meeting
ISSN:2208-7230**

Delivering the fundamental science needed to sustain Australia's resource base